STATE-OF-THE-ART REVIEW OF HYDROGEN STORAGE IN REVERSIBLE METAL HYDRIDES FOR MILITARY FUEL CELL APPLICATIONS

Prepared by

Gary Sandrock, Ph.D.

SunaTech, Inc.
113 Kraft Place
Ringwood, NJ 07456-1844 USA

for

Department of the Navy
Office of Naval Research
Ballston Tower One
800 North Quincy Street
Arlington, VA 22217-5660 USA

Dr. John Sedriks
Program Officer
ONR 332

under

Contract N00014-97-M-0001

Final Report

24 July 1997

REPORT DOCUMENTATION PAGE

Form Approved
OMB No. 0704-0188

1. AGENCY USE ONLY (Leave blank)	2. REPORT DATE	3. REPORT TYPE AND DATES COVERED
	24 July 1997	Final 11/5/96-7/24/97

4. TITLE AND SUBTITLE
STATE-OF-THE-ART REVIEW OF HYDROGEN STORAGE IN REVERSIBLE METAL HYDRIDES FOR MILITARY FUEL CELL APPLICATIONS

5. FUNDING NUMBERS
N00014-97-M-0001

6. AUTHOR(S)
Gary Sandrock

7. PERFORMING ORGANIZATION NAME(S) AND ADDRESS(ES)
SunaTech, Inc.
113 Kraft Place
Ringwood, NJ 07456-1844
USA

8. PERFORMING ORGANIZATION REPORT NUMBER

9. SPONSORING/MONITORING AGENCY NAME(S) AND ADDRESS(ES)
Program Officer
Office of Naval Research
800 North Quincy Street
Arlington, VA 2217-5660

10. SPONSORING/MONITORING AGENCY REPORT NUMBER
Final Report

11. SUPPLEMENTARY NOTES

12a. DISTRIBUTION/AVAILABILITY STATEMENT
Approved for public release; distribution unlimited

12b. DISTRIBUTION CODE

13. ABSTRACT *(Maximum 200 words)*

This report is a comprehensive review of reversible metal hydrides for possible use as hydrogen storage and supply media for proton exchange membrane (PEM) fuel cells. There is considerable interest in using fuel cells for submarine and other military power sources. First presented is a tutorial overview of the phenomenology and important technical properties of metal hydrides, followed by a guide to sources of information on the subject. The main part of the review summarizes the hydriding properties and use potential of the elements, solid-solution alloys and five classes of intermetallic compounds: AB_5, AB_2, AB, A_2B and miscellaneous others. It also briefly reviews the complex (normally nonreversible) hydrides, unconventional alloys and carbon. Emphasis is on hydrides that can use the waste heat of PEM fuel cells (0-100°C) to release H_2 in the 1-10 atmosphere pressure range, although other hydrides are also partly covered. Although there are many available alloys with useful properties, shortcomings remain especially in the areas of H-capacity, cost and resistance to impurity gases in the H_2 used. Further R&D activities aimed at overcoming some of the shortcomings are suggested.

14. SUBJECT TERMS
hydrides, hydrogen storage, fuel cells, PEM fuel cells, intermetallic compounds, solid-solution alloys, hydride properties, hydride databases, history of hydrides

15. NUMBER OF PAGES
159

16. PRICE CODE

17. SECURITY CLASSIFICATION OF REPORT	18. SECURITY CLASSIFICATION OF THIS PAGE	19. SECURITY CLASSIFICATION OF ABSTRACT	20. LIMITATION OF ABSTRACT
Unclassified	Unclassified	Unclassified	UL

NOTICE

This review was prepared by SunaTech, Inc., for the Office of Naval Research. The information included herein is taken from the published literature and was reviewed and analyzed on a best-effort basis. I believe the information is a reasonably accurate representation of the data published; however, the Office of Naval Research and SunaTech, Inc., can offer no warranty, express or implied, as to the accuracy, applicability or use of the information for the users' intended purposes.

EXECUTIVE SUMMARY

The fuel cell offers a silent and efficient source of electric power, long of interest for military applications. The fuel cell derives it power from the electrochemical reaction of hydrogen and oxygen. The storage of hydrogen is therefore important to the concept and this review considers the option of storing hydrogen in the form of reversible (rechargeable) metal hydrides. Hydrides offer compact H-storage at low pressures (high safety). The review focuses mostly on hydrides which can supply H_2 to the Proton Exchange Membrane (PEM) type of fuel cell, where waste heat is produced in the 0-100°C range and can be utilized by the hydride during H_2 desorption. In particular, the application to manned submarines is considered, but the review is applicable to most other PEM fuel cell applications operating at near-ambient temperature. This state-of-the-art review of metal hydrides was commissioned by the US Office of Naval Research.

It is assumed that the reader has little or no experience in the field of reversible hydrides, so this review begins with a tutorial introduction to their science and engineering. In addition to the most important thermodynamic pressure-composition-temperature (PCT) properties and H-capacity (gravimetric and volumetric), a number of important secondary engineering properties are defined: activation, decrepitation, H_2 absorption/desorption kinetics, impurity effects, cyclic stability, safety, raw materials cost and metallurgy. Sources of information on hydrides are summarized, including books, journals, international symposia and the new International Energy Agency Internet databases.

The main part of this report reviews in detail the large numbers of hydriding metals, elements and alloys, that will reversibly store H_2 at temperatures of 0-100°C and pressures of 1-10 atmospheres absolute. With the possible exception of vanadium, the use of elemental metals is not very practical. Fortunately there are many alloys and intermetallic compounds that combine strong hydriding elements A with weak hydriding elements B to form alloys with just the desired degrees of stability. These include solid solution alloys and intermetallic compounds of the generic families AB_5, AB_2, AB, A_2B, AB_3, A_2B_7, A_2B_{17} and others. The AB_5, AB_2 and AB offer the best combinations of PCT properties, with the AB_2 and AB compounds offering the best combinations of good H-capacity and lowest raw materials cost. However, other intermetallic compounds and V-solid solution alloys also offer possibilities. There is no perfect hydriding alloy and suggestions for further R&D to improve the state-of-the-art vis a vis fuel cell applications are listed for all of the families reviewed. For the purpose of future R&D activities, hydride laboratories in a number of countries identified by the sponsor are listed as an Appendix.

In addition to the conventional, nearly single-phase crystalline alloys that represent 90+ percent of the available H-storage alloys, more advanced materials are also briefly reviewed: multiphase alloys & composites, amorphous and nanocrystalline alloys, quasicrystalline alloys, polyhydrides and complex (chemical) hydrides. In addition, carbon (a potential competitor for metal hydrides) is also briefly reviewed in appropriate perspective.

Although all ambient temperature reversible metal hydrides have undesirably low gravimetric H-contents for their practical use in most civilian land vehicles that might use PEM fuel cells, their application to special military vehicles (such as neutral buoyancy submarines) may be practical now because of good volumetric H-capacities and safety. In fact, they are specifically included in the design of the new German U-212 class of fuel cell powered, manned submarines. It is hoped that this review can serve as a textbook and handbook for both new research activities and design engineers looking for practical applications of hydride-based H-storage.

TABLE OF CONTENTS

LIST OF TABLES

LIST OF FIGURES

1. INTRODUCTION

1.A. Fuel Cell Power

The concept of the electrochemical generation of electric power via fuel cells has had a long and variable history dating back 1.5 centuries [Appleby, 93][1] . At this moment in time, there is very strong interest in electric land vehicle propulsion using fuel cell power sources. Several major vehicle demonstration projects are either in place or being seriously planned (see monthly news reports in the Hydrogen & Fuel Cell Letter (Hoffmann, 97). In spite of the ups and downs of fuel cell history, their time seems to be finally coming with the new century and the growing need for alternate fuels and more efficient means of transportation. In fact, fuel cell power really began modestly at least 3 decades ago within the specialized needs of military and aerospace applications. More about that shortly.

The fuel cell uses the most elementary of chemical reactions:

$$H_2 + 0.5\,O_2 \text{ ----> } H_2O \qquad \text{(Eq.1)}$$

In order to generate electric power of useful emf for an external electric circuit, Reaction 1 must be performed electrolytically on two electrodes in one of several suitable electrolytes. If we assume for the moment an acidic aqueous electrolyte, then the two electrode reactions are the following:

Anode $$H_2 \text{ ----> } 2H^+ + 2e^- \qquad \text{(Eq.2)}$$

Cathode: $$0.5O_2 + 2H^+ + 2e^- \text{ ----> } H_2O \qquad \text{(Eq.3)}$$

The two electrons are driven through an external circuit connecting the anode and cathode with an emf ideally that of the oxidation potential of hydrogen (1.23 V dc), thus providing electric power for some external device. While most fuel cells are quite efficient, in fact they cannot be 100% efficient. Output emf is less than the ideal 1.23 volts and some waste heat (albeit small) is produced. As will be shown, the waste heat is an important factor in military applications and can often be utilized. Relative to this study of using metal hydrides as the source of the hydrogen input to the fuel cell, it is important to recognize at the beginning that the waste heat can be used directly by the endothermic hydride ----> H_2 desorption process.

Because operating temperature (and related waste heat temperature) is important to how fuel cells are applied to both military and civilian applications, it is important to list in Table I the main types of available fuel cells relative to that parameter (Fickett, 84). Because of the requirement to operate near room temperature and the proximity of personnel, most recent mobile fuel cell applications and demonstrations have been of the proton exchange membrane (PEM) or alkaline (AFC) types, while large stationary fuel cells (e.g., for the utility industry) have been of the phosphoric acid or molten carbonate types (Appleby, 93). Historically, almost all military and aerospace fuel cells have been of the PEM or AFC types, primarily because of the near-ambient operating conditions. Recent trends have moved more and more in the direction of the PEM types. For the purposes of this study, I will assume future military fuel cells will be of the PEM or AFC types, operating more or less in the 0-100°C temperature range.

[1] References are cited relative to the first author, followed by the year of publication. A parenthetical entry following the year, if any, represents the record number in the IEA/DOE/SNL on-line hydride reference database (cf. Section 2.C.3). An alphabetical list of references is included at the end of the report (including database numbers, if any).

Table I
Typical Operating Temperatures of Fuel Cells
(Fickett, 84)

Electrolyte	Temperature, °C
Acid	
Solid Polymer	0-120
Phosphoric	150-220
Alkaline (KOH)	-40-120
Molten Carbonate	600-700
Solid Oxide	900-1000

The PEM fuel cell consists of a polymeric electrolyte which serves as the proton exchange membrane. It typically consists of a cross-linked, PTFE-like polymer containing sulfonic acid and capable of conducting hydronium (H_3O^+) ions. In practice, the PEM fuel cell is safe and simple. The output product is very high purity, potable H_2O, i.e., there are no corrosive liquid electrolytes involved. A disadvantage of the PEM fuel cell is that it will freeze below 0°C, usually leading to permanent damage. Another significant disadvantage (at least at the present state of the art) is the fact it requires a noble metal catalyst (usually Pt) on the anode, which contributes to its relatively high cost. A related problem is the fact that impurity CO in the H_2 feed can poison the catalyst. thus leading to the need for very pure hydrogen. Anticipating later discussions, ability of hydrides to getter CO impurities and release only supra high purity hydrogen has distinct advantages for a Pt catalyzed fuel cell.

The alkaline fuel cell (AFC) typically uses a 35-50 wt.% KOH electrolyte. similar to that used in most alkaline batteries. AFCs have the advantage of storage and startup below 0°C and also consist of relatively low-cost construction materials, although small quantities of noble metals are sometimes used. In addition to the potential hazards of a corrosive liquid electrolyte, AFCs are also subject to damage from carbon oxides, especially CO_2 entering with an air-breathing unit.

If civilian fuel cell electric vehicles commercially succeed early in the new century, then significant credit for paving the way should go to those who promoted the aerospace and military development of fuel cells. The manned space program has logically and successfully used H_2-O_2 fuel cells for space power. The U.S. Department of Defense has funded fuel cell development for a diverse series of military applications, including mobile power generators. transportation vehicles, airfield lighting, communication and transmitter devices, satellite power systems, remote site generators, submerged vehicles and buoy transmitters (Appleby, 93). There are a number of inherent fuel cell properties justifying such efforts:

1. Nearly zero sound signature
2. Low infrared signature
3. High energy density relative to batteries
4. High efficiency
5. Will operates as long as fuel and oxidant is fed in
6. Good shelf life and low maintenance
7. Cogeneration potential
8. Able to use alternative fuels, e.g., methanol or NH_3
9. Independence from electric and fossil fuel interruptions, e.g., H_2 from solar PV
10. Closed cycle concepts for submersibles

This review will consider the use of rechargeable metal hydrides as H_2 storage media for

coupling with fuel cells. The primary military applications considered will be fuel cell powered vehicles, particularly manned submarines (MUV), unmanned air vehicles (UAV) and unmanned underwater vehicles (UUV). However the study will be applicable to most other military and civilian applications of fuel cells operating at near-ambient temperatures (0-100°C).

1.B. Hydrides and Fuel Cells

Fuel cell reactions 1 and 2 call for the input of molecular (or atomic) hydrogen. The most straightforward approach is to feed H_2 gas. However, it is possible to use other H-containing fuels (Fickett, 84): hydrazine (N_2H_4), ammonia (NH_3), methanol (CH_4O), ethanol (C_2H_6O), etc. All of the latter fuels must be endothermically dissociated to produce the required H atoms or H_2 molecules, either directly (within the fuel cell using catalysts) or indirectly (before the fuel cell using thermal energy and catalysts). Usually temperatures well above ambient are required and byproduct gases such as CO_2 and N_2 are produced. It would be conceptually simplest to avoid chemical reforming and catalytic dissociation technology and simply use H_2 gas as the fuel. The problem is how to store the H_2.

Like all other gases, H_2 can be stored as a gas (GH_2), liquid (LH_2) or solid (metal hydride MH). If, for the moment, we concentrate on a volume-limited submarine application, then there are rather immediate practical problems for GH_2 and LH_2. As I will show later, GH_2 requires rather large volumes and in addition poses significant compression energy penalties. The very high H_2 pressures also pose potential safety problems in manned vehicles. Cryogenic LH_2 requires liquefaction technology (and associated energy penalties) along with well-insulated containers. MH storage gives advantages in energy and volumetric efficiency, safety, shelf life but suffers from poor gravimetric efficiency (maybe not important for a submarine) and relatively high investment cost (at least relative to GH_2 containers).

At least one theoretical study for the U.S. Naval Sea Systems Command and David Taylor Research Center has considered the use of reversible and nonreversible hydrides as H_2 fuel supplies for the Autonomous Deep Diving Towed Array System (ADDTAS) (Lynch, 89). The study considered a closed-cycle internal combustion engine, not a fuel cell. Lynch found that combination of the reversible hydride $TiFeH_2$ and 12.5 MPa (1813 psia) compressed O_2 marginally met the required 30 day minimum mission duration for the vehicle. The use of LH_2 + LO_2 almost doubled the mission duration and the best durations were achieved with the combination of water reactive hydrides (MgH_2 and $LiBH_4$) and LO_2 (122 and 143 days, respectively). Of course the non-reversible water reactive hydrides are completely corroded during the H_2 generation reaction and must be completely reconstituted after each mission.

Although the use of a reversible hydride may be marginal for the unmanned ADDTAS vehicle, the story may be somewhat different for manned submarines. In fact, the German navy is building in an MH + LO_2 + PEM fuel cell combination for its new "high-tech" Class 212 submarine (Domizlaff, 96). Although a separate diesel engine is used for surface running, the hydride-LO_2-fuel cell combination is said to give the 1350 ton U-212 up to 30 days submerged time and a peak underwater speed of 20 Knots. The 34 kW fuel cell operates at 80°C, with its waste heat used to desorb the H_2 from the hydride beds .

At present there is only limited interest in coupling hydride beds to fuel cells for civilian electric vehicles. Because of the rather poor gravimetric H-content of currently available room-temperature hydrides, most recent vehicle demonstration projects have used high-pressure GH_2

tanks or methanol-reformer combinations. I would be the first to agree that a significant improvement in hydride technology is needed for its viability in the civilian transportation field.

In summary, although the use of hydrides for civilian fuel cell applications is problematical at the moment, there is more potential for fuel cell-hydride combinations in military applications. For military applications to properly develop, those involved need a clear statement of the present state of the art of rechargeable metal hydrides, as well as some feel for the future advances possible. That is the purpose of this study.

1.C. Objectives of this Review

There are four distinct objectives of this review:

1. Introduction to the Fundamentals of Hydrides - This section has two sub-objectives: First, it is intended to give a brief and efficient introduction to rechargeable hydrides for those who have had little or no experience in the field but will perhaps need to be involved in the technological aspects of coupling hydride beds to fuel cells. Second, it carefully defines the rather complex array of primary and secondary hydride properties that need to be considered in concert for the proper selection and use of an alloy for a practical device.

2. State-of-the Art Reviews of Hydriding Alloys - There are vast arrays of hydriding alloys that have been developed in recent decades. This section is structured as to generic or metallurgical alloy type. For each type, a review of history, property spectra and practicality are presented. Although most of the historical data are for conventional (equilibrium) alloys and intermetallic compounds, recent efforts directed toward nonconventional alloys and preparation techniques are also reviewed. There is some effort to concentrate on the 0-100°C operating temperature, but higher and lower temperature hydrides are also included to some extent. In addition, a brief review of carbon as a potential hydrogen storage medium is given.

3. Directions for Future R&D - Hydride property shortcomings exist for the applications of hydrides to military fuel cells. These are identified and summarized in qualitative and quantitative terms, followed by my personal suggestions for further R&D to work needed in both the present and next generations of hydrides.

4. Directory of Hydride R&D Groups - A listing of active hydride research groups in a number of countries identified by the sponsor is provided as an Appendix.

2. FUNDAMENTALS OF RECHARGEABLE HYDRIDES

This section offers a brief tutorial introduction to the general science and technology of hydrides. It is oriented toward an outline of hydride properties that are important to correctly understanding the phenomenology of these interesting materials and correctly applying them to practical applications. Other introductory articles by the author give supplementary and complementary views of the same subject (Sandrock, 81, 91, 92 (322),95; Reilly, 80).

2.A. Basic Phenomenology, Advantages and Disadvantages

Reversible metal hydrides offer a "solid" alternative to storing hydrogen in pressurized gas and cryogenic liquid forms. In a rather naive physical sense, hydride-forming metals and alloys can be considered a gaseous analogy to a water sponge. Metal crystals (or glasses) contain

interstices that will absorb and desorb hydrogen atoms just as sponges have pores that will absorb and desorb drops of water. However, unlike the purely physical action of a water sponge, hydrides involve true reversible chemical reactions. In fact, it has been known for nearly 150 years that many metals will absorb and desorb hydrogen either from the gas phase

$$M + \frac{x}{2} H_2 <----> MH_x \quad , \qquad \text{(Eq.4)}$$

or electrolytically in aqueous solutions

$$M + \frac{x}{2} H_2O + \frac{x}{2} e^- <----> MH_x + \frac{x}{2} OH^- . \qquad \text{(Eq.5)}$$

In either case, the hydrogen ends up as atomic hydrogen within the metal interstices, so there must be dissociative chemisorption (or reassociative desorption) of the H_2 (or H_2O) molecules on the surface, e.g., for gas phase absorption (--->) or desorption (<---) the reaction

$$H_2 <----> 2H. \qquad \text{(Eq.6)}$$

Although many metals and alloys form reversible hydrides given enough pressure or temperature, those in which Eq.4 can be carried out easily at modest pressures and temperatures are loosely called rechargeable or reversible metal hydrides. The practical quantification and thermodynamics of the absorption and desorption (hydriding and dehydriding) reactions will be covered in Sections 2.B.1 and 2.B.2. For the moment, suffice it to say the absorption and desorption reactions can be done with surprising ease and simplicity.

There are a number of advantages and disadvantages of storing hydrogen in hydride form that will become apparent throughout this tutorial. One of the important advantages is the highly efficient packing of H-atoms within the highly ordered interstices among the metal atoms. As shown by the elemental hydrides in Table II, this results in high volumetric densities of hydrogen, much higher than GH_2 and usually even higher than LH_2. This is an obvious advantage for volume-limited applications such as submarines. As mentioned earlier, hydride containers operate at near-ambient temperature and do not require the sophisticated thermal insulation of a cryogenic LH_2 container. There are additional safety advantages of hydride storage, as will be discussed in Section 2.B.8, p.19.

Table II also shows the single most important disadvantage of MH storage, at least for mobile terrestrial applications such as land vehicles, namely the generally poor gravimetric density (wt.%) of hydrogen. H-atoms are very light relative to the metal atoms used as storage media. Although some hydrides like LiH and MgH_2 might seem to offer respectable H weight percents (12.7 and 7.6, respectively), in fact such capacities are available only at impracticably high temperatures. As will be shown, one is hard-pressed to achieve even 2 wt.% reversible H-capacity with a near-ambient-temperature hydride. However, this is not necessarily a serious shortcoming for submarines that are purposely ballasted to achieve near-neutral buoyancy. What is considered a heavy burden to other applications can be considered part of the ballast in a submarine. Unfortunately, hydrides represent a rather expensive ballast and therein lies one of other disadvantages of hydrides (see section 2.B.9, p.20).

Table II
Gravimetric and Volumetric H-Densities
(Libowitz, 65; Hoffman, 76)

Hydrogen Form	H Weight Density, wt.%	H Volume Density, 10^{22} atoms/cm^3
Gas at 100 atm	100	0.5
Liquid (20K)	100	4.2
LiH	12.7	5.9
MgH_2	7.6	6.7
$PdH_{0.6}$	0.6	4.3
TiH_2	4.0	9.2
ZrH_2	2.2	7.3
VH_2	3.8	11.4
GdH_2	1.3	5.4
GdH_3	1.9	6.4
UH_3	1.3	8.3

2.B. Important Properties

Like any other engineering material, hydrides have a spectrum of important properties. For example, if an alloy steel is specified for a structural application, the metallurgist or design engineer must consider properties beyond tensile yield strength, e.g., corrosion properties, fatigue resistance, high-temperature creep resistance, formability, cost, etc. So it is also with hydrides. The purpose of this section is describe the various hydride properties important to applications.

2.B.1. Pressure-Composition-Temperature (PCT) Properties

The single most important area of hydride technology concerns the interrelated temperature and pressure conditions under which a hydriding alloy will absorb and desorb H_2. This section introduces the concept of P-C isotherms (ideal and real), how to measure them, and the thermodynamics associated with them.

2.B.1.a. - Pressure-Composition Isotherms (Ideal)

The hydride scientist's favorite way to quantify the absorption and desorption of hydrogen by metals is by pressure-composition isotherms which are determined experimentally (see Section 2.B.1.b, p.8). A set of somewhat idealized P-C isotherms is shown in Figure 1. They are usually plotted in the form of H_2 pressure (usually on a logarithmic scale) versus atomic hydrogen/ metal ratio (H/M). For discussion purposes, let us consider the isotherms of Fig.1 to be absorption isotherms determined at room temperature.

Using Fig.1(a) and starting with nearly H-free metal at point 1, generally called the α-phase, we apply an increasing pressure of gaseous H_2. If the surface of the metal is clean (i.e., free of oxide barriers) the H_2 molecules will dissociate and the individual H atoms will diffuse into the metal lattice to form a random M-H solid solution. That is, the H-atoms in the α solid solution do not take fixed and ordered positions and in fact are usually quite mobile, even near room temperature. The H-concentration in the α-phase (H/M) is a weak function of pressure. Because this part of the hydrogen absorption process is controlled by dissociative chemisorption (Eq.6) it

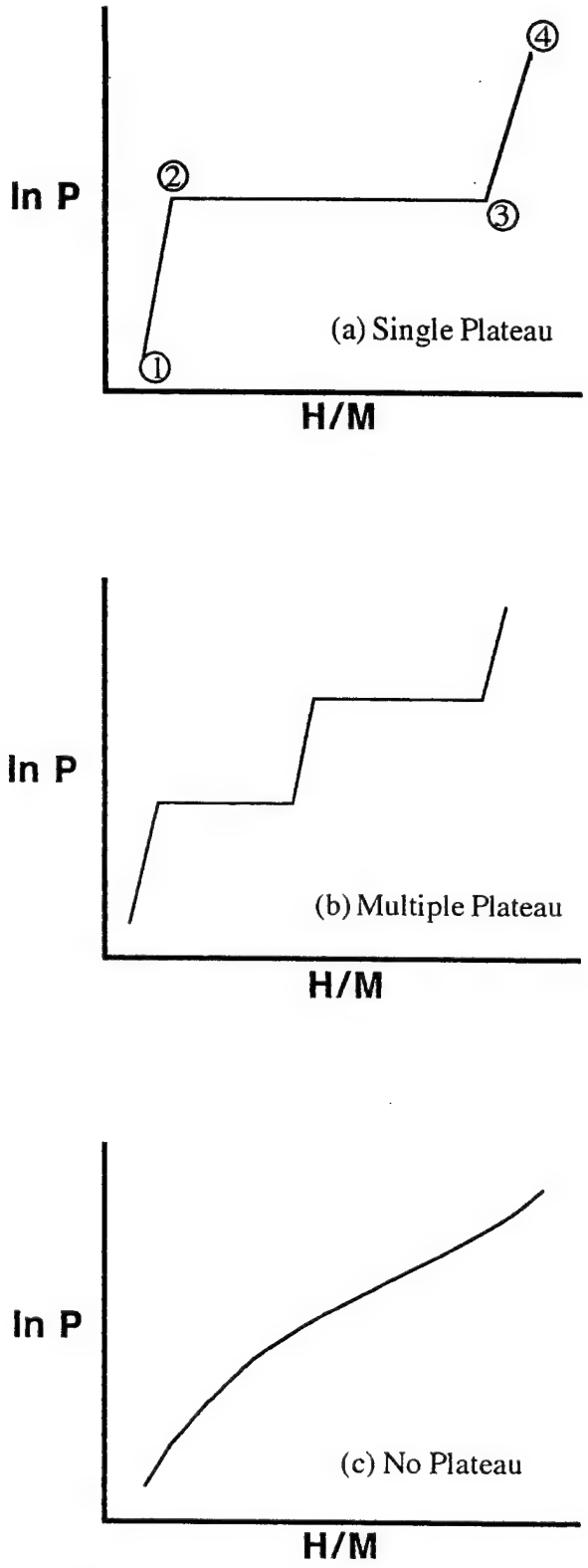

Figure 1: Types of pressure-composition isotherms

often obeys a near square root pressure dependence called Sieverts' Law:

$$H/M = kP^{0.5} \qquad \text{(Eq.7)}$$

where k is a constant dependent on temperature. At some pressure or composition (point 2), the α-phase becomes saturated with H. If the metal in question forms a hydride, a discrete, ordered hydride phase will begin to form at nearly constant pressure, called the plateau pressure. The hydride phase is usually called the β-phase so that the plateau region of H/M represents a two-phase α + β field. As the plateau is traversed by adding more and more hydrogen the β-phase grows at the expense of the α-phase. The right end of the plateau (point 3) represents 100% β-phase.

The β-phase (hydride) usually represents a discontinuous change in crystal structure (or at least in lattice parameters) from the α-phase, although the hydrides usually are closely related in structure to the parent metal phase. Many hydrides (especially interstitial hydrides) have a variable stoichiometry (i.e., x is somewhat variable in MH_x), so that further increases in pressure (to point 4) will result in slightly higher values of H/M. The upper legs of the isotherms usually do not obey Sieverts' law very well. In principal, the isotherm shown in Fig.1(a) can also represent the desorption process, i.e., starting at point 4 and ending at point 1.

An element or alloy can show multiple plateaux with a P-C isotherm, as illustrated schematically in Fig.1(b) for a 2-plateaux metal. This is an indication that more than one distinct hydride phase forms. All metals have more than one type of interstitial sites; ordered intermetallic compounds can have several. Whenever the energetics of H occupancy differs with different sites, multiple plateaux tend to occur.

Some materials show no distinct plateau, but rather a generally upward sloping P-C isotherm such as shown in Fig.1(c). Such behavior usually represents the continuous dissolution of H into the α-phase without the formation of a crystallographically distinct hydride phase. There is usually a continuous increase in lattice parameters with increasing H/M. Strictly speaking, we should not say such a material forms a hydride; however, I will make no strict semantic distinction here. Such "H-solution" metals materials can have limited utility as "hydriding" metals. In fact, a sloping isotherm can be practically useful to allow pressure to be used as an indicator the amount of hydrogen in the lattice, something you cannot easily do with a material that exhibits a flat plateau.

Many hydride-forming metals will show a distinct plateau at low temperature, but with increasing temperature that plateau will shrink in width until some temperature where the plateau disappears. This is called the critical temperature (T_c) and represents the temperature on the M-H phase diagram above which the hydride phase no longer exists, i.e., where the high thermal energy prevents the formation of an H-ordered structure and only a random solid-solution of H is possible. The element Pd is a classic example of such a material ($T_c \approx 295°C$) (Lewis, 67 (303)). Even below the Tc many practical alloys will show a somewhat sloping plateau (see Section 2.B.1.c, p.10).

2.B.1.b. Experimental Determination of P-C Isotherms and Kinetics

Although P-C isotherms can be determined by gravimetric (weight change) techniques, volumetric (pV) techniques are generally used. The volumetric method is simple. Although an apparatus may look different from lab to lab, all are basically the same. A composite apparatus, designed for three different modes of charging (or discharging) is shown schematically in Figure 2 [Sandrock, 95 (N)]. The apparatus consists of a carefully volume-calibrated gas reservoir and

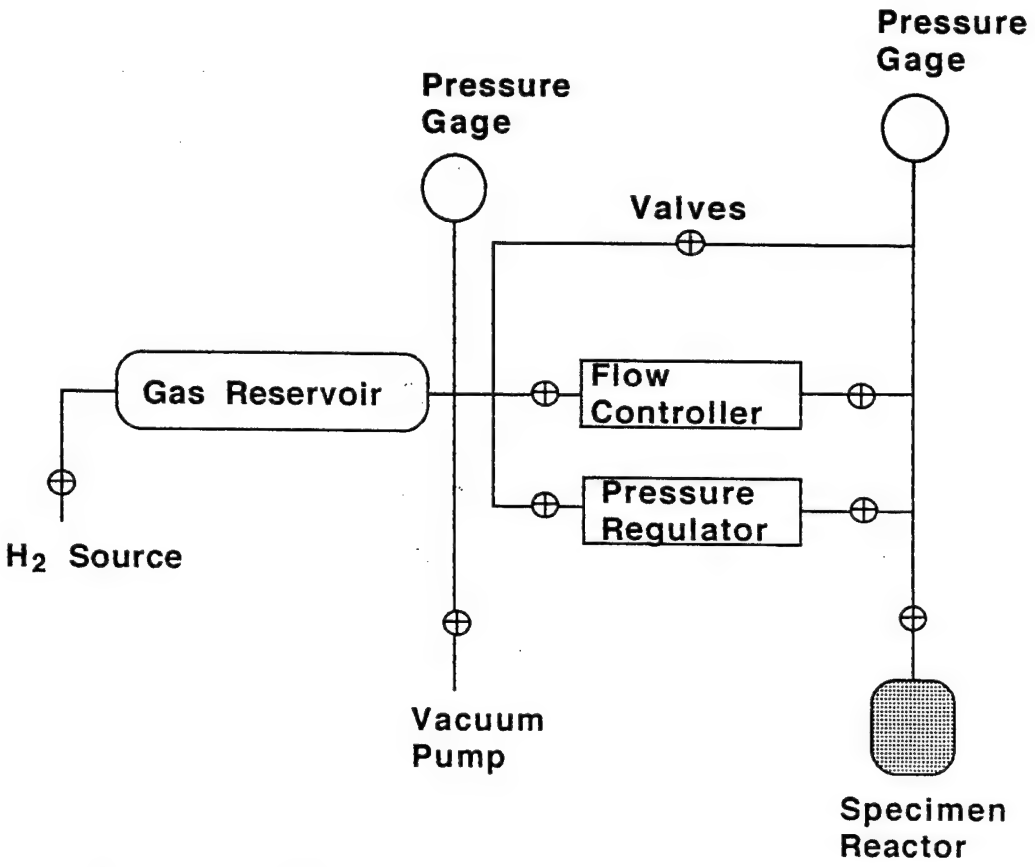

Figure 2: Multipurpose Gas Hydriding/Dehydriding Apparatus

pressure gage connected to the specimen reactor (with its own pressure gage) by gas-tight tubing. All volumes must be carefully pre-calibrated using water or He filling. The reactor is usually immersed in a water bath or furnace for temperature maintenance. The pressure gages and control instruments are usually electronic and the valves are often electrically operated so that the experiments can be controlled and analyzed by computer. If properly designed, such an apparatus can be used both for absorption and desorption experiments. In honor of his extensive and pioneering work on metal-hydrogen systems early in this century, such an apparatus is traditionally named after the German chemist Sieverts.

As shown in Figure 2, there are three possible means of transferring the H_2 gas from the reservoir to the specimen chamber. Using the top (open/close) valve, we can introduce (or remove) gas to (or from) the specimen on an aliquot by aliquot basis. For a manual absorption example, (1) the top valve is closed, (2) the gas reservoir is filled to an H_2 pressure P, (3) the top valve is opened and the H_2 allowed to react with the specimen until a static (quasi-equilibrium) pressure P′ is reached. From the temperature, pressure change (P-P′) and volumes, the amount of H that entered the specimen (ΔH/M) can be precisely calculated. If this is done repeatedly at constant temperature we obtain a plot of P′ vs. H/M, i.e., the absorption P-C isotherm discussed relative to Fig.1. Because we do this by a step-by-step procedure that waits for static quasi-equilibrium at each step we call the result a static isotherm. A similar, but reverse, procedure is used to obtain a static desorption isotherm.

Instead of the static aliquot-by-aliquot method, requiring the repeated opening and closing of

the top valve, we can slowly and continuously introduce H_2 to the specimen chamber using an electronic flow controller, while recording pressure. The result is what we call a dynamic isotherm. Static and dynamic isotherms can differ somewhat (Goodell, 80 (6)). Although dynamic isotherms are usually more representative of practical applications, static isotherms predominate in the literature.

Finally, we can use a pressure regulator to run a rapid and complete isobaric absorption experiment. The result is a plot of H/M vs. time. This technique is used to estimate absorption kinetics. If a backpressure regulator is used, isobaric desorption rate curves can be obtained. Many investigators unfortunately do not use the simple and readily available pressure regulators and perform their rate experiments with an open/close valve. Depending on the gas reservoir volume, such tests can be significantly non-isobaric and hard to relate to engineering needs. In addition, there are heat transfer problems that often make the determination of true chemical kinetics difficult (see Section 2.B.5, p.16).

2.B.1.c. Nonidealities - Plateau Slope and Hysteresis

The idealized P-C isotherms shown in Fig.1 are seldom realized with practical hydrogen storage alloys. In general we obtain isotherms such as shown schematically in Figure 3, wherein the plateaux are not completely flat and there is some pressure hysteresis between absorption and desorption.

In additional to the critical temperature phenomena discussed in section 2.B.1.a., plateau slope can be a function of metallurgy. Hydrides of pure elements, at least below T_c, tend to exhibit relatively flat plateaux because given sets of interstitial sites tend to be energetically equivalent as far as the H-atom is concerned. On the other hand, random solid solution alloys of two metals (single phase by definition) have randomly variable environments around each interstitial site, usually resulting in a variable local affinities for H, thus resulting in at least modestly sloping hydride plateaux even well below T_c. Binary, well-prepared, single phase intermetallic compounds tend to have specific interstitial environments and relatively flat plateaux. However, metallurgical segregation often occurs during preparation, especially with multicomponent intermetallics, and this leads to sloping plateaux even in predominantly single phase material (Sandrock, 78 (113 & 321)). Sloping plateaux can also develop for cyclic instability reasons (see Section 2.B.7, p.19).

As shown in Fig.3, plateau slope can be quantitatively defined from P-C isotherms:

$$\text{Slope} = \frac{d \ln P_d}{d\,(H/M)} \,. \qquad \text{(Eq.8)}$$

For most hydride applications, it is generally desired that plateau slope be minimal. As mentioned earlier, there may be cases such as fuel tanks where some plateau slope is desired so a measure of fuel level can be made from pressure and temperature.

The other important hydride nonideality is hysteresis. While hydrogen absorption and desorption can be very reversible, it is usually so with some pressure (or temperature) hysteresis. That is the plateau pressures for absorption are usually measurably higher than the plateau pressures for desorption. As shown in Fig.3, hysteresis can be quantitatively defined as

$$\text{Hysteresis} = \ln \frac{P_a}{P_d} \,, \qquad \text{(Eq.9)}$$

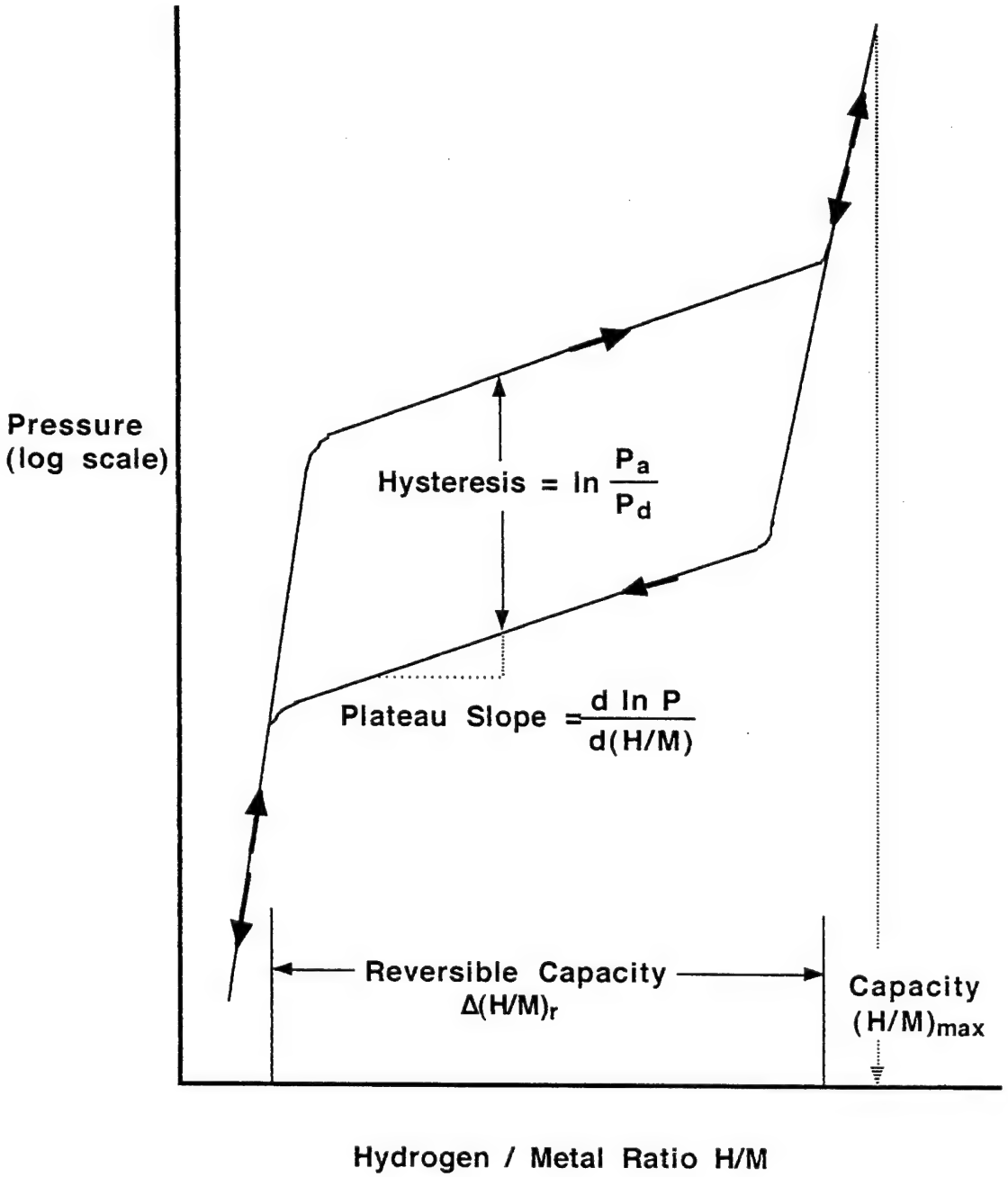

Figure 3
Schematic Isothermal Pressure-Composition Hysteresis Loop

where P_a and P_d are absorption and desorption pressures at some constant value of H/M (usually midplateau). Hysteresis is really a measure of energy loss during an absorption/desorption cycle. It has its origins in the large strains associated with the metal <----> hydride transformations and the resultant generation of internal defects such as dislocations and stacking faults. In general, hysteresis decreases with increasing temperature, probably a result of thermally activated stress relaxation processes.

Hysteresis is generally undesirable for most applications. It varies widely from hydride to hydride, from virtually 0 to 2 or more, and is an important practical parameter to quantify.

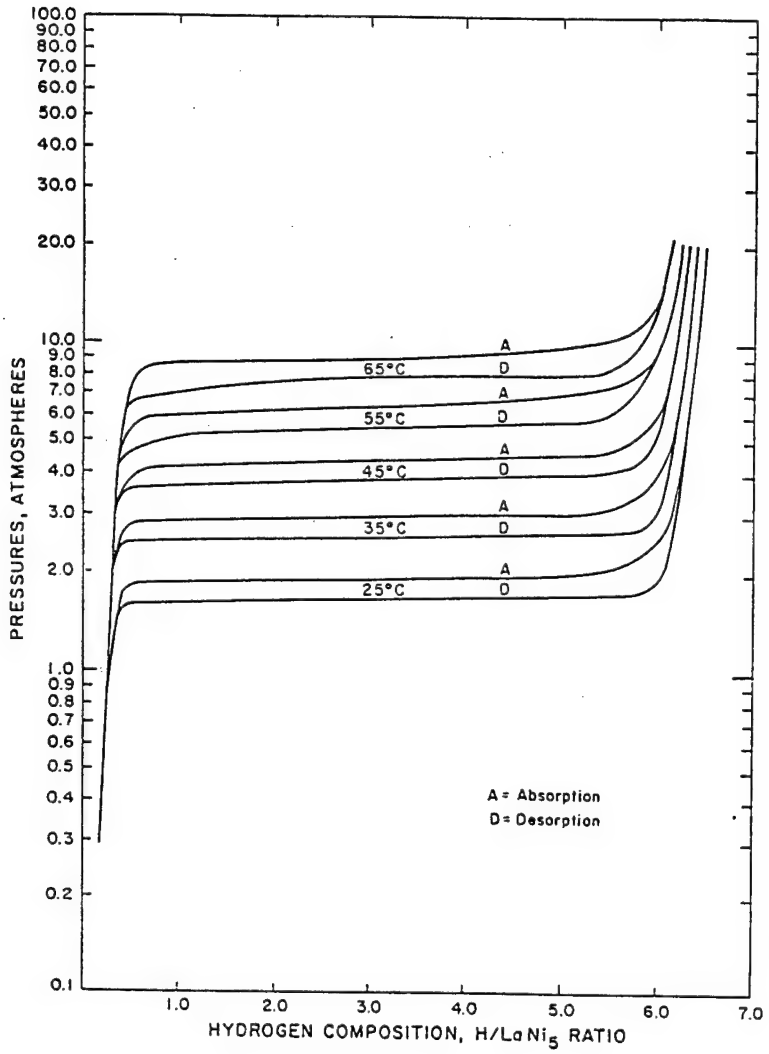

Figure 4: Hydrogen Absorption (A) and Desorption (D) Isotherms for $LaNi_5$ (Lundin. 75 (260))

Thus far we have discussed hydride PCT properties in abstract form. Actual H_2-absorption and desorption isotherms of a real material, the classic intermetallic compound $LaNi_5$, are shown in Figure 4 (Lundin, 75 (260)). Note the small, but significant, pressure hysteresis ($\approx$0.13) and the unusually small plateau slope ($\approx$0.13).

2.B.1.d. Thermodynamics - Enthalpy, Entropy and the van't Hoff Plot

An understanding of the basic fundamentals of hydride thermodynamics is extremely important for the comparison of hydrides and development of all hydride applications. Therein lie the basic principles for controlling the pressures and, through reaction heats and heat exchange, engineering rates of H_2 absorption and desorption. It may be noticed from Figure 4 that the higher the temperature the higher is the plateau pressure. This is a direct consequence of the fact the reaction in Eq.4 has enthalpy (heat) and entropy changes associated with it, as is the case for all gas-solid and gas-liquid chemical reactions. Most hydrogen-metal-hydride systems obey the van't Hoff equation which relates the plateau pressure Pp to the absolute temperature T by:

$$\ln P = \frac{\Delta H}{RT} - \frac{\Delta S}{R} , \qquad \text{(Eq.10)}$$

where ΔH is the enthalpy change (heat) of the hydriding reaction, ΔS is the entropy change and R is the gas constant.

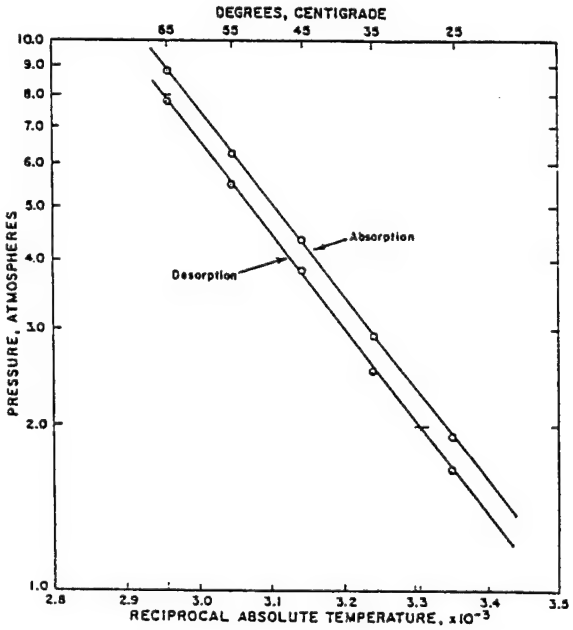

Figure 5: Van't Hoff Plots for $LaNi_5$ (Lundin, 75 (260))

ΔH is a measure of the bonding strength between hydrogen and metal atoms. It can vary over wide limits. For Eq.4, and for all practical hydrogen-metal systems we will consider, ΔH is negative. That is the hydriding reaction (-->) is exothermic and the dehydriding reaction (<--) is endothermic. ΔS, on the other hand, is roughly constant for most systems, usually within about 25 % of the -0.13 $kJmolH_2^{-1}K^{-1}$ associated with the change from gaseous to solid hydrogen (Gruen, 77 (162)).

The values of ΔH and ΔS can be easily obtained from experimental isotherms by plotting the logarithm of the plateau pressure against the reciprocal of absolute temperature. The resultant plot is commonly called a van't Hoff plot. A van't Hoff plot for $LaNi_5$, derived from the mid-plateau pressures of Fig.4, is shown in Figure 5. From the slopes of the lines, ΔH can be calculated (e.g., 30.8 $kJ/molH_2$ for H_2 desorption from $LaNi_5$). From the extrapolated intercept $1/T = 0$ (infinite temperature), ΔS can be calculated (in this case giving 0.108 $kJmolH_2^{-1}K^{-1}$). Van't Hoff plots are useful not only for determining ΔH and ΔS values, but also for graphical comparisons, interpolations and extrapolations of the P-T properties of various hydrides. They will be used extensively herein.

2.B.2. H-Capacity

Hydrogen content and capacity can be defined in various ways. The most common way of presenting hydrogen content is in terms of atomic hydrogen/total metal atom (H/M) ratio, i.e., as used above in Fig.3. Another similar way is atomic hydrogen/formula unit (H/FU) ratio, i.e., as

used in Fig.4. These two methods are simply related by

$$(H/FU) = A\ (H/M), \qquad \text{(Eq.11)}$$

where A is the total number of atoms in the H-free formula, e.g., 6 for $LaNi_5$. Occasionally an author will use the atomic H/A-atom ratio such as H/La to quantify the H-content of $LaNi_5$. In this case (where there is only one A-atom in the FU) there is equivalence with H/FU. To minimize confusion in the text and tables, I will generally try to favor H/M or the chemical formula, e.g., H/M=1.0 or $LaNi_5H_6$. The reader should remember that I will occasionally include graphs from the literature that are in the H/FU measure of H-content (e.g., Fig.4).

Another measure of H-content is weight percent (wt.% H), perhaps more practical than H/M for engineering applications. There are two ways one will find wt.% calculated. I prefer

$$\text{wt.\% H} = \frac{1.008\ N_H}{1.008\ N_H + \Sigma\ N_i W_i}\ X\ 100 \qquad \text{(Eq.12)}$$

where N_H is the number of H-atoms in the formula (H/FU) and $\Sigma\ N_i W_i$ is product of the number of specific atoms (N_i) times the atomic weight of atom (W_i) summed over all the metal atoms i of the formula unit. This is completely equivalent to

$$\text{wt.\% H} = \frac{1.008\ (H/M)}{1.008\ (H/M) + (\Sigma\ N_i W_i)/N_M}\ X\ 100 \qquad \text{(Eq.13)}$$

where N_M is the number of metal atoms in the formula unit. In both cases the number 1.008 is the atomic weight of hydrogen.

The second way of calculating wt.% H is to ignore the weight of hydrogen in the denominator of Eq. 12 and 13, e.g., wt.% H = $100(1.008\ N_H / \Sigma\ N_i W_i)$. Although commonly seen in the literature, I think this latter method is inconsistent with chemists' usual method of calculating wt.% from stoichiometry, so I will use the former method (Eq. 12 or 13) for the data presented herein. In fact, and because the weight of the hydrogen is usually small compared to the metal atoms, the two methods do not give very different values of wt.% H.

Another way of expressing H-content in in terms of H-atoms per unit volume (N_H/V). For an application with volume constraints, for example a submarine, N_H/V may be more meaningful than H/M or wt.%. Volumetric H-content is given by

$$\frac{N_H}{V} = \frac{N_H N_0 \rho}{1.008\ N_H + \Sigma\ N_i W_i} \qquad \text{(Eq.14)}$$

where N_0 is Avogadro's number ($6.024\ X\ 10^{23}$ molecules/g-mol) and ρ is the the density of the hydride (typically in g/cm^3). The main difficulty in using Eq.14 is that the precise density ρ of the hydride phase is not reported very much in the literature, especially when it comes to the multicomponent alloys of commercial interest. Densities can be calculated from reported lattice parameters or volume changes of hydriding. In the end, estimates of initial (unhydrided) density

and the volume change (ΔV) of hydriding must often be made. For the intermetallic hydrides constituting most of this review ΔV ranges from about 2.1-3.2 X 10^{-3} nm^3 per H-atom, with 2.9 X 10^{-3} a reasonable average to use [Westlake, 83 (154)].

Thus far I have talked about ways of calculating H-content. Now turn to H-capacity. Using Fig.3 as a guide, we can define H-capacity in two ways. The first is the maximum H/M that can be loaded into a material at high pressure and say room temperature. This is denoted as $(H/M)_{max}$ in Fig.3 and is most available in the literature. In general, this quantity of hydrogen cannot be easily and completely recovered in H_2 gas form without substantial heating and pumping to low pressure. So we also need to define a reversible capacity, $\Delta(H/M)_{rev}$. In a practical device, the reversible capacity really depends on the allowable pressure and temperature swings, so it is a little difficult to give a single value of reversible capacity for each material. The only thing we can consistently do is to use plateau width as a measure of $\Delta(H/M)_{rev}$, as defined in Fig.3. Even that in somewhat subjective when the ends of the plateaux are not very sharp. $\Delta(H/M)_{rev}$ as defined in Fig.3 is somewhat conservative and real usable capacity ends up being somewhere between $\Delta(H/M)_{rev}$ and $(H/M)_{max}$. For this study, I will use both $\Delta(H/M)_{rev}$ and $(H/M)_{max}$ at various times.

2.B.3. Activation

When H is first applied to a hydriding metal, reaction is usually not immediate. There is a natural oxide film barrier present on samples that have been exposed to air. The process of applying H_2 pressure and getting a metal to hydride for the first time is called activation and is important in the practical use of rechargeable metal hydrides for hydrogen storage, Activation consists of two stages. The first stage is the penetration of a small amount of molecular H_2 (or surface generated atomic H) through the natural oxide layer and the formation of the first hydride nuclei. In the case of many metals, especially rare-earth-containing AB_5 and Mn- containing AB_2 intermetallic compounds, hydrogen absorption will often begin at room temperature after an incubation time ranging from seconds to days. These materials tend to form an impurity-induced surface segregation that results in the precipitation of fine particles of the B-element which are catalytically active to H_2 dissociative chemisorption (Eq.6). For example, in the presence of O_2 and H_2 (or O_2 and H_2O) $LaNi_5$ forms a surface structure of H_2-transparent $La(OH)_3$ and catalytically active free Ni (Schlapbach, 79 (230)). On the other hand, some metals, like those high in Ti, must be heated before H_2 will be absorbed. Ti forms a tenacious oxide film which must be at least partially dissolved by heating.

Once hydrogen begins to penetrate the surface of the metal sample, a second stage of activation starts, namely the fragmentation of large particles into highly cracked smaller particles. This is caused by the stresses placed on the usually brittle metal phase by the expanding hydride phase. The cracking results in substantial increase of fresh, clean surface area. The clean, new surface is excellent for subsequent hydrogen ingress and egress, as long as it is not contaminated (see Section 2.B.6, p.17).

2.B.4. Decrepitation

Decrepitation is a term used to denote the reduction of particle size (pulverization) with hydride/ dehydride (H/D) cycling. Although we load a hydride storage tank with granular alloy (sometimes powder), activation results in cracking and initial decrepitation, as mentioned above. Because of the 15-30% volume changes during H/D cycling, further cracking and particle size breakdown can occur, although most decrepitation occurs during the first few cycles. The

decrepitation phenomenon is of mixed value. The fine powder, typically having surface areas of 0.2-2 m^2/g, is desirable for high H_2 reactivity and impurity gettering ability. On the other hand, the fine powder can progressively pack in its container (even after decrepitation has stopped), resulting in high gas impedance, container stress bulging and even container rupture (Lynch, 80). Because it is important to practical applications and because the degree of decrepitation varies from metal to metal, a review must at least address it. Engineering measures must universally be taken to avoid container packing resulting from decrepitation, migration and cyclic volume changes. There are many methods that have been tried, including compartmentalization, collapsible structures, elastic containers, fluorocarbon and silicone powder lubricants and pelletizing with plastic, rubber and metal binders, e.g., see (Sandrock, 92 (322)).

2.B.5. Intrinsic Kinetics and Heat Transfer Effects

The subject of kinetics, the intrinsic isothermal rates at which hydriding and dehydriding reactions occur, has been an area of extreme research activity throughout the history of rechargeable metal hydrides (cf. reviews (Wang, 90 (324)) and (Gérard, 92 (334))). However, much of the experimental work remains in the domain of the problematical and uncertain. This is because the area is experimentally and theoretically difficult, apparently much more than most investigators realize. Intrinsic reaction kinetics are dictated by the simultaneous effect of three things: (1) surface structures, (2) diffusion rates, and (3) heat transfer limitations. Often, the first and last of these variables are not well controlled. With all of the above affecting experimental studies, it is no wonder that the results are quite divergent and confusing. The first problem is that extremely pure H_2 is often necessary to avoid subtle contamination of the surfaces that can affect intrinsic kinetic results. The second and most serious problem seems to be the failure to establish, and carefully confirm, near-isothermal conditions during the various experiments. A hydriding or dehydriding reaction can be no faster than the macroscopic heat transfer (Goodell, 80 (7)). Many investigators fail to take the simplest of experimental precautions by including a thin, fast-response thermocouple directly in the hydride bed.

The search for the true kinetics of H/D reactions for a given alloy may not be critical to practical applications. The reason is that by using careful experimental conditions, it quickly becomes obvious that the room temperature hydrides have extraordinarily fast kinetics. The highest reaction rates for $LaNi_5$ have been achieved for a thin sample bed that also includes a 98% thermal ballast (Ni powder) to moderate the temperature swings associated with the absorption and desorption reactions (Goodell, 83 (9)). Results of this study show that, at modest applied absorption pressures or desorption backpressures, reaction rates of 40-60 $(H/M)min^{-1}$ can be easily achieved. This means most of the absorption or desorption reaction occurs in times of less than 1 second, very fast indeed! Although not all hydriding alloys are quite that fast, from the above and many other papers on hydride "kinetics", it has become evident to almost everyone in the applications field that it is not intrinsic kinetics that limit practical hydride/dehydride cycle times of room temperature intermetallics, but rather engineering heat transfer considerations and surface impurity effects (cf. Section 2.B.6, p.17, for the latter). Therefore intrinsic material kinetics will only be touched upon in this review.

As we have well established, hydriding and dehydriding reactions are associated with exothermic and endothermic heat effects, respectively. These inevitable heats of reaction range from a nuisance for one designing and using a hydride/hydrogen storage container to the desired output product of a heat pump. Thus, the handling of heat transfer becomes one of the most important of the engineering considerations necessary in the successful design of a hydride-based device. Metal powder beds have poor heat transfer properties. Hydrides are no exception. This fact led very early to the realization that rapid charge/discharge containers require some means of enhancing heat transfer. The most obvious approach, used widely in the chemical industry, was

to minimize heat transfer distance and maximize heat transfer area, for example using designs incorporating internal plates, fins, tubing or metal foams. Among this rather active engineering area considerable effort has been applied to the development of pressed composites utilizing high-conductivity metal powder additions such as Al and Cu (Ron, 80; Toepler, 80; Groll, 87; Ishikawa, 86 (291)). These composite techniques have resulted in order-of-magnitude increases of heat transfer rate, as well as improved resistance to decrepitation.

2.B.6. Gaseous Impurity Effects

Next to PCT properties, probably the most important secondary hydride property is resistance to gaseous impurities that may be in the H_2 used. No hydrogen is perfectly pure. Furthermore, there are economic incentives to use commercial purity H_2, for example as a vehicular fuel. Because of there high thermodynamic activity, traces of contaminants such as H_2O, CO, CO_2, etc., can deleteriously react with the hydriding alloy particle surfaces leading to decreased capacity and/or kinetics. This is especially the case for an "open" system, such as a hydride fuel tank or purifier that must see many charges of impure H_2. Furthermore, we must anticipate the possibility of accidental air exposure or ingress. Therefore, known impurity effects are important to this review of hydriding metals and alloys.

Alloy - gas impurity interactions are best seen from experimental H/M vs. time (rate) curves for H_2 absorption and desorption after various numbers of cycles in impure H_2. Examples of such absorption reaction-time profiles are shown in Figure 6 for $LaNi_5$ in H_2 with various impurities (Sandrock, 84 (4)). There are four classic types of alloy-impurity interaction, the first three of which are illustrated in Fig.6.

Poisoning, shown in Fig.6(a), results in a severe and rapid loss of H-capacity with cycling. The impurity is able to virtually stop hydriding with only a monolayer of surface coverage, suggesting that dissociative chemisorption (Eq.6) is deactivated. Within a macroscopic bed, poisoning is very heterogeneous with the remaining unpoisoned material showing good kinetics, i.e., the initial slope of the curves in Fig.6(a) are not greatly affected by cycling. Typical poisons include CO (near room temperature) and the S-containing gases (e.g., methyl mercaptan in Fig.6(a)). For practical purposes, it is important to know that poisoned alloys can usually be regenerated by heating and flushing with relatively pure H_2, albeit sometimes with difficulty.

Retardation, shown in Fig.6(b), is characterized by losses of absorption/desorption reaction rates without significant loss in ultimate H-capacity. Although only the first 4 minutes of absorption are shown in Fig.6(b), given enough time all the curves reach virtually full H/M. The retardant example shown in Fig.6(b) is ammonia NH_3. Other retardants include CO_2 on the AB_5 alloys or CO at temperatures above 100°C. Occasionally, retardation is followed by a recovery, as shown by the example of the short-term O_2 impurity effects in Fig.6(c). This behavior is known only for the AB_5 intermetallics and is associated with the development of a "self-restoring" surface composed of relatively transparent La_2O_3 and/or $La(OH)_3$ and fine catalytic Ni particles (Schlapbach, 79 (230)). The effects of retardation can generally be easily erased by switching back to high purity H_2.

Reaction, shown in Fig.6 (d), represents bulk corrosion loss of alloy and irreversible capacity loss. Although O_2 exhibits a short-term retardation-recovery behavior (Fig.6(c)), its long term behavior is as a reactant (Fig.6(d)). The alloy damage caused by a reactant generally cannot be recovered without complete metallurgical reprocessing.

Innocuous, not shown in Fig.6, is represented by essentially no cyclic effect on rate or

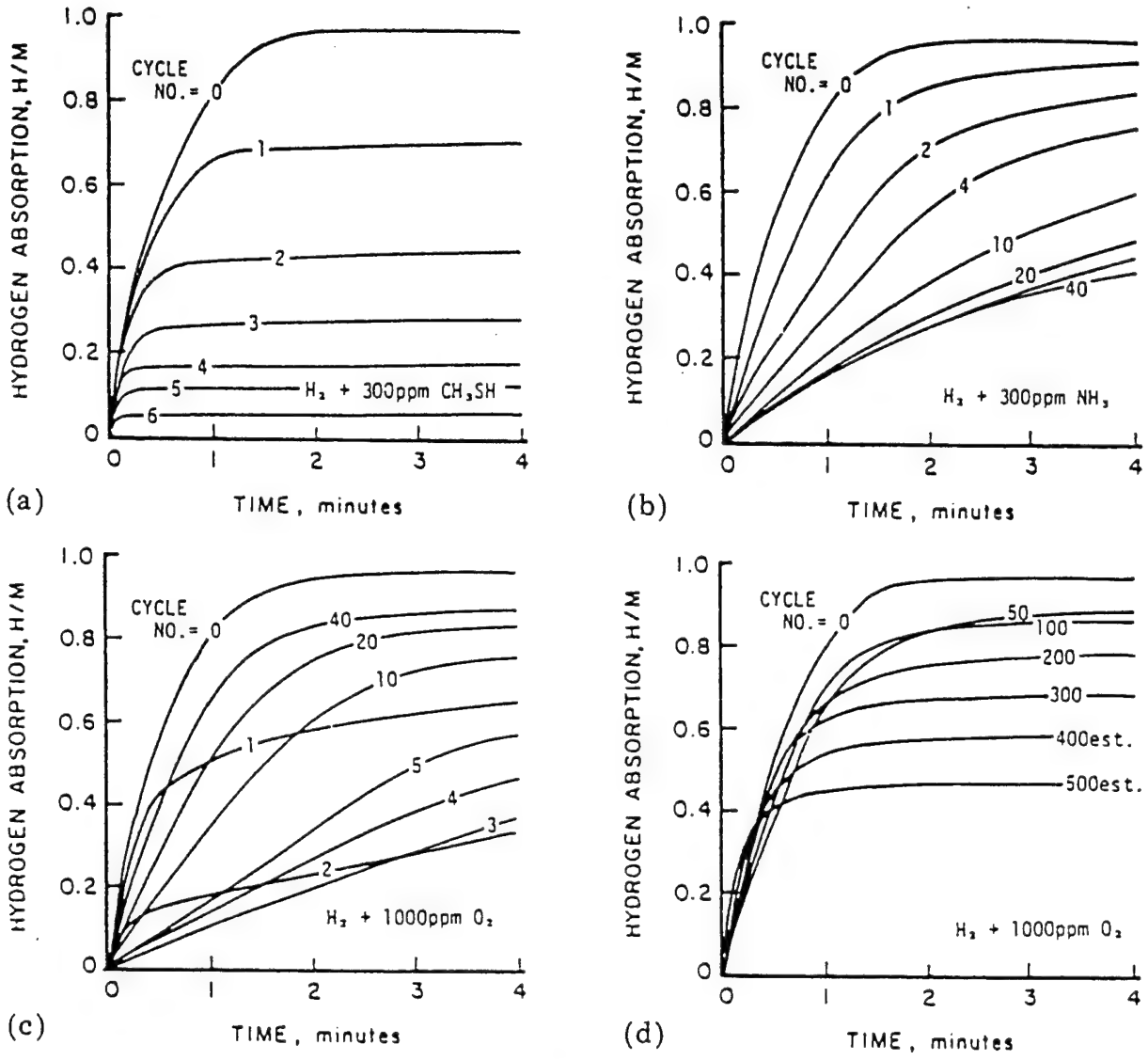

Figure 6
Effects of Different Types of $LaNi_5$ - Impurity Interactions on the Absorption H/M-Time Profiles during Repeated Cycling. (a) Poisoning; (b) Retardation; (c) Retardation-Recovery; (d) Reaction. Curves run at 25°C and 3.4 atm H_2 pressure.
(Sandrock, 84 (4))

capacity, i.e., inert. Examples of innocuous impurities include N_2 and CH_4 on AB_5 intermetallics at room temperature. Of course, it should be noted that innocuous impurities at high levels (<1%) can show exhibit what appears to be retardation during absorption. This is simple "inert gas blanketing" where the innocuous impurity gas simply collects and concentrates in the cracks and interparticle voids, resulting in a sort of H_2 diffusion barrier. Inert gas blanketing is asymmetric and is not seen on desorption as the impurity gas is quickly swept away.

I will try to cover, as best I can, the known gaseous impurity effects and regeneration

procedures for various families of materials included in this review. Unfortunately, quantitative data are limited. Although a good empirical math model for quantifying alloy-impurity effects has been developed and proposed by Goodell (Goodell, 82; see also Sandrock, 84 (4)), it has unfortunately not been followed by subsequent investigators.

2.B.7. Cyclic Stability

In addition to the above extrinsic surface effects associated with gaseous impurities, there are intrinsic effects that can lead to isotherm distortion and/or loss of H-capacity during extended cycling of intermetallic compounds even with absolutely pure H_2. These effects can be attributed to thermodynamic and structural metastabilities when alloys are H/D cycled.

The most common phenomenon involves disproportionation of the intermetallic to form a stable hydride. Using the classic $LaNi_5$ as an example, the desired reversible reaction

$$LaNi_5 + 3H_2 <-----> LaNi_5H_6 \qquad \text{(Eq.15)}$$

is really thermodynamically unstable relative to the less reversible, disproportionation reaction

$$LaNi_5 + H_2 ----> LaH_2 + 5Ni. \qquad \text{(Eq.16)}$$

We rarely see the complete disproportionation suggested by Eq.16, but rather transitional stages between Equations 15 and 16 that involve trapping sites and intermediate hydride phases. The first observable results of incipient disproportionation are distorted isotherms and an effective losses of H-capacity (Goodell, 84 (5)). Most intermetallics are inherently unstable relative to disproportionation. However, it seems to occur only in the hydrided state, and not in the solid solution region below the plateau (Sandrock, 89). It is accelerated with increasing temperature. Because Eq.16 requires the movement of metal atoms, a difficult process at low temperature, Eq.15 tends to dominate around room temperature. Even so, effects can be clearly seen with long-time cycling at near room temperature. The tendency for disproportionation varies from one intermetallic to another, so it is important to cover that topic when data is known for a particular alloy. Fortunately, most disproportionated intermetallics can be reproportionated by annealing at a few hundred degrees in an H_2-free environment such as vacuum or flowing inert gas.

There are various other cyclic alloy problems that may or may not have their origins in the thermodynamic driving forces for disproportionation. These seem to be at least partly related to the stresses and strains of H/D cycling. For one example, it will be shown later that the upper plateau pressure of AB-type intermetallic compounds (e.g., $TiFeH_2$) increases with cycling, although the lower plateau is unaffected. Another example is a tendency for certain intermetallics (e.g., the rare earth containing AB_2s) to quickly become amorphous with cycling, making them virtually unusable for hydrogen storage. In summary, all of the above cyclic instabilities must be considered when choosing an alloy for a new hydriding application. Unfortunately, detailed data on cyclic stability are sparse.

2.B.8. Safety

The generalization that metal hydrides offer a relatively safe means of storing H_2 is fundamentally correct. In an accidental container rupture situation, the discharge of H_2 gas tends to be self limiting because of the strongly endothermic nature of desorption. Compared to compressed H_2 gas or liquid H_2, it is quite difficult to quickly vent or spill H_2 from a hydride container. However, the fine powder itself can be pyrophoric, especially when most of the

hydrogen has been released. Aside from possible toxicity concerns, pyrophoricity is the only material-specific safety concern. Unfortunately, very little quantitative pyrophoricity data exists, so this review must concentrate heavily on the author's own personal experience.

2.B.9. Alloy Cost, Metallurgy and Manufacture

Alloy cost is an important property for large-scale hydrogen storage applications such as for submarine or other military fuel cell devices. On a commercial level, alloy cost is a composite of several component costs: (1) raw materials, (2) melting or other manufacturing methods, (3) metallurgy , (4) quality control, (5) grinding, (6) recycling, and (7) profit.

Raw materials costs (RMC) are the easiest to quantify and can be calculated simply as the weighted average of the weight fractions F and prices P of all the elements i in the alloy:

$$RMC = \Sigma F_i P_i \ . \qquad \text{(Eq.17)}$$

I will use RMC, or more precisely (RMC/H-capacity), in this review. For the record, the elemental prices used (typical of mid-1996) are given in Table III.

Table III
Elemental Prices used for Calculations of Alloy Raw Materials Cost

Element	$/kg	Form
Al	1.60	Ingot
Ca	4.95	Crown
Co	63.80	Electro
Cr	8.14	Electro
Cr	1.78	Lo-C Ferro
Cu	2.49	Electro
Fe	0.44	Armco (low-C Fe)
La	14.00	Ingot (CIF China)
Mg	4.25	Ingot
Mm[2]	14.30	99.8 Ingot
Mm	8.00	Standard (CIF China)
Mm	10.75	Battery Grade (CIF China)
Mm	14.00	La-rich (52%) (CIF China)
Mn	2.29	Electro
Mn	1.14	M-C Ferro
Nd	44.00	Ingot
Ni	7.92	Electro
Sn	5.60	Ingot
Ti	9.63	Sponge
Ti	3.19	Ferro
V	125.40	Lump
V	23.10	V-Ni master
V	11.39	Ferro
Zr	23.10	Sponge

[2] Mm represents mischmetal, an alloy of various rare earth elements. Standard mischmetal of Bastnasite mineral origin typically consists (in wt.%) of roughly 48-50 Ce, 32-34 La, 13-14 Nd, 4-5 Pr and 1.5 other rare earths. However other versions of mischmetal exist, depending on the ore origin and what elements have been selectively removed during processing.

There is only one broad review of the preparation methods for hydriding alloys (Percheron-Guégan, 88). Conventional vacuum induction melting is the most used technique for the commercial production of hydriding alloys today (Friedrich, 92 (342)), although I will show other possible alternatives for some alloys, such as air melting. In addition, I will address some non-conventional production techniques where appropriate, e.g., mechanical alloying, reduction-diffusion (R-D), chemical vapor decomposition (CVD), sputtering, rapid quenching, etc.

The understanding of metallurgy is important to the making of satisfactory hydriding alloys. By metallurgy, I mean the crystal structure and microstructure factors that are relevant to the achievement of the optimum hydriding properties discussed throughout Section 2.B. Microstructural factors include second phases, impurities, microsegregation, brittleness, grain sizes, metastability and others. One family of alloys has metallurgical characteristics that differ from another family. As one of the relatively few metallurgists in the field of rechargeable metal hydrides, I will often inject my own personal experience (published and unpublished) on this subject. Closely related to metallurgy is quality control which, in turn is related to the quantitative hydride property requirements of a specific application. For a given application (e.g., a hydrogen storage tank vs. a finely tuned heat pump), how precise do the PCT and H-capacity properties have to be controlled? Must we perform homogenization annealing to achieve very flat plateaux? The interactions between metallurgy and quality control dictate the specifications required of the melter, and therein lies the most difficulty in defining alloy cost. Fortunately, the relatively simple application of hydrogen storage (vs. the more exacting heat pump) gives the most in the way of tolerances.

Grinding into powder or granular form is generally straightforward and cheap because most (but not all) of the available hydriding alloys are brittle intermetallic compounds. Most of the solid solution alloys are ductile and must be converted to powder by hydride/dehydride grinding. Recycling is a future consideration but not yet a significant economic consideration because hydrides are not a large-scale industry.

The final parameter, profit to the manufacturer, depends strongly on supply and demand. It is difficult, if not impossible, to get a very firm measure of actual profit from the present manufacturers of hydriding alloys. By far, the main market for hydriding alloys today is the nickel-metal hydride (NiMH) battery which requires a few thousand tons of alloy (almost all AB_5-type) per year. This is not a large business from a production point of view. I think significant overcapacity exists in those countries that supply alloy powder to the battery industry: Austria, China, Germany and Japan[3]. Even after considering all the cost factors 1-7 above, rumors have it that the final price of battery grade hydriding alloy is approaching a value of only about two times the raw materials price (factor 1). This suggests to me that the manufacturers' profit is not very large.

2.C Sources of Information on Hydrides

Books, articles and patents on metal hydrides are numerous, certainly reaching numbers in the several thousands. Although this review will attempt to distill the most important publications from hydriding alloy and applications-related property points of view, it should be viewed as only a starting point by the reader who intends to participate in the hydride field in the future. Here is a brief overview of where more information on hydrides can be found.

[3] At this writing, a Japan Chemicals & Metals Co. hydriding alloy plant was recently completed in North Carolina, USA. This plant supplies alloy powder for a joint Toshiba-Duracell-Varta (3C) NiMH battery plant, also in North Carolina and should have enough excess capacity to supply alloy for other non-battery applications. However on July 22, 1997, the closing of the 3C battery plant was announced, so the future of the JMC plant is uncertain.

2.C.1 Books and Journals

Although several books on "hydrogen in metals" and "metal hydrides" can be found dating back to the 1940s, the following list represents what I have found to be the most useful:

The Solid State Chemistry of Binary Metal Hydrides - A concise introduction to the chemistry, thermodynamics and structural aspects of elemental hydrides (Libowitz, 65)

Metal Hydrides - The 1968 "black book" on hydrides. Although it predates the rechargeable metal hydride era, it still remains a valuable and comprehensive source of data on elemental hydrides (Mueller, 68)

Hydrogen in Metals I & II - This two-volume set gives an excellent review of the science of M-H systems as of 1978 (Alefeld, 78)

Hydrogen in Intermetallic Compounds I & II - This two-volume set represents the most comprehensive single-source of information on the rechargeable intermetallic hydrides and their applications (Schlapbach, 88&92)

The Metal-Hydrogen System - Covers the fundamental and electronic aspects of M-H systems (Fukai, 93)

Articles on rechargeable metal hydrides can be found throughout the spectrum of physics, chemistry and energy journals over the last three decades. However there are a few journals that have become more traditional outlets for hydride papers (in rough order of article frequency):

Journal of Alloys and Compounds (name of JLCM after 1991)
Journal of the Less-Common Metals (name 1991 and earlier)
International Journal of Hydrogen Energy
Zeitschrift für Physikalishe Chemie
Zhurnal Neorganicheskoi Khimii (Russian J. of Inorganic Chemistry)
Inorganic Chemistry
Izvestiya Akademii Nauk SSSR, Neorganicheskie Materialy
Nippon Kagaku Kaishi (J. of the Chemical Society of Japan)
Journal of the Electrochemical Society (battery hydrides)

Two reviews of intermetallic hydrides are especially noteworthy: (Buschow, 82 (283) and Goodell, 86 (401)).

2.C.2. M-H International Symposia

An especially fertile source of metal hydride publications are the proceedings of a long series of international symposia. The overall history of these symposia is shown schematically in Figure 7. The Hydrogen in Metals series started in 1968 without many papers on hydrides per se. With the coming of room temperature intermetallic hydrides more papers on rechargeable hydrides began to appear, so that by 1977 a separate Metal Hydride series was started, formally called International Symposia on the Properties and Applications of Metal Hydrides. For about 10 years the two series were run in parallel, although there was some overlap of the similar areas. Starting in 1988, the two series were merged under the title "METAL-HYDROGEN SYSTEMS, Fundamentals and Applications". They have so continued to this day and the 1998 Symposium will be held in Hangzhou, Zhejiang Province, China. The symposia have been run informally (independent of any professional society), yet the proceedings have all been published refereed journals (except for the 1977 symposium which was published in unrefereed book form). Table IV shows the particulars of the proceedings of the Metal Hydride and combined H-M Systems symposia.

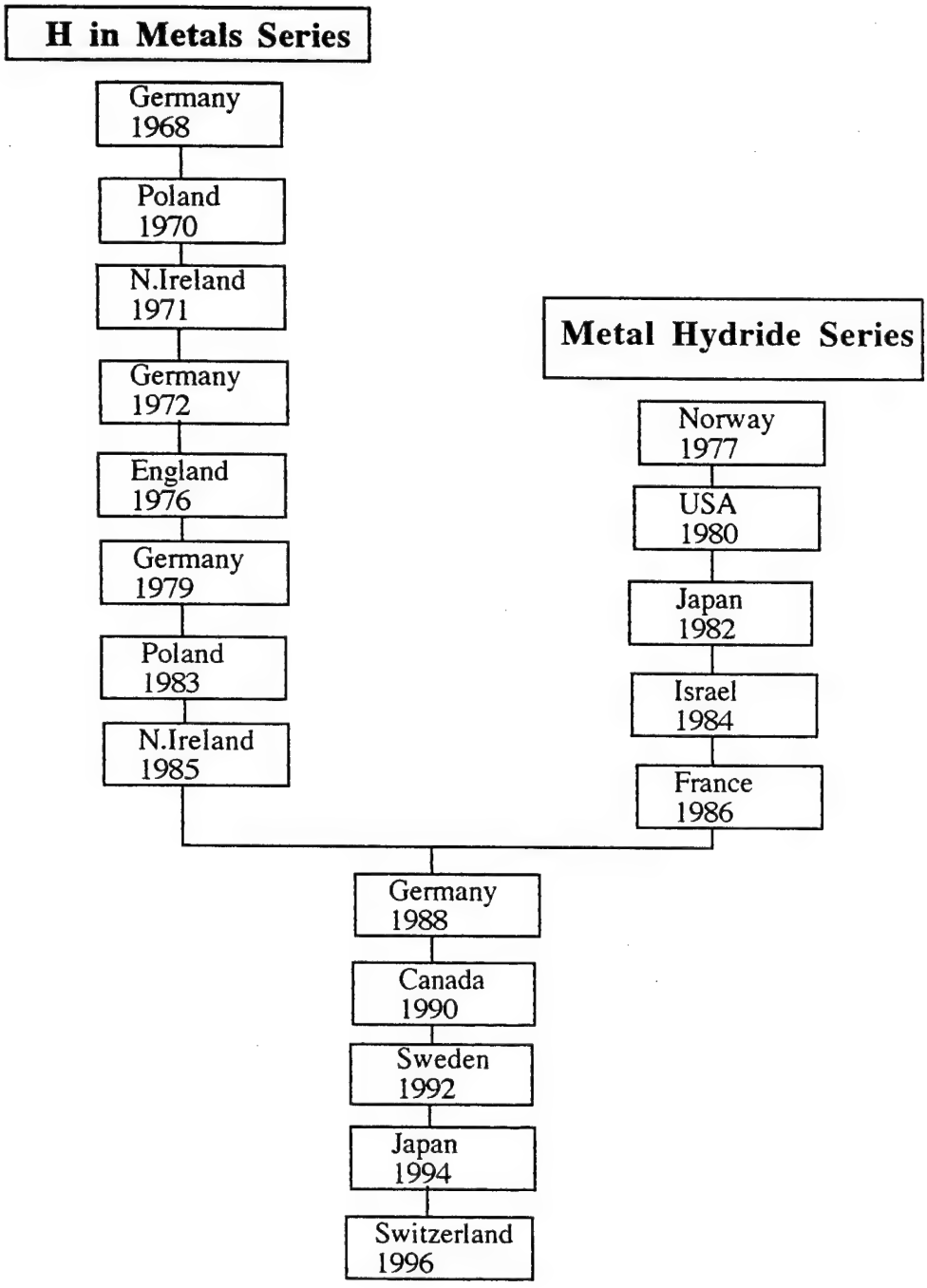

Figure 7
History of Hydrogen in Metals and Metal Hydride International Symposia

Table IV
International Symposia on the Properties and Applications of Metal Hydrides and International Symposia on Metal-Hydrogen Systems

Year Held	Place Held	Proceedings Publisher	Volume	Year	Editors
1977	Geilo, Norway	Hydrides for Energy Storage, Pergamon	--	1978	A.F. Andresen A.J. Maeland
1980	Colorado Springs, USA	J. of the Less-Common Metals	73-74	1980	G.G. Libowitz G.D. Sandrock
1982	Toba, Japan	J. of the Less-Common Metals	88-89	1982-3	W.E. Wallace T. Schober S. Suda
1984	Eilat, Israel	J. of the Less-Common Metals	103-104	1984	M. Ron Y. Josephy I. Jacob D. Shaltiel
1986	Maubuisson, France	J. of the Less-Common Metals	129-131	1987	A. Percheron-Guégan M. Gupta
1998	Stuttgart, Germany	Zeit. für Physikalische Chemie, NF	163-164	1989	R. Kirchheim E. Fromm E. Wicke
1990	Banff, Canada	J. of the Less-Common Metals	172-174	1991	F.D. Manchester
1992	Uppsala, Sweden	Zeit. für Physikalische Chemie	179-183	1993-4	D. Noréus S. Rundqvist E. Wicke
1994	Fujiyoshida, Japan	J. of Alloys and Compounds	231	1995	S. Suda Y. Fukai
1996	Les Diablerets, Switzerland	J. of Alloys and Compounds	--	1997	K. Yvon L. Schlapbach

2.C.3. IEA/DOE/SNL Hydride Databases

The author has been organizing quantitative and qualitative hydride data into a series of databases for easy access via the Internet (Sandrock, 1997). This work is being supported by the U.S. Department of Energy as a contribution to the International Energy Agency Implementing Agreement on Hydrogen Implementation. The databases are freely available to all via the Sandia National Laboratories' Hydrogen Information Center (web site http://hydpark.ca.sandia.gov). There are now three different hydride databases on-line:

1. Comprehensive Hydride Material Listings, extensive tabulations of maximum H-capacities, enthalpies of hydriding and limited pressure-temperature-composition data for the following categories of hydriding alloys (and number of entries):

AB_5 = 246
AB_2 = 406
AB = 142
A_2B = 75
Misc. other intermetallic compounds = 238
Solid-solution-alloys = 139

Total entries = 1246

The additions of the following listings are planned for the future:

Mg-Alloys
Multiphase Alloys
Composites
Amorphous and Nanocrystalline Alloys
Other Special Alloys

2. Hydride Properties, more detailed property listings for a subset of 34 well-known hydriding alloys of commercial and historical importance. The quantitative alloy properties covered include formula, names and trade names, composition, pressure at 25°C, temperature at 1 atm pressure, maximum H-capacity (H/M and wt.%), crystal structure, P-T combinations, ΔH, ΔS, plateau slope, hysteresis and plateau ranges. Additional qualitative properties include metallurgy and synthesis, activation, kinetics, cyclic stability, powder morphology, gas impurity effects, commercial suppliers and applications.

3. Hydride References, a database of 637 references containing the published data compiled in 1 and 2.

It is hoped that these extensive on-line databases will grow and serve as a convenient long-term resource for hydride scientists and applications engineers. In addition to the on-line version, there is a hardcopy version of the first (Jan. 1997) database releases (Sandrock, 97).

3. STATE-OF-THE-ART REVIEWS

This chapter represents the primary objective of this study, namely the review of the current state of hydride art. It will be presented on a class by class basis relative to the type of hydriding metals or alloys shown by the outline in Table V. As indicated earlier, it will concentrate on materials that exhibit hydride dissociation pressures of 1-10 atmospheres (absolute) in the 0-100°C temperature range, typical of operating conditions for PEM fuel cells. Of course, materials with

Table V
Class Outline of Hydriding Metals and Alloys

ELEMENTS

INTERMETALLIC COMPOUNDS
- AB_5
- AB_2
- AB
- A_2B
- Misc. Others

SOLID-SOLUTION ALLOYS

OTHER ALLOYS AND APPROACHES
- Multiphase Alloys and Composites
- Amorphous and Nanocrystalline Alloys
- Quasicrystalline Alloys
- Complex Hydrides

dissociation temperatures and pressures outside these ranges will also be considered (e.g., Mg alloys), not only for completeness but to give perspective for the future R&D needed to bring those materials into the usable pressure and temperature ranges. For each class of material, attempts will be made to summarize the known properties outlined in Section 2.B.

3.A. Elemental Hydrides

3.A.1. Overview of the Elements

Most of the elements will form hydrides under the appropriate chemical conditions (Libowitz, 65; Mueller, 68). Many (but certainly not all) will react directly and reversibly with H_2 gas at favorable temperatures and H_2 pressures. The important property then is the temperature at which the H_2 will be released for practical use. The dissociation pressures of several elemental hydrides are shown as a function of temperature (van't Hoff plots) in Figure 8. As with the van't Hoff plots to follow, the 1-10 atm / 0-100°C operation range is delineated by a superimposed box. As can be seen, only VH_2 falls within the desired range, although NbH_2 (not shown) is similar. Most of the elemental hydrides are too stable (i.e., fall far to the left of VH_2 on Fig.8) or are too unstable (e.g., NiH). The real problem is that there are only a limited number of elements and therefore a limited number of van't Hoff lines. In some sense, nature has not been kind in providing us with elemental hydrides for ambient temperature use. Fortunately, as we shall see, the science of metallurgy has provided us with many thousands of alloys and intermetallic compounds that allows us to escape this elemental dilemma. Before entering the alloy world, however, we should briefly review the elemental vanadium hydrides.

3.A.2. Vanadium

Elemental vanadium has the body-centered-cubic (A2) crystal structure with octahedral and tetrahedral interstices available for the storage of hydrogen atoms. In the practical H-storage limit

of VH_2 the metal structure transforms to face-centered cubic structure to provide enough tetrahedral sites (Schober, 78). Desorption isotherms for both hydrogen and deuterium are shown in Figure 9. V exhibits a number of hydride phases. Only the highest plateau shown in Fig.9 is really

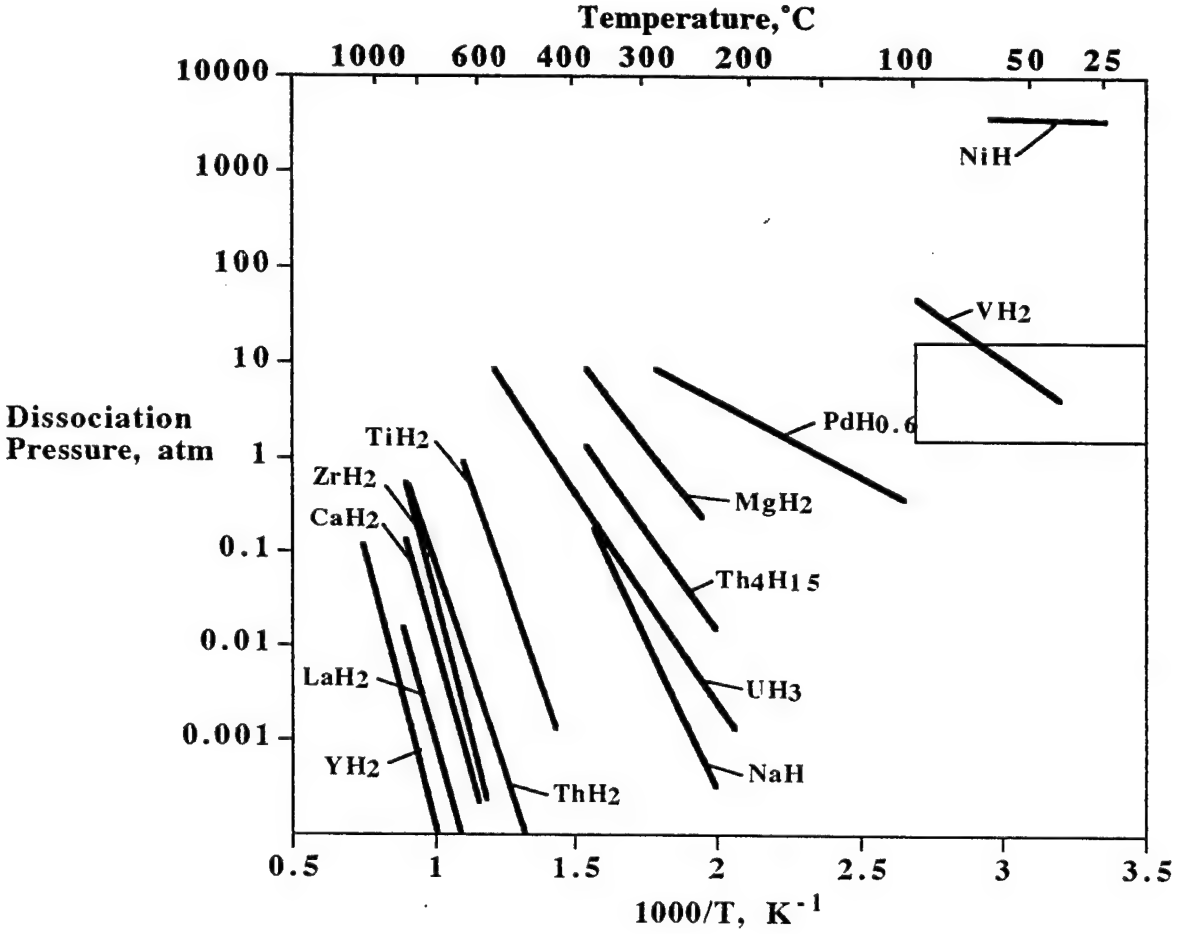

Figure 8
Van't Hoff Lines (Desorption) for Elemental Hydrides (Sandrock, 95)

usable for hydrogen or deuterium storage. For H, the usable range of stoichiometry is about $VH_{0.95}$ <----> VH_2, representing about 1.9 wt.% reversible hydrogen storage. Although Table II shows a volumetric H-density of $11.4X10^{22}$ atoms/cm^3 for VH_2, only slightly more than half of these atoms are really available in a reversible isothermal sense (i.e., about $6.0X10^{22}$ atoms/cm^3). The thermodynamics of the $VH_{0.95}$ <----> VH_2 plateau are given by ΔH = 40.1 kJ/mol and ΔS = 0.141 kJ/molK (Reilly, 72 (314)). Plateau slope is reasonably low, about 0.15 at 40°C.

V has an inverse isotope effect. Although the deuterium plateau is normally higher than the hydrogen (protium) plateau, VD_2 actually has a lower plateau than VH_2. This has led to the suggestion to use V for the chromatographic separation of hydrogen isotopes (Wiswall, 72 (318)). Because of its relatively high ΔH (van't Hoff slope) and non-disproportionation characteristic, V has been extensively studied as a possible hydride for a thermal hydrogen compressor for an

aerospace Joule-Thompson cooler (Bowman, 92).

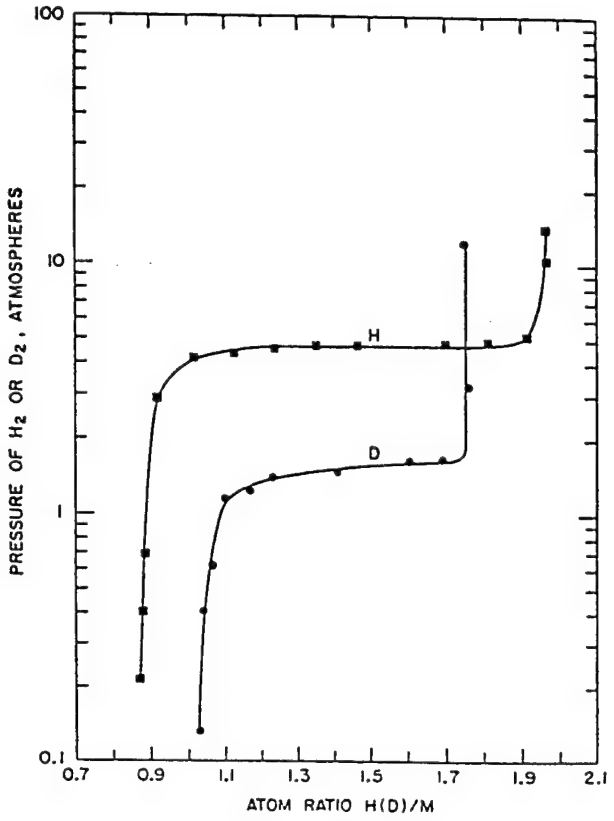

Figure 9
40°C Desorption Isotherms for the V-H and V-D Systems
(Reilly, 72 (314))

Unfortunately, V has several problems affecting its application:

1. Its hydriding properties are rather sensitive to metallic and interstitial impurities (Reilly, 72 (314)).

2. Pure V is very expensive ($125/kg from Table III, p.20). Using the 1.9 wt.% reversible capacity cited above this represents about $6.60 per gram of H_2 stored. As will be seen from the alloy hydrides to be reviewed later, pure V is prohibitively expensive. Fe-containing V alloys will allow the use of much cheaper ferrovanadium (only $11.39 per kg contained V, Table III).

3. V is relatively difficult to activate, presumably because of a rather passive oxide layer on its surface. It requires significant heating, on the order of 450°C (Reilly, 72 (314)).

4. Once activated, it is easily deactivated by O_2 or H_2O impurities in the H_2 gas used, probably for the same reason as 3.

5. The absorption/desorption hysteresis is moderately high, on the order of 0.2-0.7.

6. Even though an elemental hydride cannot disproportionate, there are significant

degradations in the plateau pressure, slope, hysteresis and H-capacity with extensive H/D cycling (Marmaro, 91 (316)). This is attributed to unusually large anisotropic plastic strains and crystal disorder that occur during cycling. An additional result is that significant H becomes "trapped" and unavailable for cyclic recovery.

7. The curious strain effects lead to the generation and growth of a low density, spongelike product that is capable of seriously straining containers, even to the point of rupture. The property and safety problems associated with 6 and 7, respectively, have apparently led to the abandonment of V-based compressors for aerospace cryocoolers (Marmaro, 91 (316)).

In summary, it is almost certainly not practical to consider the large-scale use of unalloyed vanadium for fuel cell H-storage systems, especially for submersible vehicles. However, as we shall see, V can play an important role in solid solution alloys and intermetallic compounds for hydrogen storage media.

3.B. AB_5 Intermetallic Hydrides

The hydrides based on AB_5 intermetallic compounds represent the most versatile and commercially important family of reversible hydriding alloys. For example, AB_5 hydrides are used for the anodes of most of the nickel metal hydride batteries manufactured today. A is usually taken from the rare earth (lanthanide) elements (at. no. 57-71) and/or Ca and B is Ni, usually in combination with other transition metals. The AB_5s are essentially line compounds (i.e. are rather closely restricted to the atomic A:B ratio of 1:5). They can be prepared in tonnage quantities by conventional metallurgical techniques such as vacuum induction melting. Like most intermetallic compounds, they are very brittle and easily reduced to the granular or powder form required for the filling of hydride containers. In this section I will survey the AB_5 family in terms of structure, historical evolution, PCT versatility and other important properties.

3.B.1 Crystal Structure

Almost all of the AB_5 intermetallic compounds of practical hydriding significance crystallize

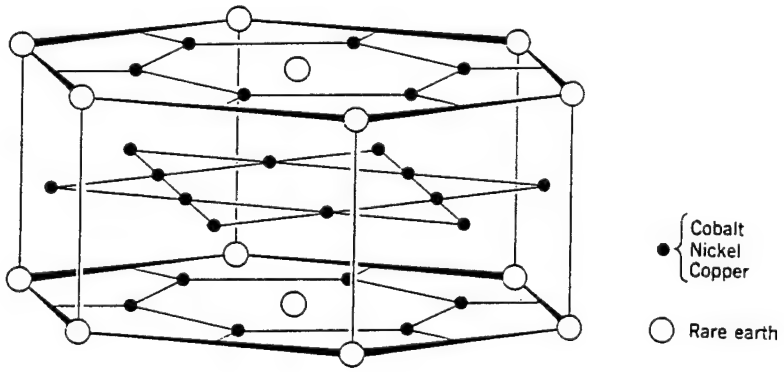

Strukturbericht = $D2_d$
Prototype = $CaCu_5$
Pearson = hP6
Space Group = P6/mmm
Generic = Haucke Phase

Figure 10
The $D2_d$ AB_5 Crystal Structure (Barrett, 80)

with the hexagonal $D2_d$ structure shown in Figure 10. It is actually a structural derivative to the C14 Laves phase AB_2 (Barrett, 80), an important family of hydriding intermetallics to be discussed later in Section 3.C. The AB_5 structure contains a variety of tetrahedral and octahedral interstices and the H-atom occupancy (usually inferred from neutron diffraction of deuterides) depends on the composition of the AB_5 and investigator (Yvon, 88 (320)). What is important is that these interstices are surrounded by both A and B atoms, such as $[A_2B_2]$, $[AB_3]$ and $[A_2B_4]$. As far as the H-atom is concerned, this results in interstitial environments that are "averages" of the very strongly bonding A-atoms and the very weakly bonding B-atoms, thus resulting in an intermediate strength bond that is so important to practical, ambient temperature reversible hydrides. The ability to vary the interstitial environments by varying the composition of the AB_5 (as well as other alloys and intermetallic compounds) has led to the modern world of rechargeable metal hydrides.

3.B.2 Historical Evolution of the AB_5 Hydrides

It is important to understand the evolution of the AB_5 hydrides from an accidental discovery in 1969 to the multicomponent alloys that are the mainstay of today's commercially available H-storage alloys. Not only is this history interesting from a technological perspective, it is helpful in picking an alloy for a new hydriding application. The overall evolution, in which the author had an active role, is shown schematically in Figure 11 as an aid to follow the presentation below.

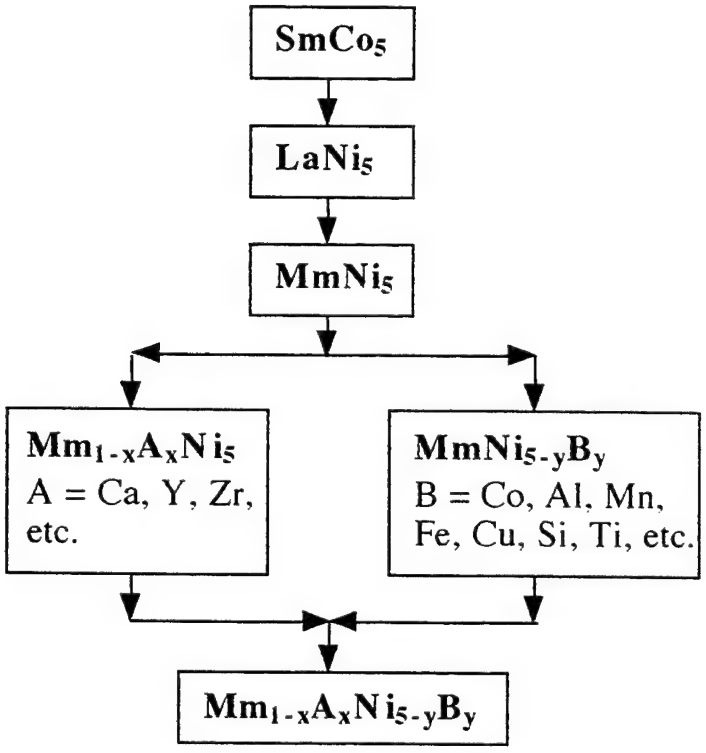

Figure 11
Schematic Flow Diagram of AB_5
Hydriding Intermetallic Compound Development

The impressive hydriding properties of AB_5 intermetallics were accidentally discovered at the Philips Eindhoven Labs about 1969 during work on AB_5 permanent magnet materials (Willems, 87 (354)). In the late 1960s the promising new high coercivity magnet material was $SmCo_5$, usually manufactured into monolithic magnets by the sintering of $SmCo_5$ powder. It was noticed that the coercivity of the powder decreased with storage time in humid air or by chemical etching and it was speculated that the following aqueous surface corrosion reaction was taking place:

$$2SmCo_5 + 3H_2O \text{ ----> } Sm_2O_3 + 10Co + 3H_2 \ . \qquad \text{(Eq.18)}$$

If so, was the H_2 so generated on the surface entering the $SmCo_5$ particles and causing the reduction of coercivity? This latter speculation was confirmed by attempts to react $SmCo_5$ directly with H_2 gas at room temperature which clearly identified not only H-pickup and coercivity loss, but a new reversible hydriding reaction

$$SmCo_5 + 1.25H_2 \text{ <-----> } SmCo_5H_{2.5} \qquad \text{(Eq.19)}$$

Eq.19 was found to be easily reversible at room temperature and a few atmospheres pressure (Zijlstra, 69 (148)). A nice flat plateau was seen but the H-capacity was not yet remarkable.

Still thinking about magnetic coercivity, the Philips researchers wanted to study the positions of the H-atoms in $SmCo_5$ hydride by NMR, but that required a sample that was not ferromagnetic. For the NMR study, they selected the isostructural AB_5 compound $LaNi_5$. The reaction of $LaNi_5$ with H_2 (van Vucht, 70 (93)) was indeed remarkable compared to $SmCo_5$:

$$LaNi_5 + 3.35H2 \text{ <-----> } LaNi_5H_{6.7} \ . \qquad \text{(Eq.20)}$$

Hydrogen capacity was high (H/M>1), reversibility was virtually complete and at ambient temperature Eq.20 could be run in either direction at pressures less than 2.5 atm absolute pressure (cf. Fig 4). Hysteresis was low and reaction kinetics were obviously rapid, even at room temperature. $LaNi_5$ could also be easily activated at room temperature. In short, a new and exciting hydrogen storage medium had been discovered in $LaNi_5$ and, to their credit, the Philips researchers recognized this fact, filed for numerous patents on AB_5 alloy compositions and practical devices, including early NiMH batteries. There was an extensive parallel effort by Philips and others to develop and scientifically understand the growing family of pure and substituted RNi_5 compounds (R = rare earth elements), examples of which will be shown later in Sections 3.B.3 and 3.B.4.

The potential for a new energy-related application for Ni attracted the author, then with the Inco R&D center, in the early 1970s. When I first began to work on AB_5 compounds in 1975, I quickly concluded that $LaNi_5$ and its close derivatives would be too expensive for most of the large scale H_2 gas storage applications that were of interest (e.g., as a vehicle H_2 fuel storage medium). Instead of using the expensive rare earth element La, I thought it better to use the much lower cost unrefined rare earth mixture commonly known as mischmetal (Mm), then used by the metallurgical and lighter flint industries. The composition of mischmetal depends on the mineral and ore body from which it is derived, but it usually contains the four main rare earth elements Ce, La, Nd and Pr. The most common and low cost Mm is derived from the fluorocarbonate mineral Bastnasite (e.g., from California and Inner Mongolia) and has the typical composition (in weight %) 48-50

Ce, 32-34 La, 13-14 Nd, 4-5 Pr and 1.5 other rare earths. $MmNi_5$ had been made by early 1973 at Brookhaven National Lab for H_2 separation trials and for a high-pressure H_2 source tank

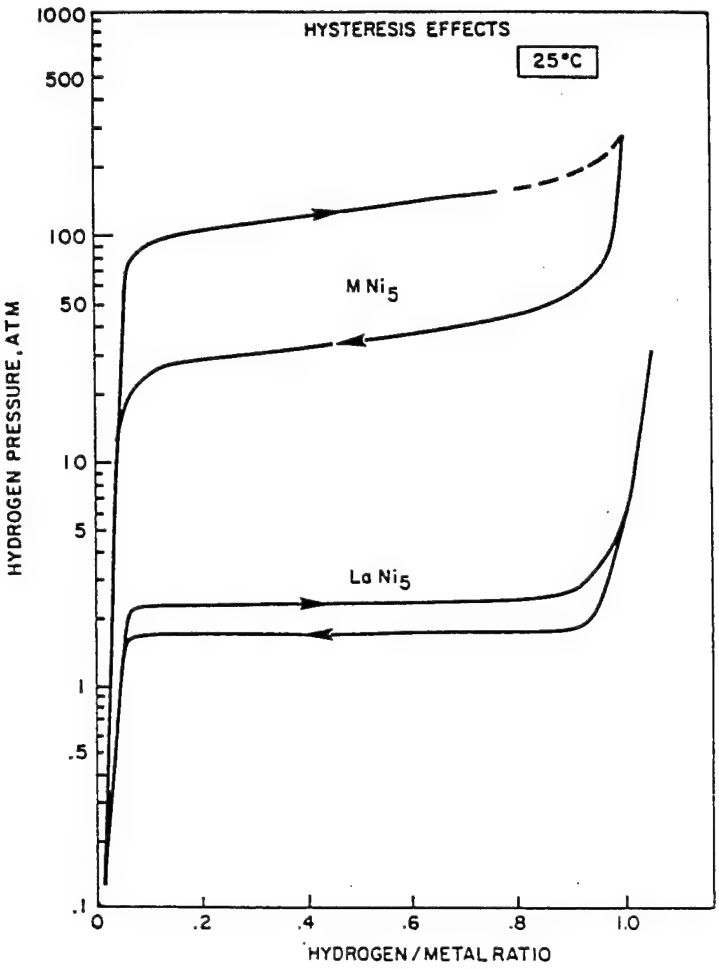

Figure 12
Hydrogen Absorption/Desorption Hysteresis Loops at 25°C for $LaNi_5$ and $MmNi_5$ (Sandrock, 81)

(Reilly, 74 (153)). As shown in Figure 12, however, the substitution of Bastnasite Mm for La results in very high plateau pressures and hysteresis . This is perhaps not surprising in view of the increases in pressure seen earlier when Ce was partially substituted for La in $La_{1-x}Ce_xNi_5$ system (van Vucht, 70 (93)).

From a practical point of view, I felt it would be best if we could learn to live with the lowest cost and most readily available form of Mm, namely Bastnasite Mm. But the high pressure, high hysteresis isotherms for Bastnasite Mm shown in Fig.12 would be very inconvenient for most gas applications and completely unusable for battery H-storage electrodes. Therefore, I started a program to look at the effects of partial ternary substitutions to both the Mm and Ni sides of $MmNi_5$ in order to lower plateau pressure and hysteresis (Sandrock, 77-78 (106,107,321,113)). Parallel work along the same line was done in Japan at the Government Industrial Research Institute Osaka (Osumi 78-83 (117,119,120,121,122,123,124,126,127,133)). This strategy, as well as a few of the many substitution elements tried, is shown in Fig.11. Although these

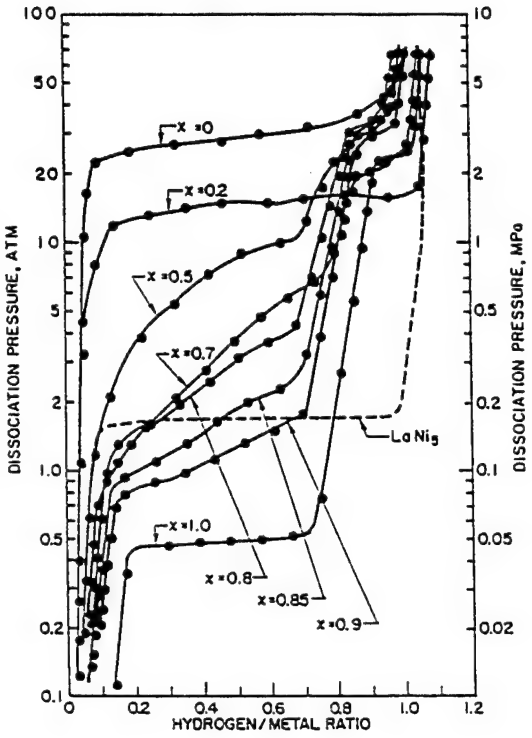

Figure 13
$Mm_{1-x}Ca_x$ Ni_5-H Isotherms at 25°C
(Sandrock, 77 (107))

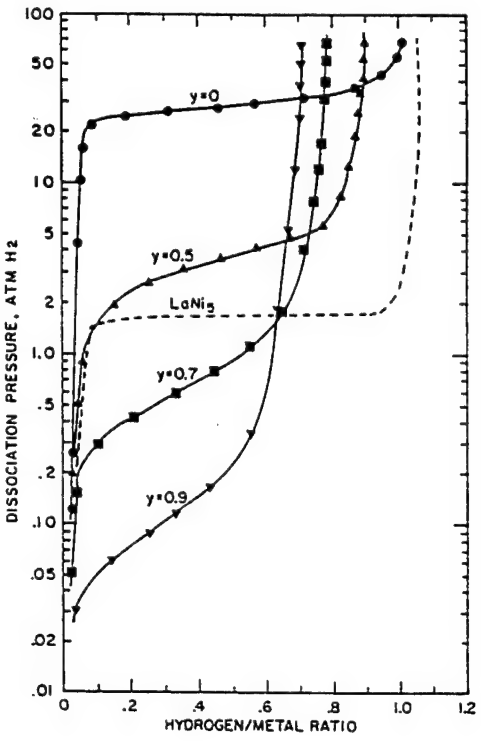

Figure 14
$MmNi_{5-y}Al_y$-H Isotherms at 25°C
(Sandrock, 78 (321))

substitutions will be discussed in more detail in Sections 3.B.3 and 3.B.4, for the purpose of illustrating examples of such partial substitutions on plateau pressure, the effects of Ca substitution on the Mm (A) side and Al on the Ni (B) side are shown in Figures 13 and 14 respectively. The effects are potent in lowering the unwieldy plateau pressure of $MmNi_5$ and (although not shown) also the hysteresis. The plateau slopes shown in Figs. 13 and 14 are a common effect seen in multicomponent AB_5s resulting from as-cast metallurgical segregation and can be reduced by homogenization annealing, as will be discussed in Section 3.B.5. Finally, as indicated by Fig.11, it is also possible to make simultaneous partial substitutions on both the Mm and Ni sides of the formula.

3.B.3. Substitutions on the A-Side of AB_5

Because numerous elements can be fully or partially substituted on the A- and B-sides of AB_5, the versatility of the family is extraordinary. The present AB_5 database lists almost 250 AB_5 alloys and families of alloys reported to form hydrides, including some duplicate investigations of the same compounds (Sandrock, 1997). This section concentrates on A-substitutions, i.e., ANi_5 alloys. It will not be complete, but rather focus on the evolution and properties of practical alloys. A more complete list of alloys and references will be found in the on-line database.

First Table VI lists examples of ANi_5 intermetallics known to hydride where A is a single element. In addition, a few basic PCT properties are listed for comparison purposes. Because some of the intermetallics show multiple plateaux (M), the capacities shown are the maximum contents (cf. Fig.3) for better comparison purposes. If multiple plateaux appear, the pressures

Table VI
Maximum H-Capacity and PCT Properties of ANi_5 Hydrides

Composition	(H-Capacity)$_{max}$ H/M	wt.%	ΔH, kJ/mol	P= (atm)	at T= (°C)	Author-Yr.	A-Atom At. No.
$CaNi_5$ (M)	1.05	1.9	31.9	0.5	25	Sandrock, 77 (106)	20
YNi_5 (M)	0.58	0.91	--	1000	21	Takeshita, 81 (128)	39
$LaNi_5$	1.08	1.5	30.8	1.8	25	Lundin, 75 (260)	57
$CeNi_5$	1.08	1.5	22.2	80	23	Klyamkin, 95 (407)	58
$MmNi_5$	1.06	1.46	21.1	23	25	Reilly, 77 (281)	--
$PrNi_5$ (M)	1.03	1.4	29	10	20	Matsumoto, 87 (568)	59
$NdNi_5$	0.93	1.27	21.6	20	20	Uchida, 82 (131)	60
$SmNi_5$	0.66	0.9	--	30	23	Anderson,73 (99)	62
$EuNi_5$	0.92	1.2	26	1.3	25	Gavra, 85 (280)	63
$GdNi_5$	0.48	0.6	--	120	23	Anderson,73 (99)	64
$YbNi_5$	0.48	0.62	--	120	23	Anderson,73 (99)	70
$ThNi_5$	0.77	0.87	--	No plateau		Takeshita, 81 (128)	90

listed represent the main plateau. The plateau pressures cited are all for desorption at temperatures near ambient, which makes comparisons easy. Most of the compositions represent rare earth elements (at. no. Z = 57-71), but Ca, Y and Th are also included. It is immediately evident that the A-atom has a large effect on plateau pressure, and to a lesser extent on H-capacity.

We should first concentrate on the compositions involving the rare earth elements (Z = 57-70 in Table VI), and particularly the four elements that constitute most of the commercial alloy mixture mischmetal (Mm): La, Ce, Pr, Nd (Z = 57-60). Fortunately all four of these A-elements result in good H-capacity (H/M≈1, wt.%≈1.5). $LaNi_5$ has an ideal plateau pressure of 1.5 atm, but $CeNi_5$, $PrNi_5$ and $NdNi_5$ all have higher plateau pressures. $MmNi_5$ represents an alloy with classic Bastnasite Mm (about 48-50 Ce, 32-34 La, 13-14 Nd, 4-5 Pr and 1.5 other rare earths, in wt.%), and it obviously inherits the high pressure of the Ce component, as well as the high hysteresis associated with Ce (cf. Fig.12). Because there is variability in the composition of commercial mischmetals, especially from mine to mine (e.g., country origin), a detailed study was made of the effect of 15 widely ranging Mm compositions on the H-content, plateau pressure ln P_d, hysteresis ln(P_a/P_d) and ΔH of hydriding for $MmNi_5$ (Liu, 83 (132)). As might be expected from Table VI, H-content is not a significant function of Mm composition. However, the other properties are. They can be approximated by simple linear regression equations as a function of the composition of the Mm (i.e., the weight fractions X of Ce, La, Nd and Pr):

$$\ln P_d = 10.60-5.70X_{Ce}-10.03X_{La}-8.46X_{Pr}-7.40X_{Nd} \quad \text{(Eq.21)}$$

$$\ln (P_a/P_d) = 12.40+0.470X_{Ce}-1.026X_{La}-0.287X_{Pr}-1.361X_{Nd} \quad \text{(Eq.22)}$$

$$\Delta H \text{ (kJ/mol } H_2) = -15.98X_{Ce}-31.2-8X_{La}-14.68X_{Pr}-25.50X_{Nd} \quad \text{(Eq.23)}$$

These equations are useful not only in understanding rare earth substitution effects in AB_5 hydrides, but also in estimating the hydriding propertied to be expected from various available rare

earth mixtures.

Partial substitutions of A-elements other than rare earths are possible, but it turns out the major control of the AB_5 properties ($LaNi_5$ and $MmNi_5$) has historically been made through B-element substitutions, to be covered in the next Section (3.B.4). However, there is one further A-substitution that should be discussed because of its potential commercial importance. That element is calcium. Ca can substitute partially or completely for La or Mm and still maintain the essentially single phase AB_5 structure. As shown in Figure 13, by varying x from 0 to 1 in $Mm_{1-x}Ca_xNi_5$, the plateau pressure can be reduced by nearly two orders of magnitude. Hysteresis is also markedly reduced.

$CaNi_5$ itself in an interesting AB_5 hydride. Figure 15 shows its desorption isotherms for both H_2 and D_2. Note the three different isotope effects for the three plateaux. Although Table VI

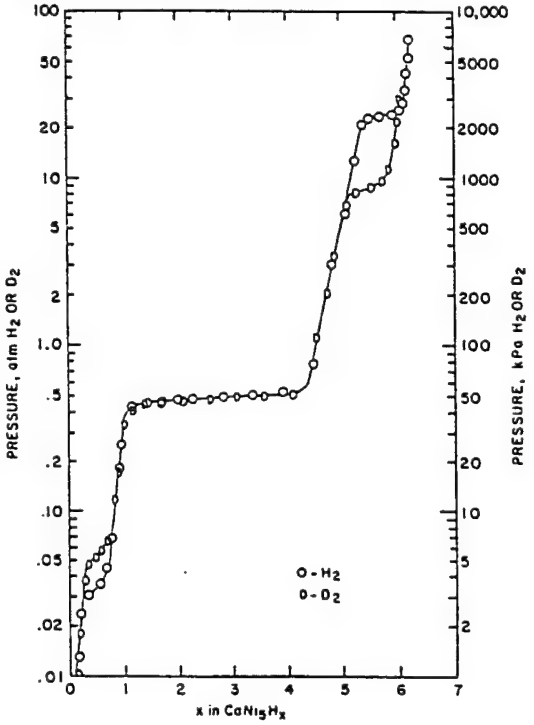

Figure 15
Desorption Isotherms for the $CaNi_5$-H and -D Systems at 25°C
(Sandrock, 82 (326))

shows that fully saturated $CaNi_5$ holds about the same amount of H as $LaNi_5$ and $MmNi_5$ on an atomic H/M basis, the wt.% is higher (1.9 vs. 1.5) because the Ca atom is much lighter than the rare earth atoms. However, this is perhaps misleading because of the three plateaux at widely differing pressures, so that the full 1.9 wt.% of $CaNi_5$ is usually not achievable on a reversible basis. On the other hand, Ca is relatively cheap and abundant so there may still be overall economic advantages of Ca substitution even if only one or two plateaux are used. These factors will be discussed in more quantitative terms in Section 3.B.5, along with $CaNi_5$'s most serious technical problem - disproportionation.

3.B.4. Substitutions on the B-Side of AB_5

As suggested in Fig.11, a large amount of experimental work has been done to control the hydriding properties of the AB_5 intermetallics by partial substitutions of other B-elements for Ni. Except for a lower pressure and hysteresis starting base for $LaNi_5$ compared to $MmNi_5$ (Fig.12), the B-substitution elements have similar effects. As a start, we can first examine the properties of the binary LaB_5 and MmB_5 hydrides shown in Table VII (i.e., single-phase compounds

Table VII
Maximum H-Capacity and PCT Properties of LaB_5 and MmB_5 Hydrides

Composition	$(H\text{-Capacity})_{max}$ H/M	wt.%	ΔH, kJ/mol	P= (atm)	at T= (°C)	Author-Yr.	B-Atom At. No.
$LaCo_5$ (M)	0.72	0.99	40	0.2	50	Kuijpers, 72 (96)	27
$LaCu_5$	0.62	0.8	42.7	5	101	Spada, 87 (255)	29
$LaNi_5$	1.08	1.5	30.8	1.8	25	Lundin, 75 (260)	28
$LaPt_5$ (M)	0.67	0.36	--	1050	21	Takeshita, 81 (128)	78
$MmCo_5$	0.5	0.7	40.2	1.8	40	Osumi, 78 (117)	--
$MmNi_5$	1.06	1.46	21.1	23	25	Reilly, 77 (281)	28

representing the complete substitution of another B-element for Ni). The AB_5s shown do form reversible hydrides with variable plateau pressures, but with lower H-capacities than their reference compounds $LaNi_5$ and $MmNi_5$. As a result all practical AB_5s are based on $LaNi_5$ and $MmNi_5$ bases with only partial replacement of Ni on the B-side. As shown by Figure 16, Philips researchers showed early on that the PCT properties of $LaNi_5$ could profoundly changed by partial substitutions (here 20%) of various elements on the Ni side.

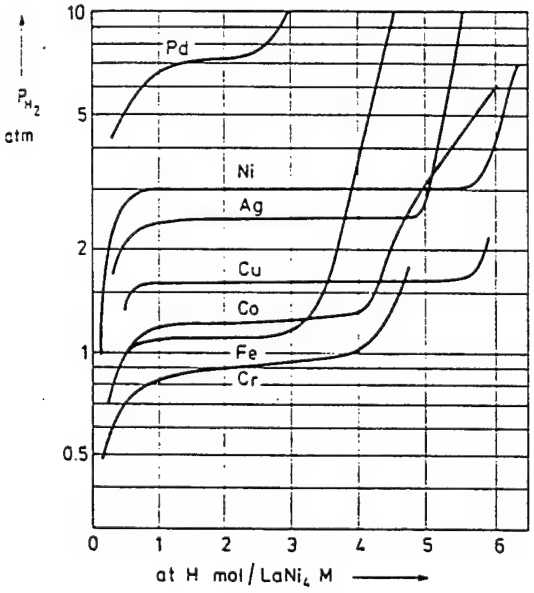

Figure 16
Effect of Substitutions M on the 40°C Desorption Isotherms of $LaNi_4M$ (van Mal, 74 (98))

An example of a partial substitution critically important to the success of NiMH battery electrode alloys is Co. The effect of Co substitution x for Ni in the formula $LaCo_{5x}Ni_{5-5x}$ is

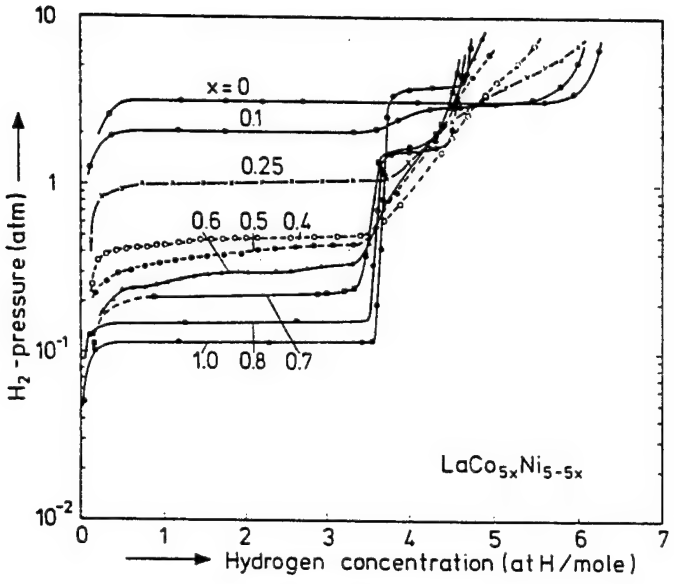

Figure 17
P-C Isotherms (40°C) for Various Co Substitutions x in $LaCo_{5\,x}Ni_{5-5\,x}$ (van Mal 73 (97))

shown in Figure 17. Small levels of Co-substitution into $LaNi_5$ (say up to 25%) lead to a reduced plateau width and a long sloping upper leg to the isotherm. At high enough pressure $(H/M)_{max}$ is not reduced. Above about 40% Co $(H/M)_{max}$ is reduced and a two-plateau isotherm shape ultimately becomes evident. As an aside, $LaCo_5$ shows additional plateaux at very high pressures (>1000 atm H_2) up to the hydride $LaCo_5H_9$ (Lakner, 76 (166)). What is important to battery electrode applications is that the reduction in the width of the main plateau by Co-substitution results in a reduced volume change (ΔV) of the hydriding reaction (van Mal 73 (97)), which in turn greatly increases electrode life by reducing the ΔV-enhanced corrosion from the KOH electrolyte (Willems, 84 (340)). The reduction in ΔV and corrosion with Co-substitution apparently also holds for $MmNi_5$. All the substituted $MmNi_5$ battery alloys commercially used today seem to have at least small levels of substituted Co (Sakai, 92 (345)). For non-battery, gas storage applications (e.g., the fuel cell), Co is not necessary. In fact Co is certainly undesirable because of its high cost and its classification as a strategic material. Most Co is derived from mining operations in the politically unstable D.R. Congo (formerly Zaire).

There are numerous other studies of partial B-substitutions to $LaNi_5$ that have been tabulated elsewhere and need not be covered here in detail. These include, in alphabetical order, at least Ag, Al, B, C, Co, Co+Al, Co+Mn+Al, Co+Sn, Cr, Cu, Fe, Ga, Ge, In, Mn, Mn+Sn, Pd, Si, and Sn. The reader is referred to the IEA/DOE/SNL Internet database for listings and references (Sandrock, 97) . The Al and Sn additions are of some interest for disproportionation resistance and will be mentioned later in that context (Section 3.B.6).

For the purpose of AB_5 intermetallics for practical (economic) large scale H-storage, I will now concentrate on B-substitutions to $MmNi_5$. The effect of Al-substitution y in $MmNi_{5-y}Al_y$ was

shown earlier in Fig.14. The dramatic ability of Al to lower the high plateau pressure and hysteresis of $MmNi_5$ is obvious, with less than 10% substitution of Al for Ni resulting in a lowering of the plateau pressure by an order of magnitude and a reduction of hysteresis by more than one order of magnitude (0.11 for $MmNi_{4.5}Al_{0.5}$ vs. 1.65 for $MmNi_5$). These benefits come at a sacrifice in H-capacity, a combination of both AB_5-phase substitution effects and the fact Al tends to form some second-phase nickel aluminides that do not hydride (Sandrock, 78 (113)). Also Al is enters the AB_5 lattice with some microsegregation during solidification from the melt, resulting in the often undesirable sloping plateaux seen in Fig.14. The Al distribution can be homogenized and the plateau flattened by heat treatment on the order of 1100°C.

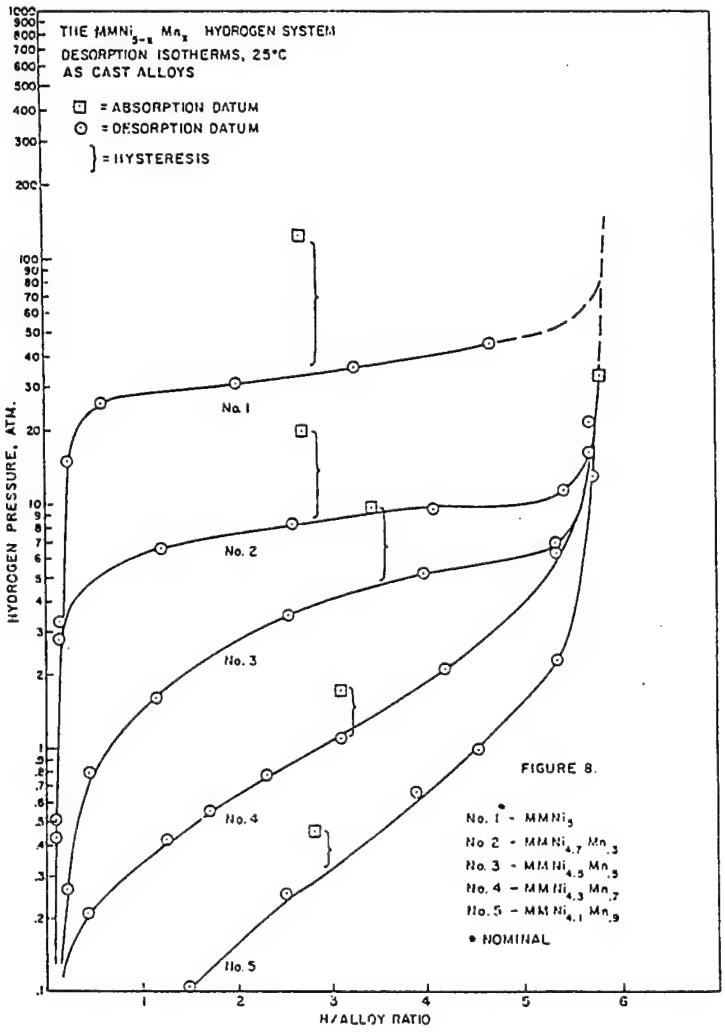

Figure 18
Effect of Mn-Content y on the 25°C Isotherm of $MmNi_{5-y}Mn_y$ (Lundin, 78 (272))

Another effective partial substitution for lowering the $MmNi_5$ plateau pressure is Mn, shown in Fig.18. Unlike Al, Mn lowers the plateau pressure without loss of H-capacity. Hysteresis is not lowered quite as dramatically as with Al-substitution. Sloping plateaux also occur and can also be flattened by homogenization annealing (Lundin, 78 (272)).

The three B-substitution elements discussed above (Co, Al, Mn) have been combined and their levels optimized to create the basic alloys used for the anodes of most of the NiMH batteries now in commercial production (Sakai, 92, 95). These alloys have levels of Co+Mn+Al to bring the plateau pressure below atmospheric, to give an low level of corrosion during battery cycling (i.e., good cyclic life) and to maximize rate capability. Although not precisely disclosed, typical commercial AB_5 battery alloys are probably on the order of $MmNi_{3.5}Co_{0.8}Mn_{0.4}Al_{0.3}$, with some variation from manufacturer to manufacturer. AB_5-based NiMH batteries have become the largest commercial application for rechargeable metal hydride batteries. For example, in Japan alone the 1995 production of NiMH cells was $306X10^6$ with a value of $95X10^9$ ¥ (about $750X10^6$ $ at the April, 1997 exchange rate)(Sakai, 96). Virtually all of this product is believed to contain AB_5 alloys of the approximate composition mentioned above. Assuming about 15g of AB_5 per battery, this represents about 4600 metric tons of alloy used for batteries in Japan during 1995. Although I do not have access to exact prices, this alloy is probably being sold to battery manufacturers at about $25-30/kg in carefully controlled powder form. All of this is used to illustrate the fact that AB_5 hydriding alloys are existing items of commerce and that a significant new market for fuel cell H-storage could probably be accommodated by the alloy manufacturers.

3.B.5. Comparisons of the Substituted $MmNi_5$ Compounds

The main purpose of this section is to give a comparative overview of the substituted $MmNi_5$ alloys in terms of PCT properties, H-capacity and raw materials cost. However for reference purposes, I will also include binary AB_5 compounds such as $LaNi_5$ and $CaNi_5$, as well as a few substituted $LaNi_5$ compounds (e.g., $La(Ni,Al)_5$).

A large and useful base of hydriding data on substituted $MmNi_5$ alloys has been developed. An outline of this work is summarized in Table VIII in terms of individual alloys and families of alloys. This historical data tends to concentrate on B-substitutions, but a few A-substitutions are also included along with a few combined A- and B-substitutions. Many of the substitutions can be made over a range of substitution levels in a true pseudobinary fashion. The overall picture is that a very wide range of hydride properties can be achieved by selecting the alloy, substitution element(s) and the level of substitution. This is important for engineering applications that alloys can be taylor-made to the P-T requirements of the application.

Let us examine in more detail a representative series of diverse AB_5 compositions that more or less cover the range of versatility of the intermetallic class. Eight selected alloys are listed in Table IX, along with their basic PCT properties in order of increasing stability. All of these alloys are included in the Hydride Properties Database (Sandrock, 97), where the original references and more detail can be found. All have been used in various hydride applications, commercial or experimental (Sandrock, 92 (322), 95). Van't Hoff plots are shown in Figure 19. H-capacity and cost-related properties are given in Table X.

A review of Table IX and Fig.19 show that a wide range of thermodynamic stabilities can be achieved. The box in Fig.19 represents the 0-100°C, 1-10 atm range we have established for PEM fuel cell supply conditions. The AB_5 family of hydrides easily covers that whole range. Other van't Hoff lines can be achieved that lie in between those chosen, by simply adjusting the levels of several possible substitution elements. Plateau hysteresis and typical slopes are listed in Table IX. Except for the aforementioned problem with the high hysteresis of binary $MmNi_5$, the substituted alloys have acceptably low hysteresis and reasonably low plateau slope. In short, the AB_5 intermetallic have excellent PCT characteristics for military fuel cell applications.

Table VIII
Summary of Substituted $MmNi_5$ Alloys

Composition	$(H\text{-}Capacity)_{max}$ H/M	wt.%	ΔH, kJ/mol	P= (atm)	at T= (°C)	Author-Yr.
$(Mm,A)Ni_5$ (A = Al, B, Mn,Cu,Si)	--	--	--	13-21	30	Osumi, 81 (124)
$Mm_{.8}Ca_{.2}Ni_5$	1.1	1.6	24.2	13	25	Sandrock, 77 (106)
$Mm_{.5}Ca_{.5}Ni_5$ (+ $Ca_{.1}$, $Ca_{.25}$, $Ca_{.75}$)	0.83	1.3	27.6	8.2	30	Osumi, 78 (117)
$Mm_{1-x}Ca_xNi_5$ (M) (x = 0.2-0.9)	0.9-1.1	1.5-1.6	22-29	1.1-13	25	Sandrock, 77 (106)
$Mm_{.8}Ca_{.2}Ni_{5-y}Al_y$ (y=0-0.5)	0.7-1.1	1.05-1.6	--	0.9-3.5	30	Rodriguez, 96 (632)
$Ml_{1-x}Ca_xNi_5$ (x = 0-0.7) (Ml=low-Ce, high-Pr Mm)	0.95-1.05	1.4-1.6	--	3-10	25	Wang, 96 (592)
$Mm_{.5}Ca_{.5}Ni_{2.5}Co_{2.5}$	0.75	1.1	34.7	9	50	Osumi, 80 (122)
$Mm_{1-x}Ca_xNi_{5-y}Cu_y$ (x = 0-1; y = 0-2.5)	0.45-1.05	0.7-1.5	--	0.1-29	25	Sandrock, 78 (107)
$Mm_{.9}Ti_{.1}Ni_5$ (+ $Ti_{.25}$ & $Ti_{.5}$)	0.7	1.3	31	16	30	Osumi, 78 (117)
$Mm_{.9}Y_{.1}Ni_{4.9}Mn_{.1}$	1.00	1.4	--	8	40	Imoto, 95 (601)
$Mm_{.82}Y_{.18}Ni_{4.95}Mn_{.05}$	1.07	1.5	--	5	25	Nakamura, 95 (414)
$MmNi_{4.5}Al_{.5}$	0.85	1.2	28	3.8	25	Sandrock, 78 (113)
$MmNi_{4.5}Al_{.5}$	0.82	1.17	23	3.2	30	Osumi, 79 (119)
$MmNi_{4.3}Al_{.7}$	0.8	1.16	--	0.6	25	Goodell, 80 (256)
$MmNi_{5-y}Al_y$ (y = 0.5-0.9)	0.7-0.9	1.0-1.3	--	0.1-3	25	Sandrock, 78(113)
$MmCFNi_{4.8}Al_{.2}$ (MmCF = cerium-free Mm)	0.95	1.33	31.4	2	25	Mendelsohn,79 (265)
$MmNi_{5-y}Al_y$ (y = 0.4 & 0.8) (Mm = Indian [high-Fe])	0.48-.6	0.7-.9	35-37	0.5-4	15	Balasubramanian, 93 (588)
$MmNi_{4.7}Al_{.3}Zr_y$ (y = 0-0.2)	0.83-1	1.1-1.35	27-33	4.5-6	25	Wang, 89 (267)
$MmNi_{4.5}Al_{.5}Zr_y$ (y = 0-0.2)	0.62-.85	0.9-1.2	--	2.5-5	30	Na, 94 (277)
$MmNi_{4.6}Al_{.2}Fe_{.2}V_{.03}$	0.98	1.4	28.1	9	30	Lee, 96 (451)
$Mm(Ni,Al,Mn,M)_5$ (M = Co, Cr, Cu, Nb,Ti,V,Zr)	--	--	--	0.2-10	30	Osumi, 83 (133)
$Mm(Ni,B)_5$ (B = Al, Co, Cr, Cu, Fe, Mn, Si, Ti, V, Zn)	--	--	--	0.1-11	30	Osumi, 81 (124)
$MmNi_3Co_2$ (+ $Co_{1.0}$ & $Co_{2.5}$)	1.05	1.4	32.7	2.9	20	Osumi, 79 (121)
$MmNi_{3.5}Co_{.7}Al_{.8}$	0.85	1.24	39.8	0.23	40	Sakai, 92 (278)

Table VIII (concluded)
Summary of Substituted $MmNi_5$ Alloys

Composition	(H-Capacity)$_{max}$ H/M	(H-Capacity)$_{max}$ wt.%	ΔH, kJ/mol	P= (atm)	at T= (°C)	Author-Yr.
$MmNi_{4.2}Co_{0.2}Mn_{.3}Al_{.3}$	0.98	1.38	36.5	0.4	40	Takeya, 93 (279)
$M1Ni_yCo_{0.5}Mn_{.3}Al_{.4}$ (y=3.8-5) (M1=La-rich Mm)	0.87-.97	1.1-1.4	--	0.06-.5	30	Hong, 95 (621)
$MmNi_{4.4-y}Co_yMn_{.3}Al_{.3}$ (y=0.2-0.8)	1.0	1.4	--	0.1-1	40	Takeya, 93 (279)
MmB_5 ($B_5 = Ni_{3.55}Co_{.75}Mn_{.4}Al_{.3}$)	0.8	1.1	--	2	30	Adzic, 95 (264)
$MmNi_{4.5}Cr_{.5}$ (+ $Cr_{.75}$ & $Cr_{1.0}$)	.92	1.2-1.3	25.5	4.8	20	Suzuki, 81 (125)
$MmNi_{4.5}Cr_{.5-z}Mn_z$ (z = 0-0.25)	0.85-.9	--	--	2-5	20	Osumi, 81 (126)
$MmNi_{3.5}Cu_{.5}$	0.83	1.13	23.4	8	25	Sandrock, 78 (113)
$MmNi_{5-y}Cu_y$ (y = 1-2.5)	0.8-.85	1.1-1.2	--	5-16	25	Sandrock, 78 (113)
$MmNi_{4.15}Fe_{.85}$	0.82	1.14	25.3	11.2	25	Huston, 80 (77)
$MmNi_{4.15}Fe_{.85}$	0.82	1.14	29	6	18	Ron, 87 (276)
$MmNi_{5-y}Fe_y$ (y = 0.5-1.5)	0.6-.95	0.8-1.3	--	4-12	25	Sandrock, 78 (113)
$MmNi_{5-y}Fe_y$ (y = 0.3-1.0)	0.7-1.02	1.0-1.4	22-29	7-14	20	Apostolov, 85 (567)
$MmNi_{4.5}Mn_{.5}$ (+ $Mn_{.25}$, $Mn_{.75}$, $Mn_{1.0}$)	0.95	1.3	17.6	2.1	20	Osumi, 79 (120)
$MmNi_{4.5}Mn_{.5}$	1.08	1.49	28	2.7	20	Wang, 89 (267)
$MmNi_{5-y}Mn_y$ (y = 0.5-0.7)	1.0	1.4	--	0.9-4	25	Sandrock, 78 (113)
$MmNi_{5-y}Mn_y$ (y = 0.3-.9)	0.97	1.3	--	0.3-9	25	Lundin, 78 (272)
$MmNi_{5-y}Mn_y$ (y = 0.4 & 0.8) (Mm = Indian [high-Fe])	0.7-.75	1.0	24-28	2-8	15	Balasubramaniam, 93 (588)
$MmNi_{4.5}Mn_{.5}Zr_y$ (y = 0.025-0.2)	0.67-1	0.9-1.25	30-32	2-2.2	25	Wang, 89 (267)
$MmNi_{4.5}Si_{.5}$ (+ $Si_{.4}$, $Si_{.6}$, $Si_{.8}$)	0.63	0.91	27.6	8	20	Osumi, 82 (127)
$MmNi_{4.6}Sn_{.4}$ (Mm = Indian [high-Fe])	0.45	0.6	29.4	4.7	15	Balasubramaniam, 93 (588)

Table IX
PCT Properties of Selected AB_5 Hydrides
(after Sandrock, 97)

Composition	ΔH, kJ/mol	ΔS, kJ/molK	25°C P_d, atm	T for 1 atm P_d	Plateau Hysteresis	Slope
$MmNi_5$	21.1	0.097	23	-56	1.65	0.54
$MmNi_{4.15}Fe_{0.85}$	25.3	0.105	11.2	-32	0.17	0.36
$MmNi_{4.5}Al_{0.5}$	28.0	0.105	3.8	-6	0.11	0.36
$LaNi_5$	30.8	0.108	1.8	12	0.13	0.13
$LaNi_{4.8}Sn_{0.2}$	32.8	0.105	0.5	39	0.19	0.22
$CaNi_5$	31.9	0.101	0.5	43	0.16	0.19
$MmNi_{3.5}Co_{0.7}Al_{0.8}$	39.8	0.115	0.11	73	0.2 est	1.2
$LaNi_{4.25}Al_{0.75}$	44.1	0.117	0.024	104	0.23	2.7

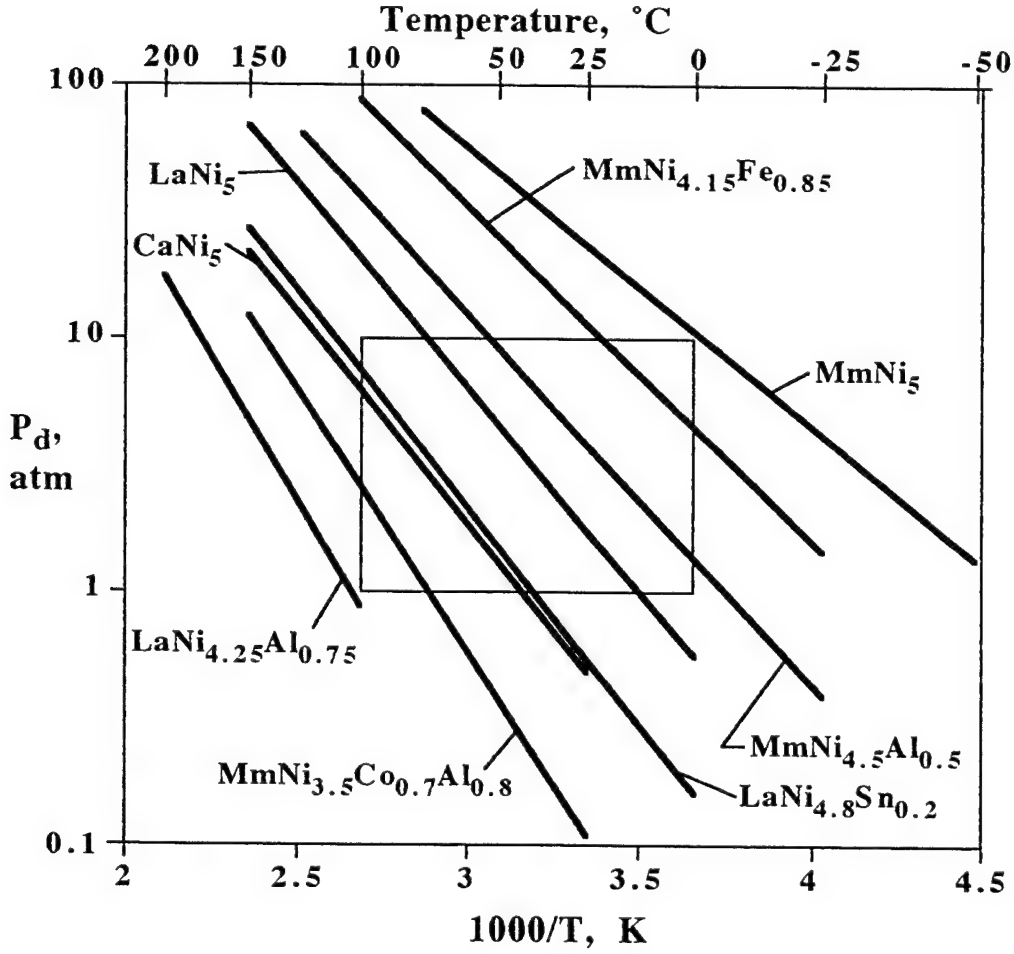

Figure 19
Van't Hoff Lines for Various AB_5 Hydrides

Table X
Capacity and Cost Properties of Selected AB_5 Hydrides

Composition	Density	$(H\text{-Capacity})_{max}$		$(H\text{-Capacity})_{rev}$			Alloy	RMC**
	g/cm^3	H/M	wt.%	$\Delta H/M$	$\Delta wt,\%$	$\Delta N_H/V^*$	$/kg	$/g H
$MmNi_5$	8.6	1.06	1.46	0.90	1.24	5.2	7.94	0.64
$MmNi_{4.15}Fe_{0.85}$	8.1	0.82	1.14	0.65	0.90	3.8	7.12	0.79
$MmNi_{4.5}Al_{0.5}$	8.1	0.85	1.2	0.58	0.83	3.5	7.17	0.86
$LaNi_5$	8.3	1.08	1.49	0.93	1.28	5.2	9.87	0.77
$LaNi_{4.8}Sn_{0.2}$	8.4	1.06	1.4	0.92	1.24	5.1	9.69	0.78
$CaNi_5$	6.6	1.05	1.87	0.55	0.99	3.4	7.56	0.76
$MmNi_{3.5}Co_{0.7}Al_{0.8}$	7.6	0.85	1.24	0.36	0.53	2.2	13.25	2.50
$LaNi_{4.25}Al_{0.75}$	7.6	0.77	1.13	0.53	0.78	3.1	9.68	1.24

* Reversible volumetric capacities are approximate and in units of 10^{22} H-atoms/crystal cm^3 (i.e., interparticle void volumes not included)
** RMC = Raw Materials Cost; $/g H based on $(H\text{-Capacity})_{rev}$

The H-capacities of the eight example alloys, along with the raw materials costs (RMC), are shown in Table X. The capacities are given in both atomic H/M and wt.% for both the maximum and reversible definitions given in Fig.3. The reversible capacities are closer to what might be achieved in practice, but are probably slightly conservative. A little more than the plateau is used for most applications, especially hydrogen storage. In any event, the basic problem that has limited the mobile applications of the AB_5s is seen, namely the rather low gravimetric H-capacities. The best reversible capacity shown is only about 1.3 wt.% H and some of the compositions fall below 1 %. When considering the overly optimistic $(H\text{-capacity})_{max}$, the highest value is nearly 1.9 wt.% for $CaNi_5$. Because of the very light A-element Ca, compared to the heavy rare earth A-elements, $CaNi_5$ stands out in its potential for higher gravimetric H-capacity for an equivalent H/M. Unfortunately, $CaNi_5$ exhibits several plateaux (cf. Fig.15) and using only the main plateau results in the 1.9 wt.% $(H\text{-capacity})_{max}$ being reduced to only about 1.0 wt.% $(H\text{-capacity})_{rev}$, a level comparable to the rare earth based AB_5s.

Volumetric, not gravimetric, H-capacity may be a more important parameter for neutral buoyancy submersible applications. The volumetric capacity $\Delta N_H/V$ (H-atoms/cm^3) is also shown in Table X for the reversible (plateau width) method of calculating capacity. The values of $\Delta N_H/V$ are approximate and some explanation should be given on how they were calculated. $\Delta N_H/V$ was calculated from the reversible H/M using Eq.14. The problem with using Eq.14 is the fact the hydride density ρ is often not exactly known, especially for the ternary and higher substituted alloys. The starting (H-free) intermetallic densities can easily be calculated exactly from generally available crystal lattice parameter data by the formula

$$\rho = \frac{11.499 A_{av}}{a^2 c} \qquad \text{(Eq.24)}$$

where A_{av} is the average atomic weight for the AB_5 formula and the hexagonal lattice parameters a and c are given in angstroms (0.1 nm) (Sandrock, 77 (106)). It is these values of metal density that are given in Table X. For the purpose of Eq.14, the hydride densities were then estimated by assuming that all AB_5 compounds expand about 24 vol.% per 1.0 H/M absorption, as is the case for the archetypical $LaNi_5$ (van Vucht, 70(93)). Although this procedure is not exact, it should give accurate enough values of $\Delta N_H/V$ for comparison purposes. As shown in Table X, the values of estimated $\Delta N_H/V$ correlate with $\Delta H/M$ and scatter around the value for liquid H_2 listed in Table II, $4.2X10^{22}$ H-atoms/cm^3. Comparisons with the other classes of alloys and intermetallic compounds will be made later in this review (Section 4, p.117).

The final two columns of Table X deal with alloy raw materials cost. The last column gives raw material cost in terms of dollars per gram of reversible H-storage, a more meaningful measure than dollars per kilogram of alloy. All alloys show uncomfortably large RMCs for one interested in large scale H-storage. It might be noted that the La- and Mm-based AB_5s are comparable in cost on an H-capacity basis, in spite of my arguments earlier for the economic advantages of Mm over La. This apparent equivalence is probably misleading. The base prices used for both La ($14/kg) and Mm ($8/kg) are based on actual 1996 prices for both materials from China (Table III), which has dominated rare earth pricing in recent years. In fact, there is no significant commercial market for La-based AB_5s at this time, whereas Mm-based AB_5s are widely used in battery alloys today. It is therefore argued that if a large market developed for La-based AB_5s, the real price for refined La (separated from Mm) would greatly increase and the apparent equivalence shown in the right column of Table X would no longer hold.

$MmNi_{3.5}Co_{0.7}Al_{0.8}$, the battery alloy shown in Table X, has by far the highest reversible-capacity-normalized raw material cost. This reflects two factors: (1) the very high price of the strategic element Co, needed for electrode stability and (2) the relatively narrow plateau shown by this alloy. Although $MmNi_{3.5}Co_{0.7}Al_{0.8}$ has a reasonably good $(H\text{-capacity})_{max}$, the narrow plateau results in a low $(H\text{-capacity})_{rev}$ for gas storage applications. The alloy, like most Co-containing AB_5s, has long sloping upper and lower isotherm legs (Sakai, 92 (278)) which are at least partially usable for electrochemical H-storage.

$CaNi_5$ hydride, originally developed by this reviewer (Sandrock, 77 (106)), has some potential as a large-scale, low-cost H-storage medium. In spite of the fact its main plateau is rather narrow on an H/M basis, Table X shows that it still offers 1 wt.% reversible capacity that is cost competitive to the rare earth based AB_5s. If future R&D could achieve enlargement of the main plateau at the expense of the low- and high-pressure side plateaux (cf. Fig.15, p.35), then $CaNi_5$ could be the AB_5 of economic choice. However, it should still be mentioned that $CaNi_5$ has a disproportionation problem that must be addressed (see following Section 3.B.6).

3.B.6. Other Properties

The purpose of this section is to briefly cover the non-PCT properties of AB_5 alloys that are defined in Sections B.3 to B.9.

Activation

Activation of the AB_5 compounds is generally easy. Freshly crushed alloy will usually activate at room temperature without prior heating, so long as the applied H_2 pressure is well above the absorption plateau. There is always an incubation time, ranging from seconds to several hours depending on the applied pressure and the time the as-crushed granules or powder have been

stored in air. High-pressure, high-hysteresis alloys like binary $MmNi_5$ need high activation pressure and may have to be cooled to 0°C or lower if the applied activation pressure is close to the room temperature plateau.

Decrepitation

AB_5 compounds quickly decrepitate into powder with particle sizes on the order of a few to a few tens of μm (not including internal cracks) with surface areas on the order of 0.2 m^2/g. Ni-rich alloys, or other alloys consisting of a two-phase brittle AB_5 + ductile Ni solid solution microstructure, do not decrepitate as much. The eutectic $LaNi_5$-Ni (7 at.%La) decrepitates very little, but this is accomplished only with about 50% loss of H-capacity because the Ni-phase does not hydride at LaNi5 temperatures and pressures (Goodell, 80 (256)). The fine AB_5 powder usually resulting from decrepitation does mandate careful engineering considerations as to filtration, gas flow impedance and packing/expansion problems.

Intrinsic Kinetics and Heat Transfer

The intrinsic H_2 absorption/desorption kinetics of AB_5 compounds are obviously very high, at least after initial activation and if high purity H_2 is used. It was shown early on that the practical reaction rates possible in a hydride bed can be no higher than the reaction heat transfer of that reactor (Goodell, 80 (6&7)). So it is clear that numerous "intrinsic kinetic" studies done over the years have been compromised by reactor heat transfer limitations and are not reliable (e.g., see reviews by Wang, 90 (324) and Gérard, 92 (334)). If great care is taken to mix the AB_5 powder with a thermal ballast material (e.g., 95% Ni or Al powder), then reaction times of only a few seconds can be accomplished (Goodell, 83 (9); Huang, 89; Clay, 90), perhaps approaching the obviously high intrinsic kinetics. In any event, intrinsic kinetics are more than adequate for any anticipated application and we need worry only about the heat transfer design of the hydride container.

Gaseous Impurity Effects

One of the reasons for the general success of AB_5 intermetallics in applications is the fact they are relatively resistant to common impurities that might be present in the H_2 used (i.e., relative to other alloys and intermetallics). Earlier in Fig.6 we saw the effects of interactions between various gas impurities and $LaNi_5$. Although there is little quantitative impurity data on the substituted $MmNi_5$ alloys, limited data obtained on $MmNi_{4.5}Al_{0.5}$ and $MmNi_{4.15}Fe_{0.85}$ suggest that all the AB_5s can be considered qualitatively similar (Kim, 88; Han, 89). O_2 (or H_2O vapor) results in first a retardation effect followed by recovery (Fig.6c) and then a long-term reaction effect (Fig.6d). The partial substitution of Al into $LaNi_5$ or $MmNi_5$ results in increased resistance to O_2 (Han, 89). O_2 and H_2O are clearly and fortunately not poisons to AB_5 intermetallics because they do not form a passive oxide or hydroxide surface layer but rather a "self-restoring" surface structure of non-passive oxide/hydroxide and catalytically active fine Ni particles (Siegmann, 78; Schlapbach, 79 (230); Wallace, 79).

CO is an important impurity to consider, not only from the hydride's point of view but also because it is an important impurity from the PEM fuel cell's point of view. Just as CO is a serious poison to the Pt H_2-dissociation catalyst used in the fuel cell, so it is a poison to AB_5 hydrides, at least at low temperatures (Eisenberg, 83 (208), Han, 89). Reaction-time profiles for H_2-CO look similar to those show in Fig.6a for CH_3SH-H_2. The effects of CO levels and test temperature on the cyclic degradation of $LaNi_5$ capacity are shown in Figure 20. At room temperature (25°C) damage is immediate and severe and is proportional to the CO-content of the H_2 used. It has been

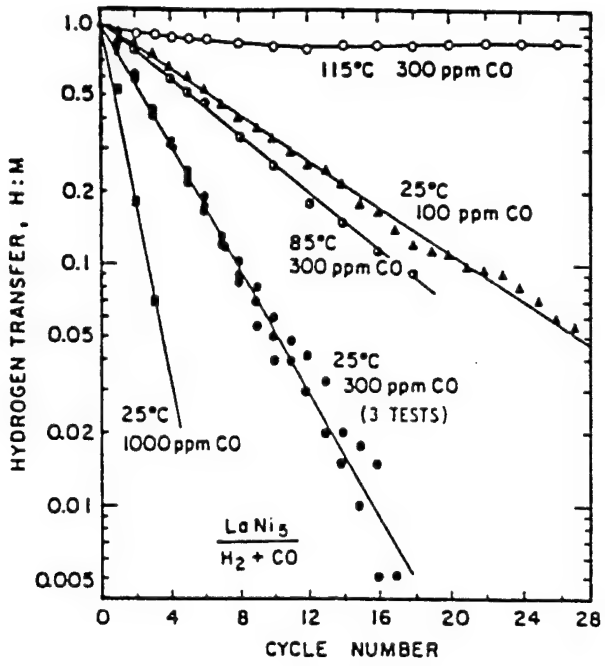

Figure 20
Effect of Cycling $LaNi_5$ in CO-Contaminated H_2
(Eisenberg, 83 (208))

suggested that only one monolayer of CO chemisorption is able to deactivate $LaNi_5$ to hydrogen absorption, probably by forming Ni-carbonyl bonds which destroy the critical H_2<---->2H dissociative properties of the Ni (Sandrock, 80 (203)). The same effect was seen with $MmNi_{4.5}Al_{0.5}$ with evidence partial Al substitution is somewhat beneficial to CO-resistance (Han. 89). What is very important to note in Fig.20 is that CO damage decreases with increasing temperature, virtually disappearing by 115°C. It is also important to understand that CO damage done at 25°C can be easily erased by heating the damaged sample to 100+°C during a desorption cycle. The Ni-CO bond becomes unstable at high temperature and the CO monolayer is removed either by non-dissociative desorption of the CO molecule itself or by dissociative desorption in the form of CH_4 (Eisenberg, 83 (208)). Although one might consider the high room-temperature sensitivity to CO to be a disadvantage for AB_5 hydrides, it is actually an advantage when used as a storage medium for PEM fuel cells. The AB_5 storage bed can act as a CO getter or purifier and prevent trace CO from reaching the sensitive Pt catalyst in the fuel cell thus prolonging its life, or more importantly allowing safe use of lower Pt loadings. As we see, when the CO level of the AB_5 bed gets too high it can easily be regenerated with a simple thermal cycle, during which the desorbed CO or CH_4 is discarded.

Cyclic Stability

Like most intermetallic hydrides, the AB_5s are subject to disproportionation, but at widely varying degrees. Sloped or stepped plateaux ultimately develop with effective loss of reversible capacity. While a stepped plateau can be crystallographically interpreted as a new hydride phase (e.g., Matsumoto, 86), it is also likely associated with the early stages of the significant capacity

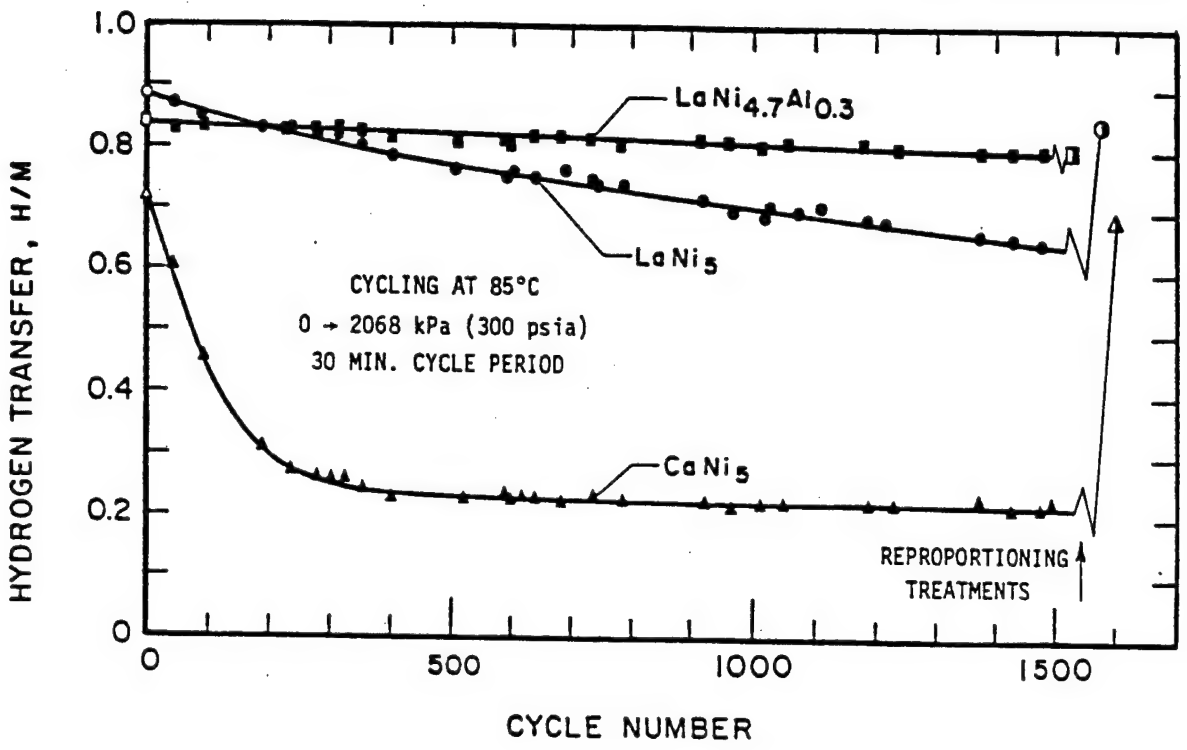

Figure 21
Effect of 85°C Pressure Cycling on the (H-Capacity)$_{rev}$ of Three AB_5 Alloys (Goodell, 84 (5))

loss we call disproportionation (Goodell, 84 (5)). The process is diffusion controlled and is accelerated by increasing temperature. Disproportionation does not require cycling and seems to depend on the time the AB_5 is in the fully hydrided state at pressures above the plateau (Sandrock. 89). Because of this, pressure cycling (as opposed to temperature cycling) generally gives more severe disproportionation. Figure 21 shows the effect of 85°C pressure cycling $LaNi_5$. $LaNi_{4.7}Al_{0.3}$ and $CaNi_5$ on the H-capacity. Lesser, but similar, effects can be seen at 25°C. Both $LaNi_5$ and $CaNi_5$ show disproportionation with the latter suffering much more severe damage. The small partial substitution of Al for Ni gives a dramatically improved resistance to disproportionation. This is believed to be the result of strong Al ordering in the B(Ni)-sublattice that increases its stability (Goodell, 84 (5)). $MmNi_{4.5}Al_{0.5}$ also seems to be reasonably disproportionation resistant, at least relative to thermal cycling (Kim, 87). In any event, and as shown in Fig.21, disproportionation can be almost completely erased by a thermal reproportionation treatments (e.g., 500°C) in vacuum.

The strong beneficial effect of Al has been widely noted and most AB_5 hydride applications that require extensive cycling use Al-containing alloys (e.g., the NiMH batteries discussed earlier). Recently it has been shown that partial Sn-substitution to $LaNi_5$ gives possibly even greater resistance to disproportionation than Al (Marmaro, 91 (316); Lambert, 92 (348); Bowman, 95 (349)). Unfortunately, the one attempt to partially substitute Sn into $MmNi_5$ led to significantly decreased H-capacity (Balasubramaniam, 93 (588)), so it is not clear Sn will be as effective in the commercial Mm-alloys as the La-alloys. More experimental work is needed.

The poor disproportionation resistance of $CaNi_5$ is disappointing given its potential as a low-cost H-storage medium. That fact has greatly limited its application, although although one solar energy storage project claimed good results with $CaNi_5$ hydride used in a thermal cycling environment (Bawa, 82 (155)). It seems possible that substitutional efforts to change the multiplateau characteristic of $CaNi_5$ might also help disproportionation resistance.

Safety

AB_5 hydrides and decrepitated powder are gently pyrophoric when exposed suddenly to air (Sandrock, 81). By "gently pyrophoric", I mean they spontaneously ignite and smolder slowly without explosion or significant flame. They can be deactivated without burning by slowly exposing to air several times in a confined space (e.g. a reactor). Mn-substituted AB_5s are more pyrophoric and more difficult to stabilize. Detailed quantitative safety studies of $LaNi_5$ have been performed in terms of standard powder tests: electrostatic ignition energy, impact and friction, dust explosion indices, ignition temperature, etc. (Lundin, 75 (260)). In general, the results were rather mild compared to many metal powders and the long-used UH_3, but they do require careful consideration when using $LaNi_5$ and related AB_5 materials. Water should not be used in fire situations; Type D dry powder fire extinguishers or dry sand should be used to smother AB_5 fires. There is need for more quantitative safety data on the substituted $MmNi_5$ hydriding alloys.

The inhalation and ingestion toxicities of AB_5 intermetallics are unknown. In the absence of other information, it is generally assumed the toxicity is dominated by the properties of the principal elemental component, nickel (Anon., 88). From a dust inhalation point of view, both the US Occupational Safety and Health Administration (OSHA) and the US National Toxicology Program consider Ni to be a "possible cancer hazard" with the OSHA Permissible Exposure Limit in air set at 1 mg/m^3. The International Agency for Research on Cancer (IARC) has concluded that nickel and certain Ni compounds are probably carcinogenic to humans but could not say which specific compounds are carcinogenic, saying that "...metallic Ni seems less likely to be so than nickel subsulphide or nickel oxides." Epidemological studies of workers exposed to Ni powder or workers exposed to dust and fumes generated in the production of Ni alloys and stainless steel have not indicated the presence of a significant respiratory cancer hazard. As far as ingestion is concerned, the US National Institute for Occupational Safety and Health (NIOSH) have concluded that Ni and its organic compounds are not carcinogenic when ingested. The US Food and Drug Administration (FDA) has affirmed that Ni is generally recognized as safe as a direct human food ingredient. Like the ubiquitous presence of NiCd and NiMH batteries, the use of AB_5 storage tanks for fuel cell applications should involve virtually complete containment of the alloy powder. Toxicity concerns exist only for accidental spill situations and the initial filling of the containers. Properly designed containers should be adequately filtered to prevent powder particles from leaving with the H_2 gas stream. As with the use of all metal powders, adequate precautions should be taken in the handling of AB_5 powders. Users should follow the Material Safety Data Sheets (MSDS) provided by the alloy producers.

Metallurgy, Manufacture and Recycling

The metallurgy of the AB_5 intermetallic compounds can be at least partly discussed in terms of the La-Ni phase diagram, shown in Figure 22. The AB_5 phase is essentially a line compound and therefore it is important to prepare alloys to close tolerances to maximize the amount of that phase. Ni-rich alloys give some second-phase Ni (or Ni solid solution) that does not hydride at the normal temperature and pressure of the AB_5s (cf. Fig.8). Similarly, A-rich alloys result in second phase A_2B_7 which hydrides but is generally not useful for reversible room temperature storage. In

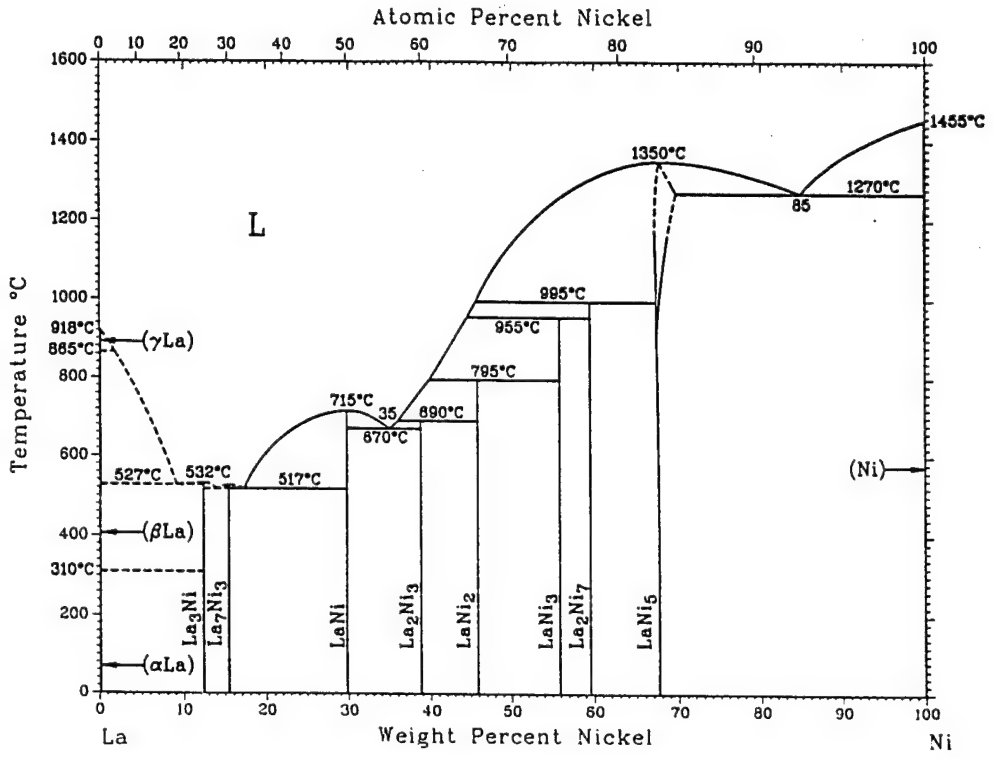

Figure 22
The La-Ni Phase Diagram
(Pan, 90)

general, for gas storage applications it is best to have a microstructure that is as close as possible to single phase AB_5, although it has been argued that some second-phase Ni particles are useful to electrochemical applications (Notten, 91 (294)). At high temperature (>1000°C), $LaNi_5$ does have a small homogeneity range ($LaNi_{4.9-5.4}$) so that the plateau pressure can be varied by adjusting stoichiometry and solution treating about 1200°C (Buschow, 72 (95)).

A-substitutions, at least rare earth elements, do not change the phase diagram of Fig.22 very much. Ternary, or higher order, B-substitutions sometimes do apparently change the phase diagram, e.g. Al and Fe. The $LaNi_5$ melting point (1350°C) can be lowered, the alloy my develop distinct liquidus and solidus temperatures (i.e., is no longer congruent) and second phases my form on solidification reducing H-capacity (Sandrock, 78 (113)). Elements like Co, Cu and Sn seem to substitute well into the AB_5 without producing significant amounts of second phases. However, because the A-substitution Ca and many of the B-substitutions result in a liquidus ----> solidus gap, solidification occurs with a metallurgical coring or microsegregation within the AB_5 phase, in turn giving it an often undesirable sloping plateau. Post-solidification homogenization heat treatments are used to reduce this segregation and flatten the plateau.

AB_5 alloys are usually made commercially by vacuum induction melting of the elements, although the author has had some success with air induction melting. Ca and Mn have high vapor pressure and alloys with significant levels of these elements require an Ar pressure in the vacuum chamber. $CaNi_5$ requires air or argon blanket melting (Sandrock, 77 (106)). AB_5 alloys can also be made by the solid state reduction-diffusion (R-D) process involving the calciothermic reduction of the low-cost rare earth oxide with Ca or CaH_2 in the presence of Ni powder (Martin, 75 (152)):

$$5Ni + 0.5La_2O_3 + 1.5CaH_2 \text{ ---> } LaNi_5 + 1.5CaO + 1.5H_2 \qquad \text{(Eq.25)}$$

The CaO is separated from the $LaNi_5$ by water flotation and mild acid leaching. The R-D process has also been applied to multicomponent $Mm(Ni,Co,Mn,Al)_5$ battery alloys (Takeya, (93)).

The AB_5 family of hydrogen storage compounds do not depend strongly on critical strategic elements, at least for gas storage applications such as for the fuel cell. Present electrochemical applications (NiMH battery) do seem to require small amounts of Co, a strategic element. But gas storage applications can easily get by without Co. Rare earth elements (especially mischmetal) are not really rare and are available from numerous places: USA, China, Brazil, India and Norway, at least. Nickel is a widely available, London-traded commodity, but not much comes from the USA. Canada is the largest supplier. Although the spectrum of AB_5 elements are not in short supply, they are expensive and that remains one of the disadvantages of the family.

Spent AB_5 alloy can be recycled. The procedures for recycling NiMH batteries have been demonstrated (Lyman, 94), but are probably not in place yet commercially. It is possible to directly rejuvenate O-damaged dry $LaNi_5$ powder by the calciothermic procedure of Eq.25 (Zhang, 89 (262)).

3.B.7 Summary and Suggested R&D

The AB_5 family of intermetallic hydrides is large and very versatile. The PCT properties are ideal for PEM fuel cell applications and are easily fine tuned to the precise desired properties. Volumetric H-contents are good but gravimetric H-densities are limited to the order of 1-1.25 wt.% on a reversible (plateau width) basis. In general, impurity resistance is good and resistance to disproportionation is good if stabilized with Al or Sn ternary additions. Alloys based on partially substituted $MmNi_5$ are made commercially in large quantities for NiMH battery uses. Except for Co (used only in battery applications) no critical strategic elements are really needed. The AB_5s are borderline expensive, even when Mm is used as the A-element. They are safe to use, but are mildly pyrophoric when suddenly exposed to air.

From a future alloy development point of view, other substitutional elements and levels can certainly be tried. But it is probably safe to say that the AB_5 family is close to reaching the limits of its potential, at least with the rare earth - Ni systems. Small further improvements can likely be made but major increments seem unlikely. There are a few areas of AB_5 R&D this reviewer would suggest, especially relative to the application of such alloys as H_2 storage media for PEM fuel cells and closely related applications:

1. Develop $CaNi_5$ into a viable and competitive AB_5. By systematically surveying ternary substitutions, try to enlarge the main plateau and increase the disproportionation resistance. An improved $CaNi_5$ could become the lowest cost and highest capacity AB_5.

2. Develop a full understanding of the ability of AB_5s to getter CO, thus protecting the fuel cell from CO damage. Quantify poisoning and regeneration for substituted $MmNi_5$ alloys. Determine if it is possible for $Ni(CO)_4$ (a highly toxic gas) to be formed and released.

3. Generate more quantitative safety data, especially on the substituted $MmNi_5$ alloys.

3.C AB_2 Intermetallic Hydrides

The AB_2 family of intermetallic compounds, like the AB_5s, represents a large and versatile group of hydriding materials with properties of value for the ambient temperature realm. The IEA/DOE/SNL database presently includes more than 400 AB_2 entries, including multiple data on certain binary and multicomponent compounds by various investigators (Sandrock, 97). The A-elements are often from the IVA group (Ti, Zr, Hf) and/or rare earth series (at. no. 57-71) or Th. The B-elements can be a variety of transition or nontransition metals with something of a preference for atomic numbers 23-26 (V, Cr, Mn, Fe). As will be shown, a very wide variety of substitutions are possible for both A- and B-elements, thus providing a high degree of fine tuning of PCT properties.

3.C.1 Crystal Structure

Almost all of the practical AB_2 hydriding intermetallic compounds come from the Laves phases. There are three Laves phase structures: C14, C15 and C36 (Wernick, 67). The C14 and C15 are the most important and their structures are shown in Figures 23 and 24, respectively.

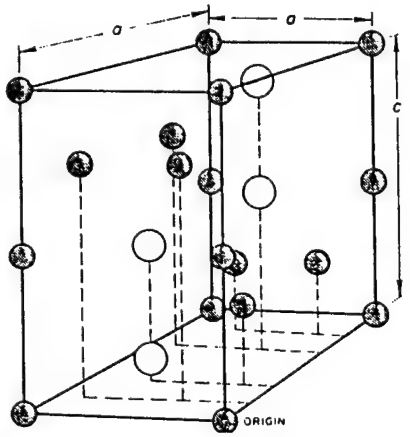

Strukturbericht = C14
Prototype = $MgZn_2$
Pearson = hP12
Space Group = $P6_3/mmc$
Generic = Laves Phase

Figure 23
Structure of the C14 Laves Phase
(Barrett, 73)

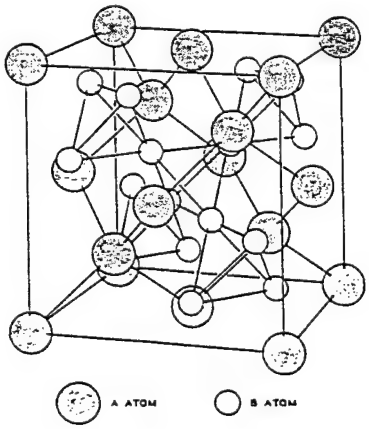

Strukturbericht = C15
Prototype = $MgCu_2$
Pearson = cF24
Space Group = Fd-3m
Generic = Laves Phase

Figure 24
Structure of the C15 Laves Phase
(Wernick, 67)

The C14 (Fig.23) structure is hexagonal, with 4 AB_2 formula units per equivalent trigonal unit cell shown (4 A-atoms and 8 B-atoms). A classic C14 hydriding phase is $ZrMn_2$. The C15 structure (Fig.24) is cubic with eight AB_2 formula units per unit cell shown (8 A-atoms and 16 B-atoms). A classic C15 hydriding phase is ZrV_2. In both cases H-atoms tend to occupy $[A_2B_2]$ tetrahedral interstices (Yvon, 88 (320)). Unlike the AB_5 line compounds, the AB_2 intermetallics often have some homogeneity range (i.e., A:B need not be exactly 1:2; cf. Section 3.C.6, p.70).

3.C.2 Historical Background of the AB_2 Hydrides

The first known demonstration that intermetallic compounds could be intentionally hydrided (Trzeciak, 56 (483)) reported the formation of two AB_2 hydrides: $ZrCr_2H_{3.6}$ and $ZrV_2H_{4.14}$. This early study focused mostly on high temperature (≥538°C) properties and did not include lower temperature PCT data in the contemporary sense. Six years later a major pioneering hydriding survey of many binary intermetallic compounds was reported (Beck, 62 (45)). Although that work was done at 1 atm pressure (glass apparatus) and did not include PCT isotherms, a promising number of AB_2 compounds were found to hydride. They are summarized in Table XI for historic interest and also to show that at this early time the concept of disproportionation was recognized. In particular several AB_2s with rare earth, Th or Y A-elements were seen to disproportionate.

Table XI
Hydridable AB_2 Compounds from the 1962 Beck Survey
(Beck, 62 (45))

Composition	Structure Type	$(H\text{-Capacity})_{max}$ H/M	wt.%	Disproportionation Products (if disproportionation occured)
$CaAl_2$	C15	0.19	0.6	
$CeNi_2$	C15	>0.5	--	$CeH_x + CeNi_5$
$DyMn_2$	C15	>0	>0	$DyH_x + Mn$
$GdCo_2$	C15	>.5	--	$GdH_x + GdCo_5$
$GdFe_2$	C15	>1	--	$GdH_x + Fe$
$GdMn_2$	C15	>0	>0	$GdH_x + Mn$
HfV_2	C15	1.06	1.1	
$PrGa_2$	C32	0.11	0.1	
$SmMg_2$	C15	>0	>0	$SmH_x + Mg$
$ThMn_2$	C14	1.19	1.0	
$ThNi_2$	C32	0.7	0.6	$Th_7Ni_3H_x + ThNi_5$
$TiCr_2$	C14	0.22	0.4	
UMn_2	C15	0.18	0.16	
YFe_2	C15	>1	--	$YH_x + Fe$
YNi_2	C15	>0.5	--	$YH_x + YNi_3$
$ZrCr_2$	C15	1.16	1.8	
$ZrMn_2$	C14	0.67	1.0	
$ZrMo_2$	C15	0.27	0.3	
ZrV_2	C15	1.38	2.1	

The first detailed PCT data were obtained for AB_2 hydrides ($ZrCr_2$, ZrV_2 and $ZrMo_2$) about 1966 (Pebler, 66 (12), 67 (13)). However, AB_2 hydride activity was virtually dormant for next decade. Perhaps stimulated by the AB_5 and AB hydride successes of the early 1970s, AB_2 hydride R&D became quite active at several laboratories in the late 1970s:

Academy Sciences USSR (Burnasheva, 77 (520), 79 (519); Paderets, 78 (513); Kost, 79 (515))
Brookhaven National Laboratory (Reilly, 76 (490); Johnson, 78 (330, 335), 80 (42))
Hebrew University (Shaltiel, 77 (14), 78 (66), 79 (51); Jacob, 77 (47), 78 (15,16), 79 (361), 80 (65))
Matsushita (Machida, 78 (371), Gamo, 79 (33-35), 80 (36,37))
Philips (Buschow, 76 (518), 77 (52,54); van Mal 76 (44))
University of Pittsburgh (Gualtieri, 76 (516), 77 (50); Malik, 77 (514))

Most of these efforts continued strongly into the 1980s with the notable major added AB_2 contributions from the following laboratories:

Argonne National Laboratory (Kierstead 79 (458), 80 (356), 82 (61, 374); Mendelsohn, 81 (21); Shenoy 81, (445); Vicarro, 80 (359))
Daimler Benz (Bernauer, 89 (341, 344), 84 (521), 87 (610))
University of Winsor (Ivey, 82 (58), 83 (251), 84 (29), 86 (285, 377); Qian. 89 (376, 559))

AB_2 R&D has continued to this day in many laboratories around the world. Many others beyond those listed above deserve credit. More activities are cited below and a much more complete list of references can be found in the AB_2 on-line database (Sandrock, 97).

3.C.3 Binary AB_2 Hydriding Compounds

We should begin our review of the AB_2 hydrides with a comparison of the capacity and PCT properties of the binary compounds. Although many have been reported to hydride, only a limited subset have been quantified relative to useful PCT measurements. These are listed in Table XII. Table XII lists both binary AB_2 intermetallic that have been studied in considerable detail (i.e., enough to have ΔH reported), as well as some which have only semiquantitative PCT data or estimated data reported. Compounds that show multiple plateaux are marked with an (M) and those with calorimetric values of ΔH are marked with a (cal). Particularly sloping plateaux are noted. Some listed compounds are off-stoichiometric, which is one way to control PCT properties of AB_2 hydrides (cf. Section 3.C.6, p.70).

It should be immediately evident from Table XII that a large range of PCT properties are available. As a measure of stability, ΔH ranges from 20 kJ/mol to more than 150.[4] H-capacities (by the maximum definition) are reasonably high, usually exceeding 1 on an H/M basis. However on a weight percent basis, H-capacities are not very impressive when heavy A-atoms are involved (e.g., the rare earth elements or Zr). Using the lighter Ti as the A-element helps with weight percent. The highest wt.% shown is 4.4 for $TiBe_2H_3$ (Maeland, 83 (362)), but this is an unlikely candidate because of Be-toxicity reasons, among others. It can be seen from Table XII that higher pressure (more unstable) hydrides result from Ti-Cr combinations, whereas Zr-Mn combinations tend toward the opposite. This sets part of the stage for multicomponent alloy PCT control.

[4] The two values of ΔH below 20 kJ/mol (Pourarian, 81 (19)) for $ZrMn_{2+x}$ compounds are considered anomalously low compared to data by other investigators on similar alloys (see discussion on page 64). These data may be in error and should be experimentally checked before using them for any application.

Table XII
Hydride PCT Properties of Binary AB_2 Compounds

Composition	(H-Capacity)$_{max}$ H/M	wt.%	ΔH, kJ/mol	P= (atm)	at T= (°C)	Author-Yr.
$CaNi_2$	1.13	2.1	85 (cal)	<0.05	25	Oesterreicher, 80 (43)
$DyFe_2$ (M)	1.4	1.5	58	0.0001	80	Kierstead, 80 (356)
$DyFe_2$ (M)	2.5 (1400 atm)	2.7	--	0.03	21	Pourarian, 80 (357)
$ErFe_2$ (M)	1.4	1.5	57.9	0.001	80	Kierstead, 80 (356)
$ErFe_2$ (M)	1.07	1.1	56.2	0.013	130	Flanagan, 87 (358)
$ErMn_2$	1.63	1.75	--	0.02	22	Viccaro, 80(359)
$GdCo_2$ (M)	1.37	1.5	48	2	200	Jacob, 79 (361)
$GdFe_2$	1.37	1.5	29	<1 (Sloping plateau)	292	Jacob, 79 (361)
$GdFe_2$ (M)	1.46	1.6	--	0.0001 (Sloping plateau)	20	Kierstead, 82 (61)
GdFeAl	1.0	1.2	--	0.75	27	Drulis, 84 (553)
$GdMn_2$	1.0	1.1	87.5	1 (Sloping plateau)	360	Shaltiel, 79 (361)
$GdNi_2$	1.37	1.5	90	<1 (Sloping plateau)	300	Jacob, 79 (361)
$GdRh_2$	1.1	0.9	--	0.8	100	Shaltiel, 77 (14)
$GdRh_2$	1.07	0.9	49	6	142	Jacob, 79 (361)
$GdRu_2$	1.23	1.0	--	0.7	200	Shaltiel, 77 (14)
$GdRu_2$	1.23	1.0	60	3	225	Shaltiel, 79 (361)
$HoRu_2$	1.4	1.1	--	1	155	Shilov, 81 (530)
$LaRh_2$	1.63	1.4	--	0.7	200	Shaltiel, 77 (14)
$LaRh_2$ (M)	1.63	1.4	44.3	2 (Sloping plateau)	244	Jacob, 79 (361)
$LaRu_2$	1.5	1.3	--	Low	<200	Shaltiel, 77 (14)
$LiPd_2$	0.56	0.8	51	0.16	300	Sakamoto, 95 (411)
$PrCo_2$	1.33	1.5	>67	<0.001	100	Clinton, 75 (102)
$ScFe_2$	1.03	2.0	--	1	140	Shilov, 81 (530)
$ScMn_2$	1.27	2.4	--	--	--	Kost, 79 (515)
$ScMn_2$	1.27	2.4	--	1	140	Shilov, 81 (530)
$SmCo_2$	1.33	1.5	--	0.01	40	Kanematsu, 89 (558)
$ThNi_2$	1.33	1.1	44.7	No plateau		Buschow, 75 (187)
$ThZr_2$	2.0	0.5	413	0.08	910	Bartscher, 88 (556)
$TiBe_2$	1.0	4.4	--	>1	22	Maeland, 83 (362)

Table XII (concluded)
H-Capacities and Hydride PCT Properties of Binary AB_2 Compounds

Composition	(H-Capacity)$_{max}$ H/M	wt.%	ΔH, kJ/mol	P= (atm)	at T= (°C)	Author-Yr.
$TiCr_{1.8}$ (M)	1.25	2.43	20.2	40	-20	Johnson, 78 (335)
$TiCr_2$	0.67	1.3	--	30 (Sloping plateau)	-16	Reilly, 76 (490)
$TiCr_2$	0.4	0.8	23	40 (Sloping plateau)	20?	Machida, 78 (371)
$TiMn_{1.5}$	0.99	1.9	28.7	7	20	Gamo, 81(31)
$TiMn_{1.5}$	1.0	1.9	27.9	1.8	0	Andreev, 82 (522)
$TiMn_{2-y}$ (y = 0.3-0.75)	0.4-1.2	0.8-2.3	--	4-40	50	Someno, 80 (381)
$TmFe_2$ (M)	1.47	1.6	56.8	0.003	80	Kierstead, 82 (374)
UTi_2	2.16	1.9	--	0.2	400	Asada, 95 (628)
YCo_2	1.23	1.8	--	0.05	25	Shaltiel, 77 (14)
YFe_2 (M)	1.43	2.1	--	0.001	20	Kierstead, 82 (61)
YRu_2	1.1	1.1	--	Low	<200	Shaltiel, 77 (14)
$ZrAl_2$	0.17	0.35	--	<0.1	20	Jacob, 78 (16)
ZrNiAl	0.18	0.3	--	<0.001	40	Yoshida, 95 (622)
$ZrBe_2$	0.77	2.1	--	<0.01	22	Maeland, 83 (362)
$ZrCr_2$	1.2	1.8	46	0.03	27	Pebler, 67 (13)
$ZrCr_2$	1.2	1.8	--	0.3	100	Perevesenzew, 88 (557)
$ZrMn_{1.8}$	0.82	1.2	--	0.06	50	van Essen, 80 (17)
$ZrMn_{1.8}$	1.09	1.6	38.8	0.1	50	Luo, 92 (582)
$ZrMn_2$	1.2	1.8	53.2	0.03 (Absorption)	80	Shaltiel, 77 (14)
$ZrMn_2$	1.0	1.5	36	3	210	Fujii, 87 (369)
$ZrMn_2$	0.9	1.4	--	1	150	Yonezu, 91 (563)
$ZrMn_2$	1.15	1.7	37.4	0.01	50	Luo, 92 (582)
$ZrMn_{2.4}$	1.06	1.6	--	0.7	50	van Essen, 80 (17)
$ZrMn_{2.5}$	0.94	1.4	32	0.07	50	Luo, 92 (582)
$ZrMn_{2.7}$	0.82	1.3	33.6	3 (Sloping plateau)	100	Uchida, 86 (370)
$ZrMn_{2.8}$	--	--	29.9	0.3 (Sloping plateau)	23?	Pedziwiatr, 83 (28)
$ZrMn_{2.8}$	1.05	1.6	--	2	50	van Essen, 80 (17)
$ZrMn_{2.8}$	0.95	1.5	18.4	0.4	23	Pourarian, 81 (19)
$ZrMn_3$	0.82	1.3	29.2	0.6	50	Luo, 92 (582)
$ZrMn_{3.8}$	0.75	1.2	17	0.7 (Sloping plateau)	30	Pourarian, 81 (19)
$ZrMo_2$	0.27	0.3	38.5	No plateau		Pebler, 67 (13)
ZrV_2	1.55	2.4	≈150	No plateau		Pebler, 67 (13)

3.C.4 Multicomponent Substituted AB_2 Hydriding Compounds

Like the AB_5 hydriding compounds, the AB_2s also have a high degree of PCT versatility that can be achieved by partial substitutions for both A- and B-atoms. One of the most useful means of control is by the use of both Ti and Zr on the A-side and varying the ratio of the two elements. For example, Figure 25 shows the PCT effects of Zr-content y in the formula $Ti_{1-x}Z_xCrMn$ over the

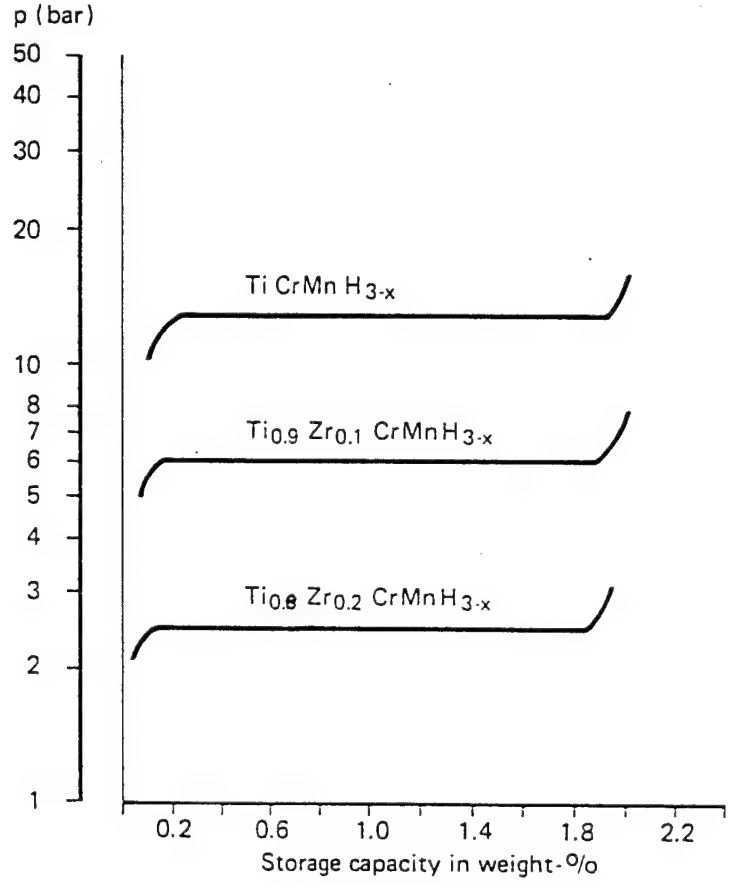

Figure 25
Effect of Zr-Content x on the -20°C Isotherm of $Ti_{1-x}Z_xCrMn$
(Bernauer, 89 (344))

range x = 0-0.2. First of all Zr-substitution decreases plateau pressure rather strongly. This might be intuitively expected from the fact the elemental hydride ZrH_2 is significantly more stable than TiH_2 (Fig.8), but it can also be related to the C14 cell volume (Bernauer, 89 (344)). Second, plateau pressure can be controlled without loss of H-capacity, at least up to x = 0.2 Zr. This is always useful from a practical perspective. Third, note that the plateaux shown in Fig.25 are quite flat. Flat plateaux can be achieved only by carefully annealing the as-cast alloys of the TiCrMn family (Reilly, 78).

Numerous partial substitutions are also possible on the B-side of AB_2. For an historic early example of this, Table XIII lists the PCT properties of a number of substituted ternary ZrB_2 compounds adapted from what is one of the earliest patent claiming multicomponent Laves phase

Table XIII
PCT Properties of $Zr(A_{1-y}B_y)_2$ Compounds
(after Shaltiel, 79 (51))

Composition	(H-Capacity)$_{max}$ H/M	(H-Capacity)$_{max}$ wt.%	ΔH, kJ/mol	ΔS, kJ/molK	Plateau Pressure, atm 50°C	Plateau Pressure, atm 80°C
$Zr(Fe_{0.5}V_{0.5})_2$	1.07	1.6	48.1	0.094	0.0012	0.0056
$Zr(Fe_{0.75}V_{0.25})_2$	1.07	1.6	32.2	0.088	0.25	0.7
$Zr(Fe_{0.5}Cr_{0.5})_2$	1.13	1.7	49.4	0.134	0.1	0.6
$Zr(Fe_{0.75}Cr_{0.25})_2$	0.95	1.4	24.3	0.092	5.5	12
$Zr(Fe_{0.4}Mn_{0.6})_2$	1.07	1.6	33.1	0.096	0.4	1.4
$Zr(Fe_{0.5}Mn_{0.5})_2$	0.97	1.4	30.1	0.090	0.65	1.65
$Zr(Co_{0.5}V_{0.5})_2$	1.23	1.8	49.4	0.102	0.0023	0.01
$Zr(Co_{0.75}V_{0.25})_2$	1.0	1.45	34.3	0.113	1.5	4.5
$Zr(Co_{0.5}Cr_{0.5})_2$	1.07	1.6	40.2	0.121	0.7	2.5
$Zr(Co_{0.75}Cr_{0.25})_2$	0.53	0.8	--	--	No plateau	
$Zr(Co_{0.25}Mn_{0.75})_2$	1.13	1.65	44.4	0.117	0.08	0.3
$Zr(Co_{0.4}Mn_{0.6})_2$	1.3	1.5	36.0	0.105	0.5	1.6
$Zr(Co_{0.5}Mn_{0.5})_2$	1.3	1.5	34.8	0.109	1.2	3.7

hydrides. Although not clearly indicated in the reference, the plateau pressures are believed to be for desorption. Note the wide differences in hydride stability (as measured by ΔH and plateau pressure) than can be accomplished with reasonable H-capacity by varying the B-elements and their levels. The 50°C pressures vary over three orders of magnitude.

The multicomponent AB_2 work which Shaltiel and coworkers and Gamo and coworkers started in the late 1970s (typified by Table XIII) was continued by many investigators throughout

Table XIV
Hydride PCT Properties of Multicomponent AB_2 Compounds

Composition	(H-Capacity)$_{max}$ H/M	(H-Capacity)$_{max}$ wt.%	ΔH, kJ/mol	P= (atm)	at T= (°C)	Author-Yr.
$CaAl_{1.8}B_{.2}$ (M)	0.2	0.7	--	3	40	Tanaka, 95 (416)
$CeAlAl_{1.25}Cr_{.75}$	0.45	0.6	--	<0.05	21	Gross, 96 (630)
$Ca_{.5}Mg_{.5}Ni_2$	0.87	1.7	--	No plateau		Oesterreicher, 80 (43)
CeMnAl	0.67	0.9	--	<0.05	21	Gross, 96 (630)
GdFeAl	1.0	1.2	--	0.75	27	Drulis, 84 (553)
GdNiAl	0.67	0.8	--	0.5	27	Drulis, 84 (553)
$Ho_{.6}Zr_{.4}Co_2$	0.83	1.0	33	0.2	50	Ramesh, 93 (363)
$Ho_{.8}Zr_{.2}Co_2$	1.1	1.2	25	0.2	50	Ramesh, 93 (363)
$Ho_{.6}Zr_{.4}Fe_2$	1.83	2.2	18	40	25	Kesavan, 95
$Ho_{.8}Zr_{.2}Fe_2$	2.7	3.0	6	60	27	Kesavan, 96

Table XIV
Hydride PCT Properties of Multicomponent AB_2 Compounds (continued)

Composition	(H-Capacity)$_{max}$ H/M	wt.%	ΔH, kJ/mol	P= (atm)	at T= (°C)	Author-Yr.
LaMnAl(M)	0.92	1.2	--	15 (Absorption, upper plateau)	21	Gross, 96 (630)
MmMnAl	0.75	1.0	--	<0.05	21	Gross, 96 (630)
$Tb_{.27}Dy_{.73}Fe_2$	1.36	1.5	--	0.15	200	Manwaring, 93 (379)
TiCrMn	0.91	1.7	--	15 (S)	-16	Reilly, 76 (490)
$Ti_{1.2}CrMn$	1.05	2.0	25.5	5.7	-10	Osumi, 83 (40)
$Ti_{1.2}Cr_{1.9}Mn_{.1}$	0.91	1.8	20.1	19.4	-10	Osumi, 83 (40)
$Ti_xCr_{1.2}Mn_{.8}$ (x = 1.1-1.3)	0.94-1	1.8-2.1	25-26	4.6-10	-10	Osumi, 83 (40)
$TiMn_yB_{.1}$ (y = 1.3-1.4; B = Co, Cu, Fe, Ni, V)	0.92-1	1.7-1.9	--	4-10	20	Gamo, 80 (31)
$TiMn_{1.25}Cr_{.25}$	1.1	2.1	--	6	20	Hong, 91 (365)
$TiMn_{1.2}Fe_{.37}$	0.72	1.4	--	9	10	Gamo, 80 (36)
$TiMn_{1.3}Fe_{.11}$	0.89	1.7	32.7	6	24	Gamo, 80 36)
$TiMn_{1.4}Fe_{.11}$	0.88	1.7	--	4.5	0	Gamo, 80 (36)
$TiMn_{1.2}V_{.8}$	1.10	2.1	--	4.5 (S)	50	Bernauer, 84 (521)
$TiMn_{1.4}V_{.62}$	1.14	2.15	--	3.5	20	Bernauer, 84 (521)
$TiMnV_{.9}Cr_{.1}$	1.28	2.45	--	0.8	45	Bernauer, 84 (521)
$TiMn_{1.28}V_{.6}Fe_{.15}$	1.13	2.15	--	8	20	Bernauer, 84 (521)
$TiV_{1.5}Fe_{.4}Mn_{.1}$	1.7	3.3	--	7	50	Bernauer, 87 (610)
$TiV_{2-y}Mn_y$ (y = 0.4-1)	1.17-2.0	2.2-3.8	--	--	--	Jacob, 81 (459)
TiVMn	1.24	2.4	--	2	70	Bernauer, 89 (344
$Ti_{.98}Zr_{.02}B_{2.07}$ ($B_{2.07} = Mn_{1.5}V_{.43}Fe_{.09}Cr_{.05}$)	0.99	1.9	27.4	9	20	Bernauer, 89 (341)
$Ti_{1-x}Zr_xCr_2$ (x = 0-0.3)	0.4	0.8	--	3-40	20?	Machida, 78 (371)
$Ti_{1-x}Zr_xCrMn$ (x = 0-0.2)	1.0	2.0	--	2.5-13	-20	Bernauer, 89 (344)
$Ti_{1-x}Zr_xMn_y$ (x = 0-0.2, y = 1.5-1.8)	0.9-1	1.7-1.8	--	2-6.5	20	Gamo, 80 (31)
$Ti_{1-x}Zr_xMn_{2-y-z}Cr_yCu_z$ (x = 0-1, y = 0.5-1, z = 0-0.2)	0.9-1.1	1.6-1.9	--	<1-30	30	Moriwaki, 91 (366)
$Ti_{.5}Zr_{.5}Mn_{.9}Cr_{.9}Ni_{.4}$	1.05	1.6	--	3 (S)	40	Liu, 96 (526)
$Ti_{.5}Zr_{.5}(Mn_{.5}Cr_{.5})_{1-y}Ni_y$ (x=0-1.4)	1.05	1.6	--	1-60 (S)	40	Liu, 96 (526)
$Ti_{1-x}Zr_xNiV_{.6}Mn_{.2}Fe_{.2}$ (x = 0.2-0.4)	0.9-1.0	1.6-1.7	--	0.7-2 (S)	30	Gao, 95 (403)
$Ti_{.5}Zr_{.5}Mn_2$	1.1	1.8	40?	1.5 (S)	70	Gamo, 79 (34)

Table XIV
Hydride PCT Properties of Multicomponent AB_2 Compounds (continued)

Composition	(H-Capacity)$_{max}$ H/M	wt.%	ΔH, kJ/mol	P= (atm)	at T= (°C)	Author-Yr.
$Ti_{.5}Zr_{.5}Ni_{1.3}V_{.7}B_{.2}$ (B = Al, Cr, Fe, Mn)	0.86-1.08	1.4-1.8	--	No plateaux		Miyamura, 93 (372)
$Ti_{1-x}Zr_xMn_{1.7}Cu_{.3}$ (x = 0.3-0.5)	0.88-1.05	1.5-1.7	--	0.1-1	20	Gamo, 80 (31)
$Ti_{.6}Zr_{.4}Mn_{1.9}Cu_{.1}$	1.0	1.7	40.6?	0.5	20	Gamo, 79 (34)
$Ti_{.8}Zr_{.2}Mn_{1.2}Cr_{.8}$	1.1	2.0	28.9	5	20	Machida, 78 (371)
$Ti_{.6}Zr_{.4}Mn_{1.4}Cr_{.4}Cu_{.2}$	1.07	1.8	48?	0.3	20	Gamo, 79 (35)
$Ti_{.5}Zr_{.5}Mn_{1.2}Fe_{.3}$	1.14	1.9	39	1.5 (S)	120	Komazaki, 83 (29)
$Ti_{.5}Zr_{.5}Mn_{1.36}Fe_{.34}$	0.94	1.5	--	3 (S)	100	Komazaki, 83 (29)
$Ti_{.5}Zr_{.5}(Mn_{1-y}Fe_y)_{1.5}$ (y = 0.2-0.8)	0.5-1.1	0.8-1.8	--	4-70+	100	Komazaki, 83 (29)
$Ti_{.475}Zr_{.475}La_{.05}Mn_{.8}$ - $Cr_{.8}Ni_{.4}$	1.08	1.8	--	2	40	Liu, 95 (415)
$Ti_{.8}Zr_{.2}Mn_{1.5}Fe_{.5}$	0.95	1.7	25.4	11	30	Hong, 93 (373)
$Ti_{.7}Zr_{.3}Mn_{1.9}Mo_{.1}$	1.07	1.7	41?	0.9	17	Gamo, 79 (34)
$Ti_{.8}Zr_{.2}Mn_{1.5}Cr_{.5}$	1.1	2.0	27.5	10	30	Hong, 93 (373)
$Ti_{.77}Zr_{.23}Mn_{.67}Cr_{.67}Cu_{.67}$	0.94	1.6	--	8	30	Zhan, 95 (627)
$Ti_{.8}Zr_{.2}Mn_{1.5}Cu_{.5}$	0.9	1.6	27	3	30	Hong, 93 (373)
$Ti_{.8}Zr_{.2}Mn_{1.8}Mo_{.2}$	1.0	1.7	29	4	20	Gamo, 80 (31)
$Ti_{.8}Zr_{.2}Mn_{2-y}Mo_y$ (y = 0.1-0.3)	0.99-1.03	1.65-2.5	--	2-6	20	Gamo, 80 (31)
$Ti_{.8}Zr_{.2}Mn_{1.5}V_{.5}$	1.1	2.0	45.6	0.5	30	Hong, 93 (373)
$Ti_{.8}Zr_{.2}Mn_{1.6}V_{.2}Cr_{.2}$	1.07	1.9	30.5	2	20	Gamo, 79 (35)
$Ti_{.8}Zr_{.2}Mn_{1.7}V_{.2}Mo_{.1}$	1.13	2.0	35	1	14	Gamo, 79 (35)
$Ti_{.8}Zr_{.2}Mn_{1.4}V_{.2}Cr_{.4}$	1.07	1.9	29	9	20	Gamo, 80 (31)
$Ti_{.8}Zr_{.2}Mn_{1.2}V_{.2}Cr_{.6}$	1.07	1.9	30.5	2.2	20	Gamo, 79 (35)
$Ti_{.8}Zr_{.2}Mn_{.8}Cr_{1.0}Fe_{.2}$	0.97	1.8	28	12	20	Gamo, 79 (35)
$Ti_{.6}Zr_{.4}NiV_{.6}Mn_{2+y}Fe_{.2}$ (y = 0-0.4)	0.95	1.6-1.7	--	0.4-3 (S) (slopimg plateaus)	30	Gao, 95 (403)
ZrNiAl	0.18	0.3	--	<0.001	40	Yoshida, 95 (622)
$Zr(B_{1-y}C_y)_2$ (B = Fe, Co; C = V, Cr, Mn; y = 0.25-0.75)	0.97-1.23	1.4-1.8	30-49	0.001-5	50	Shaltiel, 79 (51)
$ZrCo_{1.5}Al_{.5}$	0.63	1.0	--	0.4	20	Jacob, 78 (16)
$Zr(Co_{1-y}Al_y)_2$ (y = 0-1)	0.12-.67	0.2-1.05	--	<0.1-30	20	Jacob, 78 (16)
ZrCoCr	1.07	1.6	40.2	0.7	50	Shaltiel, 77 (14)
ZrCoV	1.23	1.8	49.4	0.0023	50	Shaltiel, 77 (14)
$ZrCo_{1.5}V_{.5}$	1.0	1.5	34.3	1.5	50	Shaltiel, 77 (14)
$ZrCr_2Co_{.8}$	0.66	1.0	45.3	2	100	Drasner, 91 (564)
$ZrCrCo_{.6}V_{.4}$	1.1	1.6	--	1 (S)	180	Bououdina, 96 (585)

Table XIV
Hydride PCT Properties of Multicomponent AB_2 Compounds (continued)

Composition	(H-Capacity)$_{max}$ H/M	wt.%	ΔH, kJ/mol	P= (atm)	at T= (°C)	Author-Yr.
$ZrCr_{.8}Co_{.8}V_{.4}$	1.22	1.8	--	1 (S)	130	Bououdina, 96 (585)
$ZrCr_2Fe_{.8}$	0.79	1.2	46.5	0.8	100	Drasner, 91 (564)
ZrCrFe	1.07	1.6	36	2	51	Yu, 85 (555)
$ZrCr_{1.2}Fe_{.8}$ (+ $Fe_{1.2}$ & $Fe_{1.5}$)	0.95	1.4	50.2	0.75	70	Boulghallat, 93 (375)
$ZrCr_{1-y}Fe_{1+y}$ (y = 0.2-0.5)	0.9-1	1.3-1.5	24-29	0.4-5	30	Lee, 90(378)
$ZrCrFe_{1.6}$	0.75	1.2	29.1	2.5	30	Uchida, 86 (370)
$ZrCr_{1.75}Ge_{.25}$	0.87	1.3	--	<1	200	Drasner, 93 (583)
$ZrCr_{1.2}Ni_{.8}$	1.33	2.0	56.4	0.25 (S)	70	Boulghallat, 93 (375)
$Zr(Cr_{1-y}Ni_y)_2$ (y=0.125-0.5)	1.1-1.2	1.6-1.8	--	<2	23	Drasner, 90 (561)
$ZrCr_2Ni_{.8}$	0.92	1.4	37.9	1	100	Drasner, 91 (564)
$ZrCr_{2-y}Si_y$ (y=0.25-0.5)	0.6-.9	1.0-1.4	--	<1	200	Drasner, 93 (583)
$Zr(Cr_{1-y}V_y)_2$ (y=0.2-0.4)	1.27-1.33	1.9-2.0	--	No plateau		Perevesenzew, 88 (557)
$ZrFe_{1.6}Al_{.4}$	>0.67	>1.0	36	10	24	Fujii, 82 (22)
$ZrFe_{1.5}Al_{.5}$	0.65	1.0	--	0.1	20	Jacob, 78 (16)
$Zr(Fe_{1-y}Al_y)_2$ (y = 0-1)	0.05-.73	0.1-1.1	--	<0.1-25	20	Jacob, 78 (16)
$ZrFe_{1.4}Cr_{.6}$	1.0	1.5	29.9	3	20	Ivey, 84 (29)
$ZrFe_{1.5}Cr_{.5}$	1.03	1.5	25.6	5	20	Ivey, 84 (29)
$Zr(Fe_yCr_{1-y})_2$ (y = 0.45-0.8)	0.84-1	1.2-1.5	--	0.15-3	20	Ivey, 86 (377)
$ZrFe_{1.4}Cr_{.6}$	--	--	--	0.8	23?	Pedziwiatr, 83 (28)
ZrFeCr	1.13	1.7	49.4	0.1	50	Shaltiel, 77 (14)
$ZrFe_{1.5}Cr_{.5}$	0.95	1.4	24.3	5.5	50	Shaltiel, 77 (14)
$ZrFe_{1.4}Cr$	1.12	1.7	21	1	23	Sinha, 85(554)
$ZrFe_{1.5}Cr$	0.97	1.5	23	1.5	23	Sinha, 85 (554)
$Zr(Fe_yCr_{1-y})_2$ (y = 0.5-0.8)	0.97-1.1	1.4-1.6	--	0.1-5	30	Qian, 89 (376)
ZrFeMn	0.93	1.6	31	10	150	Suzuki, 82 (27)
$Zr(Fe_yMn_{1-y})_2$ (y = 0.5-0.8)	0.63-1	0.9-1.5	24-35	0.2-20	40	Suzuki, 83 (30)
$Zr(Fe_yMn_{1-y})_2$ (y = 0.3-0.9)	0.68-1.13	1.0-1.7	6.5-22	2.5-60	100	Shitikov, 84 (552)
$ZrFeMnCr_{.25}$	1.05	1.6	--	0.5	45	Sinha, 85 (554)
$ZrFeMnNi_{.4}$	0.5	0.8	--	5	23	Sinha, 85 (554
ZrFeMo	0.97	1.2	29.8	0.6	30	Semenenko, 80 (638)

Table XIV
Hydride PCT Properties of Multicomponent AB_2 Compounds (continued)

Composition	(H-Capacity)$_{max}$ H/M	(H-Capacity)$_{max}$ wt.%	ΔH, kJ/mol	P= (atm)	at T= (°C)	Author-Yr.
ZrFeV	1.07	1.6	48.1	0.0012	50	Shaltiel, 77 (14)
$ZrFe_{1.5}V_{.5}$	1.07	1.6	32.2	0.25	50	Shaltiel, 77 (14)
$ZrMn_2Co_{.8}$	--	--	20.9	4	23?	Pedziwiatr, 83 (28)
$ZrMn_2Co_{.8}$	0.58	0.9	19.3	3.5	23	Pourarian, 84 (551)
$ZrMn_{1.8}Co_{0.2}$	0.81	1.2	--	6	200	Fujitani, 91 (368)
$ZrMn_{1.6}Co_{.4}$	0.9	1.3	--	3	150	Yonezu, 91 (563)
$ZrMn_{2-y}Co_y$ (y = 0.5-1.0)	1.03-1.13	1.5-1.7	35-44	0.08-1	50	Shaltiel, 77 (14)
$ZrMn_{1.52}Co_{.4}V_{0.08}$	0.8	1.2	--	8	200	Yonezu, 91 (563)
$ZrMn_2Cu_{.8}$	--	--	31.6	0.06	23?	Pedziwiatr, 83 (28)
$ZrMn_2Cu_{.8}$	0.92	1.4	27	0.06	50	Pourarian, 84 (551)
$ZrMn_{1.2}Fe_{0.4}$ (+ ZrMnFe)	1.07	1.5	33	0.4	50	Shaltiel, 77 (14)
$ZrMn_2Fe_{.8}$	0.89	1.4	12.7	0.7 (S)	23	Sinha, 82 (509)
$ZrMn_2Fe_{.8}$	--	--	25	0.5	23?	Pedziwiatr, 83 (28)
$ZrMn_2Fe_{.8}$	0.75	1.2	29.3	2 (S)	30	Uchida, 86 (370)
$ZrMn_{1.8}Fe_{0.2}$	--	1.2	--	8	200	Fujitani, 91 (368)
$ZrMn_2Fe_{1.2}$	0.48	0.7	6.8	3 (S)	25	Sinha, 82 (509)
$ZrMn_{1.53}Fe_{1.27}$	0.68	1.0	9	4	23	Sinha, 83 (23)
$ZrMn_{1.22}Fe_{1.11}$	0.99	1.5	13	1	23	Sinha, 83 (23)
$ZrMn_{1.22}Fe_{1.14}$	0.82	1.2	31	2	40	Uchida, 86 (370)
$ZrMn_{1.11}Fe_{1.22}$	0.99	1.5	13.3	5	100	Sinha, 83 (23)
$ZrMn_{1.11}Fe_{1.22}$	0.84	1.3	29.4	2	30	Uchida, 86 (370)
$ZrMn_{2.6}Fe_{.2}$	0.92	1.4	15	0.12 (S)	100	Pourarian, 82 (512)
$ZrMn_{2.8}Fe_{.4}$	0.76	1.2	23	0.12 (S)	100	Pourarian, 82 (512)
$Zr(Mn_{1-y}Nb_y)_{2.2}$ (y=0-0.2)	1.08-1.18	1.6	--	0.6-3(S)	200	Kodama, 96 (584)
$Zr(Mn_{1-y}Nb_y)_{2.9}$ (y=0-0.2)	0.78-1.05	1.2-1.5	--	5-10 (S)	200	Kodama, 96 (584)
$ZrMn_2Ni_{.8}$	--	--	25	1.6	23?	Pedziwiatr, 83 (28)
$ZrMn_{2.8}Ni_{.4}$	0.83	1.3	--	4 (S)	23	Pourarian, 84(551)
$ZrMn_2Ni_{.8}$	0.84	1.3	18.6	3 (S)	23	Pourarian, 84 (551)
$ZrMn_{1.8}Ni_{0.2}$ (M)	0.74	1.1	--	6	200	Fujitani, 91 (368)
$ZrMn_{1.8}V_{0.2}$	0.87	1.3	--	1	200	Fujitani, 91 (368)
$ZrMn_{2-x}V_x$ (x=0.1-0.2)	0.8	1.2	--	1-2	200	Yonezu, 91 (563)
$Zr_xNi_{1.2}Cr_{.4}Mn_{.4}$ (x = 0.8-1.1)	1-1.15	1.4-1.7	--	1-50	45	Moriwaki, 91 (367)
$Zr(Ni_{.6}V_{.4})_{2.4}$	1.08	1.6	--	No plateau		Gao, 96 (586)

Table XIV
Hydride PCT Properties of Multicomponent AB_2 Compounds (concluded)

Composition	(H-Capacity)$_{max}$ H/M	(H-Capacity)$_{max}$ wt.%	ΔH, kJ/mol	P= (atm)	at T= (°C)	Author-Yr.
$Zr(Ni_{.6}V_{.2}Mn_{.2})_{2.4}$	1.05	1.6	39.9	0.3	30	Gao, 95 (404)
$ZrNi_{1.2}Mn_{.6}Cr_{.2}$	1.0	1.45	--	4.5	70	Moriwaki, 91 (367)
$ZrNi_{1.2}Mn_{.5}Cr_{.2}V_{.1}$	1.08	1.6	--	3	70	Moriwaki, 91 (367)
$Zr_{.8}Ce_{.2}Mn_2$	1.13	1.6	--	0.25	100	Wallace, 83 (528)
$Zr_{.7}Ce_{.3}Mn_2$ (M?)	1.1	1.6	--	0.6	100	Wallace, 83 (528)
$Zr_{.6}Ho_{.4}Co_2$	0.8	1.0	29.3	2	50	Ramesh, 93 (363)
$Zr_{.7}Ti_{.3}CrFe$	1.07	1.7	30	0.8 (S)	23	Yu, 85 (555)
$Zr_{.5}Ti_{.5}CrFe$	1.1	1.8	27	4 (S)	23	Yu, 85 (555)
$Zr_{1-x}Ti_xCr_{.8}Fe_{1.2}$ (y = 0-0.2)	0.9-1.03	1.4-1.55	26-29	0.31.5	30	Lee, 90 (378)
$Zr_{.8}Ti_{.2}Cr_{1.25}Mn$	1.11	1.8	--	0.08	65	Sinha, 85 (554)
$Zr_{1-x}Ti_xNi_{1.1}Mn_{.6}V_{.1}Fe_{.2}$ (x = 0-0.4)	1.0-1.15	1.6-1.7	26-35	1.2-10	30	Morii, 95 (410)
$Zr_{.9}Ti_{.1}Cr_{1-y}Fe_{1+y}$ (y = 0-0.4)	0.93-1	1.4-1.5	24-31	0.2-4	30	Lee, 90 (378)
$Zr_{.8}Ti_{.2}Cr_{1-y}Fe_{1+y}$ (y = 0-0.4)	0.8-.9	1.2-1.4	26-29	0.4-6 (S)	30	Lee, 90 (378)
$Zr_{1-x}Ti_xCr_{1-y}Fe_{1+y}$ (x=0-0.5; y = 0-0.5)	0.9-1.0	1.4-1.6	30-36	0.2-10 (Some sloping plateaus)	30	Park, 90 (560)
$Zr_{.8}Ti_{.2}FeMn_yCr_{1-y}$ (y=0-1)	0.9-.97	1.4-1.5	30-33	0.4-1.6 (Some sloping plateaus)	30	Park, 91 (562)
$Zr_{.8}Ti_{.2}FeMn$	0.9	1.4	30	1.6	30	Park, 91 (562)
$Zr_{1-x}Ti_xFe_{1.5}V_{.5}$ (x=0-0.3)	0.87-1.03	1.4-1.5	--	0.2-1(S)	50	Park, 92 (581)
$Zr_{.6}Ti_{.4}Mn_2$	1.07	1.7	--	0.2	23	Fujii, 81 (18)
$Zr_{.79}Ti_{.21}MnFe_{1.02}$	0.95	1.5	33	1.5	30	Uchida, 86 (370)
$Zr_{.5}Ti_{.5}Mn_{1.2}Fe_{.3}$	1.0	1.6	--	3 (S)	150	Suzuki, 82 (26)
$Zr_{.75}Ti_{.25}Mn_{1.1}Fe_{.9}$	--	--	--	0.9	23?	Pedziwiatr, 83 (28)
$Zr_{.7}Ti_{.3}Mn_2Fe_{.8}$	0.5	0.8	14	2.6 (S)	25	Sinha, 82 (20)
$Zr_{.7}Ti_{.3}MnFe$	1.1	1.7	10	2	23	Sinha, 82 (25)
$Zr_{1-x}Ti_xMnFe$ (x=0-0.3)	0.7-.93	1.1-1.4	28-34	0.4-9	30	Park, 92 (581)
$Zr_{.8}Ti_{.2}Ni_{1.3}Mn_{.7-y}V_y$ (y = 0-0.2)	--	1.62-1.7	31-35	1-4	30	Morii, 95 (410)
$Zr_{.8}Ti_{.2}Ni_{1.1+y}Mn_{.8-y}V_{.1}$ (y = 0-0.32)	--	1.6-1.72	29-37	0.6-7	30	Morii, 95 (410)
$Zr_{.76}Ti_{.24}Ni_{1.16}Mn_{.63}$ - $V_{.14}Fe_{.18}$	--	1.6	29.7	5	30	Morii, 95 (410)
$Zr_{.65}Ti_{.35}Ni_xV_{2-x-y}Mn_y$ (x = 1.0-1.2, y = 0.2-0.4)	0.76-.94	1.2-1.5	36-39	0.05-0.4	40	Yang, 95 (402)

the 1980s and 1990s even to this day. A tabulation of the numerous multicomponent AB_2 alloys and families of alloys developed is given in Table XIV, at least for those materials where some PCT data are available. The parenthetical abbreviation (S) following the plateau pressure P indicates a sloping plateau or plateaux and (M) indicates multiple plateaux. The quantity of data that has been generated is quite impressive and presents a large number of choices. We will compare some of these alloys relative to our PEM fuel cell targets in the next section (3.C.5). However, before doing that some of the results shown in Table XIV must be briefly discussed relative to this reviewer's cautions on certain data.

The first concern centers around the two $Ho_{1-x}Zr_xFe_2$ alloys shown in Table XIV at the bottom of page 57 (Kesavan, 95&96). For example, consider the $Ho_{0.8}Zr_{0.2}Fe_2$ alloy. The P-C isotherms (absorption?) recently published for this alloy are shown in Figure 26 to aid in the

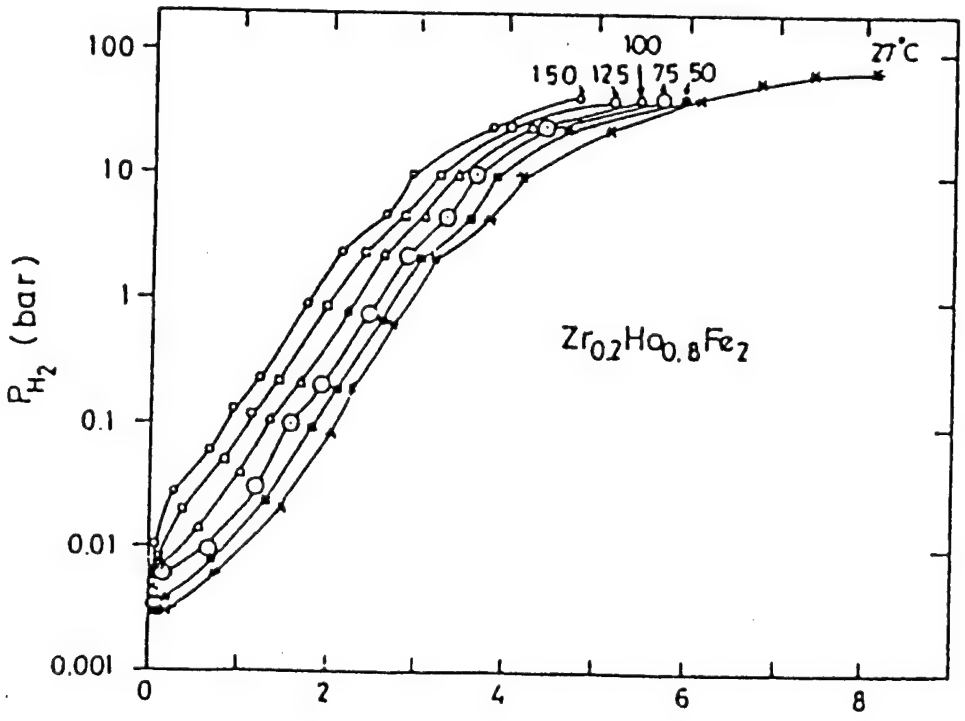

Figure 26
P-C Isotherms of $Ho_{0.8}Zr_{0.2}Fe_2$
(Kesavan, 96)

following discussion. The isotherms show a long sloping solution lines followed by plateaus above about 4.5 n(H)/n(fu). The highest H-content shown at 67 bar and 27°C, namely $Ho_{0.8}Zr_{0.2}Fe_2H_{8.1}$ or H/M=2.7. In fact, the 27°C isotherm shown in Fig.26 was apparently still on the plateau at the maximum test pressure of 70 bar and the implication is that even higher H-contents are possible. As can be seen from Tables XII, XIII and XIV (and also noted by the authors), this is the highest H-content ever seen for an AB_2 intermetallic. It seems unreasonable to me that an alloy of the three elements Ho (max. H/M=3.0), Zr (max. H/M=2) and Fe (Max.

H/M≈0) can form a hydride with nearly 3 H/M average, at least at such modest pressure. However, $DyFe_2$ has been hydrided to 1.4 H/M at 0°C and 13 atm pressure (Kierstead, 80 (356)) and 2.5 H/M at 21°C and 1400 atm (Pourarian, 80 (357)), so the formation of $Ho_{0.8}Zr_{0.2}Fe_2H_{8.1}$ is not inconceivable. The high principal plateau pressure for a rare earth based AB_2 is somewhat unexpected (see Table XII), but again the 70 bar region of Fig.26 is similar in shape to the 1400 atm region for $DyFe_2$ (Pourarian, 80 (357)). In summary, confirmation of the interesting data of Fig.26 is much desired and would give hope for future improvements of interest to H-storage applications. $Ho_{0.8}Zr_{0.2}Fe_2H_{8.1}$ itself would be difficult to apply to fuel cell H_2 storage for three reasons: (1) Much of the useful capacity is outside the 0-100°C, 1-10 atm T-P range of interest; (2) Ho is one of the rarest of the rare earth elements and has no significant metallic use or availability (i.e., would be very expensive, even if there was a large demand); and (3) the rare earth AB_2 compounds generally have a tendency to disproportionate or become quickly amorphous (see Section 3.C.6, p.69). Further R&D on this family of alloys is suggested in Section 3.C.7.

Another area of Table XIV where caution should perhaps be used is a number of B-rich ZrB_{2+} compounds that have unexpectedly low values of ΔH reported (i.e., Sinha, 82 (25, 509), 83 (23); Pourarian 81 (19), 82 (512)), at least compared to similar compositions reported by other investigators. For example, in an attempt to resolve such apparent discrepancies, PCT measurement of $ZrMn_{1.11}Fe_{1.22}$ at Kogakuin University Japan by (Uchida. 86 (370)) gave ΔH=24.9 kJ/molH_2 versus the previously reported value of 13.3 for the same $ZrMn_{1.11}Fe_{1.22}$ by (Sinha, 83 (23)) of the University of Pittsburgh USA (cf. Table XIV, page 61). There seems to be a general feeling among the hydride community that there may have been systematic experimental errors in some of the Pittsburgh data. In any event, caution should be used in accepting the PCT data for these materials and results should be experimentally reconfirmed before using them to design hydride devices.

3.C.5. Comparisons of Commercially-Oriented AB_2 Hydrides

Table XV lists the PCT-related properties of six selected AB_2 hydrides that have been used in commercial applications or have properties or economics of interest to future applications. Most examples are taken from the current Hydride Properties Database (Sandrock, 97). $TiMn_{1.4}V_{0.62}$ is calculated from (Bernauer, 84 (521)). The $TiCr_{1.8}$ data are for the low temperature C15 form of the compound (Johnson, 78 (335). Van't Hoff lines for all six alloys are shown in Figure 27.

Table XV
PCT Properties of Selected AB_2 Hydrides

Composition	ΔH, kJ/mol	ΔS, kJ/molK	25°C P_d, atm	T for 1 atm P_d	Plateau Hysteresis	Plateau Slope
$TiCr_{1.8}$	20.2	0.111	182	-91	0.11	0.12
$Ti_{0.98}Zr_{0.02}V_{0.43}Fe_{0.09}Cr_{0.05}Mn_{1.5}$	27.4	0.112	11	-28	--	1.1
$TiMn_{1.5}$	28.7	0.114	8.4	-21	0.93	0.57
$ZrFe_{1.5}Cr_{0.5}$	25.6	0.097	4.0	-10	0.34	1.26
$TiMn_{1.4}V_{0.62}$	28.6	0.107	3.6	-5	--	1.4
$ZrMn_2$	53.2	0.121	0.001	167	0.99	0.74

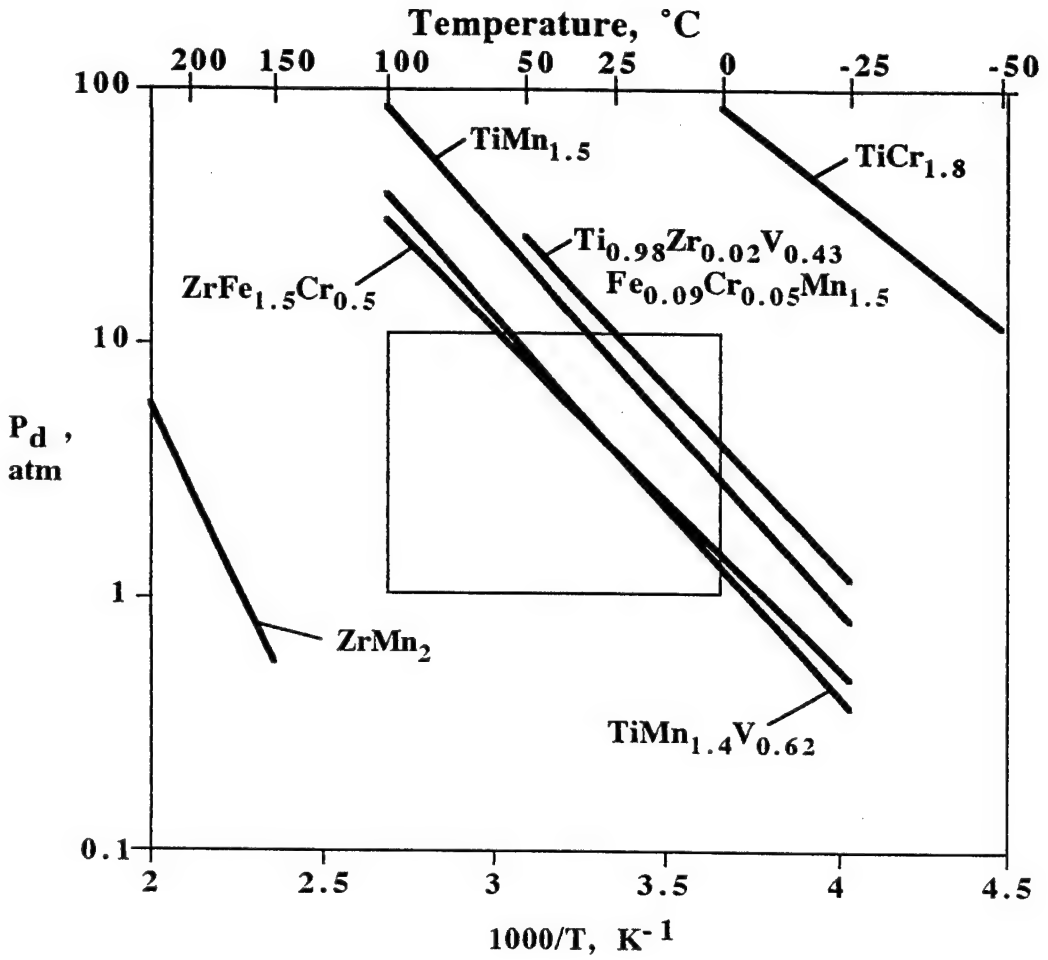

Figure 27
Hydride van't Hoff lines for Selected AB_2 Compounds

The utility of the AB_2 intermetallic family for PEM fuel cells is clear with alloys falling within the 0-100°C, 1-10 atm box superimposed on Fig.27. Other alloys falling outside the desired fuel cell range are also included for interest. For example, $TiCr_{1.8}$ might be useful for very high pressure applications such as a thermal compressor. At the other extreme, $ZrMn_2$ has been used for low partial pressure gettering of contaminant H_2 from closed NH_3 heat pipes (Franco, 86 (337)).

Capacities and alloy raw materials costs for the same six selected alloys are shown in Table XVI. These data were calculated in a similar manner to the AB_5 data (Table X, p.43) and can be directly compared to that data. Although the AB_2 compounds tend generally have higher values of $(\text{H-capacity})_{max}$ than the AB_5s, the values of $(\text{H-capacity})_{rev}$ are similar on a weight basis by our definition of Fig.3. The AB_2s may be slightly lower than the AB_5s in reversible volumetric H-capacities, an important property for submarine application. The AB_2s often suffer from less distinct, narrower plateaux and a residual, essentially non-reversible "heel" compared to AB_5s. All-in-all, a broad comparison of Tables X and XIV (along with the other Tables and Figures) shows the two families are comparable.

Table XVI
Capacity and Cost Properties of Selected AB_2 Hydrides

Composition	Density	$(H\text{-Capacity})_{max}$		$(H\text{-Capacity})_{rev}$			Alloy	RMC**
	g/cm^3	H/M	wt.%	ΔH/M	Δwt,%	$\Delta N_H/V^*$	$/kg	$/g H
$TiCr_{1.8}$	6.0	1.25	2.43	0.45	0.85	2.7	8.64	1.02
$Ti_{0.98}Zr_{0.02}V_{0.43}Fe_{0.09}Cr_{0.05}Mn_{1.5}$	5.8	0.99	1.9	0.7	1.3	3.8	4.82	0.37
$TiMn_{1.5}$	6.4	0.99	1.86	0.65	1.15	3.8	4.99	0.44
$ZrFe_{1.5}Cr_{0.5}$	7.6	1.03	1.5	0.62	0.9	3.3	10.90	1.21
$TiMn_{1.4}V_{0.62}$	5.8	1.14	2.15	0.56	1.1	3.1	29.40	2.67
$ZrMn_2$	7.4	1.2	1.77	0.6	0.9	2.9	11.29	1.25

* Reversible volumetric capacities are approximate and in units of 10^{22} H-atoms/crystal cm^3 (i.e., interparticle void volumes not included)
** RMC = Raw Materials Cost; $/g H based on $(H\text{-Capacity})_{rev}$

The AB_2 alloys do offer a significant advantages over the AB_5s in cost, at least if the A-element is mostly Ti and not Zr. As shown in Table XVI, $Ti_{0.98}Zr_{0.02}V_{0.43}Fe_{0.09}Cr_{0.05}Mn_{1.5}$ and $TiMn_{1.5}$ have have $(H\text{-capacity})_{rev}$-normalized raw materials costs about half those of the best AB_5s (Table X). The higher price of Zr, compared to Ti (Table III), makes $ZrFe_{1.5}Cr_{0.5}$ and $ZrMn_2$ less competitive on a cost basis. To make an important point on the use of V, $TiMn_{1.4}V_{0.62}$ should be compared to $Ti_{0.98}Zr_{0.02}V_{0.43}Fe_{0.09}Cr_{0.05}Mn_{1.5}$. Both alloys are similar in composition (including V-content) and have similar capacities, but $TiMn_{1.4}V_{0.62}$ is 6-7 times the raw materials cost. Why? Pure V is very expensive compared to ferrovanadium, a low-cost product used by the steel industry ($125.40/kg vs. $11.39/kg, Table III, p.20). Therefore, a V-containing alloy should also have some Fe present to allow the use of low-cost ferrovanadium. $TiMn_{1.4}V_{0.62}$ does not have Fe co-present with V and $Ti_{0.98}Zr_{0.02}V_{0.43}Fe_{0.09}Cr_{0.05}Mn_{1.5}$ does, and therein lies all the difference.

Given an examination of the AB_2 properties discussed above in relation to composition, it should not be surprising that $Ti_{0.98}Zr_{0.02}V_{0.43}Fe_{0.09}Cr_{0.05}Mn_{1.5}$, and alloys very similar to it, have led the way to AB_2 commercialization. A short history may be of interest because it likely leads to the hydride storage tanks in the upcoming German PEM fuel cell submarine (Domizlaff, 96), at least in this reviewers opinion. $Ti_{0.98}Zr_{0.02}V_{0.43}Fe_{0.09}Cr_{0.05}Mn_{1.5}$ and closely related AB_2s were originally developed at Daimler Benz (Bernauer, 84 (521)). PCT isotherms for $Ti_{0.98}Zr_{0.02}V_{0.43}Fe_{0.09}Cr_{0.05}Mn_{1.5}$ are shown in Figure 28. Its properties are ideal for ambient temperature H-storage, so it was used as the alloy of choice for a German Government sponsored, multi-vehicle (IC engine) demonstration program in Berlin from 1984-1986 (Bernauer, 87 (610); Feucht, 88 (343)). During this period Daimler Benz and Mannesman formed a joint company called Hydrid Wasserstoff Technologie (HWT) which commercialized hydride alloy and container technology based on $Ti_{0.98}Zr_{0.02}V_{0.43}Fe_{0.09}Cr_{0.05}Mn_{1.5}$ and related alloys. A few years ago HWT was acquired by GfE Gesellschaft für Electrometallurgie which has continued the

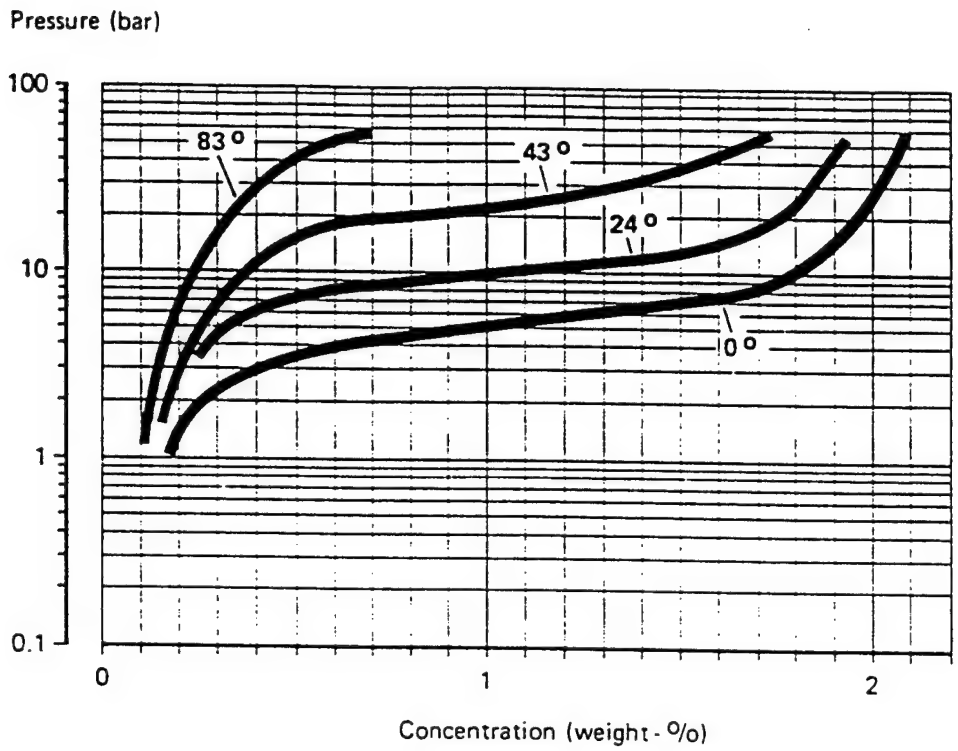

Figure 28
Hydrogen P-C Isotherms for $Ti_{0.98}Zr_{0.02}V_{0.43}Fe_{0.09}Cr_{0.05}Mn_{1.5}$
(Bernauer, 87 (610))

manufacture of AB_2 hydriding alloys (for both battery and gas applications) and hydride containers (Friedrich, 92 (342)). Although the hydride alloy composition for the hydrogen store of the new U-212 Class German submarine has not been announced, GfE is supplying it. Therefore it is reasonable to believe the alloy is $Ti_{0.98}Zr_{0.02}V_{0.43}Fe_{0.09}Cr_{0.05}Mn_{1.5}$ or something similar. The alloy system is low in cost and PCT properties shown in Fig.28 can be easily adjusted to any pressures desired by adjusting the Zr/Ti ratio. GfE offers alloys with various plateau pressures, although specific compositions are usually not specified.

3.C.6. Other Properties

As done for the AB_5 hydrides (Section 3.B.6), a brief summary of non-PCT properties of the AB_2 hydrides is given here.

Activation

As a general rule, most AB_2 intermetallic compounds will activate at room temperature given sufficient H_2 pressure and time, suggesting the air exposed surfaces are not completely passivated. There are certainly exceptions to this general rule, for example high-Al AB_2s (Jacob, 78 (16)), where some heating must be used. It is the author's general experience that alloys high in Ti, Cr and V are somewhat slower to activate than alloys high in Zr, Mn and Ni. With occasional exceptions, most of the ZrB_2 compounds activate at room temperature (Shaltiel, 77 (14)). It always helps to have a freshly crushed sample that has not been stored too long in air. Heating is recommended for activation of some of the commercial GfE alloys. The user will occasionally find AB_2s that do not seem to activate at room temperature. If so, try heating to a few hundred °C under H_2. For AB_2s where the A-element is a rare earth or mixture of rare-earths, activation seems to very rapid at room temperature.

Decrepitation

Like the AB_5 compounds, the AB_2 compounds decrepitate into powder with the first hydrogen absorption. This reviewer's feeling is that the decrepitated powder particle sizes of AB_2s are generally smaller than AB_5s. Although quantitative data is sparse, this seems to have been confirmed by a comparison of $ZrFe_{1.5}Cr_{0.5}$ with $LaNi_5$ (Ivey, 86 (377)). A high level of Mn seems to guarantee an especially fine powder. For example, the well-used commercial alloy $Ti_{0.98}Zr_{0.02}V_{0.43}Fe_{0.09}Cr_{0.05}Mn_{1.5}$ is reported to decrepitate to less than 1 μm in particle size, which can result in packing and container expansion problems if the powder is not properly demobilized (Bernauer, 87 (610)). The finer particle size for AB_2 hydrides may be a result of higher volume changes during hydriding. Although the volume change for AB_2 hydriding averages about the same as AB_5 hydriding per unit H (roughly 25% per 1.0 H/M), the AB_2s tend to reach somewhat higher values of $(\text{H-content})_{max}$, so the overall expansion of a given AB_2 is generally somewhat greater than an AB_5. When cycled 20000 cycles over the relatively low 0.4 wt.% H range, $Ti_{1.2}Cr_{1.9}Mn_{0.1}$ did not show much decrepitation and retained an mean particle size on the order of 100 μm (Lupu, 88).

Intrinsic Kinetics and Heat Transfer

Work with activated AB_2 compounds of practical interest (i.e., $(Ti,Zr)(Mn,Cr,V)_2$) quickly convinces one the intrinsic H/D kinetics are obviously high. For the well-used multicomponent $Ti_{0.98}Zr_{0.02}V_{0.43}Fe_{0.09}Cr_{0.05}Mn_{1.5}$, it has been stated that the intrinsic kinetics are faster than the heat transfer (Bernauer, 89 (344)). Thus the situation for AB_2 hydrides is similar to that of the AB_5s, namely practical charging and discharging rates are dictated by heat transfer and gas impedance properties of the container and internal powder configuration.

Gaseous Impurity Effects

The general feeling in the hydride community is that the AB_2 alloys are somewhat more sensitive to gaseous impurities than the AB_5s. It is hard to be certain on that because there is much less good quantitative data on the AB_2s. Fortunately, some good quantitative data has been developed for the important commercial alloy $Ti_{0.98}Zr_{0.02}V_{0.43}Fe_{0.09}Cr_{0.05}Mn_{1.5}$. These data are

Table XVII
Gas Impurity and Reactivation Effects for
$Ti_{0.98}Zr_{0.02}V_{0.43}Fe_{0.09}Cr_{0.05}Mn_{1.5}$ (Bernauer, 89 (344))

Impurity (50 ppm)	Residual H-Capacity*(loss) after 100 cycles, wt.%	Reactivation without heating	
		Cycles	Capacity
CO	0.85 (-54%)	10	1.8
CO_2	1.35 (-27%)	100	1.65
O_2	1.65 (-11%)	90	1.8

* Initial capacity 1.85 wt.% H

shown in Table XVIII. Significant losses in capacity were seen at 50 ppm CO, CO_2 or O_2, in order of decreasing severity. The effect of CO is probably comparable to $LaNi_5$ (cf. Fig.20,

p.46). However, if we compare the O_2 data of Table XVII with $LaNi_5$ (Goodell, 83 (8)), we would conclude $LaNi_5$ is much more tolerant to O_2 than $Ti_{0.98}Zr_{0.02}V_{0.43}Fe_{0.09}Cr_{0.05}Mn_{1.5}$. It would take at least 300 ppm O_2 to cause an 11% loss in $LaNi_5$ capacity in 100 cycles. In any event, Table XVII shows $Ti_{0.98}Zr_{0.02}V_{0.43}Fe_{0.09}Cr_{0.05}Mn_{1.5}$ can be reactivated to nearly full capacity after impurity damage by cycling in pure H_2. Although CO-contaminated AB_5 alloys can be fully reactivated, O_2-contaminated AB_5s cannot be recovered in the same manner as AB_2s. This ability of AB_2s to recover capacity has also been noted with $TiMn_{1.25}Cr_{0.25}$ (Hong, 91 (365). Although an H-capacity loss of 40% resulted from 20 cycles in H_2-650 ppm O_2, all but about 3% could be recovered by 300°C reactivation. In summary, and assuming some generalizations, the AB_2s seem to be more sensitive to O_2 than the AB_5s. O_2 behaves more like a poison to AB_2s (as opposed to a reactant to AB_5s) so recovery is possible. It can be assumed H_2O vapor has similar effects to O_2. Finally, the AB_2s seem to have significant immunity to N_2 and CH_4 (Bernauer, 89 (344)), as do the AB_5s.

Cyclic Stability

As indicated in Table XI, it has long been known that the AB_2 intermetallics containing A-elements that are rare earths (R) tend to disproportionate or become amorphous on hydriding (Beck, 62 (45); Oesterreicher, 76 (524); Cohen, 78; Shilov, 81 (530); among others). This can occur even at room temperature or below. $CeNi_2$ becomes amorphous even when it is hydrided at -76°C (Kim, 91). Some RB_2s show some stability at room temperature but begin to disproportionate at modestly elevated temperature, e.g., $ErFe_2$ (Flanagan, 87 (358), Ahn, 93). The instability of the RB_2 compounds is not surprising, give the fact they generally solidify by a relatively low-temperature peritectic reaction (cf. Fig.22), an indication of weak bonding between the A and B atoms within the intermetallic compound itself. This, combined with the fact the RB_2 hydrides have generally low dissociation pressure (cf. Table XII), lends doubt to their practical potential. Hopefully, exceptions can be found, for example with $Zr_{0.2}Ho_{0.8}Fe_2$ discussed earlier for its high reported H-capacity (Kesavan, 96). It seems to be stable enough to obtain isotherms over the 27-150°C range (Fig.26), but its longer-term cyclic stability has needs to be determined.

The AB_2s of more commercial interest, i.e., based on $(Ti,Zr)(Mn,Cr,X)_2$, fortunately have much better stability than the RB_2 phases. Unfortunately there is less quantitative data for the AB_2s than the AB_5s, but we do know $Ti_{0.98}Zr_{0.02}V_{0.43}Fe_{0.09}Cr_{0.05}Mn_{1.5}$ loses less than 5% of its capacity to disproportionation during 2000 A/D cycles with high purity H_2 (1-50 atm, 20-80°C) (Bernauer, 89 (344)). The H/D cycling of $Ti_{1.2}Cr_{1.9}Mn_{0.1}$ for 20000 times (50-60 atm, 20-60°C) resulted in a disproportionation capacity reduction of about 25%, virtually all of which could be regained by a 380°C reproportionation treatment under vacuum (Lupu, 88). In summary, the practical AB_2s seem to have adequate cyclic stability for storage applications.

Safety

The AB_2 compounds exhibit pyrophoric behavior, the degree of which is dependent on the composition. Alloys that are high in Zr and Mn are much more pyrophoric than those high in Ti and Cr. $ZrMn_2$, for example, decrepitates into a fine powder that is instantly pyrophoric when exposed to air. As far as I can see, it cannot be passivated without resorting to S-containing gases such as SO_2. Again this is a problem only in a container rupture situation. There is a general absence of quantitative safety data on the AB_2s. Most of the practical AB_2 compounds do not contain toxic metals. However, the usual precautions with handling metal powder should be

taken, including adherence to the manufacturer's MSDS (cf. AB_5 safety discussion on p.48).

Metallurgy, Manufacturing and Recycling

There are important differences in the metallurgy of AB_2 compounds vs. AB_5 compounds. Although the AB_5s tend to be line compounds (Fig.22) the AB_2s of practical interest tend to have a finite single-phase homogeneity range. For example, the Zr-Mn phase diagram of Figure 29 clearly shows the wide homogeneity range. This has advantages and disadvantages. The advantage,

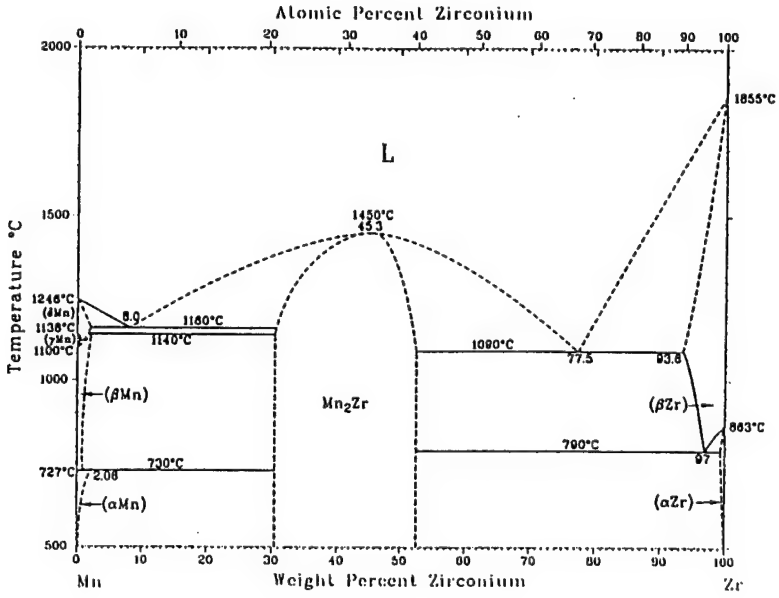

Figure 29
The Zr-Mn Phase Diagram
(Lasocka, 90)

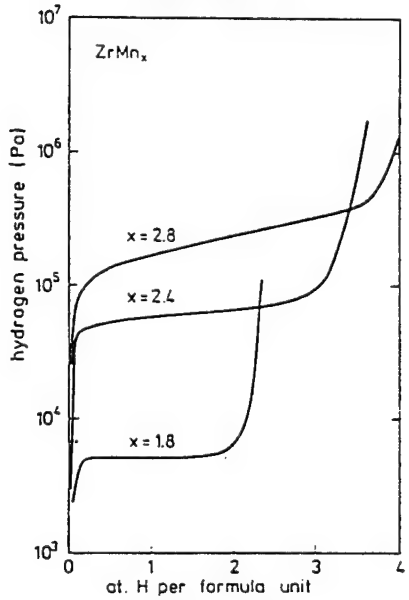

Figure 30
Effect of Mn-Content x on the 50°C Absorption Isotherm of $ZrMn_x$ (van Essen, 80 (17))

shown in Figure 30, is that the PCT properties can be manipulated by adjusting the stoichiometry in the phase field (i.e., B:A ratio). Conversely, small errors in melting can cause significant variations in PCT properties, particularly undesirable for those applications that require precision.

The commercial production of AB_2 compounds is more difficult than AB_5 compounds and requires great metallurgical care. Because of the high melting points of the principal elements (Ti = 1670°C; Zr = 1855°C; Cr = 1863°C), along with their high reactivities, it is very difficult to use standard vacuum induction melting (VIM) in a conventional oxide crucible. If the AB_2 has a high level of relatively low-melting Mn (1246°C), then a two-step VIM procedure can be used, but only with the use of last-minute mischmetal deoxidation to reduce the O-contamination from the crucible (Percheron-Guégan, 88). I have successfully induction-melted $ZrMn_2$ (melting temperature 1450°C) under argon in Al_2O_3 crucibles. However, the typical $(Ti,Zr)(Mn,Cr,X)_2$ commercial alloys should be melted by the vacuum-arc or argon-arc skull technique using a cold copper crucible that minimizes contamination (Friedrich, 92 (342)). Because the multicomponent alloys can form either the C14 or C15 structures a rapid quench after solidification may be needed to achieve the C14 structure, if desired. Mn has a high vapor pressure and corrections must be made for evaporation during melting. As mentioned earlier (p.66), if V is present then Fe should also be present so that cheap ferrovanadium can be used. GfE and Japan Metals and Chemicals, principal AB_2 manufactures, make their own ferrovanadium by aluminothermic reduction of vanadium oxide (Friedrich, 92 (342)). At least for gas applications, the final AB_2 product should generally be as close as possible to single phase microstructure to maximize reversible H-capacity. Minor second phases are inevitable in commercial melting practice (Bernauer, 87 (610)). Annealing is often used to reduce plateau slope and reduce the content of undesired second phases. In summary, although the production of practical AB_2 alloys is difficult, it has been done in tonnage quantities as witnessed by the successful Berlin vehicle demonstration (Bernauer, 87 (610); Feucht, 88 (343)) and the present German submarine program (Domizlaff, 96).

Recycling procedures have been established for an AB_2-containing multiphase alloy used for some NiMH batteries (Lyman, 94). These procedures should be applicable to any practical AB_2. In general, the commercial AB_2 family is free of critical or strategic metals, although Mn may be considered somewhat strategic because of its foreign origins.

3.C.7 Summary and Suggested R&D

Like the AB_5s, the AB_2 family of intermetallic hydrides is large and very versatile. The PCT properties are ideal for PEM fuel cell applications and can be fine tuned to the precise desired properties. Volumetric H-contents are not quite as good as the AB_5s, but gravimetric H-densities are up to 1.3 wt.% on a reversible (plateau width) basis and potentially better than the AB_5s given an appropriate thermal and pressure cycle. In general, impurity resistance of the AB_2s appears to be not quite as good as the AB_5s, although there is scant data. Resistance to disproportionation seems to be good for the practical $(Ti,Zr)(Mn,Cr,X)_2$ family, but poor for the RB_2 family, where R = rare earth elements. AB_2 alloys are made commercially in large quantities. No critical strategic elements are really needed, save perhaps for Mn. The AB_2s are considerably less expensive than the AB5s. They are safe to use, but are generally pyrophoric when suddenly exposed to air. Although extensively researched in the past, AB_2 intermetallics still have the potential for significant further improvement in the H-capacity area, which is probably not so certain for the AB_5 family of hydriding compounds.

There are a few areas of AB_2 R&D this reviewer would suggest, especially relative to the application of such alloys as H_2 storage media for PEM fuel cells. In some ways, these areas are parallel to those I gave for the AB_5s (p.49):

1. The reported hydride properties of $Ho_{0.8}Zr_{0.2}Fe_2$ (Kesavan, 96) must be independently confirmed. The unexpectedly high H-capacity reported, $Ho_{0.8}Zr_{0.2}Fe_2H_{8.1}$, gives hope for the practical development of AB_2s with much higher capacity. However, assuming confirmation of the high H-capacity with $Ho_{0.8}Zr_{0.2}Fe_2$ and closely related alloys, this reviewer feels practicality cannot be achieved with the truly rare element Ho. Ho represents only 1.2 ppm of the earth's crust whereas the components of mischmetal (Ce, La, Nd, Pr) represent 126 ppm (Kilbourn, 93) and its present price is on the order of $1800/kg. Therefore R&D should be directed toward substituting low-cost Mm for the extremely expensive Ho. This will probably require significant composition changes and other multicomponent substitutions. Because all prior information on RB_2 intermetallics suggests $Ho_{0.8}Zr_{0.2}Fe_2$ will probably be susceptible to disproportionation or amorphization with H/D cycling, the substitutions used must also stabilize the intermetallic structure against those deleterious effects.

2. The Laves phases $TiFe_2$ and $ZrFe_2$ do not hydride to any significant capacity. If they did, they would represent low cost hydrogen storage materials. Work is needed to determine why these AB_2s do not absorb H_2 and how they can be made to with minor substitutions.

3. Because of its importance to PEM fuel cell performance, a full understanding of the ability of AB_2s to getter CO must be developed, along with methods of regeneration.

4. The impurity effects of O_2 and especially H_2O should be better quantified for the AB_2 compounds. Good quantitative data is scarce. If there is success with Recommendation 1, then impurity data should be generated for the RB_2 intermetallics.

5. Quantitative safety data should be generated, especially on the Mn-containing AB_2 alloys.

3.D. AB Intermetallic Hydrides

The third group of intermetallic compounds of possible interest to ambient temperature fuel cell applications is the AB family. Most of the practical AB compounds are based on TiFe and therefore represent low raw materials costs. They are historically important to the early development of ambient temperature hydrides and their application to the first H_2-fueled vehicles. Because of technical problems to be reviewed below, AB hydriding compounds have not survived the test of time and are now seldom used. However, it will be argued that the relatively low cost of AB alloys justified their reconsideration for large-scale H_2 storage, such as for submarines.

3.D.1. Crystal Structure

There are a number of AB structures (e.g., the common B_f CrB-type structure), but most of the practical hydriding compounds are of the relatively simple B2 structure shown in Figure 31. It is essentially a body-centered-cubic cell with one formula unit per unit cell. One A-atom is shared by the cell corners and one B-atom resides at the center of the cubic cell. Each cell contains 12 tetrahedral and 6 octahedral interstices. Only the octahedral sites become occupied with H-atoms with strong preference to those that have $[Ti_4Fe_2]$ co-ordination (Reilly, 80; Yvon, 88 (320)). At

high H/M some [Ti_2Fe_4] octahedral sites may possibly also fill.

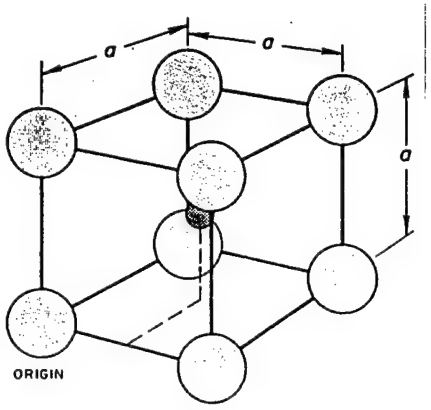

Strukturbericht = B2
Prototype = CsCl
Pearson = cP2
Space Group = Pm-3m

Figure 31
The B2 AB Crystal Structure
(Barrett, 73)

3.D.2. Historical Background of the AB Hydrides

The first detailed PCT data for an intermetallic hydride was published in 1958, by which it was clearly demonstrated that the AB compound ZrNi (orthorhombic B_f structure) could be easily and reversibly hydrided to form a true reversible intermetallic hydride ($ZrNiH_3$) that had a thermodynamic stability that was intermediate between the very stable ZrH_2 and very unstable NiH elemental hydrides (Libowitz, 58 (68)). Figure 32 reproduces the original $ZrNiH_3$ isotherms which may be compared with the van't Hoff lines of Fig.8. ZrH_2 requires about 900°C to achieve

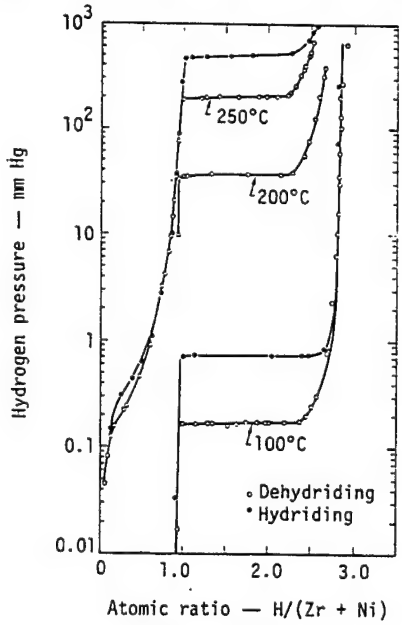

Figure 32
ZrNi-H Isotherms
(Libowitz, 58 (68))

a desorption plateau pressure of 1 atmosphere and NiH exhibits a 25°C plateau of more than 3000 atm. Yet the intermetallic hydride $ZrNiH_3$ exhibits its main desorption plateau at 1 atm around 300°C, a rather profound "interpolation" between a very stable and a very unstable hydride. Although the major significance of this discovery was not fully appreciated for another decade, the stage had been set for the liberation of hydride technology from the very limited and restrictive domain of the elemental hydrides. This discovery went largely unappreciated, probably because the 300°C temperature required for H_2 desorption was too high for most practical use. The practical AB was still a decade away in 1958.

The first really practical room temperature AB hydride was TiFe, discovered at Brookhaven National Lab in the U.S. around 1969 (Hoffman, 69; Reilly, 74 (319)). An absorption/desorption hysteresis loop (40°C) for TiFe is shown in Figure 33. Two distinct hydrides (TiFeH and $TiFeH_{1.95}$) resulting in two separate plateaus. Unlike ZrNi, dissociation pressures are very convenient, a few atmospheres at 40°C. Hysteresis is significant, on the order of 0.6.

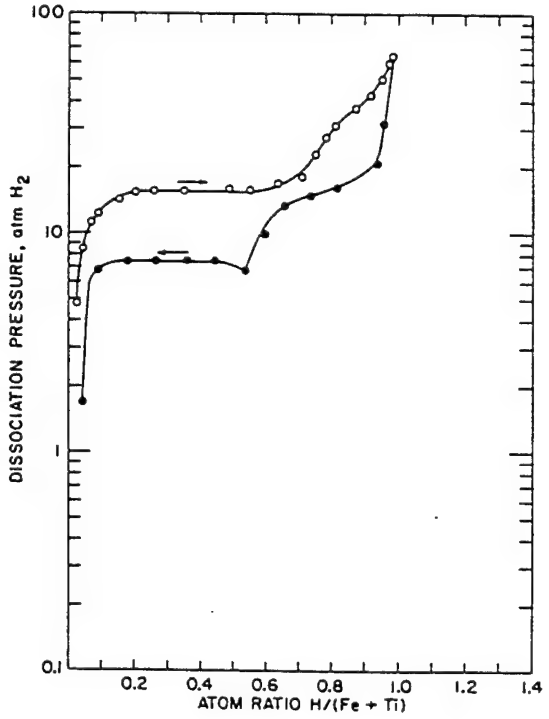

Figure 33
40°C Hysteresis Loop for TiFe-H
(Reilly, 74 (319))

3.D.3 Binary AB Hydriding Compounds

A large number of AB intermetallics form hydrides (Sandrock, 97), but only a fraction of those have reported PCT data. Those AB compounds where at least some PCT data are available are listed in Table XVIII. Note there is a general absence of ABs where A is a rare earth element. Although RB intermetallics are common, they tend to disproportionate when hydrided (Beck, 62 (45)). The van't Hoff lines for selected AB hydrides are shown in Figure 34. These three alloys

Table XVIII
Hydride PCT Properties of Binary AB Compounds

Composition	(H-Capacity)$_{max}$ H/M	wt.%	ΔH, kJ/mol	P= (atm)	at T= (°C)	Author-Yr.
ErAg	0.47	0.3	35.2	0.01	790	Philipp, 91 (384)
HfAl	0.5	0.5	--	1	50	van Essen, 79 (386)
HfCo	1.6	1.3	59 (calc)	0.001	50	van Essen, 79 (386)
HfCo	1.5	1.3	43 (cal)	1	270	Nemirovskaya, 91 (606)
HfNi (M)	1.6	1.3	50 (calc)	0.02	50	van Essen, 79 (386)
HfNi (M)	1.5	1.3	40 (cal)	1	190	Nemirovskaya, 91 (606)
$Li_{.94}Pd$	0.5	0.9	69.2	0.02	300	Sakamoto, 95 (411)
ThCo	2.0	1.4	46.8	<0.05	40	Buschow, 75 (187)
ThNi	1.8	1.2	45.3	0.01	40	Buschow, 75 (187)
TiCo	0.76	1.4	57.4	4	155	Yamanaka, 75 (73)
TiCo (M)	0.72	0.7	--	5.2	116	Reilly, 76 (490)
TiCo	0.58	1.1	61.1	2.2	150	Someno, 79 (381)
TiCo (M)	0.78	1.45	54	2	152	Burch, 79 (500)
TiCo	0.7	1.3	57.8	2.2	150	Osumi, 80 (80)
TiCu (M)	0.88 (Dp)	1.6	126	0.15	500	Kadel, 78 (523)
TiCu	0.97 (Dp)	1.7	75	0.004	200	Maeland, 78 (389)
TiCu	0.7 (Dp)	1.3	--	0.2	500	Someno, 79 (381)
TiCu	0.31 (Dp)	0.6	--	0.19	500	Arita, 79 (495)
TiFe (M)	0.98	1.9	28.1	5.2	30	Reilly, 74 (319)
TiFe (M)	0.9	1.7	26.7	11	51	Yamanaka, 75 (73)
TiFe (1 wt.% Mm)	0.9	1.7	--	7	40	Sandrock, 78 (321)
TiFe (+4.5 w/o Mm)	0.85	1.6	--	3	27	Bronca, 85 (549)
TiNi	0.7	1.3	--	Sloping plateau 1	200	Yamanaka, 75 (73)
TiNi	0.77	1.4	58-60	Sloping plateau No plateau		Burch, 79 (500)
TiNi	0.7	1.3	--	1	200	Hata, 80 (74)
UCo	0.9	0.6	55	Sloping plateau 0.08	150	Yamamoto, 91 (398)
ZrAg (M)	0.5	0.5	--	$<10^{-3}$	280	Deschanvres, 64(497)
ZrCo	1.11	0.7	--	0.4	365	Reilly, 66 (489)
ZrCo (M)	1.22	1.6	67	0.013	200	Irvine, 78 (70)
ZrCo	0.87	1.2	90	0.05	252	Devillers, 89 (399)
ZrCo	1.5	2.0	66 (cal)	1	430	Nemirovskaya, 91 (606)
ZrNi (M)	1.4	1.8	76.8	0.26	250	Libowitz, 58 (68)
ZrNi (M)	0.9 Lower plateau	--	47.5	0.005 Sloping plateau	300	Luo, 90 (550)
ZrNi (M)	1.5	2.0	64 (cal)	1	300	Nemirovskaya, 91 (606)
ZrNi (M)	1.28	1.7	40.1	0.2	250	Cantrell, 95 (409)

(M) = Multiple plateau
(Dp) = Disproportionates
(cal) = Calorimetric determination of ΔH
(calc) = Calculated (non-van't Hoff) value of ΔH

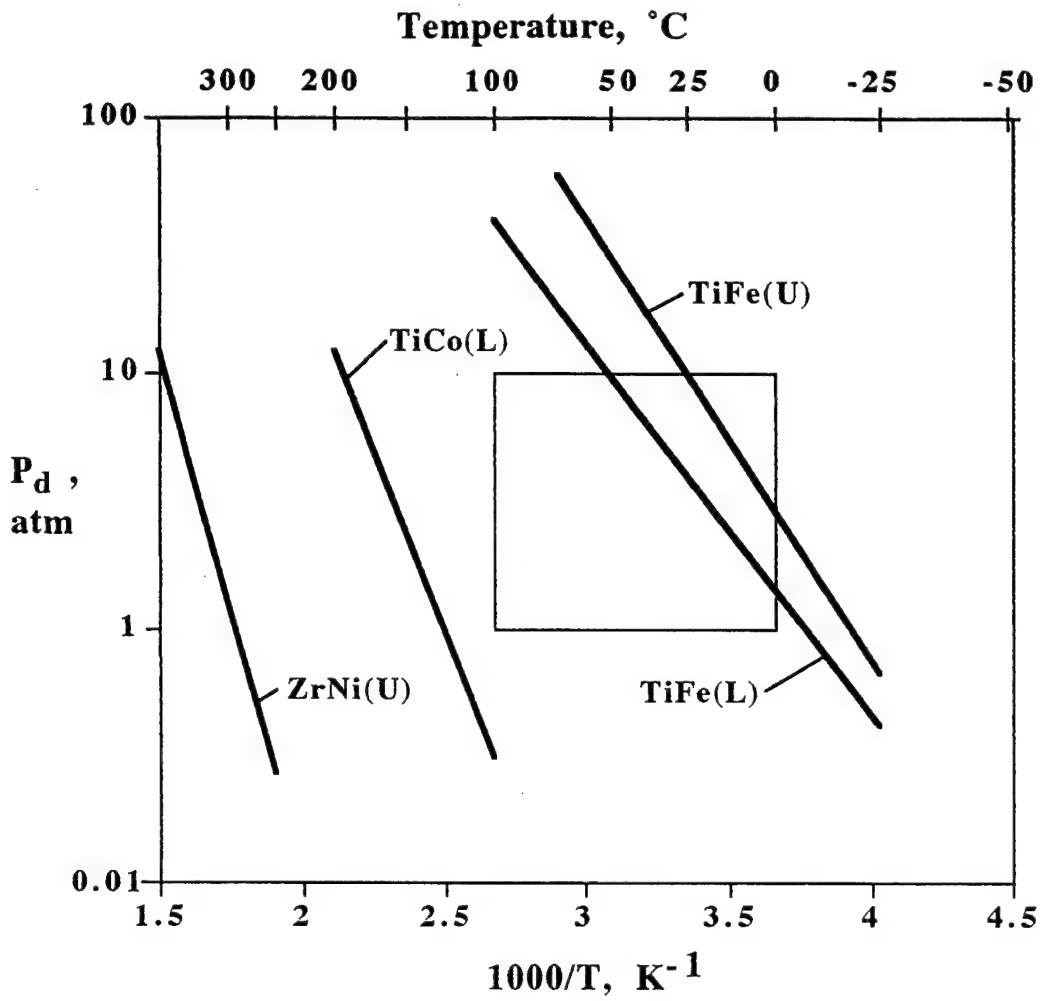

Figure 34
Hydride van't Hoff Lines for Selected Binary AB Compounds
Sources: ZrNi=(Libowitz, 58 (68)); TiCo=(Burch, 79 (500)); TiFe=(Reilly, 74 (319))

represent materials with significant PCT data and have been of interest for applications over the years. All three exhibit multiple plateaux, two for ZrNi and TiFe and three for TiCo. In Fig.34 (L) denotes the lower plateau and (U) denotes the upper plateau. Van't Hoff lines for both plateaux are shown for TiFe.

3.D.4 Multicomponent Substituted AB Hydriding Compounds

It is evident from Table XVIII and Fig.34 that most of the binary AB hydrides are rather stable and have desorption temperatures that fall outside the 1-10 atm, 0-100°C range we have used as a criterion for useful PEM fuel cell parameters (i.e., the superimposed box in Fig.34). The one exception is TiFe which has has the appropriate P-T properties. It is also convenient that TiFe consists of two elements that are relatively low in cost and are widely available. This was recognized early in reversible hydride history and spurred a number of prototype applications that used TiFe and related alloys (Sandrock, 92 (322)). It also stimulated a number of research efforts to modifying TiFe with ternary and higher order substitutions. (Ti,X)(Fe,Y) alloys and families of

Table XIX
Summary of Substituted $Ti_{1-x}A_xFe_{1-y}B_y$ Hydrides

Composition	(H-Capacity)$_{max}$ H/M	wt.%	ΔH, kJ/mol	P= (atm)	at T= (°C)	Author-Yr.
TiFe (M)	0.98	1.9	28.1	5.2	30	Reilly, 74 (319)
TiFe (M)	0.9	1.7	26.7	11	51	Yamanaka, 75 (73)
$TiFe_{1-y}Al_y$ (y=0.04-0.1)	0.65-.7	1.3-1.4	--	4-7 (Sloping plateau)	40	Sandrock, 78 (321)
$TiFe_{.76}Al_{.24}$	0.53	1.1	--	No plateau		Sandrock, 78 (321)
$TiFe_{.9}Al_{.1}$	0.65	1.3	30	1.2	25	Bruzzone, 81 (422)
$TiFe_{.94}Al_{.06}$	0.6	1.2	--	5 (Sloping plateau)	30	Lim, 1984 (548)
$TiFe_{1-y}Al_y$ (y=0.02-0.1)	0.55-.59	1.1	21-29	3-8	30	Lim, 1984 (547)
$TiFe_{.8}Be_{.2}$	0.67	1.4	30.5	0.7	21	Bruzzone, 80 (421)
$TiFe_{.9}Co_{.1}$	0.94	1.8	--	3.3	40	Reilly, 76 (383)
$TiCo_{.5}Fe_{.5}$	0.6	1.1	42.3	4 (Sloping plateau)	100	Suzuki, 81 (82)
$TiFe_{.5}Co_{.5}$	0.58 (Lower plateau only)	1.1	41.4	12	150	Someno, 79 (381)
$TiFe_{1-y}Co_y$ (y = 0.25-0.75)	0.52-0.58 (Lower plateau only)	1.0-1.1	31-47	4-30	150	Someno, 79 (381)
$TiFe_{1-y}Co_y$ (M?) (y = 0.1-0.2)	--	--	31-33	0.9-1.6	25	Mintz, 81 (390)
$TiFe_{1-y}Cr_y$ (M) (y = 0.1-0.2)	--	--	30-36	0.2-1	25	Mintz, 81 (390)
$TiFe_{.95}Cr_{.05}$ (M)	0.90	1.7	--	4	40	Reilly, 76 (383)
$TiFe_{.9}Cr_{.1}$ (M)	0.88	1.7	--	1.6	40	Reilly, 76 (383)
$TiFe_{.9}Cr_{.1}$	0.58 (Lower plateau only)	1.1	30.5	20 (Sloping plateau)	150	Someno, 79 (381)
$TiFe_{.8}Cr_{.2}$ (M)	.95	1.8	--	0.4	40	Reilly, 76 (490)
$TiFe_{1-y}Cr_y$ (M) (y = 0.05-0.1)	0.83	1.6	--	2-5 (Sloping plateaux)	50	Lee, 94 (391)
$TiFe_{.9}Cu_{.1}$	0.62	1.2	--	2.3 (Sloping plateaux)	40	Reilly, 76 (383)
$Ti_{1-x}Cu_xFe$ (x = 0.02-0.1; + 0.5%Fe_2O_3)	0.4-.65	0.8-1.2	--	0.8-3 (Sloping plateau)	30	Nagai, 86 (392)
TiFe (1 w/o Mm)	0.9	1.7	--	7	40	Sandrock, 78 (321)
TiFe (+4.5 w/o Mm)	0.85	1.6	--	3 (Sloping plateau)	27	Bronca, 85 (549)
$TiFe_{1-y}Mn_y$ (y = 0.1-0.3)	0.92-0.98	1.8-1.9	--	1-6	40	Johnson, 77 (393)
$TiFe_{.9}Mn_{.1}$ (M)	1.0	1.9	29.5	2.6	25	Johnson, 78 (330)

Table XIX
Summary of Substituted $Ti_{1-x}A_xFe_{1-y}B_y$ Hydrides

Composition	(H-Capacity)$_{max}$ H/M	wt.%	ΔH, kJ/mol	P= (atm)	at T= (°C)	Author-Yr.
$TiFe_{.9}Mn_{.1}$	0.6	1.2	27.2	30	100	Someno, 79 (381)
	(Lower plateau only)					
$TiFe_{.7}Mn_{.2}$	1.0	2.0	34.7	1.4	40	Reilly, 76 (383)
				(Sloping plateau)		
$TiFe_{.7}Mn_{.3}$	0.83	1.6	--	1.3	40	Sandrock, 76 (76)
				(Sloping plateau)		
$TiFe_{.95}Mn_{.05}$ (M)	0.8	1.6	29.3	9	50	Mintz, 81 (390)
$TiFe_{1-y}Mn_y$ (M)	--	--	28-32	0.8-3.4	25	Mintz, 81 (390
(y = 0.05-0.2)						
$TiFe_{1-y}Mn_y$ (M)	0.9-.98	1.7-1.9	--	4-6	50	Lee, 94 (391)
(y = 0.1-0.2)						
$TiFe_{1-y}Mn_y$	0.84-.92	1.6-1.8	--	0.5-2	27	Mitrokhin, 93 (593)
(y=0.1-0.3)				(Sloping plateaux)		
$TiFe_{.9}Mo_{.1}$	0.93	1.7	--	3	40	Reilly, 76 (383)
				(Sloping plateau)		
$TiFe_{.96}Nb_{.04}$	0.92	1.7	--	4	40	Sasaki, 81 (394)
				(Sloping plateau)		
$TiFe_{.9}Ni_{.1}$	0.85	1.6	--	0.9	40	Reilly, 72 (195)
$TiFe_{.8}Ni_{.2}$	0.7	1.3	41.2	0.33	50	Huston, 80 (77)
$TiFe_{1-y}Ni_y$	--	--	35-45	0.005-.6	25	Mintz, 81 (390)
(y = 0.1-0.5)						
$TiFe_{.8}Ni_{.2}$	0.5	1.0	41.9	0.28	50	Mintz, 81 (390)
$TiFe_{.8}Ni_{.2}$	0.63	1.2	--	9	150	Oguro, 83 (78)
$TiFe_{1-y}Ni_y$	--	--	49-54	--	--	Bershadsky, 93 (395)
$TiFe_{.6}Ni_{.4}$	0.77	1.5	48.6	0.035	50	Bershadsky, 93 (395)
$TiFe_{.8}Ni_{.15}Nb_{.05}$	0.56	1.1	--	7	150	Oguro, 83 (78)
$TiFe_{.8}Ni_{.15}V_{.05}$	0.68	1.3	41	7	150	Oguro, 83 (78)
$TiFe_{1-y}Si_y$	0.65-.88	1.3-1.7	--	2-3.5	40	Sandrock, 78 (321)
(y=0.02-0.1)						
$TiFe_{.95}V_{.05}$ (M)	0.97	1.7	--	5	40	Reilly, 76 (383)
				(Sloping plateau)		
$Ti_{.46}Fe_{.45}V_{.05}Mn_{.05}$	0.9	1.7	28.6	2	22	Mitrokhin, 93 (396)
$Ti_{1-x}Nb_xFe$	0.56-.66	1.0-1.2	--	2.5-4	30	Nagai, 86 (392)
(x = 0.04-0.12; + 1.0% Fe_2O_3)						
$Ti_{1-x}V_xFe_{1-y}Mn_y$	0.8-.93	1.5-1.8	--	--	--	Liu, 82 (499)
(x=0.01-0.04, y=0-0.2)						
$Ti_{1-x}Zr_xFe$	0.56-.9	1.0-1.7	--	3-7	30	Jang, 86 (397)
(x = 0-0.2)						
$Ti_{.9}Zr_{.1}Fe$	0.56	1.0	28.9	3.3	30	Jang, 86 (397)
$Ti_{.96}Zr_{.04}Fe_{.95}Nb_{.04}$	0.9	1.7	31.8	1.4	30	Sasai, 83 (79)

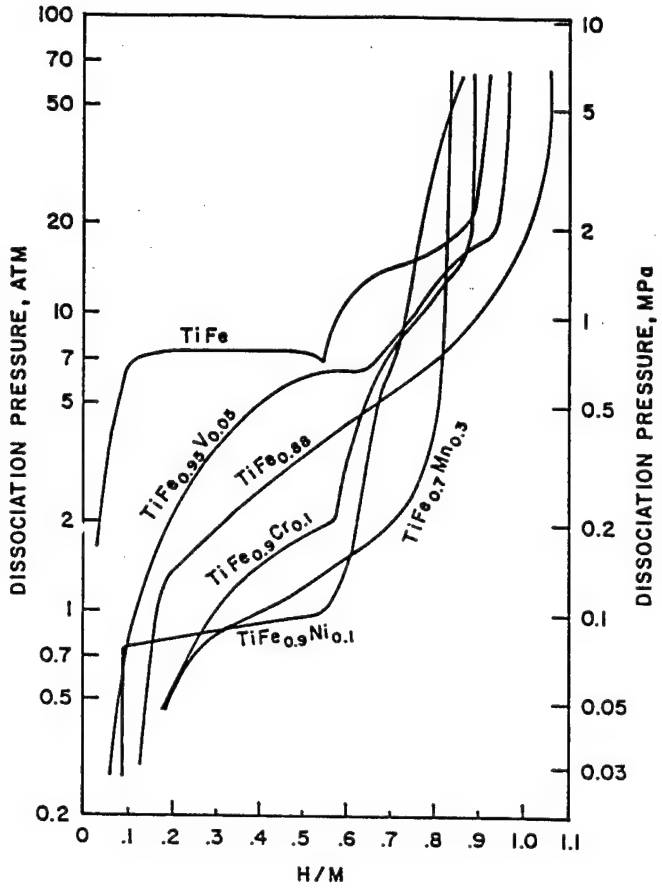

Figure 35
Desorption Isotherms (40°C) for Partially Substituted AB Compounds
(Sandrock, 76 (76))

alloys are summarized from those works in Table XIX. Isotherms for selected alloys with partial ternary substitutions for Fe are compared to binary TiFe in Figure 35. Both Table XIX and Fig.35 indicate that most substitutions lower the plateau pressures (increase |ΔH|) and result in sloping plateaux. Generally substitutions tend to lower capacity, but not always. In the case of Ni-substitution ($TiFe_{0.8}Ni_{0.2}$ in Fig.35), the lower plateau is substantially reduced in pressure and the upper plateau is increased beyond accessibility, so effectively there is a significant loss of usable capacity. It may be noticed that the $(H/M)_{max}$ for the binary TiFe is lower in Fig.35 than the highest values shown for that compound in Tables XVIII and XIX. That is because the sample used for Fig.35 was made by commercial melting techniques which leads to lower H-capacities than high purity samples (see discussion in Section 3.D.6, p.79). In summary, like the other intermetallics we have reviewed earlier, the PCT properties TiFe can be widely tailored by partial substitutions.

Although it is almost entirely the TiFe-type intermetallic hydrides that are of practical interest for H_2 storage under ambient conditions, it is useful to note that ZrNi also has uses in other pressure and temperature realms. Because it has low pressure PCT properties (cf. Figs. 32&34), it has been used successfully as a reusable H_2 getter for insulated steam injection tubing (Sandrock, 87 (336)), NH_3 heat pipes (Franco, 86 (337)) and tritium systems (Nakamura, 85 (338)). It has also been used for Joule-Thompson cryoabsorption systems (Freeman, 94 (350), but application appears to have been unsuccessful because ZrNi tends to disproportionate above about 400°C (Cantrell, 95 (409)).

3.D.5. Comparisons of Commercially-Oriented TiFe Hydrides

TiFe itself and Mn- and Ni-substituted versions of it seem to have had the most commercial interest of the ABs. In this section we will compare the hydride properties of the following three alloys using data from the sources indicated: TiFe (Reilly, 74 (319)); $TiFe_{0.85}Mn_{0.15}$ (Johnson, 78 (330)); $TiFe_{0.8}Ni_{0.2}$ (Huston, 80 (77)). The H-capacity data for TiFe and $TiFe_{0.85}Mn_{0.15}$ represents carefully prepared, high-purity laboratory material and are perhaps 10% higher than what might be achieved in commercial practice, but they represent reasonable ideals. TiFe and $TiFe_{0.85}Mn_{0.15}$ exhibit two plateaux, both of which are more or less within the range of our fuel cell PCT range, so both plateaux will be included in $(\text{H-capacity})_{rev}$. This may a little misleading when comparing to other alloy families with single plateaux, especially in view the upper plateau instability for ABs that will be discussed later in Section 3.D.6, p.85. Table XX gives the PCT properties and Table XXI the capacity and cost properties for the three alloys. Figure 36 shows the desorption van't Hoff lines for the lower hydride of each alloy.

Table XX
Lower Plateau PCT Properties of TiFe-Type Hydrides

Composition	ΔH, kJ/mol	ΔS, kJ/molK	25°C P_d, atm	T for 1 atm P_d	Plateau Hysteresis	Plateau Slope
TiFe	28.1	0.106	4.1	-8	0.64	0.0
$TiFe_{0.85}Mn_{0.15}$	29.5	0.107	2.6	3	0.62	0.92
$TiFe_{0.8}Ni_{0.2}$	41.2	0.119	0.1	73	0.05	0.36

Table XXI
Capacity and Cost Properties of TiFe-Type Hydrides

Composition	Density	$(\text{H-Capacity})_{max}$		$(\text{H-Capacity})_{rev}$			Alloy	RMC**
	g/cm^3	H/M	wt.%	ΔH/M	Δwt,%	$\Delta N_H/V$*	$/kg	$/g H
TiFe	6.5	0.975	1.86	0.79	1.5	5.0	4.68	0.31
$TiFe_{0.85}Mn_{0.15}$	6.5	1.0	1.9	0.80	1.5	5.0	4.83	0.32
$TiFe_{0.8}Ni_{0.2}$	6.5	0.7	1.3	0.42	0.8	2.9	5.5	0.68

* Reversible volumetric capacities are approximate and in units of 10^{22} H-atoms/crystal cm^3 (i.e., interparticle void volumes not included)
** RMC = Raw Materials Cost; $/g H based on $(\text{H-Capacity})_{rev}$

TiFe and $TiFe_{0.85}Mn_{0.15}$ show good volumetric and gravimetric reversible H-capacities, competitive with the best of the AB_5s and AB_2s, along with PCT properties that are good for fuel cell applications. However, $TiFe_{0.8}Ni_{0.2}$ is not so useful because of its low capacity and low plateau pressure. The low capacity of $TiFe_{0.8}Ni_{0.2}$ is due to the fact the upper plateau is absent in this alloy, i.e., is at too high a pressure range to be useful. TiFe and $TiFe_{0.85}Mn_{0.15}$ offer low price, lower on a per unit H_2 storage capacity than anything heretofore presented[5]. As will be

[5] The Ti used in determining the raw materials costs in Table XXI was standard sponge Ti ($9.63/kg in Table III). The alloy price can be greatly lowered by using commercial ferrotitanium ($3.19/kg Ti), but Al and O impurities in that Ti source cause significant capacity loss and isotherm distortion (Sandrock, 78 (321)).

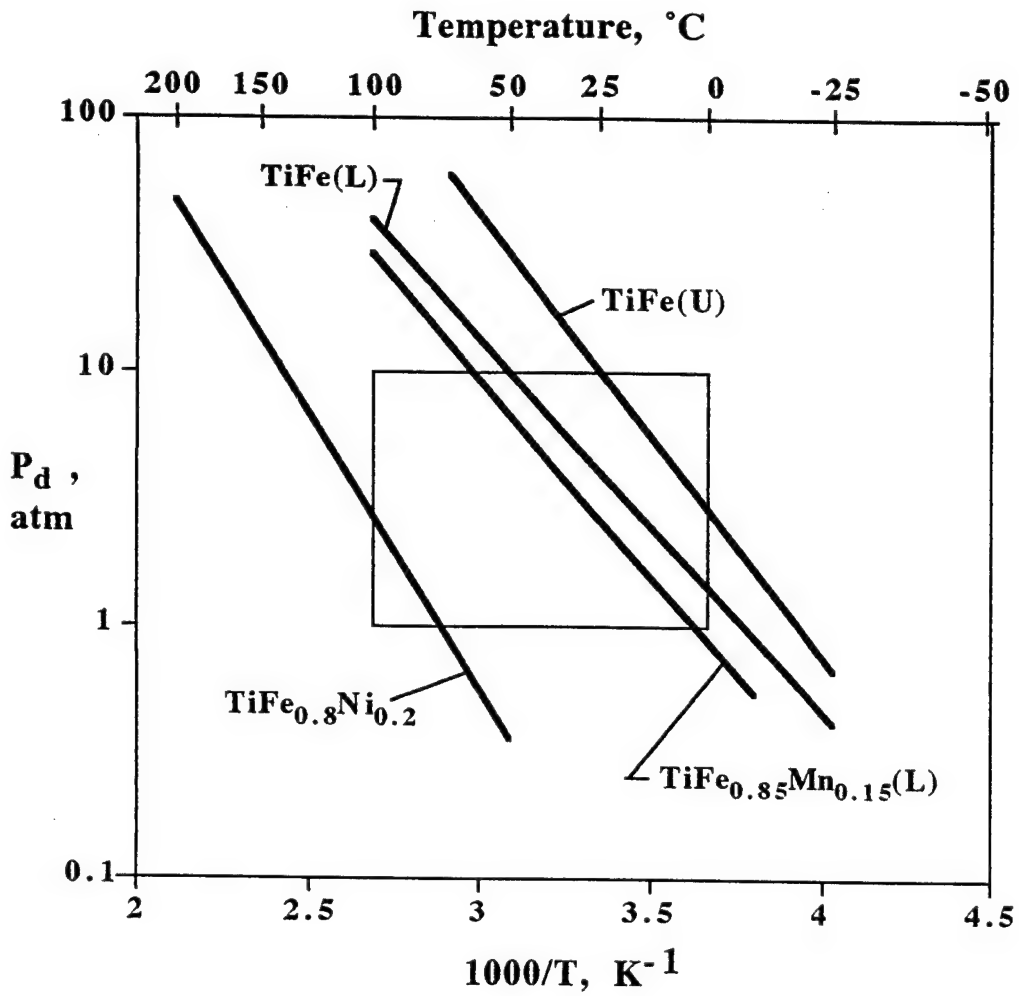

Figure 36
Desorption van't Hoff Lines for TiFe-Type Hydrides
(L) indicates lower plateau; (U) indicates upper plateau

shown in Section 3.D.6, however, the capacity and cost advantages of TiFe and $TiFe_{0.85}Mn_{0.15}$ may be short lived and not sustainable.

3.D.6 Other Properties

In spite of the favorable PCT, capacity and alloy cost properties of TiFe-type alloys, their practicalities are unfortunately dictated by a variety of problems related to other properties, the sum of which have greatly limited their use in recent years.

Activation

The AB compounds (especially the TiFe-type) are generally much more difficult to activate than the AB_5 and AB_2 compounds, partly a result of more passive and dissociatively inactive natural oxide films on the surface of air-exposed particles and partly the result of higher toughness. Binary TiFe does not activate at room temperature and must be heated to about 300-400°C before hydrogen begins to penetrate the passive surface layer as the first stage of activation. What happens during this step was the subject of more than 100 papers by 1983 (Schlapbach, 83), but in

general the surface apparently become segregated into Ti-oxides and catalytically active Fe so that atomic H can be made which easily penetrates through the surface layer into the bulk. Fortunately, almost any ternary substitution one makes to TiFe virtually eliminates the need for heating to get the reaction started, e.g., Mn, Ni, Al, Mm.

Once H-atoms begin to enter the bulk of an TiFe particle, a second stage of activation begins. It takes the form of cracking the alloy particles and exposing new surfaces. TiFe-type alloys have significant fracture toughness and the second stage can be agonizingly slow. The more single-phased the microstructure the longer is the time for complete activation. High purity TiFe can take 200 hours to fully activate, and then only when repeated, high pressure A/D cycling is done to assist in the cracking (Sandrock, 78 (321)). This is shown in Figure 37. Also shown in Fig.37 is

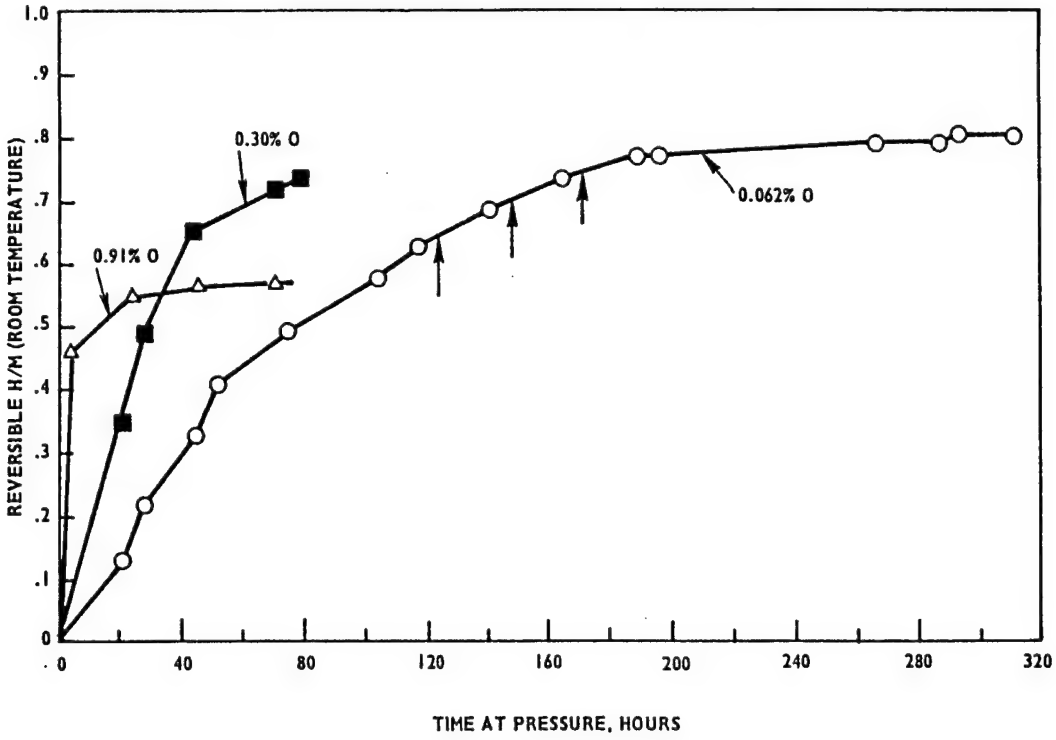

Figure 37
Effect of O-Content on the Second Stage Activation of TiFe
Initial particle size = -30+50 mesh; P_{H2} = 67 atm at room temperature;
data points and arrows each represent an absorption/desorption cycle.
(Sandrock, 78 (321))

the fact that O-contaminated TiFe (containing a eutectic distribution of $Fe_7Ti_{10}O_3$ particles) activates much faster, albeit with lower ultimate capacity. Insoluble mischmetal particles in the microstructure (resulting from Mm deoxidation) greatly aid in the activation of otherwise pure TiFe (Sandrock, 78 (321)); Bronca, 85 (549)). Mn-containing alloys tend to have $TiFe_2$ second phase particles in the microstructure which facilitate cracking and activation, even though the $TiFe_2$ particles do not hydride themselves. A small starting particle size (e.g., -100 mesh) helps speed activation. In any event, activation of TiFe-type alloys typically takes tens of hours at high pressure vs. tens of minutes at lower pressures for many of the AB_5 and AB_2 compounds.

Decrepitation

The pattern of decrepitation in the TiFe-type AB intermetallics is somewhat different than the AB_5 and AB_2 compounds. At first, the ABs give the impression they do not pulverize as much during activation by retaining more or less what appears to be the original particle size. In fact each particle becomes highly cracked internally and actually develops a specific surface area that is higher than the AB_5s (0.5 m^2/g for FeTi vs. 0.2 m^2/g for $LaNi_5$). The macroscopic particles have enough strength to hold together, at least to some degree. Figure 38 shows an unetched metallographic cross section of TiFe particles A/D cycled 1500 times. Although some inevitable

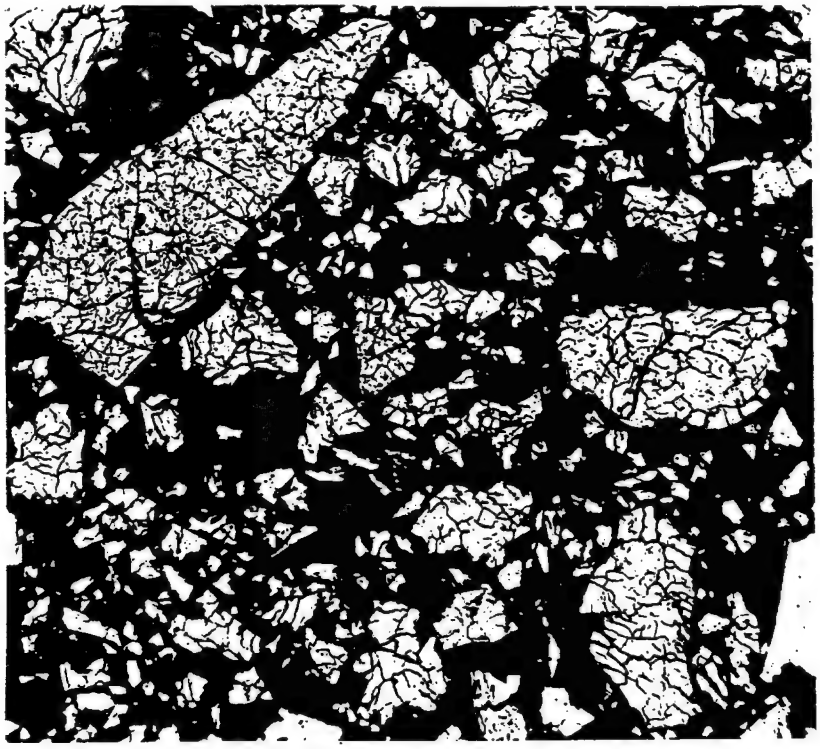

Figure 38
Polished Cross Section (Unetched) of TiFe Particles after 1500 Absorption/Desorption Cycles
(Sandrock, 76)

fragmentation occurred, many of the internally cracked particles retained particle sizes that were near their originals. This ability to maintain a rather coarse macroscopic particle size is an advantage for TiFe-type hydrides because it gives high surface area in a sponge-like structure with relatively low gas impedance. However, the many small particles that ultimately do detach (cf. Fig.38) can migrate, fill interparticle spaces, thus causing the usual packing and its associated problems. The actual decrepitation of a TiFe-type AB depends on the microstructure, especially second phases.

Intrinsic Kinetics and Heat Transfer

Although the intrinsic kinetics of TiFe and related alloys are slower than the AB_5s, it is clear they are rapid relative to practical heat transfer (Goodell, 80 (6), 80; Gérard, 92 (334)). Therefore, like the AB_5s and AB_2s discussed earlier, we can say that the heat transfer design of the storage vessel will dictate all practical uses of the TiFe-type AB compounds. However, as shown in the next topic, this situation will change quickly if impure H_2 is used.

Gaseous Impurity Effects

The TiFe-type AB hydrogen storage compounds have less resistance to gaseous impurities (especially O_2 and H_2O) than the AB_5s. Figure 39 shows the cyclic damage to TiFe, $TiFe_{0.85}Mn_{0.15}$ and $LaNi_5$ as a result of 300 ppm O_2, H_2O and CO in the H_2 used. For CO, all

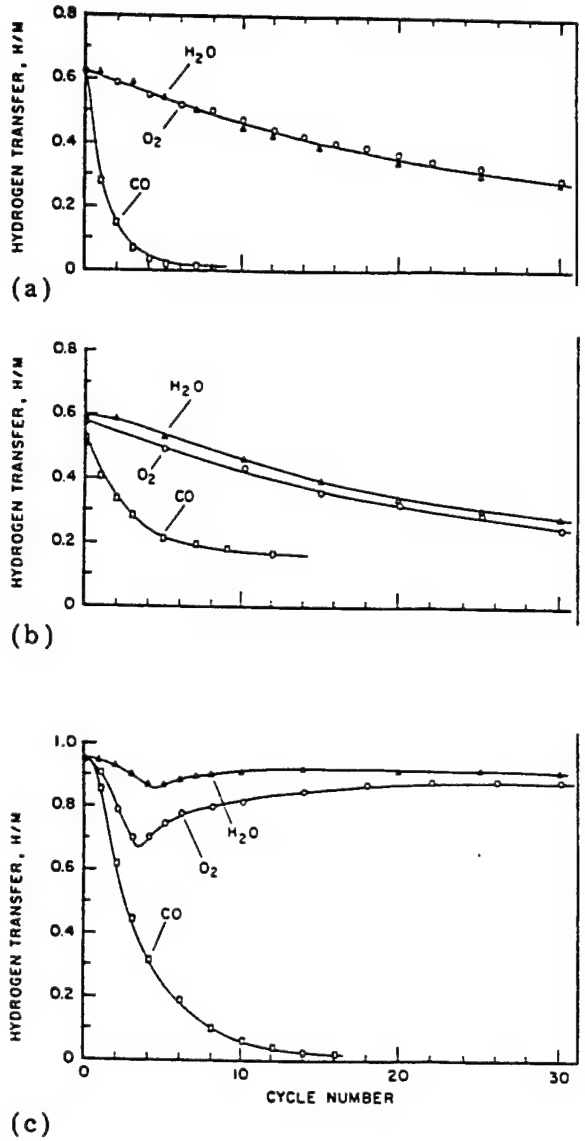

Figure 39
Effect of 300 ppm O_2, H_20 and CO on the 25°C $(H\text{-}Capacity)_{rev}$ of TiFe(a), $TiFe_{0.85}Mn_{0.15}$(b) and $LaNi_5$(c)
(Sandrock, 80 (203))

three alloys are poisoned more or less the same, although $TiFe_{0.85}Mn_{0.15}$ seems to have some terminal resistance to complete capacity loss. The main problem is the fact that the two AB compounds exhibit a steady loss of effective capacity with cycling in 0_2- and H_20-containing H_2.

As mentioned earlier, $LaNi_5$ exhibits a temporary loss, followed by recovery and a relatively good resistance with only a long-term reaction effect present (cf. Fig.6 c and d). It takes only about 10 monolayers of O-coverage to deactivate TiFe (Sandrock, 80 (203)). Although the TiFe-type compounds can be reactivated by significant heating, their strong sensitivity to such a common impurities as H_2O has contributed to the loss of interest in these H-storage materials, in this reviewer's opinion.

Cyclic Stability

TiFe-type alloys have excellent cyclic stability if only the lower plateau is used. The closed-volume thermal cycling of $TiFe_{0.85}Mn_{0.15}$ nearly 30000 times back and forth through the lower plateau only resulted in no loss of capacity (Johnson, 77 (393)). Unfortunately that is not the case when cycling through the upper plateau. As shown in Figure 40, the upper plateau pressure of

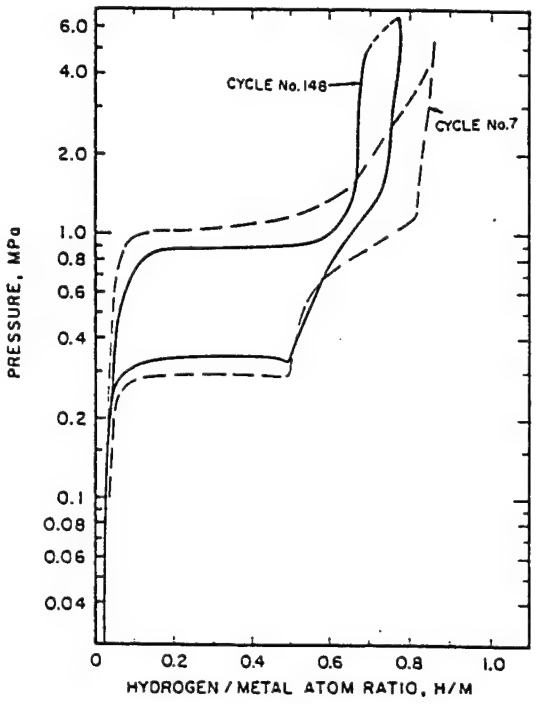

Figure 40
Effect of Absorption/Desorption Cycling on the 25°C Dynamic Hysteresis Loop of TiFe
(Goodell, 80 (6))

TiFe increases with cycling. Apparently the lattice strains of A/D cycling affect only those interstitial site associated with the upper plateau. The effect is quite apparent with only 148 cycles and results in an effective reduction of reversible capacity below that cited in Table XXI. This problem probably contributes to the low utilization of the alloy family.

Safety

TiFe-type alloys are not pyrophoric, probably a result of the thin passive oxide layer that quickly forms with exposure to the air. A detailed quantitative and qualitative safety study of TiFe and TiFe hydride powder (including dust clouds) has be made with the conclusion there are no

significant safety hazards associated with normal use of the the material for hydrogen storage (Lundin, 75). The two alloys of most commercial interest TiFe and $TiFe_{0.85}Mn_{0.15}$ do not contain toxic elements. Like all metallic powders, TiFe-type powders should not be inhaled or ingested and the manufacturer's MSDS should be followed during handling.

Metallurgy, Manufacturing and Recycling

A significant portion of the metallurgy and manufacturing information on TiFe-type alloys was developed by this reviewer at the Inco R&D Center with the support of the DOE Brookhaven National Laboratory (Sandrock, 76, 77, 78 (321)). Most of this section is based on this work. TiFe has a strong thermodynamic affinity for oxygen and is easily contaminated during melting or other synthesis techniques. As shown in Figure 41, a small amount O-contamination results in a significant loss in H-capacity. The loss is the result of the formation of an O-stabilized phase $Fe_7Ti_{10}O_3$ that hydrides, but not reversibly. Thus, one of the main objects of any alloy preparation procedure must be to minimize the minimize the final O-content in the product. A second important object, of course is to be as close as possible to the 1:1 A:B stoichiometry.

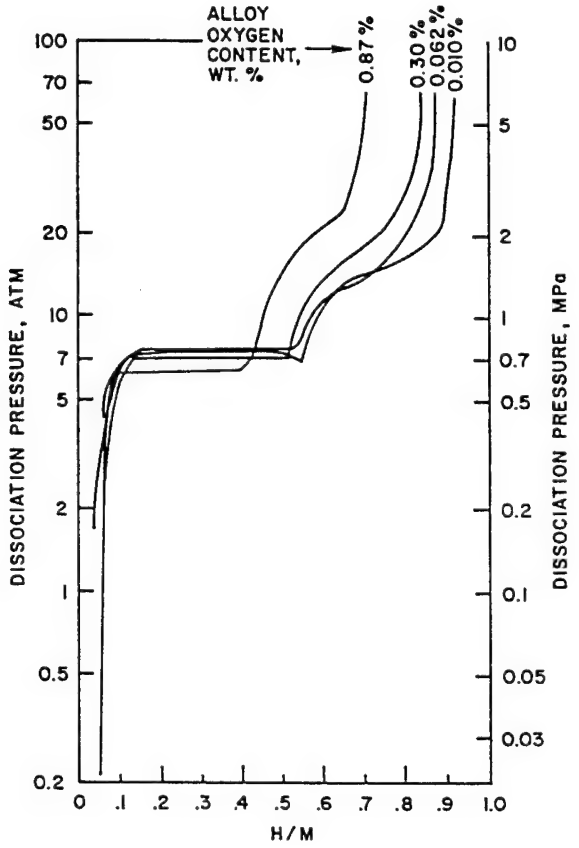

Figure 41
Effect of Oxygen Content on the 40°C Desorption Isotherm of TiFe
(Sandrock, 78 (321))

TiFe-type alloys can be melted by the cold crucible, conventional vacuum arc processes commonly used in the Ti industry. Melting of TiFe-type alloys in conventional oxide crucibles (e.g., Al_2O_3, MgO, ZrO_2) is difficult, if not impossible, because of crucible reduction and O-contamination. They can be vacuum induction melted in pure graphite crucibles. There is some C-

contamination, ending up as TiC particles, but it is minimal. The above vacuum melting processes require significant capital investment in expensive furnaces. As a lower-cost alternative, it is possible to prepare tonnage quantities of TiFe-alloys in air induction furnaces using an argon cover and deoxidizing the melt with about 4% mischmetal a few minutes before casting. TiFe of quality equal to arc melted material can be made by this technique. In addition, as mentioned earlier, isolated insoluble Mm particles that remain in the final product greatly aid activation without affecting PCT properties (Sandrock, 78 (321)); Bronca, 85 (549)). The air/argon melting, Mm deoxidation procedure can also be used to prepare the H_2-gettering alloy ZrNi.

Two decades ago there was interest in the possibility of making TiFe by the direct reduction of Ilmenite $FeTiO_3$. We examined this suggestion in considerable thermodynamic and economic detail, concentrating on metallothermic reduction with the relatively low cost reductants Si, Mg, Ca and Al (Sandrock, 77). Thermodynamics or economics do not favor Si, Mg or Ca, but the study suggested that aluminothermic reduction could result in TiFe with a price as low as $3.56/kg (cost and markup included). While this was somewhat lower than direct melting of Fe with sponge Ti ($4.84/kg), the thermodynamics required an excess of Al reductant, much of which ends up in the final product. Unfortunately, as shown in Figure 42, Al severely distorts TiFe isotherms and effectively reduces capacity.

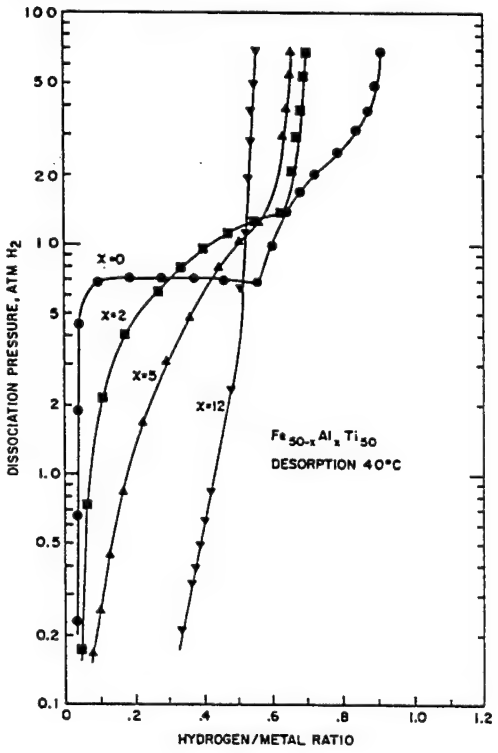

Figure 42
Effect of Al-Content on the 40°C Desorption Isotherms of TiFe
(Sandrock, 78 (321))

3.D.7 Summary and Suggested R&D

Among the AB intermetallic compounds, only those based on TiFe have PCT properties that are useful to PEM fuel cell applications. They can be easily modified for selected PCT properties

by the partial substitutions of Mn or Ni. Other advantages include low cost, safety, and good initial H-capacity (both gravimetric and volumetric). Unfortunately the TiFe-subfamily of AB compounds is hindered by the following problems (in order of decreasing importance): (1) high sensitivity to gaseous impurities in the H_2 used, especially O_2 and H_2O vapor; (2) cyclic instability associated with the upper plateau; (3) slow activation. The following suggestions for new R&D center around the first two of these problems.

1. The resistance of TiFe-type alloys to common gaseous impurities (especially O_2 and H_2O vapor) must be improved if the family is to see a renaissance in practical interest. Some improvements can possibly be made by partial substitutions, but it is probable that improved impurity resistance will come at the expense of H-capacity or PCT properties. A second approach may be surface coating or surface modification procedures. For reasons of importance to the downstream PEM fuel cell, the interaction of CO with alloy particle surfaces should be fully understood and quantified.

2. The upper plateau instability must be understood and preferably eliminated. It is known that the first careful absorption of TiFe shows only a single long plateau. The two-plateau isotherm develops only on the first desorption and, as shown in Fig.39, increases in pressure with further cycling. What is the origin of this deleterious effect? Can it be halted or minimized by alloy modification with ternary or higher order additions? Can the single plateau of the first absorption be extended through desorption and stabilized for many cycles?

3.E. A_2B Intermetallic Hydrides

The A_2B family of compounds represent the fourth group of intermetallic in terms of activity. Various crystal structures are represented. Unfortunately, the A_2Bs offer little in the 0-100°C, 1-10 atm range useful for PEM fuel cells, at least with the present state of the art. Because of the past historic and practical interest in the A_2Bs, as well as their arguable potential for the future, a brief review of them is justified here.

A number of A_2B intermetallics are known to form hydrides, as can be seen from the IEA/DOE/SNL on-line databases (Sandrock, 97). Those with at least some reported PCT data are listed in Table XXII. A quick scanning of this table quickly identifies the problem with all the

Table XXII
Hydride PCT Properties of A_2B Compounds

	(H-Capacity)$_{max}$		ΔH,	P=	at T=	
Composition	H/M	wt.%	kJ/mol	(atm)	(°C)	Author-Yr.
Hf_2Co	1.21	0.9	--	$<10^{-5}$	50	van Essen, 79 (386)
Hf_2Cu	0.97	0.7	--	$<10^{-5}$	50	van Essen, 79 (386)
Hf_2Cu (M)	2.13	1.5	--	1500	20	Klyamkin, 94 (595)
	(2000 atm at 20°C)			(high-P plateau)		
Hf_2Fe	1.03	0.75	--	$<10^{-5}$	50	van Essen, 79 (386)
Hf_2Fe	1.53	1.1	60-80	0.38	277	Aubertin, 89 (425)
Hf_2Mn	1.3	0.95	--	$<10^{-5}$	50	van Essen, 79 (386)
Hf_2Ni	1.03	0.75	--	$<10^{-5}$	50	van Essen, 79 (386)

Table XXII (concluded)
Hydride PCT Properties of A_2B Compounds

Composition	(H-Capacity)$_{max}$ H/M	wt.%	ΔH, kJ/mol	P= (atm)	at T= (°C)	Author-Yr.
Hf_2Pd (M)	1.52 (2000 atm at 20°C)	1.0	--	1000 (high-P plateau)	20	Klyamkin, 94 (595)
Hf_2Rh	0.7	0.45	--	$<10^{-5}$	50	van Essen, 79 (386)
Mg_2Co	1.67	4.5	--	--	--	Selvam, 91 (426)
(Mg_2Co phase not stable without H)						
Mg_2Co (M)	1.57	4.2	108	5.7	418	Yoshida, 93 (594)
(Mg_2Co phase not stable without H)						
Mg_2Cu	1.0 (Dp)	2.6	72.9	6	295	Reilly, 67 (87)
Mg_2Fe	2.0	5.5	--	--	--	Selvam, 91 (426)
(Mg_2Fe phase not stable without H)						
Mg_2Ni	1.33	3.6	64.5	3.2	299	Reilly, 68 (88)
Mg_2Ni	1.33	3.6	64.6	2.5 (Dynamic PCT)	300	Lutz, 77 (420)
$Mg_{1.92}Al_{.08}Ni$	1.3	3.5	70.5	4	295	Hirata, 83 (427)
$Mg_2Ni_{1-y}Be_y$ (y = 0.15-0.25)	1.33	3.9-4.1	71-80	3-6	337	Lupu, 82 (419)
$Mg_2Ni_{1-y}Cu_y$ (y = 0-1)	1-1.3	2.6-3.5	53-73	3.5-8	300	Darnaudery, 83 (417)
$Mg_2Ni_{.75}Cu_{.25}$	--	--	53.2	1	227	Darnaudery, 83 (418)
$Mg_2Ni_{.75}Co_{.25}$	1.15	3.1	64.5	1	279	Darnaudery, 83 (418)
$Mg_2Ni_{.75}Cr_{.25}$	1.1	3.0	59.9	1	248	Darnaudery, 83 (418)
$Mg_2Ni_{.75}Fe_{.25}$	1.03	2.8	63.2	1	253	Darnaudery, 83 (418)
$Mg_2Ni_{.75}V_{.25}$	1.06	2.9	62.4	1	250	Darnaudery, 83 (418)
$Mg_2Ni_{.75}Zn_{.25}$	1.22	3.3	61.5	1	246	Darnaudery, 83 (418)
Th_2Al	1.25	0.8	130	0.001 (Sloping plateau)	500	Van Vucht, 63 (492)
$Th_{1.5}Ce_{.5}Al$	0.58	0.4	133	0.0003	650	Van Vucht, 63 (492)
Th_2Al	1.33	0.8	--	$<10^{-9}$	50	Buschow, 82 (283)
Ti_2Cu (M)	1.17 (Dp)	2.2	130	0.12	500	Kadel, 78 (523)
Ti_2Cu	0.53 (Dp)	1.0	--	0.02	500	Arita, 79 (495)
Ti_2Ni (M)	0.83	1.6	--	0.11	150	Buchner, 72(71)
Zr_2Cu (M)	1.1	1.3	144	0.003	600	Pebler, 66 (12)
Zr_2Cu (M)	1.1 (Dp)	1.3	142	0.02	700	Kadel, 79 (429)
Zr_2Ni	1.04	1.3	183	0.003	604	Pebler, 66 (12)
Zr_2Pd	1.6	1.6	--	<0.1	25	Spada, 87 (424)
Zr_2Pd (M)	1.83 (2000 atm at 20°C)	1.9	--	500 (High-P plateau)	20	Klyamkin, 94 (595)

A_2B intermetallics, namely that they form very stable hydrides relative to the AB_5, AB_2 and AB compounds previously discussed. Nothing comes close to offering a desorption pressure of 1 atm at 100°C or less. The possible exception to this last statement are the very high pressure A_2B plateaux recently reported by (Klyamkin, 94 (595)), to be discussed later.

Historically Mg_2Ni was one of the earliest intermetallic compounds that was shown to be usable as a rechargeable hydride (Reilly, 68 (88)). Isotherms from the original publication are reproduced in Figure 43. A single hydride of composition about Mg_2NiH_4 is formed along a long flat plateau.

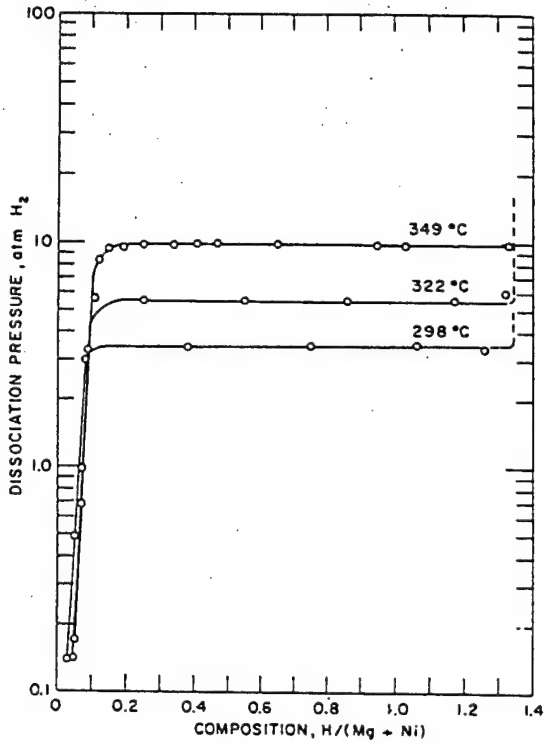

Figure 43
P-C Isotherms for the Mg_2Ni-H System
(Reilly, 68 (88))

It should be mentioned that Mg_2NiH_4 is really not a metallic hydride in the sense of the other intermetallic compounds we have discussed heretofore. It is really a more complicated hydride where Mg donates electrons to stabilize an $[NiH_4]^{-4}$ complex. In effect 4 hydrogen atoms bond with a single Ni atom and the two Mg atoms donate two electrons each to stabilize that high-H transition metal complex (Noréus, 89 (331)). It is not an interstitial hydride. The structure is antifluorite, quite different from the starting Mg_2Ni (hexagonal structure related to the the C16 Al_2Cu type). Most of the many such "low-valence hydride complexes" are not very reversible (cf. Section 3.H.5.A). Mg_2NiH_4 is a rather unusual exception where the basic A_2B stoichiometry is maintained between the intermetallic and hydride phases. More typical examples include Mg_2FeH_6 and Mg_2CoH_5 in Table XXII. These A_2B stoichiometries are present only as hydride complexes. The corresponding H-free phases Mg_2Fe and Mg_2Co do not exist in the binary metal systems.

Thus the poorly reversible absorption/desorption cycle is controlled by slow metal atom diffusion.

Mg_2NiH_4 requires about 300°C to dehydride at a few atmospheres pressure, as seen from Fig.43. Such levels of waste heat are not available from a PEM fuel cell. Ignoring that problem for the moment, the other H-storage properties of Mg_2Ni are very attractive:

$(H/M)_{max} = 1.33$
$(wt.\%)_{max} = 3.6$
$(\Delta H/M)_{rev} = 1.23$
$(\Delta wt.\%)_{rev} = 3.3$
$(\Delta H/V)_{rev} = 5.2X10^{22}$ H-atoms/cm^3
Alloy Raw Materials Cost = $6.26/kg
Alloy Raw Materials Cost = $0.19/g H stored

Note the particularly low cost compared to the alloys we have previously discussed.

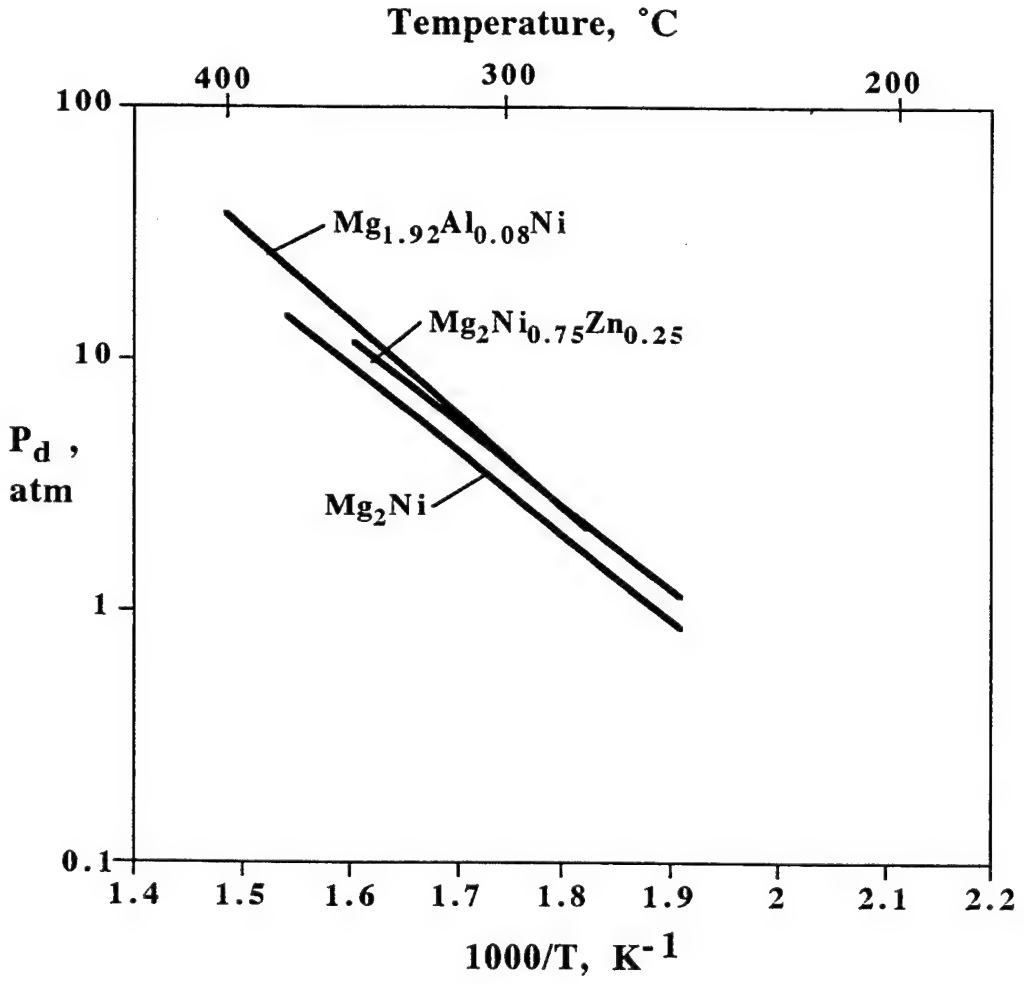

Figure 44
Van't Hoff Lines for Substituted Mg_2Ni-H Systems

Knowing the history of the AB_5, AB_2 and AB hydrides, the reader might speculate that increasing the desorption pressure of Mg_2NiH_4 might be simply a matter of partial substitution of other elements, a procedure shown to be so powerful for the other systems. Unfortunately, the substitution effects are rather small, as shown in Table XXII and the van't Hoff lines of Figure 44. Partial substitution of Al for Mg and Zn for Ni does lower the desorption temperatures of Mg_2Ni a little, but there seems to be little hope that 1 atm at 100°C can be reached (off scale to the right of Fig.44). The are fundamental differences in the metallurgy of Mg-systems, as well as the basic chemistry of the hydrides, compared to the AB_5, AB_2 and AB families. This reviewer believes that the limits of conventional metallurgy are being reached for the Mg-based A_2Bs and the other approaches of Section 3.H are required.

Although the A_2B alloys have principal plateaux at very low pressures, recent work has shown that Zr_2Pd, Hf_2Pd and Hf_2Cu have additional plateaux at very high pressures (ca. 1000 atm) and room temperature, as shown in Table XXII (Klyamkin, 94 (595)). These interesting intermetallics have the "non-close-packed" tetragonal $C11_b$ $MoSi_2$ structure with various available interstitial sites (Maeland, 80 (428); Spada, 87 (424)). The additional plateaux cover about 0.3-0.6 H/M, i.e., a relatively small part of the maximum capacity. The high pressures involved, coupled with the relatively expensive elements involved, give doubt as to whether they will be practical for H-storage; however, further exploratory work on other A_2Bs with this structure would probably be useful.

A brief review of the manufacturing techniques of Mg_2Ni-type A_2Bs is perhaps in order. The alloys can be made by air or inert gas melting. However, the stoichiometric composition solidifies by a peritectic reaction, first precipitating $MgNi_2$ crystals so that the final product is typically a three-phase mixture of Mg_2Ni, $MgNi_2$ and Mg. In order to avoid the MgNi2 phase, which apparently does not hydride, the alloy is usually melted to slightly higher Mg-levels than the stoichiometric Mg_2Ni. The result is some eutectic Mg-Mg_2Ni in additional to the predominant Mg_2Ni phase. The Mg results in an additional small lower plateau associated with MgH_2 (Reilly, 68 (88)). Very fine, nearly single phase $MgNi_2$ can be made by mechanical alloying (high-energy ball milling) of elemental Mg and Ni powders (Song, 85; Singh, 95). Recently, good single-phase Mg_2Ni has been made by the reaction of Ni powder with Mg vapor (Thomas, 96).

3.F. Miscellaneous Other Intermetallic Hydrides

In addition to the AB_5, AB_2, AB and A_2B intermetallic compounds discussed above, several other families of intermetallics have been shown capable of reversible hydriding/dehydriding reactions (Sandrock, 97). Examples include AB_3, A_2B_7, A_6B_{23}, A_2B_{17}, A_3B and others. Although none of these have attained commercial levels of interest, at least the AB_3 and A_2B_7 phases are deserve brief inclusion in this review because PCT properties are in the range of interest for PEM fuel cell applications. In addition, there has been some controversy centered around the La_2Mg_{17} phase, and this material will be briefly discussed.

3.F.1. AB_3 Compounds

The structures of the AB_3 compounds, listed in Table XXIII, are closely related to the AB_5 and AB_2 structures in that they are simply stacking of equal numbers of AB_5 and AB_2 units (Dunlop, 80 (447)). The two common types of AB_3 structures ($CeNi_3$ and $PuNi_3$) simply

represent differences in the long-period AB_5 and AB_2 stacking sequences. In effect one-third of the interstitial sites are AB_5-like and two-thirds are AB_2-like.

Table XXIII
Crystal Structures of the AB_3 Phases

Prototype = $CeNi_3$	Prototype = $PuNi_3$
Pearson = hexagonal	Pearson = hR12
Space Group = $p6_3/mmc$	Space Group = R-3m

Table XXIV
Hydride PCT Properties of AB_3 Compounds

Composition	(H-Capacity)$_{max}$ H/M	wt.%	ΔH, kJ/mol	P= (atm)	at T= (°C)	Author-Yr.
$CeCo_3$ (M)	0.82	1.0	38.1	0.3	79	Tauber, 76 (529)
$CeCo_3$	1.22	1.6	38.1	0.2	50	Burnasheva, 77 (543)
$CeCo_3$	1.05	1.3	--	0.2	50	van Essen, 80 (355)
$CeNi_3$	0.75	0.9	--	0.09	50	van Essen, 80 (355)
$CeNi_3$	1.4 (2000 atm and -78°C)	1.8	--	No plateau		Verbetsky, 96 (636)
$CeNi_{2.2}Mn_{.8}$	1.56 (2000 atm and -78°C)	1.7	--	No plateau		Verbetsky, 96 (636)
$DyCo_3$	1.2	1.4	42.7	0.3	50	Burnasheva, 77 (543)
$DyCo_3$	1.07	1.3	42	3	100	Wallace, 80 (439)
$DyCo_3$(M)	1.00	1.2	--	0.02	0	Dunlap, 80 (447)
$DyFe_3$	0.8	1.0	47.1	0.4	150	Goudy, 76 (186)
$DyFe_3$(M)	0.95	1.1	45.7	0.001	20	Kierstead, 80 (449)
$ErCo_3$	1.17	1.3	39.8	0.2	50	Burnasheva, 77 (543)
$ErCo_3$	1.05	1.2	38	10	100	Wallace, 80 (439)
$ErCo_3$	1.07	1.2	--	1	120	Shilov, 81 (530)
$ErFe_3$	0.7	0.8	42.9	1.15	150	Goudy, 76 (186)
$ErNi_3$	0.88	1.0	--	1.3	25	Goudy, 76 (186)
$ErNi_3$	1.27 (2000 atm and -78°C)	1.5	23.8	1.2	-40	Verbetsky, 96 (636)
$GdCo_3$ (M)	1.15	1.4	45	3	150	Wallace, 80 (439)
$GdCo_3$(M)	1.07	1.3	--	0.01	80	Dunlap, 80 (447)
$GdCo_3$ (M)	1.12	1.3	42.6	0.015	20	Kierstead, 81 (444)
$GdFe_3$	0.8	1.0	50.4	0.18	150	Goudy, 76 (186)
$HoCo_3$	1.05	1.2	36	6	100	Wallace, 80 (439)
$HoFe_3$	0.8	1.0	44.6	0.63	150	Goudy, 76 (186)
$LuCo_3$ (M)	0.9	1.0	32	5.9	20	Kierstead, 84 (571)

Table XXIV (concluded)
Hydride PCT Properties of AB_3 Compounds

Composition	(H-Capacity)$_{max}$ H/M	wt.%	ΔH, kJ/mol	P= (atm)	at T= (°C)	Author-Yr.
$NdCo_3$(M)	1.07	1.3	--	0.02	80	Dunlap, 80 (447)
$NdCo_3$ (M)	1.07	1.3	54.5	0.29	20	Kierstead, 81 (444)
$SmCo_3$	0.5	0.6	59.4	0.2	69	Tauber, 76 (529)
$SmCo_3$	1.32	1.6	--	1	175	Shilov, 81 (530)
$TbCo_3$ (M)	1.2	1.4	46.9	0.6	75	Burnasheva, 77 (543)
$TbCo_3$ (M)	1.12	1.3	44	1.5	100	Wallace, 80 (439)
$TbFe_3$	0.9	1.1	48	0.23	150	Goudy, 76 (186)
$ThFe_3$	0.75	0.7	--	<0.1	40	Buschow, 77 (187)
ThNiAl	0.99	0.9	47	0.007	40	Drulis, 82 (434)
$TiCu_3$	0.2 (Dp)	0.3	0.56	500	--	Arita, 79 (495)
UNiAl	0.91	0.8	48	No plateau		Drulis, 82 (434)
YCo_3 (M)	0.5	0.6	--	0.6	43	Tauber, 76 (529)
$YCo_{2.9}Ni_{.1}$ (M)	0.47	0.6	--	0.27	28	Tauber, 76 (529)
YCo_3	0.25	0.4	--	$5x10^{-3}$	50	van Essen, 80 (355)
YCo_3	1.02	1.5	44	0.45	75	Yamaguchi, 85 (573)
$YCo_{2.4}Fe_{.6}$ (M)	1.0	1.5	--	0.8	120	Yamaguchi, 89 (615)
$YCo_{2.4}Ni_{.6}$ (M)	0.92	1.4	--	3.5	120	Yamaguchi, 89 (615)
YFe_3	1.2	1.9	--	$<10^{-5}$	50	van Essen, 80 (355)
$YFe_{1.5}Ni_{1.5}$ (M)	0.87	1.3	--	2	120	Yamaguchi, 89 (615)
YNi_3	0.3	0.45	--	0.25	50	van Essen, 80 (355)

A list of AB_3 compounds, where hydride PCT data are available, is given as Table XXIV. In almost all cases the A species is a rare earth or rare-earth-like element and B is a transition element, particularly Co, Fe or Ni. A quick review of Table XXIV indicates most AB_3 hydrides are on the stable side, but clearly some have at least 1 atm dissociation pressure within the 100°C limit we have chosen for fuel cell applications. There is an undesirable tendency for the AB_3s to either show multiple plateaux (e.g., $NdCo_3$ shown in Figure 45) or a short plateau with a sloping upper leg and a low-pressure offset (e.g., $GdFe_3$ in Figure 46). On the positive side, note the low absorption/desorption hysteresis shown for $GdFe_3$ in Fig.46.

There are little data to be found on the practical properties of the AB_3 hydrides such as gaseous impurity effects and cyclic stability. With regard to the stability of the rare earth AB_3 hydrides, there have been few reports of disproportionation, but it should be noted that the phase forms from the melt by peritectic reactions (cf. $LaNi_3$ in Fig.22, p.49). This is usually taken as an indication that the intermetallic itself has marginal stability. If AB_5 hydrides show some tendency for disproportionation with long-term cycling, it might be argued that the AB_3s will show as much or more. Their peritectic formation also makes it hard to produce single phase AB_3 without significant annealing of as-cast alloy.

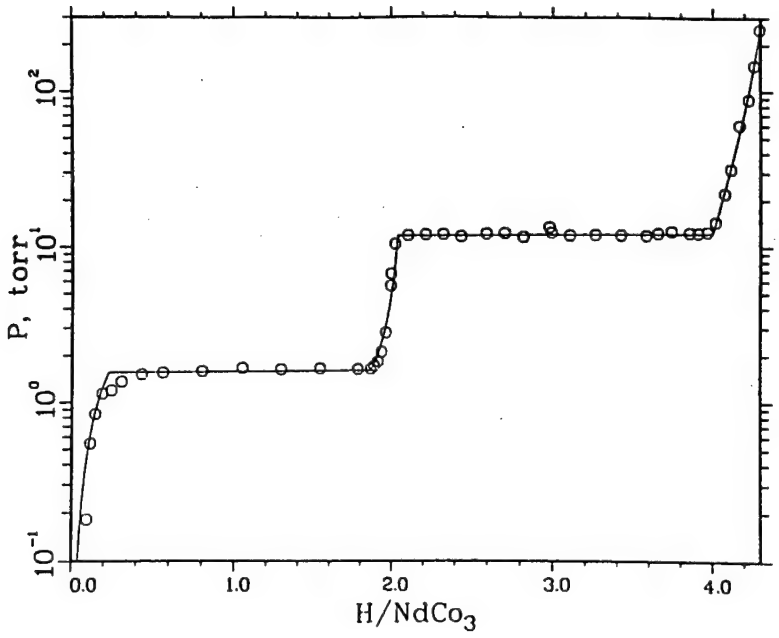

Figure 45
H_2 Desorption Isotherm of $NdCo_3$ at 80°C (Kierstead, 81 (444))

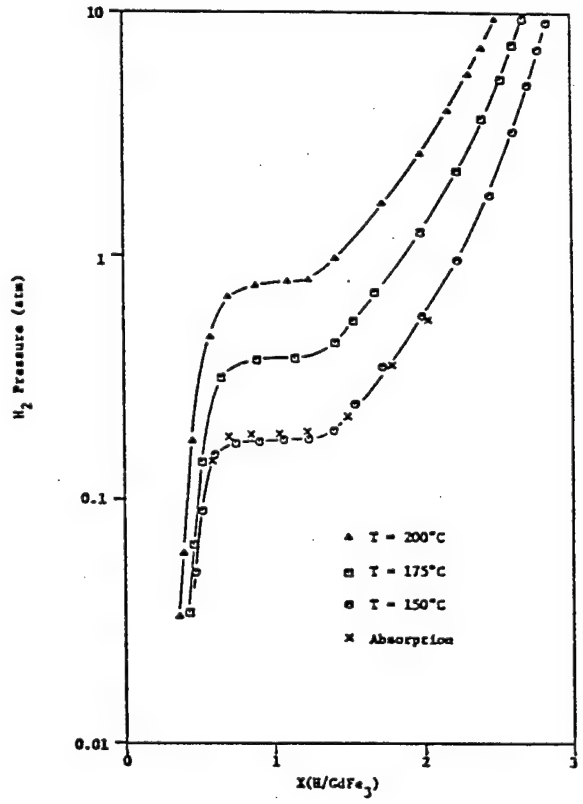

Figure 46
H_2 Isotherms of $GdFe_3$ (Goudy, 76 (186))

The fact the AB_3 intermetallics have PCT properties that are near those useful for fuel cell applications, yet there is little in the way of past applications or engineering data, suggests at least some further R&D on this family is desirable:

1. $CeFe_3$ (and probably $MmFe_3$) does not exist on the ternary phase diagram. Can it be stabilized with partial ternary substitutions? $MmFe_3$, especially, would represent the basis of a potential low-cost H-storage alloy if it could be made appropriate properties result.

2. There is little data on ternary and higher component AB_3 intermetallics. How can PCT and other properties be controlled by the partial substitution of such things as Al, Sn, etc.?

3. The long-term, room-temperature cyclic stability of a few representative AB_3s should be determined. Are they inherently unstable like the AB_5s? Does partial Al- or Sn-substitution impart disproportionation resistance?

4. Basic gaseous impurity resistance of the family should be determined, especially CO and H_2O. What are the inherent differences among ANi_3, AFe_3 and ACo_3, where A is a rare earth like Ce or a RE mixture like Mm?

3.F.2. A_2B_7 Compounds

Similar to the AB_3 phases, A_2B_7 phases consist of sequenced stacking of 2 AB_5 and 1 AB_2 layers, again giving essentially the same interstitial environments (Dunlop, 80 (447)). Resulting is the structure designated by prototype Ce_2Ni_7 and space group $P6_3/mmc$. There is a general

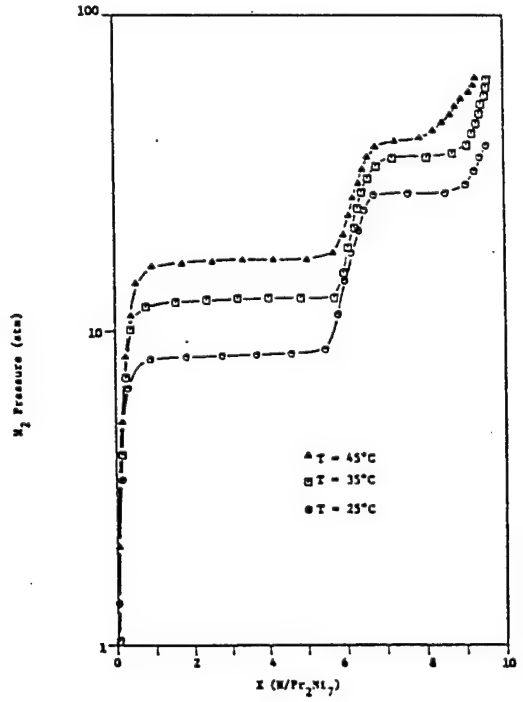

Figure 47
H_2 Isotherms of Pr_2Ni_7 (Goudy, 76 (186))

tendency for the A_2B_7 phases to show multiple plateaux, e.g. two plateaux shown for Pr_2Ni_7 in Figure 47. The PCT properties of several A_2B_7 hydrides are tabulated in Table XXV (with pressures shown for the largest plateau in multiple plateau (M) materials). Like the AB_3s, most of the the A_2B_7 compounds reported to hydride consist of rare earth or similar A-elements and Ni, Fe or Co B-elements. Plateau pressures are generally in the useful range for PEM fuel cells; however, the capacities are not particularly good. Bear in mind that the reversible H-capacities are considerably lower than values of $(\text{H-capacity})_{max}$ shown in Table XXV, especially when only one plateau is used in a multiple plateau alloy.

Table XXV
Hydride PCT Properties of A_2B_7 Compounds

Composition	$(\text{H-Capacity})_{max}$ H/M	wt.%	ΔH, kJ/mol	P= (atm)	at T= (°C)	Author-Yr.
Ce_2Co_7	0.74	1.0	--	0.5	50	van Essen, 80(355)
Ce_2Co_7	0.7	0.9	43.3	0.9	100	Goudy, 76 (186)
Ce_2Ni_7	0.49	0.6	--	0.2	50	van Essen, 80 (355)
Dy_2Co_7 (M)	0.89	1.1	35.8	2	50	Goudy, 76 (186)
Er_2Co_7 (M)	1.07	1.3	29.6	8	50	Goudy, 76 (186)
Gd_2Co_7 (M)	0.76	0.9	40	6	100	Goudy, 76 (186)
La_2Ni_7	1.11	1.4	--	3	50	Osterreicher, 76 (524)
Nd_2Co_7 (M)	0.96	1.2	56.7	0.9	125	Goudy, 76 (186)
Pr_2Co_7	0.56	0.7	33.3	10	100	Clinton, 75 (102)
Pr_2Co_7 (M)	0.9	1.1	54.6	2	150	Goudy, 76 (186)
Pr_2Ni_7	1.11	1.4	--	8.3	25	Goudy, 76 (186)
Tb_2Co_7 (M)	0.86	1.1	40.4	2	50	Goudy, 76 (186)
Th_2Co_7	0.53	0.5	--	0.25	40	Buschow, 75 (187)
Th_2Fe_7 (M)	0.68	0.7	--	0.6	40	Buschow, 77 (187)
Y_2Co_7	0.17	0.3	--	10^{-2}	50	van Essen, 80 (355)
Y_2Co_7	0.89	1.3	38	0.25	20	Yamaguchi, 85 (573)

Although the PCT properties of the A_2B_7 hydrides are more appropriate to PEM fuel cell applications than are those for AB_3s, the A_2B_7s also suffer from lack of data on properties other than PCT, such as cyclic stability and impurity effects. Suggested R&D on the A_2B_7 hydriding compounds is essentially the same as given for the AB_3 compounds on page 96.

3.F.3. La_2Mg_{17}

The intermetallic compound La_2Mg_{17} deserves a brief review of its own because of its controversial history and reported potential for high capacity room temperature H-storage. The structure of La_2Mg_{17} is related to the AB_5 structure and given by the following designations: prototype Th_2Ni_{17}, Pearson hP38 and space group $P6_3/mmc$.

The first data on the hydriding properties of La_2Mg_{17} was reported by Brookhaven in 1972

and said have an H-capacity of 5.3 wt.% with a desorption pressure about 10% higher than MgH_2, i.e., unremarkable over Mg (Reilly, 72 (195)). Then, in 1977, a short paper suggested significant

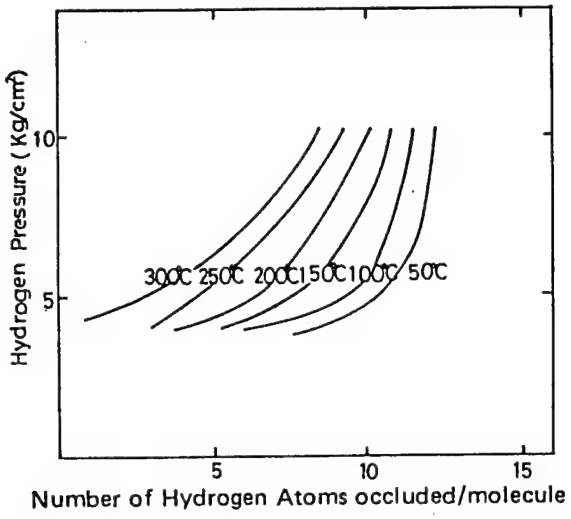

Figure 48
H_2 Absorption Isotherms for La_2Mg_{17} (Yajima, 77 (188))

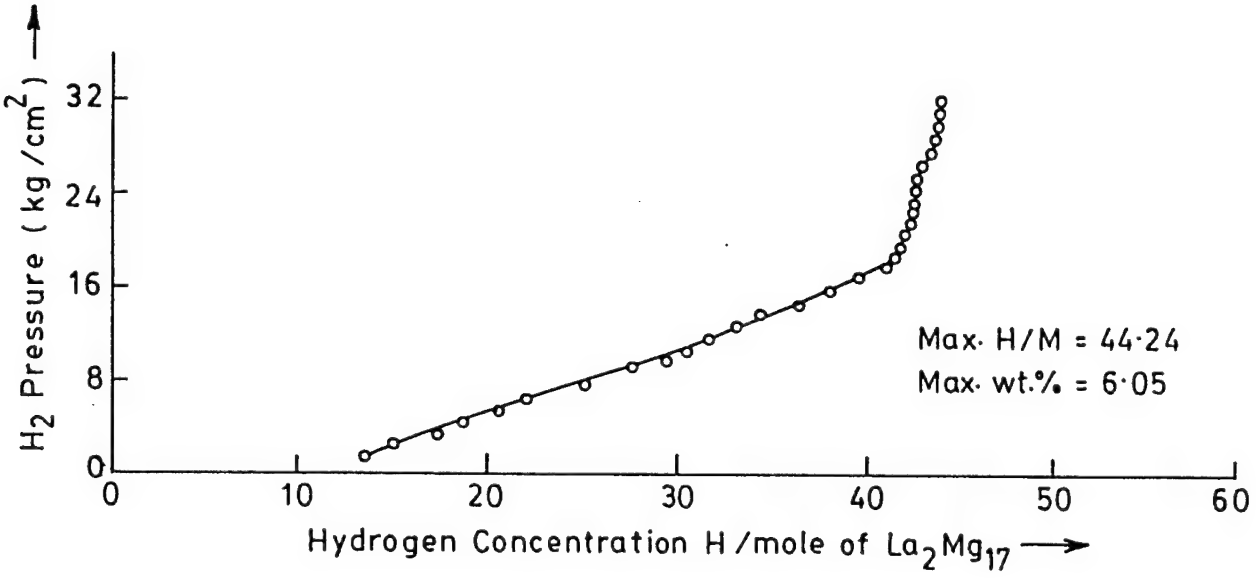

Figure 49
Ambient Temperature H_2 Desorption Isotherm for La_2Mg_{17}
(Dutta, 90 (442))

potential for the reversible storage of H in La_2Mg_{17} at temperatures well below the 300°C needed for Mg (Yajima, 77 (188)). P-C isotherms from that paper are reproduced as Figure 48. These isotherms show rather unusual characteristics for a reversible hydride. Although they show the

beginning of a plateau-like behavior at about 4 kg/cm^2 (≈4 atm), the plateau pressure seems to be largely independent of temperature. Curiously, no data was presented below 4 atm pressure so the full profile of the isotherm was not defined. In any event, the 50°C isotherm suggests considerable pressure and reversibility near room temperature. The maximum hydrogen content shown in Fig. 48 at 50°C, $La_2Mg_{17}H_{12}$, represents only 1.7 wt.%.

Later work in Bulgaria and France reported that a two-step series of disproportionation reactions was involved in the absorption and desorption of H_2 in La_2Mg_{17}, at least at temperatures well above ambient (Darriet, 80 (433); Khrussanova, 85 (436)):

$$La_2Mg_{17} + 20H_2 \text{ ----> } 2LaH_3 + 17MgH_2 \qquad \text{(Eq.26)}$$

$$2LaH_3 + 17\,MgH_2 \text{ <----> } 2LaH_x + 17Mg + (20\text{-}x)H_2. \qquad \text{(Eq.27)}$$

Capacities reported were up to 5.5wt.% with implications of desorption pressures similar to MgH_2 (≈3.5 atm at 325°C) , thus confirming the earlier Brookhaven work (Reilly, 72 (195)). There was no indication of room temperature reversibility.

A dramatically different picture for the hydriding properties of La_2Mg_{17} was given in 1990, incidentally at a conference session this reviewer chaired. Using La_2Mg_{17} prepared by a careful melting and homogenization technique, researchers from the Banaras Hindu University in India claimed reversible "ambient temperature" H-capacity of more than 6 wt.% (Dutta, 90 (442)). The desorption isotherm reported is reproduced as Figure 49. Needless to say, this presentation generated a considerable interest and stimulated further work by others. With all other intermetallic compounds, the hydride PCT properties fall in between those of the corresponding elements. Referring to Fig.8, p.27, how can the combination of a very strong hydride former (La) and a moderately strong hydride former (Mg) result in an intermetallic with an unstable hydride of room temperature utility? If La_2Mg_{17} behaved as reported by Dutta and Srivastava (Dutta, 90 (442)), a major theoretical anomaly would be born and the practical culmination of decades-long Mg-alloy hydride quests would be at hand. La_2Mg_{17} would represent the best hydride for PEM fuel cells.

Unfortunately, ambient temperature La_2Mg_{17} hydride has not been independently confirmed. This reviewer is aware of at least two or three attempts (unsuccessful) to reproduce the Banaras Hindu University results. Except for one negative result that has been published in the open literature, these private experiments remain unpublished. The one detailed published work (Slatterly, 95 (433)) failed to confirm any of the hydriding and dehydriding results of the Banaras Hindu University group. In particular, temperatures of 275+°C were needed for significant H_2 release from La_2Mg_{17}-hydride.

Because of the importance of this controversy to the application of hydride storage to fuel cell devices, this reviewer recommends one further attempt at understanding La_2Mg_{17}-hydride. Because the Banaras Hindu University group is a contractor to the U.S. Naval Research Laboratory, it is recommended that some of these contract activities be aimed at settling the "ambient temperature" La_2Mg_{17} questions, once and for all. In particular, the work should not only be aimed at understanding the lack of reproducibility by researchers at BHU and NRL, but to provide BHU-qualified alloy and specific instructions for activation and testing to a few well-known experts for independent confirmation.

3.G. Solid Solution Alloy Hydrides

Metallurgically speaking, the term "solid solution alloy" designates a primary element (solvent) into which one or more minor elements (solutes) are dissolved. Unlike the intermetallic compound, the solute need not be present at an integer or near-integer stoichiometric relationship to the solvent and is present in a random (non-ordered) substitutional or interstitial distribution within the basic crystal structure. Several solid solution alloys form reversible hydrides, in particular those based on the solvents Pd, Ti, Zr, Nb and V.

3.G.1. Pd, Ti and Zr Solid Solutions

Perhaps the largest family of solid solution hydrides consists of the face-centered-cubic (A1) Pd-based alloys, summarized in the IEA/DOE/SNL Internet Database (Sandrock, 97). Although the PCT properties of many of the Pd solid solution alloys are compatible with our PEM fuel cell range of 1-10 atm at 0-100°C, they are of generally low gravimetric and volumetric H-capacity, e.g., seldom exceeding 1.0 wt.%H. In addition they are prohibitively expensive and using them for H-storage would add further to the cost burden of the precious metals already required in the PEM fuel cell for electrocatalysis. Therefore Pd alloys will not be considered further in this review.

Ti- and Zr-base solid solution alloys form hydrides that are too stable for PEM fuel cell application, even when highly alloyed. They will also not be further reviewed. Those interested in such stable Ti and Zr alloy hydrides can also find property summaries in the solid solution listing of the Internet database.

3.G.2. Nb and V Solid Solutions

Because Nb and V (cf. Section 3.A.2, p.26) have dihydride properties compatible with H-storage for PEM fuel cells, it is logical that binary and higher component solid solutions based on those elements offer further opportunities. These alloys are all based on the simple body-centered-cubic (A2) crystal structure and their dihydrides generally form a face-centered cubic structure

Table XXVI
Dihydride PCT Properties of Nb and V Solid Solution Alloys

Composition	(H-Capacity)$_{max}$ H/M	wt.%	ΔH, kJ/mol	P= (atm)	at T= (°C)	Author-Yr.
$Nb_{1-x}Fe_x$ (x=0.004-0.01)	1.85-1.90	2.0-2.1	--	2.2-2.4	40	Reilly, 72 (314)
$Nb_{.994}Ge_{.006}$	1.95	92.1	--	3.4	40	Reilly, 72 (314)
$Nb_{1-x}Si_x$ (x=0.01-0.026)	1.85-1.92	2.0-2.1	--	2.8-4.0	40	Reilly, 72 (314)
$V_{.99}B_{.01}$	1.94	3.72	--	4.8	40	Reilly, 72 (314)
$V_{1-x}C_x$ (x=0.005-0.008)	1.98-2.03	3.8-3.9	--	5.3-5.8	40	Reilly, 72 (314)
$V_{.99}Co_{.01}$	1.94	3.69	--	6.9	40	Reilly, 72 (314)
$V_{1-x}Cr_x$ (x=0.01-0.049)	1.99-2.15	3.8-4.1	--	6.4-11	40	Reilly, 72 (314)
$V_{1-x}Cr_x$ (x=0-0.1)	1.9-2	3.6-3.8	33-39	5-25	50	Lynch, 78 (84)

Table XXVI (concluded)
Dihydride PCT Properties of Nb and V Solid Solution Alloys

Composition	$(H\text{-}Capacity)_{max}$ H/M	wt.%	ΔH, kJ/mol	P= (atm)	at T= (°C)	Author-Yr.
$V_{.855}Cr_{.145}$	1.2	2.3	29.7	50	50	Lynch, 78 (84)
$V_{1-x}Fe_x$ (x=0.001-0.009)	1.99-2.01	3.8-3.9	--	5.3-7.4	40	Reilly, 72 (314)
$V_{1-x}Ge_x$ (x=0.003-0.011)	1.61-1.98	3.1-3.8	--	7.4-9.0	40	Reilly, 72 (314)
$V_{.99}Mo_{.01}$	2.02	3.81	--	8.0	40	Reilly, 72 (314)
$V_{.99}Nb_{.01}$	1.95	3.69	--	5.3	40	Reilly, 72 (314)
$V_{.8}Nb_{.2}$	1.9	3.1	--	2	45	Wiswall, 72(318)
$V_{.991}Ni_{.009}$	1.90	3.62	--	6.9	40	Reilly, 72 (314)
$V_{1-x}Si_x$ (x=0.001-0.017)	1.85-2.03	3.5-3.9	--	5.3-18	40	Reilly, 72 (314)
$V_{.96}Si_{.04}$	1.59	3.1	--	13	0	Reilly, 72 (314)
$V_{1-x}Sn_x$ (x=0.004-0.006)	1.97-2.01	3.7-3.7	--	5.8	40	Reilly, 72 (314)
$V_{.983}Ta_{.013}$	1.77	3.28	--	5.8	40	Reilly, 72 (314)
$V_{.992}Ti_{.008}$	2.03	3.86	--	4.2	40	Reilly, 72 (314)
$V_{.8}Ti_{.2}$	1.55	3.0	48.1	2	80	Ono, 80 (452)
$(V_{.9}Ti_{.1})_{.9}Al_{.05}Fe_{.05}$	--	--	42.8	--	--	Libowitz, 88 (353)
$(V_{.9}Ti_{.1})_{.91}Al_{.05}Fe_{.04}$	1.47	2.6	--	5	25	Libowitz, 85 (471)
$(V_{.8}Ti_{.2})_{.9}Al_{.05}Fe_{.05}$	--	--	46.8	--	--	Libowitz, 88 (353)
$(V_{.85}Ti_{.15})_{1-x}Cr_x$ (x=0.1-0.2)	--	--	39-49	0.1-1.5	25	Libowitz, 88 (353)
$(V_{.9}Ti_{.1})_{.95}Fe_{.05}$	1.95	3.7	43.2	9.3	80	Lynch, 85 (351)
$(V_{.9}Ti_{.1})_{1-x}Fe_x$ (x=0-0.075)	1.8-1.95	3.4-3.7	40-51.8	1.5-20	80	Lynch, 85 (351)
$(V_{.8}Ti_{.2})_{1-x}Fe_x$ (x=0.02-0.1)	--	--	50-55	0.15-3.4	80	Libowitz, 88 (353)
$(V_{.9}Ti_{.1})_{.95}Ge_{.05}$	--	--	47.3	--	--	Libowitz, 88 (353)
$(V_{.85}Ti_{.15})_{.92}Mn_{.08}$	--	--	50.6	0.06	25	Libowitz, 88 (353)
$(V_{.8}Ti_{.2})_{.86}Mn_{.14}$	--	--	48.6	0.04	25	Libowitz, 88 (353)
$(V_{.59}Ti_{.41})_{.74}Mn_{.26}$	--	--	52.7	0.03	25	Libowitz, 88 (353)
$(V_{.8}Ti_{.2})_{.88}Mn_{.08}Fe_{.04}$	--	--	48.5	0.08	25	Libowitz, 88 (353)
$(V_{.63}Ti_{.37})_{.8}Mn_{.1}Fe_{.1}$	--	--	44.7	0.03	25	Libowitz, 88 (353)
$(V_xTi_{1-x})_{1-y-z}Mn_yFe_z$ (x=0.59-0.85; y=0.08-0.26; z=0-0.1)	--	1.6-2.5	45-52	0.03-.08	25	Libowitz, 85 (471)
$V_{1-x}W_x$ (x=0.008-0.01)	1.96-2.0	3.7	--	8.0-8-5	40	Reilly, 72 (314)
$V_{.99}Zr_{.01}$	2.02	3.8	--	3.7	40	Reilly, 72 (314)

(Strukturbericht C1, prototype CF_2, Pearson cF12 and space group Fm-3m). Numerous examples of hydrides of these alloys exist, especially for V-based solid solution alloys. Like elemental V (cf. Fig.9, p.28), only the upper dihydride plateau is usable for H-storage. Many of the Nb and V solid solution alloys, were PCT properties are available, are listed in Table XXVI. Note that most of the hydriding alloys shown in Table XXVI derive from the Brookhaven group (leader Reilly) and Allied Chemical group (leader Libowitz) Most are based on V, not the similar but more expensive Nb.

Although there are many possibilities, this reviewer argues that the only practical V-based solid solution alloys must contain the solute element Fe because this allows the alloys to be made with relatively inexpensive ferrovanadium (cf. Table III). Because of its strong ability to control PCT properties, Ti is also useful as a solute element. Thus, the most practical solid solution alloy family for PEM fuel cell H-storage is V-Ti-Fe, developed in the late 1980s by the Allied group. The ability to control the plateau pressure of $V_{0.9}Ti_{0.1}$ by small additions of Fe is shown in Figure 50. The higher the Fe-content, the higher the plateau pressure. Up to the level of x=0.075 in $(V_{0.9}Ti_{0.1})_{1-x}Fe_x$, there is no serious loss of reversible H-capacity, but there is at higher levels.

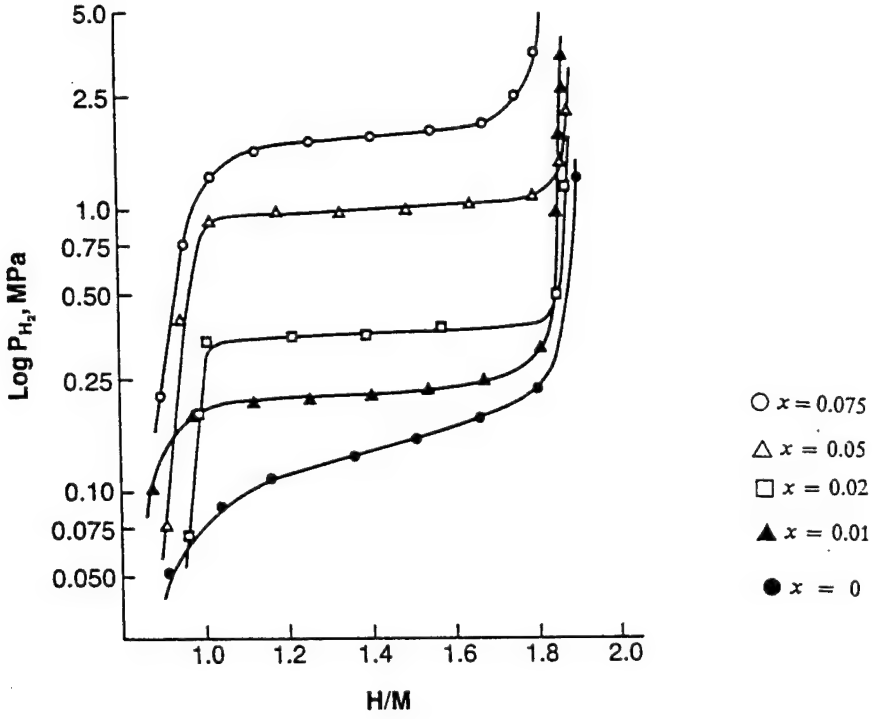

Figure 50
Effect of Fe-Content x on the 80°C Desorption Isotherm of $(V_{0.9}Ti_{0.1})_{1-x}Fe_x$ (Lynch, 85 (351))

It would be instructive to compare the H-storage properties of a representative V solid solution alloy with those of the various intermetallic compounds presented earlier. For that purpose, I choose $(V_{0.9}Ti_{0.1})_{0.95}Fe_{0.05}$, the properties of which are calculated from (Lynch, 85 (351)) for an annealed sample and tabulated as follows:

$\Delta H = 43.2$ kJ/mol H_2
$\Delta S = 0.140$ kJ/molK
25°C Pd = 0.5 atm
T for 1 atm Pd = 36°C
Hysteresis = 0.80
Plateau Slope = 0.45
$(H/M)_{max} = 1.95$
$(wt.\%)_{max} = 3.7$
$(\Delta H/M)_{rev} = 0.95$
$(\Delta wt.\%)_{rev} = 1.8$
$(\Delta H/V)_{rev} = 4.9X10^{22}$ H-atoms/cm^3
Alloy Raw Materials Cost = \$10.63/kg
Alloy Raw Materials Cost = \$0.59/g H stored

The alloy raw materials cost was calculated assuming low-cost ferrotitanium as the source of V and sponge Ti. A comparison of these properties with AB_5, AB_2 and AB hydrides indicates the following relative properties for $(V_{0.9}Ti_{0.1})_{0.95}Fe_{0.05}$:

1. Reversible gravimetric and volumetric H-capacities are very competitive.

2. Hysteresis is high.

3. Raw materials cost, even using low-cost ferrovanadium, is higher than the best AB_2 and AB alloys, but competitive with the AB_5 alloys.

The comparison of this typical V solid solution alloy with the intermetallics may suffer when other qualitative properties are considered. Some of the negative factors listed on pages 28-29 for elemental V hydride probably also hold for V alloys: sensitivities to alloy and gaseous impurities, as well as strain effects associated with cycling, for example. Although gaseous impurity effects have not been quantified for for the V alloys, they are apparently much easier to activate than elemental V (Libowitz, 88 (353)), so there may be some hope that they have greater resistance to gaseous impurities such as O_2 or H_2O vapor. The high melting temperatures and high reactivities of V alloys probably restrict the available melting techniques to "cold crucible" methods such as vacuum arc or electron beam melting. No large-scale commercial batches of such alloys have been produced and hydrided. There has been no long-term cycling of V alloy hydrides, so it is uncertain if disproportionation or other metallurgical instabilities occur.

In summary, V solid solution alloys offer potential alternatives to the commercially established intermetallic compounds for H-storage media for PEM fuel cells. However, before the term "potential" can be removed from that last statement, the following R&D on typical V solid solution alloys is needed:

1. Resistance to typical gaseous impurities must be determined, especially CO, CO_2, O_2, H_2O and N_2. Are there composition effects, e.g., the role of Fe-content?

2. Perform long-term H/D cycling. Are there problems with disproportionation or cyclic strain effects?

3. Do the V alloys pose the same potential container expansion problems as elemental V (cf. Section 3.A.2, p.28-29).

4. Make commercial size lots of V-Ti-Fe alloys, using ferrovanadium. How will the high oxygen and aluminum levels typical of ferrovanadium affect the hydriding properties of the final alloy? Can large batches be made without significant segregation in the ingot, i.e., without variable PCT properties and highly sloping plateaux?

3.H. Magnesium Alloy Hydrides

Mg alloys, in the present state of the the art, do not offer hydrogen storage properties within the 1-10 atm / 0-100°C envelope for PEM fuel cell applications. Unlike the predominantly metallic hydrides discussed heretofore, Mg and its alloys and intermetallic compounds tend to form covalent or complex hydrides. This, coupled with the fact Mg does not alloy with with as many elements as the transition metal, limits the metallurgical possibilities for hydride property tailoring. Although very extensive research on Mg alloy hydrides has been done in the past, no conventional Mg alloys are capable of forming hydrides that will release H_2 anywhere near ambient temperatures. An excellent review of Mg-alloy hydrides covers the history up to 1986 (Selvam, 86). The state of the art has not greatly improved since 1986. The lowest temperature Mg-alloy hydrides to date center around the ß-phase of the Mg-Al-Zn system where H-capacities of about 3 wt.% and 1 atm/200°C desorption conditions are estimated.(Thomas, 97). The above discussion is relative to conventional metallurgical alloys. Some interesting Mg possibilities exist in the areas of composite materials and nanocrystalline materials, discussed below in Section 3.H.

It should be mentioned that this reviewer in involved in an international R&D effort to develop improved hydriding alloys as part of the International Energy Agency Hydrogen Implementing Agreement (see Section 2.C.3, p.25, for associated IEA Internet databases). This effort includes some Mg alloy studies and is aiming at a hydride that will desorb 5 wt.% hydrogen at 150°. Although this target is far from being met, success would bring the state of the Mg art closer to the properties needed for fuel cell H-storage.

3.I Other Approaches

Thus far we have reviewed predominantly single phase alloys and intermetallic compounds made by more or less conventional metallurgy. Other approaches have been considered, especially in recent years. Some of the more important "other approaches" will be briefly reviewed in this section. Because these approaches are experimental and generally incomplete relative to practical H-storage, this review will not be as comprehensive as given earlier for the conventional alloys. However, it is important to identify potential for future progress.

3.I.1. Multiphase Alloys and Composites

It is quite easy to make multiphase alloys by normal melting and/or heat treatment, in fact it is generally easier than making single phase alloys. For the purpose of electrochemical applications (e.g., NiMH batteries), multiphase hydriding alloys are sometimes said to offer advantages as to capacity, charge/discharge rate capability or cyclic capacity retention, the second phases apparently acting as beneficial electrocatalysts or preferred paths for hydrogen penetration (Gutjahr, 73 (72); Notten, 91 (294) & 95 (412); Fetecenko, 92; Tsukahara, 95 & 96; Joubert, 96). For the purpose of gas storage (e.g., for PEM fuel cells), there are modest disadvantages and advantages of multiple phases. The principal disadvantages are losses in reversible capacity (if the second phases do not hydride) or multiple plateaux (if the second phases form hydrides with different PCT properties than the primary phase). An advantage of second phases is they generally make activation easier by providing paths for initial H penetration (see Section 3.D.6, for example). If

the second phase is ductile and of significant amount, then decrepitation-resistant structures can result (Goodell, 80 (256); Ogawa, 88). In the case of AB_5 compounds, an early study of purposely introduced second phases did not identify particular advantages in capacity and post-activation kinetics due the presence of those second phases; in fact the effects were generally the opposite (Goodell, 80 (256)). Thus, for gas applications, I doubt if multiphase alloys made by conventional metallurgy offer significantly increased practical potential over nominally single phase alloys and intermetallic compounds.

There are more interesting possibilities in the area of composite hydrides. By "composite", I mean a mixture of phases (at least one hydriding) that is not in metallurgical equilibrium. Composites are made by powder plating or mechanical mixing that may or may not be followed by sintering or partial melting. For example, the simple blending of two hydriding alloys to produce custom PCT properties such as stepped plateaux has been known for nearly two decades (Suda, 78 & 81 (288)). Another composite class is the "microencapsulated" hydrides. Here hydriding alloy powder particles are plated with Cu or Ni to improve thermal and electrical conductivity, corrosion resistance and decrepitation resistance (Ishikawa, 85 (290) & 86 (291)). A similar approach, especially useful in making MH electrodes, is to dry-blend the hydriding alloy (usually AB_5 or AB_2) with Ni or Cu flake (Yoshinaga, 95 (298)). Non-metallic coatings, particularly fluorides made by surface reactions in aqueous solutions, have been applied to AB_5 and A_2B compounds to impart corrosion resistance and improved activation properties (Suda, 93, Liu, 92 & 94). The addition of rare earth oxides to TiFe (Suzuki, 87 (292)) increases the ease of activation, much like the addition of the rare earth itself (see Section 3.D.6, p.81).

An especially active area of composite research has been a number of attempts to improve the hydriding properties of Mg by various physical additions: $LaNi_5$ (Song, 83), $TiO_2/V_2O_5/Cr_2O_3$ (Khrussanova, 89 (293)), $ZrFe_{1.4}Cr_{0.6}$ or $TiMn_{1.5}$ (Fujii, 91 and Ye, 94), Ni (Bogdanovic´, 93 (485)), $Ti_{0.6}Zr_{0.4}Mn_{0.8}CrCu_{0.2}$ (Orimo, 94 (297)), YNi_2 (Orimo, 94). TiFe (Liang, 95), C (Imamura, 96). With all these composite cases the low temperature Mg hydriding kinetics where greatly improved over those of pure Mg and often also the cyclic life. However, there were no clear and significant increases in H-capacity or MgH_2 desorption temperatures needed to apply Mg to PEM fuel cells.

In striking contrast to the above cited results for Mg composites, a group at the Banaras Hindu University recently reported reversible room-temperature capacities of 3.0-3.6 wt.% for composites of Mg and the AB alloy Ti(Fe,Mn) (Mandel, 94; Dutta, 94 (296)). For example, a typical room temperature desorption isotherm for a 50 wt.% Mg - 50 wt.% Ti(Fe,Mn) composite is shown in Figure 51. The composites were made by the careful melting (partial melting?) of a Mg pellet surrounded by Ti(Fe,Mn) powder, a procedure similar to that also used to make the controversial low temperature hydriding alloy La_2Mg_{17} reported by the same laboratory (see Section 3.F.3, p.97). The authors admit to not understanding the origins of the unexpectedly high capacity, but suggest it is related to the complex multiphase nature of the composite (Mg + Ti(Fe,Mn) as major phases with Ti, TiMg and Ti_2Fe reported as variable minor phases). Both TiMg and Ti_2Fe do not exist on my 1990 binary phase diagrams (Murray, 90), so the metallurgy must be complex indeed. A more recent paper from the same University covers similar composites of Mg and $CFMmNi_5$, where CFMm means cerium-free mischmetal (Sai Raman, 96). Although up to 5.6 wt.% is claimed, such levels of H-capacity are apparently not recoverable at room temperature because only 400-500°C data are shown.

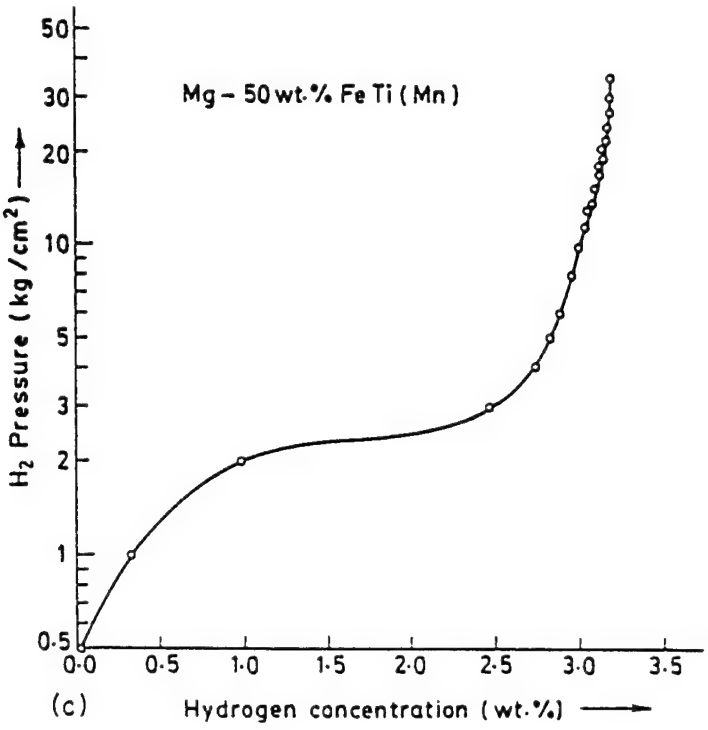

Figure 51
Room Temperature Desorption Isotherm of a Mg-Ti(Fe,Mn) Composite (Mandal, 94)

If the Mandel and Srivastava 1994 room-temperature results on Mg-Ti(Fe,Mn) composites shown in Fig.51 can be confirmed and the material made in practical quantities, then the concept would be of very significant importance to potential military (and civilian) PEM fuel cell use. I am not aware of any confirmations independent of Banaras Hindu University, but would strongly recommend follow-up on this new class of hydride composites. Because the University has contract activities for the US Naval Research Laboratory, a possible mechanism exists for the important distribution of samples to independent researchers.

3.I.2. Amorphous and Nanocrystalline Alloys

Certain amorphous and glassy metals can be made in thin film or ribbon form by sputtering or rapid quenching from the melt, respectively. The subject of amorphous or glassy hydrides has been an active research area for many years, perhaps more for academic than practical reasons. A number of useful reviews exist from the 1980s that are still appropriate to the state of the art: the 1986 NATO Proceedings (Bambakidis, 1986), that of the Allied Chemical group (Libowitz & Maeland, 84) and that of (Bowman, 88). From this reviewer's practical perspective, the following general observations on amorphous and glassy metal hydriding properties are offered:

1. Compared to identical crystalline compositions, amorphous or glassy metals always exhibit P-C isotherms that have no plateau, a consequence of the broad range of interstitial environments. For example, Figure 52 compares the 300°C isotherms of glassy vs. crystalline ZrNi. The complete absence of a plateau is usually undesirable for gas-based practical hydride devices like H-storage where limited charging and discharging pressure ranges are imposed. The absence of a plateau is not necessarily a barrier to the use of amorphous or glassy alloys in a battery (Sapru, 86; Ryan, 91).

2. As also shown in the Fig.52 example, the maximum H-capacity is almost always lower for an

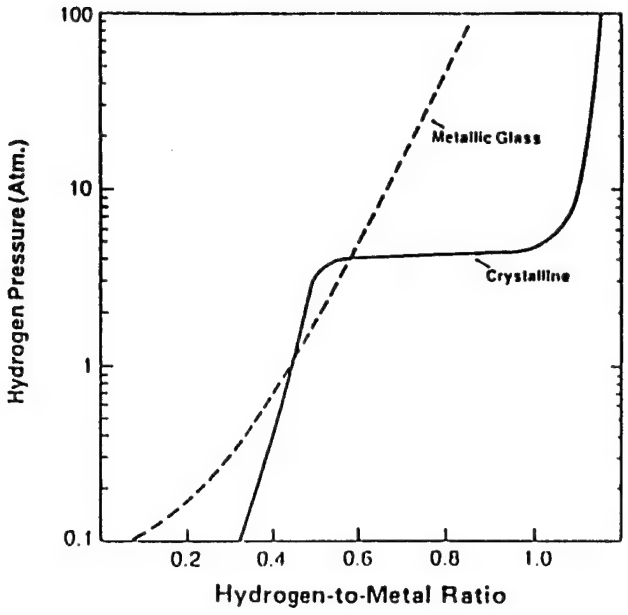

Figure 52
300°C Isotherms of Glassy and Crystalline ZrNi
(Libowitz, 84 after Aoki, 82)

amorphous or glassy alloy than its crystalline counterpart. One rare exception is TiCu where the amorphous phase absorbs about 35% more H than the crystalline phase (Maeland, 80).

3. It is apparently difficult to keep most amorphous alloys amorphous. They are metastable and there is a tendency for them to crystallize with H-absorption or modest heating. Most work has centered on certain alloy systems like Zr-Ni, Ti-Cu and Zr-Pd that are easy to make into glass form and will tend to keep their glassy structure with some H/D cycling.

4. Although the disordered amorphous structure generally shows a higher H-diffusion rate than its crystalline counterpart, this may not be reflected in actual kinetics because of surface effects associated with sample manufacture (Spit, 82 (446)).

5. Amorphous/glassy alloys do tend to have resistance to H/D decrepitation (Spit, 80; Ryan, 91) probably because of their relatively high ductility and fracture toughness combined with the fact a first-order hydride transformation (plateau) does not occur.

In summary, past work has not shown overall advantages for amorphous/glassy hydrides and I am not aware of any practical hydride devices that use them today. However, a very recent report from Toshiba has suggested that the stability of Mg_2Ni-hydride can be greatly reduced if the alloy is mechanically ground (ball milled) to the "amorphous-like", highly strained state (Kohno, 96). An 80°C isotherm for the "first absorption stage" of mechanically ground Mg_2Ni is shown in Figure 53. Compared to crystalline Mg_2Ni (Fig.43&44, pp.90-91), the capacity of amorphous Mg_2Ni is similar and its pressure is indeed much higher, perhaps 250 times higher. However, the reader should be cautioned in reading Fig.53. A virgin absorption curve is not necessarily a measure of desorption pressure, i.e., proof that the desorption pressure has really been raised to similar useful levels and can be sustained through multiple cycles. However, the approach is intriguing enough to deserve further R&D aimed at confirmation and evaluation of practical potential.

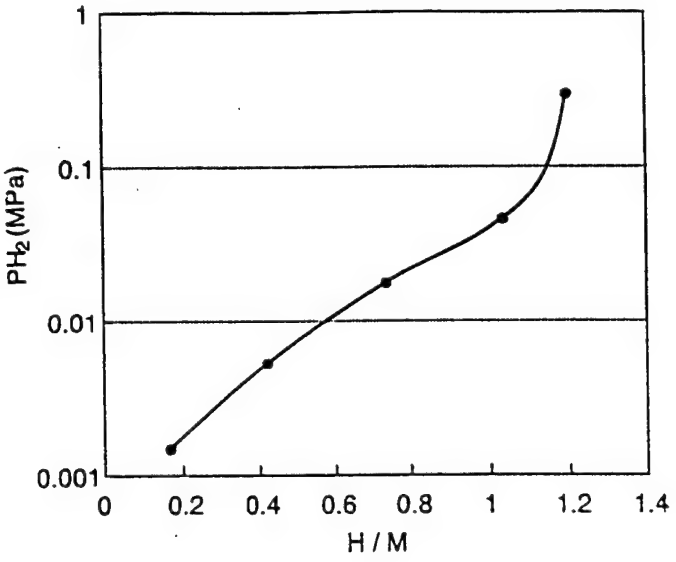

Figure 53
First Absorption Isotherm (80°C) for Amorphous Mg_2Ni
(Kohno, 96)

In recent years, there has been growing interest in hydrides based on nanocrystalline structures. What is usually meant by nanocrystalline (or microcrystalline) structures are very fine crystallites (typically less than 50 nm in size) that are surrounded by essentially amorphous grain boundaries (Zaluski, 97). As the crystallite size becomes smaller and smaller the ratio of grain boundary material to crystalline material increases. Thus, as shown in Figure 54 for TiFe, a nanocrystalline alloy shows hydrogen PCT properties that are intermediate between conventional

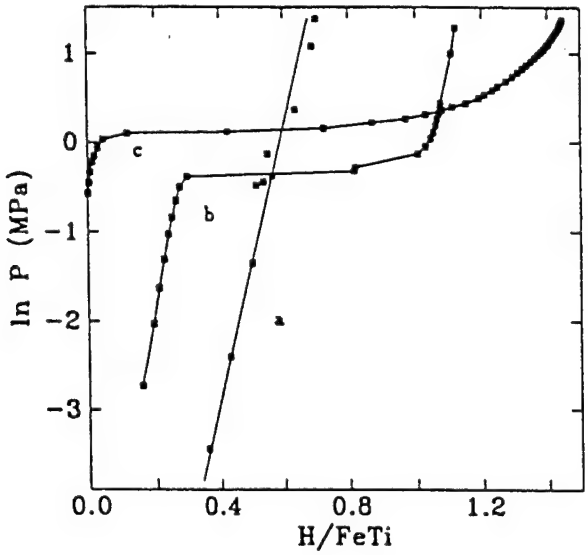

Figure 54
Room Temperature Hydrogen P-C Isotherms for TiFe
(a) amorphous, (b) nanocrystalline, (c) crystalline
(Zaluski, 93)

crystalline and amorphous alloy. Nanocrystalline materials are most conveniently made by high energy ball milling, sometimes called mechanical alloying, a process long known to be useful in synthesizing fine H-active powders of both crystalline and metastable structures directly from the elements, e.g., crystalline Mg_2Ni (Song, 85&87; Stephanov, 87), crystalline $MmNi_{4.5}Al_{0.5}$ (Singh, 93) and metastable Mg-Fe (Konstanchuk, 87).

Although the classic intermetallic compounds $LaNi_5$, TiFe and Mg_2Ni have been successfully made into nanocrystalline structures (see review, Zaluski, 97), most recent reported activity has been directed toward nanocrystalline Mg_2Ni (Zaluski, 95; Fujii, 97; Orimo, 97). The most dramatic effect invariably seen with nanocrystalline alloys is a rapid increase in low temperature kinetics (even room temperature), associated with the fine, clean particles and the disordered grain boundary material. It has been postulated that there is a "cooperation" between the crystallites and disordered inter-grain regions to facilitate hydrogen absorption and desorption at low temperatures (Fujii, 97). In addition, high strain energies associated with ball milling may aid the absorption and/or desorption processes. Unfortunately for our interest in PEM fuel cell H-storage, however, nanocrystalline Mg_2Ni has not yet been made that demonstrates desorption conditions within our 1-10 atm / 0-100°C envelope of interest. The recent progress is in the right direction and should be continued.

Multiphase or composite nanocrystalline materials are also of interest. Examples include Mg with Ni and other catalytic transition metals (Ivanov, 87; Stepanov, 87; Holtz, 97), Mg_2Ni, TiFe & $LaNi_5$ with Pd (Zaluski, 95), La_2Ni_{17} with $LaNi_5$ (Gross, 96) and V with $LaNi_5$ (Lü. 93), among others. In all cases, nanocrystalline kinetics are profoundly improved and activation eased in comparison to the conventional phases. Often resistance to gaseous impurities is improved. In the cases of the room temperature hydrides (TiFe, $LaNi_5$ and V), there may be immediate applicability to fuel cell storage.

Continued R&D is recommended in the area of amorphous, nanocrystalline and other metastable alloys as an alternative to the obvious limits to conventional metallurgy. Can the absorption results shown in Fig.53 for amorphous Mg_2Ni be practically achieved in the desorption mode? Can other amorphous or nanocrystalline materials be engineered to achieve useful room temperature properties as well as have reasonable economics of production? Can the strain energies of ball milling be used to decrease the desorption temperatures of Mg and its alloys? If so, can these metastable structures be hardened against recrystallization, grain growth and other undesirable conversions to metallurgical equilibrium?

3.I.3 Quasicrystalline Alloys

Quasicrystals, offering icosahedral symmetry, offer the possibility of interstitial environments somewhat different from the classic crystal structures. Unfortunately, the number of alloys that form quasicrystals is limited; most are Al-based, unlikely to form hydrides. Recently, however, some Ti-based quasicrystals have been shown to hydride (Viano, 95). Compositions such as $Ti_{45}Zr_{38}Ni_{17}$ and $Ti_{53}Zr_{27}Ni_{20}$ have been hydrided up to 1.6 H/M. As might be expected from the high Ti+Zr contents, temperatures for the desorption of the H_2 are impracticably high (<650°C) and disproportionation is sometimes apparent at such temperatures. The addition of small amounts of Si to $Ti_{53}Zr_{27}Ni_{20}$ results in amorphous (glassy) structures that also hydride. Work on quasicrystal hydrides is in the very early stages and it is far from certain if compositions are possible that will result in practical, easily reversible hydrides.

3.H.4 Polyhydrides

In recent years Jensen and coworkers at the University of Hawaii have identified the potential of certain nonclassical metal complex hydrides for H_2 storage (Mediati, 90 & 92). They have concentrated on Group VIIIA based materials such as $IrH_aX_b(H_2)(PR_3)_2$, where X = Cl, Br or I; R = C_6H_{11}, $C(CH_3)_3$ or $CH(CH_3)_2$; a = 1-2; and b= 1-2. In this general formula (H_2) represents a dihydrogen species (a sort of H_2 molecule) that can bound to the Ir metal atom to form a weak ligand. This ligand can be easily broken and reformed during the reversible H_2 desorption / absorption storage reactions. For example, in the X = Cl version, the reversible reaction with H_2 can be written as

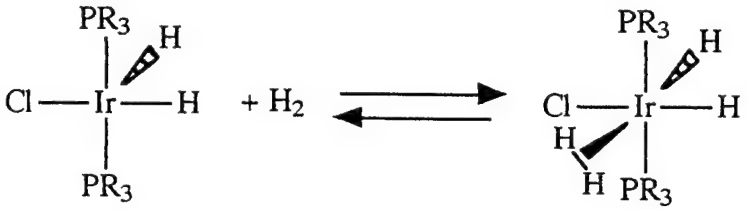

(Eq.28)

The thermodynamics of the storage reaction is controlled by the strength of the dihydrogen ligand with the transition metal atom (Ir) which in turn can be strongly influenced by varying the PR_3 (phosphine alkyl) ligands to that atom. The enthalpies of H_2 absorption and desorption can be adjusted to reasonable levels for ambient temperature use of the concept, but there two problems remain at this writing: (1) The reversible H-contents are disappointingly low, less than 0.5 wt.% (Zidan, 96); and (2) it remains uncertain if useful polyhydrides can be made with other than impracticably expensive noble metal species such as Ir (Jensen, 95). However, a new concept has surfaced for using the polyhydrides not as storage media, but as catalysts for the reversible hydrogenation/dehydrogenation of unsaturated hydrocarbons (Jensen, 96). In this case reversible H-contents of 7wt.% are theoretically possible using only limited amount of the expensive PM-containing polyhydride catalysts. It is too soon to judge if this concept will be useful for fuel cell H_2 storage, but the R&D approach is an interesting and different one.

3.H.5 Complex Hydrides

The metallic hydrides we have discussed earlier, although nicely reversible, have rather low hydrogen storage capacities, at least as measured in weight percent. There are families of more complex hydrides that offer the potential of higher H-capacities, although they are generally less reversible. Some of these complex hydrides are new and some are old. Some have R&D potential for future storage applications and deserve a brief review, at least. The complex hydrides fall in two main categories: transition metal and non-transition-metal complexes.

3.H.5.A. Transition Metal Complex Hydrides

When certain transition metals are combined with a Group IA or IIA element in the presence of hydrogen, a low valence complex of the transition metal and multiple H atoms will form. Such complexes are stabilized by the donation of electrons from the more electropositive IA or IIA elements (e.g., Noreus, 89 (331)). A well used example of this is Mg_2NiH_4, where Mg donates electrons to stabilize the $[NiH_4]^{-4}$ complex. In effect 4 hydrogen atoms bond with a single Ni atom and the two Mg atoms donate two electrons each to stabilize that high-H transition metal complex. There are a number of such transition metal complex hydrides that have been discovered around the world and are at least four groups that have contributed much of the historical activity in this area:

(1) the Yvon group at the University of Geneva, (2) the Noréus group at Stockholm University, (3) the Bronger group at the Technische Hochschule Aachen and (4) the Moyer group at Trinity College (USA).

Table XXVII
Transition Metal Complex Hydrides
Studied at the University of Geneva (Yvon, 97)

Compound	Space Group	Structure*	(H-Content)$_{max}$ wt.%	g H/L	Desorption Temp., °C	Reference
$BaReH_9$	$P6_3/mmc$	$[ReH_9]^{2-}$ ttp	2.7	134	<100	Stetson, 94
$NaKReH_9$	Pnma	$[ReH_9]^{2-}$ ttp	3.5	117	<100	Gingl, 95
Mg_3ReH_7	$P6_3/mmc$	$[ReH_6]^{5-}$ oct	2.7	108	>300	Huang, 93
Mg_2FeH_6	Fm-3m	$[FeH_6]^{4-}$ oct	5.5	150	320	Didisheim, 84
$Ca_4Mg_4Fe_3H_{22}$	P-43m	$[FeH_6]^{4-}$ oct	5.0	122	395	Huang, 92
$SrMg_2FeH_8$	P-3m1	$[RuH_6]^{4-}$ oct	4.0	115	440	Huang, 92
$LiMg_2RuH_7$	$P6_3/mmc$	$[RuH_6]^{4-}$ oct	4.3	113	>400	Huang, 94
Mg_2RuH_4	Cmcm	$[RuH_4]_n$ sad	2.6	95	>400	Bonhomme, 92
Mg_3RuH_3	$P4_2/mnm$	$[Ru_2H_6]^{12-}$ ts	1.7	54	>400	Bonhomme, 92
Mg_2CoH_5	P4/nmm	$[CoH_5]^{4-}$ spy	4.5	126	280	Zolliker, 85
$Mg_6Co_2H_{11}$	Pnma	$[CoH_4]^{5-}$ sad	4.0	97	370	Cerny, 92
Mg_2NiH_4	C2/c	$[NiH_4]^{4-}$ tet	3.6	98	280	Zolliker, 86
$CaMgNiH_4$	$P2_13$	$[NiH_4]^{4-}$ tet	3.2	87	405	Huang, 92
$LiSr_2PdH_5$	P4/mmm	$[PdH_3]^{3-}$ oct	1.7	74	>400	Yoshida, 93
K_2ZnH_4	Pnma	$[ZnH_4]^{2-}$ tet	2.7	57	310	Bortz, 94
K_3ZnH_5	I4/mcm	$[ZnH_4]^{2-}$ tet	2.7	56	360	Bortz, 94

* Geometry of transition metal complex: oct=octahedral, sad=saddle like, spy=square pyramidal, tet=tetrahedral, ts=t-shaped, ttp=tricapped trigonal prismatic

A list of some of the TM complex hydrides studied at Geneva is shown as Table XXVII (Yvon, 97). The structure column gives an indication of the chemical and crystallographic variety of anion complexes that can be formed between the transition metal atom and the hydrogen atoms, the main reason there has been so much academic interest in these materials. The H-capacities of some of these compounds are if interest for fuel cell applications, but generally the desorption temperatures are higher than desired.

Mg_2NiH_4 is an exception to the general situation of TM complex hydrides in that it has a corresponding Mg_2Ni intermetallic. It is very significant that transition metal complex hydrides can be synthesized from combinations of electropositive elements and transition metals that do not form intermetallic compounds. For example, it is well known that Mg and Fe do not alloy at all in the H-free solid metallic state (Nayeb-Hashemi, 90). Yet when Ni and Fe powder are sintered in

H_2, the high-H complex hydride Mg_2FeH_6 forms (Didisheim, 84). Because the formation and decomposition of transition metal complex hydrides usually require some metal atom diffusion, the kinetics tend to be rather slow compared to the traditional interstitial hydrides and high temperatures are needed for H_2 desorption. However the high hydrogen contents possible (e.g. Mg_2FeH_6 = 5.5 wt.% H) give potential to these materials as storage hydrides. Recent work in Geneva on $[ReH_9]^{2-}$ complexes has identified $BaReH_9$, a compound with the largest H/M ratio of any known metal hydride (Stetson, 94). Made by wet chemistry, the H/M ratio of $BaReH_9$ is 4.5 and the volumetric hydrogen packing density is twice that of LH_2. Although $BaReH_9$ would be very expensive because it contains rare Re, Mg_2FeH_6 would be attractive for both low cost and high volumetric capacity.

Continued R&D on the transition metal complex hydrides is recommended. Selective searches should aimed at new materials with better reversibility at low temperatures, if possible. Recent work at Stockholm has examined this class of hydrides as a function of transition metal (d-electron content) and has discovered a number of new materials and structures (Kadir, 94), one of which is $NaPd_3H_2$ which has hybrid characteristics intermediate between interstitial and transition metal complex hydrides (Kadir, 93). Increases in such fundamental chemical and structural understanding could lead to the control necessary for new generations of practical storage hydrides.

3.H.5.B. Non-Transition-Metal Complex Hydrides

This family of hydrides can be described with the general formula $M(M'H_4)_n$, where M is a metal (typically Group IA or IIA) with valence n and M′ is a trivalent Group IIIB metal (typically B, Al or Ga) (Sullivan, 80). Typical examples are shown in Table XXVIII. They consist of M^+

Table XXVIII
Properties of Some Non-Transition-Metal Complex Hydrides
After (Sullivan, 80)

Compound	Density g/cm³	$(H\text{-Content})_{max}$ wt.%	Dissociation Temp., °C	Melting Point, °C
$LiBH_4$	0.66	18.5	--	278
$NaBH_4$	1.074	10.7	--	505
KBH_4	1.177	7.5	--	585
$Be(BH_4)_2$	0.702	20.8	123	--
$Mg(BH_4)_2$	--	14.9	320	--
$Ca(BH_4)_2$	--	11.6	260	--
$Zn(BH_4)_2$	--	8.5	>50	--
$Al(BH_4)_3$	0.549	16.9	--	-64.5
$Zr(BH_4)_4$	1.113	10.8	--	28.7
$Th(BH_4)_4$	2.59	5.5	204	--
$LiAlH_4$	0.917	10.6	190	--
$NaAlH_4$	1.28	7.5	--	178
$Mg(AlH_4)_2$	--	9.3	140	--
$Mg(AlH_4)_2$	--	7.8	>230	--

cations and $M'H_4^-$ anions (i.e., BH_4^- and AlH_4^-), where the H atoms are tetrahedrally coordinated around the M' atom and have a distinct electron-rich character. In addition to the examples shown, there are related cyanoborohydride and alkoxyborohydride derivatives (e.g., $NaBH_3CN$ and $NaBH(OCH_3)_3$, respectively). They are long standing hydrides of commercial importance and are used as reducing agents (H-donors) for the production of specialty chemicals, pharmaceuticals, precious metals and other products.

As can be seen from Table XXVIII, the non-TM-complex hydrides offer high hydrogen weight percents, e.g., $LiBH_4$=18.5 wt.%H. In addition, they are quite reactive with water, hydrolyzing and liberating even more hydrogen gas than suggested from their stoichiometry alone:

$$LiBH_4 + 2H_2O \text{ ----> } LiOH + H_3BO_3 + 4H_2. \qquad \text{(Eq.29)}$$

The water reaction of Eq.29 is not reversible, of course, but these materials have been used for disposable (one-time) sources of H_2 gas. When used in this way, there is a tendency to use the term "chemical hydrides". Eq.29 liberates 4.1 L (STP) of H_2 per gram of $LiBH_4$ (Sullivan, 80). As mentioned in Section 1.B (p.3), this fact has led to non-TM metal complex hydrides being suggested as a high energy density source of H_2 fuel for submersible vehicles (Lynch, 89).

Ideally for a fuel cell application, we do not want to destroy the rather expensive hydride each time by the above hydrolysis reaction. The main problem is that these hydrides cannot be easily made by direct reaction of the metals with gaseous H_2, but are usually synthesized by various solvent chemical reactions. However, as implied in Table XXVIII, they can sometimes be thermally decomposed at reasonable temperatures in the absence of H_20. The challenge is how to make this class of hydrides more reversible. Fortunately, there has been very recent progress in this direction for the catalyzed Na-Al hydrides.

3.H.5.C. Ti-doped Na-Al Hydrides

$NaAlH_4$ can be made from the elements (molten Na and Al) by a direct one-step reaction with H_2, but at inconveniently high temperatures (200-400°C) and pressures (100-400 atm) (Dymova, 74). It can then be thermally decomposed at 210°C in a two-step reaction with the intermediate product being Na_3AlH_6 (Dymova, 75). But apparently Na_3AlH_6 cannot be made by direction reaction with the elements, at least in the uncatalyzed state (Ashby, 66). Recently, Bogdanovic' has importantly discovered that the entire two-step reaction can be made reversible (absorption and desorption) by the addition of Ti-catalysts, e.g. ß-$TiCl_3$ (Bogdanovic', 97). Thus the entire two-step reaction

$$NaAlH_4 \text{ <---> } 1/3\ Na_3AlH_6 + 2/3\ H_2 \text{ <---> } NaH + Al + 3/2\ H_2 \qquad \text{(Eq.30)}$$

becomes usable in a reversible storage sense. Isotherms for both absorption and desorption are shown in Figure 55. Note the two plateaux and the lack of A/D pressure hysteresis. The H-capacity for Eq.30 is about 5.6 wt.%; under cyclic conditions a respectable range of 3.1-4.2 wt.% reversible capacity is achieved. Equilibrium pressures are significant. Unfortunately, kinetics are low even with catalysis, desorption requiring 10s of hours below 160°C. This may be partly a result of the diffusion changes in metal atom stoichiometry during the reactions. Although the required temperatures are higher that we have available from a PEM fuel cell, Bogdanovic' has made significant progress in converting what has been considered a classic non-reversible hydride system into one that shows clear potential for practical H-storage at very attractive weight percents.

Further work is clearly warranted and should be directed in improving the catalysis for improved

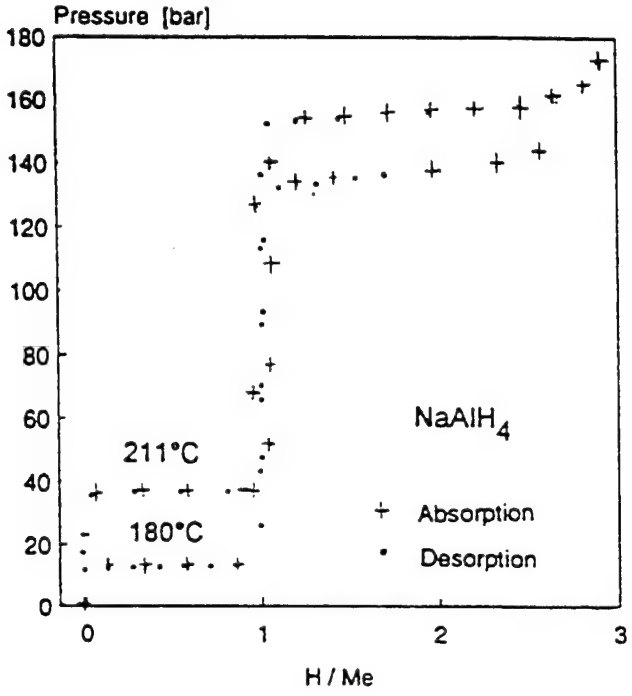

Figure 55
Hydrogen P-C Isotherms for Ti-Catalyzed $NaAlH_4$
(Bogdanovic´, 97)

kinetics. There were also cyclic losses in capacity noted, and these must be understood. The potential for potential control of the thermodynamics were shown by Bogdanovic´(e.g., partial substitution of Na by Li). Other substitutional possibilities probably exist in this and other non-transition-metal hydrides.

3.H.6 Carbon

It might be argued that because carbon is not a metal and does not fit in a review on metal hydrides, However, C does have some real possibilities for hydrogen storage and therefore it deserves a brief introduction and comparison to hydride storage.

It has long been known that high surface area "activated" carbon will physisorb molecular H_2 and serve as a storage medium for the gas (Carpetis, 80). However, because adsorption is by relatively weak Van der Walls interactions, significant storage of H_2 on C occurs only when the C is cold and high pressures are applied. Using the best activated carbon of 1980, H_2 weight percents of 6.4 were accomplished at 77K and 41 atm pressure. The disadvantages of a cryogenic system in terms of cost, insulation, refrigeration, etc., are obvious. Recent carbon work has employed KOH treated carbons that have cage-like structures and surface areas on the order of 3000 m^2g^{-1} (Chahine, 94). With these carbons, significant H_2 adsorption can be accomplished at higher temperatures, e.g., 2-3 wt.% at 175K and 50 atm. The problem with all the activated carbons, however, is that they have low bulk densities and the result is poor volumetric H-density compared to hydrides or even LH_2. For example, if an H_2 storage tank were made of the 175K

example just given, about half of the H_2 would be on the C-surface and half in the gas phase. Thus for a volume-limited submarine fuel cell application, or even a land vehicle, the addition of carbon and its required cooling would not offer major improvements over conventional compressed gas storage.

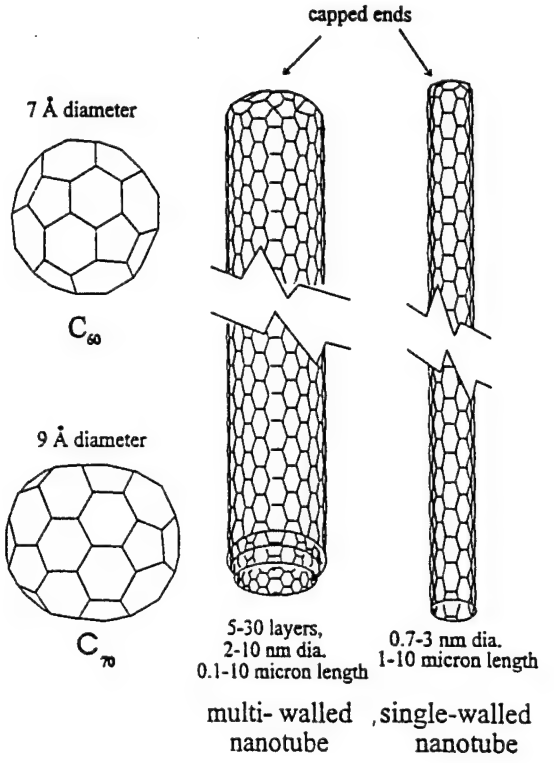

Figure 56
Types of Fullerene Carbon (Withers, 97)

The last few years have seen a dramatic increase in work on fullerene carbons, a special variety of C resulting from the condensation of its gaseous phase (e.g., near a C-arc). It is said that the first few years after the discovery of fullerenes, a new paper on the subject appeared on the average of every 13 hours (Withers, 97). A small fraction of this massive activity is looking at the possibility of hydrogen storage. Of the most common forms of fullerenes shown in Figure 56, H-storage is being considered with the C60 "buckyballs" and the single-walled nanotubes (SWNTs).

Single-walled nanotubes have internal dimensions on the order of 1-2 nm, about what is needed for the capillary "condensation" of H_2 near room temperature. For this reason, Heben an co-workers at the National Renewable Energy Laboratory (USA) have been examining the potential of using SWNTs for H-storage (Dillon, 97). The situation is shown rather nicely by the temperature programmed desorption (TPD) curves of Figure 57 which compares the desorption of H_2 from an activated carbon (AC) (b) with two forms of SWNTs, (a) and (c). Except for the much higher quantity of H_2 desorbed from the SWNT, the TPD profile of the as-prepared SWNT (Fig.57(a)) is similar to the AC (Fig.57(b)) with peaks in desorption about 150K. However, when SWNTs are heated under vacuum or an oxidizing atmosphere the end caps shown in Fig.56 are removed and the bore of the SWNT then becomes available for H_2 filling. The result, shown in Fig.57(c), is an additional broad TPD peak centered around room temperature, 300K. Although 100% "uncapped" SWNTs have not yet been made, quantitative measurements of the

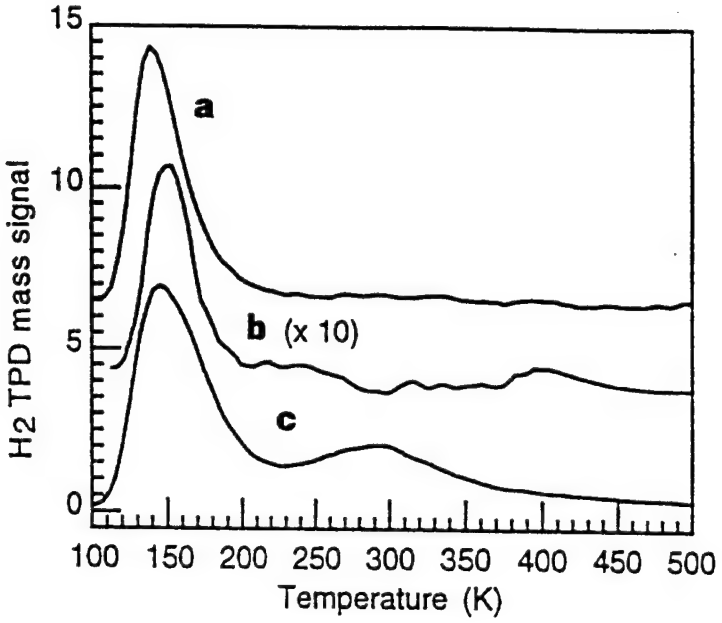

Figure 57
Temperature Programmed H_2 Desorption Spectra of Carbons
(a) as-produced single-wall nanotube sample,
(b) activated carbon (signal magnified 10 times),
(c) 970K vacuum treated single-wall nanotube sample
(Dillon, 97)

300K peak on partial SWNT samples suggest that if 100% SWNTs samples could be made, then 5-10 wt.% room temperature H-storage capacity might be possible. As will be discussed in Section 4, volumetric H-densities of SWNTs are good and would be competitive with existing metal hydrides. Therefore the potential for room-temperature H_2 storage has clearly been shown for SWNT carbon and R&D in the area should continue to evaluate this potential. It remains to be seen if high-volume, low-cost production of nearly pure SWNTs can be accomplished, but at this moment progress is being made in that direction (Withers, 97); however, target fullerene prices of $250/kg still sounds to expensive for tonnage applications for fuel cell H-storage.

As outlined by (Withers, 97), the C_{60} fullerenes ("buckyballs") can be hydrogenated with gaseous H_2 using high pressures (135 atm) and temperatures (200°C), although "catalysts" can reduce the necessary conditions to the more practical levels of 8 atm and 120°C. H-contents as high as $C_{60}H_{48}$ (6.3 wt.%H) have been achieved. Unlike the purely physisorption process with SWNTs, C_{60} carbon atoms form relatively strong covalent bonds with H atoms. In effect, the normal C=C double bonds of the C_{60} molecule are converted to C-C and C-H single bonds preserving the fullerene structure and chemically binding H. Although the gravimetric H-capacity is high for $C_{60}H_{48}$, unfortunately the C-H bond is uncomfortably strong, on the order of 285 kJ/mol. This means that temperatures on the order of 400°C are needed for the breaking of that bond and the desired desorption of H_2 gas (Wang, 96), temperatures too high for PEM fuel cells. The key for the practical development of fullerene "hydrides" will be to decrease the C-H bond strength so that practical desorption temperatures (hopefully ambient) can be accomplished. As shown throughout this review, this "destabilization" process has been successfully achieved with metal hydrides. Hopefully, history can be repeated with fullerenes.

One final form of carbon proposed for near ambient temperature H-storage applications are "graphite nanofibres", developed by Rodriguez and Baker of Northeastern University, Boston (Hill, 96). The new form of graphite is made by reacting hydrocarbons and CO on Ni-and Fe-based catalysts. By a mechanism not fully understood by the developers, this form of carbon is said to be capable of "condensing" extraordinary amounts of molecular H_2 within the graphite layers, namely up to levels of CH_{36} (75 wt.% hydrogen)! Because H-contents of strongly bonded C-H chemical compounds do not even exceed methane CH_4 (25 wt.%H), the proposal of CH_{36} for physically intercalated H_2 has been met with some skepticism, to say the least. To my knowledge, the claims of Rodriguez and Baker have not been independently substantiated to date, but I understand attempts are being made. If even partially confirmed, this new form of graphite would obviously be of great interest for H-storage. As always in science, time will be the great resolver of this interesting controversy.

4. COMPARATIVE OVERVIEW

A rather detailed review of hydrides and their properties have been given. Although comparisons were made during that review, it is perhaps worthwhile to stand back and make a comparative summary. First, it may be useful to compare hydride-based H-storage with other options using Figure 58, which is a map of volumetric vs. gravimetric H-densities (Dillon, 97).

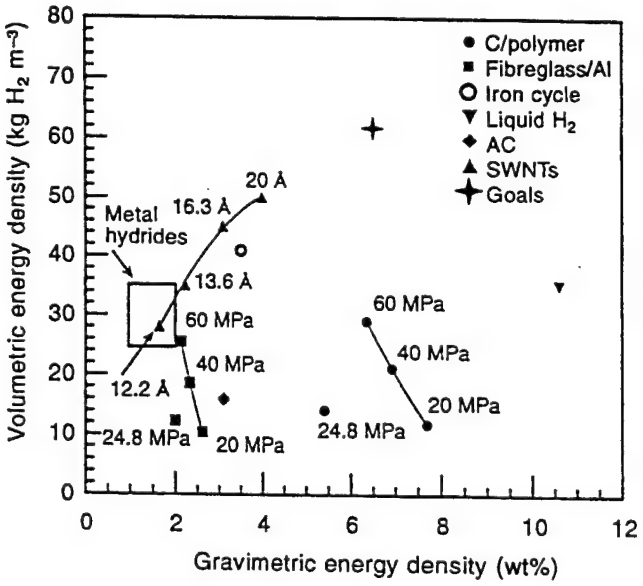

Figure 58
Volumetric and Gravimetric H-Densities for H-Storage Systems
Storage Methods: C/polymer = C-wrapped polymer gas cylinders;
Fiberglass/Al = fiberglass-wrapped Al gas cylinders;
Iron cycle = steam-Fe reaction; AC = activated C;
SWNTs = single-walled nanotubes (Dillon, 97)

Each data point represents an estimate of the system, H-storage medium and container. Metal hydrides are included as a box representing a range of storage systems containing both ambient and high dissociation temperature materials (DeLuchi, 89; T-Raissi, 96). Such a comparison as Fig.58

is dependent on many assumptions as to the systems design and pressure-code safety factors, but for our purposes gives a good reference frame. The goal shown is for fuel powered land vehicles (DeLuchi, 89). The metal hydride options offer good volumetric H-densities but poor gravimetric densities, as we have long known. Although far from perfected at this moment, the authors of Fig.58 feel that SWNTs have the potential to exceed hydrides in both volumetric and gravimetric H-densities. If one does not care about volumetric density and very high required pressures (200-600 atm), then C-wrapped polymer gas tanks offer the best gravimetric densities other than LH_2, namely several wt.%. Although each of the H-storage techniques shown in Fig.28 may have its own place within the spectrum of possible military fuel cell applications, it was argued in Section 1.A (p.3) that rechargeable metal hydrides are probably the best option for manned submarines.

The hydriding alloys that provide the most useful PCT properties for ambient temperature application to PEM fuel cells are of the AB_5, AB_2, AB and V-based solid solution families. Although the data were shown earlier in each alloy section, Tables XXIX and XXX below compare selected alloys from these systems on a side-by-side basis with regard to PCT and H-capacity properties, respectively. In choosing the alloys shown for these comparisons over many other possibilities, some consideration was given to better H-capacity, past commercial experience and low alloy cost within each family. They should be considered to be reasonable "practical" representations of the more favorable members of the respective families.

From the general view of PCT (Table XXIX) properties, all of the alloys shown have properties within the range of applicability to PEM fuel cell waste heat and input pressure requirements. Which in particular would be the most appropriate depends on the exact engineering parameters of the particular application, details of which are beyond the scope of this broad review. For example, the AB_5s tend to have less plateau hysteresis and slope and favorable secondary properties but may suffer from capacity and cost disadvantages. H-capacity and cost considerations alone (Table XXX) favor the AB and AB_2 compounds.

Table XXIX
Comparative PCT Properties of Selected Hydrides

Composition	ΔH, kJ/mol	ΔS, kJ/molK	25°C P_d, atm	T for 1 atm P_d	Plateau Hysteresis	Plateau Slope
AB_5-Type						
$MmNi_{4.5}Al_{0.5}$	28.0	0.105	3.8	-6	0.11	0.36
$LaNi_5$	30.8	0.108	1.8	12	0.13	0.13
$CaNi_5$	31.9	0.101	0.5	43	0.16	0.19
AB_2-Type						
$Ti_{0.98}Zr_{0.02}V_{0.43}Fe_{0.09}Cr_{0.05}Mn_{1.5}$	27.4	0.112	11	-28	--	1.1
$TiMn_{1.5}$	28.7	0.114	8.4	-21	0.93	0.57
AB-Type						
TiFe	28.1	0.106	4.1	-8	0.64	0.0
$TiFe_{0.85}Mn_{0.15}$	29.5	0.107	2.6	3	0.62	0.92
SS-Type						
$(V_{0.9}Ti_{0.1})_{0.95}Fe_{0.05}$	43.2	0.140	0.5	36	0.80	0.45

Table XXX
Comparative Capacity and Cost Properties of Selected Hydrides

Composition	Density	$(\text{H-Capacity})_{max}$		$(\text{H-Capacity})_{rev}$			Alloy RMC**	
	g/cm^3	H/M	wt.%	ΔH/M	Δwt,%	$\Delta N_H/V^*$	$/kg	$/g H
AB_5-Type								
$MmNi_{4.5}Al_{0.5}$	8.1	0.85	1.2	0.58	0.83	3.5	7.17	0.86
$LaNi_5$	8.3	1.08	1.49	0.93	1.28	5.2	9.87	0.77
$CaNi_5$	6.6	1.05	1.87	0.55	0.99	3.4	7.56	0.76
AB_2-Type								
$Ti_{0.98}Zr_{0.02}V_{0.43}Fe_{0.09}Cr_{0.05}Mn_{1.5}$	5.8	0.99	1.9	0.7	1.3	3.8	4.82	0.37
$TiMn_{1.5}$	6.4	0.99	1.86	0.65	1.15	3.8	4.99	0.44
AB-Type								
TiFe	6.5	0.975	1.86	0.79	1.5	5.0	4.68	0.31
$TiFe_{0.85}Mn_{0.15}$	6.5	1.0	1.9	0.80	1.5	5.0	4.83	0.32
SS-Type								
$(V_{0.9}Ti_{0.1})_{0.95}Fe_{0.05}$	6.0	1.95	3.7	0.95	1.8	4.9	10.63	0.59

* Reversible volumetric capacities are approximate and in units of 10^{22} H-atoms/crystal cm^3 (i.e., interparticle void volumes not included)
** RMC = Raw Materials Cost; $/g H based on $(\text{H-Capacity})_{rev}$

Table XXXI
Qualitative Overview of Hydride Types as to Attributes
Attribute Key: - = problem; 0 = neutral; + = good; ? = uncertain

Attribute	AB_5	AB_2	AB	A_2B	V-SS
Versatility	+	+	+	-/0	0
H-Capacity	0	0/+	0/+	+	+
PCT	+	+	+	-	+
Activation	+	0	-/0	0	0
Impurity Effects	+	0	-	0	-/?
Cyclic Stability	-/0/+	-/0/?	-/0	0/?	?
Ease of manufacture	+	0	+	0	?
Pyrophoricity	0	-	+	+	+/0
Cost	0	+	+	+	-/0

A complete story is not possible with only the quantitative PCT, H-capacity and cost parameters listed in Tables XXIX and XXX. As discussed in the detailed sections on each family of materials, there are a number of "other properties" that must be taken into consideration when trying to decide which alloy fits best for a particular application. An attempt to create a qualitative matrix of such properties and attributes is shown in Table XXXI. It should be understood that such a matrix is quite subjective an somewhat dependent on the reviewer, including personal experience that might be involved. This is my own version and it should not be considered absolute or perfect. It is included simply as a reminder that the world of hydride technology is a complex one and requires detailed consideration, literature searching and even experimental data verification and analysis when a specific new application arises.

5. SUMMARY OF SUGGESTED R&D WORK NEEDED

Detailed suggestions for further R&D directed toward the remaining problems of hydride storage of hydrogen for PEM fuel cells are given in each section of this report. This section summarizes those suggestions, with reference to the earlier pages where more detail can be found.

5.A. AB_5 Compounds (Section 3.B.7, p.50)

1. Improve $CaNi_5$ disproportionation resistance and enlarge the main plateau.
2. Develop a full understanding of the action of CO impurities on AB_5 surfaces.
3. Generate more quantitative safety data, especially on the substituted $MmNi_5$ alloys.

5.B. AB_2 Compounds (Section 3.C.7, p.71)

1. Confirm the reported hydride properties of $Ho_{0.8}Zr_{0.2}Fe_2$. If confirmation is positive, develop lower-cost alternatives to Ho.
2. Find modifications that make the Laves phases $TiFe_2$ and $ZrFe_2$ hydride.
3. Develop a full understanding of the ability of AB_2s to getter CO, along with determining methods of regeneration.
4. Quantify the impurity effects of O_2 and H_2O for the AB_2 compounds.
5. Generate quantitative safety data, especially for the Mn-containing AB_2 alloys.

5.C. AB Compounds (Section 3.D.7, P.87)

1. Improve the resistance of TiFe-type alloys to common gaseous impurities (especially O_2 and H_2O vapor). Understand the reactions with CO.
2. Work on the upper plateau instability. Try substitutions and other approaches to merge the two plateaux into one.

5D. AB_3 Compounds (Section 3.F.1, p.96)

1. Can $CeFe_3$ (and $MmFe_3$) be stabilized with partial ternary substitutions?
2. How can PCT and other properties of AB_3s be controlled by the partial substitution of such things as Al, Sn, etc.?
3. Determine the long-term, room-temperature cyclic stability of a few representative AB_3s.
4. Quantify the basic gaseous impurity resistance of the AB_3 family, especially for impurities such as CO and H_2O.

5.E. A_2B_7 Compounds (Section 3.F.2. p.98)

Determine secondary (non-PCT) properties for the A_2B_7 family, essentially similar R&D to the AB_3 compounds (see Section 5.D).

5.F. La_2Mg_{17} (Section 3.F.3, p.99)

Attempt to confirm the extraordinary room temperature hydriding properties reported for La_2Mg_{17}.

5.G. V-Solid Solution Alloys (Section 3.G.2, p.103)

1. Determine resistance to typical gaseous impurities, especially CO, CO_2, O_2, H_2O and N_2.
2. Perform long-term H/D cycling to quantify possible disproportionation or cyclic strain effects?
3. Do the V alloys pose the same potential container expansion problems as elemental V?
4. Make commercial size lots of V-Ti-Fe alloys, using ferrovanadium.

5.H. Composites (Section 3.H.1, p.106)

Try to confirm the unexpectedly high room temperature H-capacity of Mg-Ti(Fe,Mn) composites.

5.I. Amorphous and Nanocrystalline Alloys (Section 3.H.2, p.109)

1. Can the low-temperature absorption results reported for amorphous Mg_2Ni be practically achieved in the desorption mode?
2. Can amorphous or nanocrystalline materials be engineered to achieve useful room temperature properties as well as have reasonable economics of production?
3. Can the strain energies of ball milling be used to decrease the desorption temperatures of Mg and its alloys and if so, can these metastable structures be stabilized against conversion to metallurgical equilibrium?

5.J Quasicrystalline Alloys (Section 3.I.3, p.109)

Search for new families of hydridable quasicrystals beyond the overly stable Ti-Zr-Ni system.

5.K Polyhydrides (Section 3.H.4, p.110)

Continue exploratory work on their application as catalysts for reversible organic hydrogenation and dehydrogenation.

5.L Transition Metal Complex Hydrides (Section 3.H.5.A, p.112)

Further develop understanding of this large class of hydrides and search for more reversible species.

5.M Na-Al and other Non-Transition-Metal Hydrides (Section 3.H.5.B, p.113 and 3.H.5.C, p.114)

1. Search for improved catalysts for the reversible Na-Al hydride system.
2. Search for possible catalyzed reversibility in other systems of this class.

REFERENCES

References are presented primarily in alphabetic order of the surname of the first author, with secondary ordering as to the year published. The number in parentheses at the end of the citation, if any, is the IEA/DOE/SNL Reference Database Number (see Section 2.C.3, p.25).

Ahn, H.-J.; Kim, Y.-G.; and Lee, J.Y., J. Alloys and Compounds, **196** (1993), 45-53. "Structural changes of the Laves phase $ErFe_2$ during static and cyclic hydrogenation treatments"

Adzic, G. D.; Johnson, J. R.; Reilly, J. J.; McBreen, J.; Mukerjee, S.; and et al, J. Electrochem. Soc., **142** (1995), 3429-3433 "Cerium Content and Cyclic Life of Multicomponent AB_5 Hydride Electrodes" (264)

Alefeld, G.; Völkl, J., Eds., Hydrogen in Matals I & II, Topics in Appl. Phys., **28 - 29** (1978)

Anderson, J. L.; Wallace, T. C.; Bowman, A. L.; Radosevich, C. L.; and Courtney, M. L., Los Alamos Informal Report UC-4, LA-5320-MS (1973) "Hydrogen Absorption by AB_5 Compounds" (99)

Andreev, B. M.; Dobryanin, O. V.; Magomedbekov, E. P.; Pak, Yu. S.; and Shitikov, V. V., Russian J. Phys. Chem., **56** (1982), 283-284 "The Interaction of Hydrogen with the Intermetallic Compound Titanium Manganide ($TiMn_{1.5}$)" (522)

Anon., Inco Material Safety Data Sheet, DOT I.D. No. NA 9188, International Nickel, Saddle Brook, NJ, Jan. 1, 1988, "Inco Nickel Powder Type 123"

Aoki, K.; Horata, A.; and Matsumoto, T., Proc. 4th Int. Conf. on Rapidly Quenched Matals, T. Matsumoto and K. Suzuki, Eds., Japan Inst. of Metals, Sendai, 1982, 1649-1652

Apostolov, A.; Stanev, N.; and Tcholakov, P., J. of Less-Common Metals, **110** (1985), 127-129 "Hydrogen Desorption Characteristics of $MmNi_{5-x}Fe_x$ Compounds" (567)

Appleby, A. J.; Foulkes, F. R., Fuel Cell Handbook, Krieger Pub., Malabar, FL, 1993

Arita, M.; Kinaka, R.; and Someno, M., Met. Trans. A, **10A** (1979), 529-534 "Application of the Metal-Hydrogen Equilibrium for Determining Thermodynamic Properties in the Ti-Cu System" (495)

Asada, K.; Ono, K.; Yamaguchi, K.; Yamamoto, T.; Maekawa, A.; Oe, S.; and Yamawaki, M., J. of Alloys and Compounds, **231** (1995), 780-784 "Hydrogen absorption properties of uranium alloys" (628)

Ashby, E. C.; Kobetz, P., Inorg. Chem., **5** (1966), 1615-1617, "The Direct Synthesis of Ni_3AlH_6"

Aubertin, F.; Gonser, U.; Becker, G.; and Detemple, I., Z. Phys. Chem. NF, **163** (1989), 243-248 "Phase Separation in Hf_2Fe Hydrides" (425)

Balasubramaniam, R.; Mungole, M. N.; and Rai, K. N., J. of Alloys and Compounds, **196** (1993), 63-70 "Hydriding properties of $MmNi_5$ system with aluminum, manganese and tin substitutions" (588)

Bambakidis, G.; Bowman, R. C., Eds., Hydrogen in Disordered and Amorphous Solids, Plenum Press (1986)

Barrett, C. S., Metallography, Structures and Phase Diagrams, Metals Handbook, T. Lyman, Ed., **8**, 1973, ASM, Metals Park, OH, 233-250. "Crystal Structure of Metals"

Barrett, C. S.; Massalski, T.B., Structure of Metals, 3rd Ed., Pergamon, Oxford, 1980

Bartscher, W.; Rebizant, J., J. of Less-Common Metals, **136** (1988), 385-394 "Equilibria and Thermodynamic Properties of the $ThZr_2$-H System" (556)

Bawa, M. S.; Ziem, E. A., Int. J. Hydrogen Energy, **7** (1982), 775-781 "Long Term Testing and Stability of $CaNi_5$ Alloy for a Hydrogen Storage Application" (155)

Beck, R.; Mueller, W. M., Summary Report, AEC Contract AT(33-3)-3, Denver Research Institute (1962) "Investigation of Hydriding Characteristics of Intermetallic Compounds" (45)

Bernauer, O.; Ziegler, K., U. S. Pat. 4,457,891 (1984) "Hydrogen Storage Alloy" (521)

Bernauer, O.; Halene, C., J. of Less-Common Metals, **131** (1987), 213-224 "Properties of Metal Hydrides for Use in Industrial Applications" (610)

Bernauer, O., Z. Phys. Chem. NF, **164** (1989), 1381-1390 "Metal Hydride Storages" (341)

Bernauer, O.; Topler, J.; Noreus, D.; Hempelmann, R.; and Richter, D., Int. J. Hydrogen Energy, **14** (1989), 187-200 "Fundamentals and Properties of some Ti/Mn Based Laves Phase Hydrides" (344)

Bogdanovic, B.; Hartwig, T. H.; and Splietoff, B., Int. J. Hydrogen Energy, **18** (1993), 575-589 "The development, Testing and Optimization of Energy Storage Materials Based on the MgH_2-Mg System" (485)

Bogdanovic´, B.; Schwickardi, M.; J. of Alloys and Compounds, 1997, in press, "Ti-doped alkali metal aluminum hydrides as potential reversible hydrogen storage materials"

Bonhomme, F.; Yvon, K.; Triscone, G.; Jansen, K.; Auffermann, G.; Müller, W.; Bronger, W.; and Fischer, P., J. of Alloys and Compounds, **178** (1992), 161-166, "Orthorhombic dimagnesium ruthenium tetrahydride containing a diamagnetic $[RuH_4]^{-4}$ complex ion with C_{2v} symmetry"

Bonhomme, F.; Yvon, K.; and Fischer, P., J. of Alloys and Compounds, **186** (1992), 309-314, "Tetragonal trimagnesium ruthenium trideuteride, Mg_3RuD_3, containing dinuclear $[Ru_2D_6]^{12-}$ complex ions"

Bortz, M; Yvon, K.; and Fischer, P., J. of Alloys and Compounds, **216** (1994), 39-42, "Synthesis and structure determination of complex zinc hydrides. Part 1: Dipotassiumtetrahydridozincate (II) hydride, $K_2[ZnH_4]H$"

Bortz, M; Yvon, K.; and Fischer, P., J. of Alloys and Compounds, **216** (1994), 43-45, "Synthesis and structure determination of complex zinc hydrides. Part 2:

Tripotassiumtetrahydridozincate (II) hydride, $K_3[ZnH_4]H$"

Boulghallat, M.; Gerard, N.; Canet, O.; and Percheron-Guegan, A., Z. Phys. Chem. NF, **79** (1993), 199-209 "Correlation Between structure and Hydriding Behaviors in Laves Phases: $Zr(M_xCr_{1-x})2$, M=Fe,Ni" (375)

Bououdina, M.; Soubeyroux, J. L.; Fruchart, D.; Akiba, E.; and Nomura, K., J. of Alloys and Compounds, **235** (1996), 93-96 "Study of the System $Zr(Cr_{0.8-x}Co_xV_{0.2})_2$-$H_2$" (585)

Bowman, R. C., Material Science Forum, **31** (1988), 197-228, "Preparation and Properties of Amorphous Hydrides"

Bowman, R. C.; Freeman, B. D., and Philips, J. R., Cryogenics, **32** (1992), 127-137, "Evaluation of metal hydride compressors for applications in Joule-Thompson cryocoolers"

Bowman, R. C.; Luo, C. H.; Ahn, C. C.; Witham, C. K.; and Fultz, B., J. of Alloys and Compounds, **217** (1995), 185-192 "The effect of tin on the degradation of $LaNi_{(5-y)}Sn_y$ metal hydrides during thermal cycling" (349)

Bronca, V.; Bergman, P.; Ghaemmaghami, V.; Khatamian, D.; and Manchester, F. D., J. of Less-Common Metals, **108** (1985), 313-325 "Hydrogen Absorption Characteristics of an FeTi+Misch Metal Alloy" (549)

Bruzzone, G.; Costa, G.; Ferretti, M.; and Olcese, G. L., Int. J. of Hydrogen Energy, **5** (1980), 317-322 "Hydrogen Storage in a Berryllium Substituted TiFe Compound" (421)

Bruzzone, G.; Costa, G.; Ferretti, M.; and Olcese, G. L., Int. J. of Hydrogen Energy, **6** (1981), 181-184 "Hydrogen Storage in Aluminum-Substituted TiFe Compounds" (422)

Buchner, H.; Gutjahr, M. A.; Beccu, K.; and Saufferer, H., Z. Metallkunde, **63** (1972), 497-500 "Hydrogen in Intermetallic Phases: The System Titanium-Nickel-Hydrogen" (71)

Burch, R.; Mason, N. B., J. Chem. Soc., Faraday Trans. I, **75** (1979), 561-577 "Absorption of Hydrogen by Titanium-Cobalt and Titanium-Nickel Intermetallic Alloys, Part 1 - Experimental Results" (500)

Burch, R.; Mason, N. B., J. Chem. Soc., Faraday Trans. I, **75** (1979), 578-590 "Absorption of Hydrogen by Titanium-Cobalt and Titanium-Nickel Intermetallic Compounds, Part 2 Thermodynamic Parameters and Theoretical Models" (501)

Burnasheva, V. V.; Klimeshin, V. V.; and Semenenko, K. N., Izvestiya Akademii Nauk SSSR, Neorganicheskie Materialy, **15** (1977), 251-255 "Equilibria in the Systems RCo_3-H_2, Where R is Ce, Pr, Tb, Dy, or Er" (543)

Burnasheva, V. V.; Ivanov, A. V.; and Semenenko, K. N., Izvestiya Akademii Nauk SSSr, Neorganicheskie Materialy, **14** (1978), 1302-1307 "Reaction of Hydrogen with Intermetallic Compounds of Composition(Ln)M_2, where M is Fe, Co, or Ni" (520)

Burnasheva, V. V.; Yartys', V. A.; Ivanov, A. V.; and Semenenko, K. N., Russian J. Inorganic Chem., **24** (1979), 1130-1132 "Hydride Phases Based on Intermetallic Compounds with a Laves Phase structure Formed by Yttrium, Lanthanum, and the Lanthanides" (519)

Buschow, K. H. J.; van Mal, H. H., J. of Less-Common Metals, **29** (1972), 203-210 "Phase Relations and Hydrogen Absorption in the Lanthanum-Nickel System" (95)

Buschow, K. H. J.; Mal, H. H. Van; and Miedema, A. R., J. of Less-Common Metals, **42** (1975), 163-178 "Hydrogen Absorption in Intermetallic Compounds of Thorium" (187)

Buschow, K. H. J.; van Diepen, A. M., Solid State Comm., **19** (1976), 79-81 "Effect of Hydrogen Absorption on the Magnetic Properties of YFe_2 and $GdFe_2$" (518)

Buschow, K. H. J.; Cohen, R. L.; and West, K. W., J. of Appl. Phys., **48** (1977), 5289 "What is the Mechanism of Hydrogen Absorption in Rare Earth Intermetallics?" (52)

Buschow, K. H. J., J. of Less-Common Metals, 51 (1977), 173-175 "Note on the Change in Magnetic Properties of $GdCo_2$ on Hydrogen Absorption" (54)

Buschow, K. H. J.; Bouten, P. C. P.; and Miedema, A. R., Rep. Prog. Phys., **45** (1982), 937-1039 "Hydrides formed from intermetallic compounds of two transition metals: a special class of ternary alloys" (283)

Cantrell, J. S.; Bowman, R. C.; Wade, L. A.; Luo, S.; Clewley, J. D.; and Flanagan, T. B., J. of Alloys and Compounds, **231** (1995), 518-523 "Thermodynamic properties and the degredation of $ZrNiH_x$ at elevated temperatures" (409)

Carpetis, C.; Peschka, W., Int. J. Hydrogen Energy, **5** (1980), 539-554. "A Study on Hydrogen Storage by use of Cryoadsorbants"

Cerny, R.; Bonhomme, F.; Yvon, K.; Fischer, P.; Zolliker, P.; Cox, D. E.; and Hewat, A., J. of Alloys and Compounds, **187** (1992), 233-241, "Hexamagnesium dicobalt undecadeuteride $Mg_6Co_2D_{11}$ containing $[CoD_4]^{5-}$ and $[CoD_5]^{4-}$ complex ions conforming to the 18-electron rule"

Chahine, R.; Bose, T. K., Int. J. Hydrogen Energy, **19** (1994), 161-164, "Low-Pressure Adsorption Storage of Hydrogen"

Clay, K. R.; Goudy, A. J.; Schweibenz, R. G.; and Zarynow, A., J. of Less-Common. Met., **166** (1990), 153-162, "The Effect of Partial Replacement of Lanthanum in $LaNi_5$-H with Cerium, Praseodymium, and Neodymium on Absorption and Desorption Kinetics"

Clinton, J.; Bittner, H.; and Oesterreicher, H., J. of Less-Common Metals, **41** (1975), 187-189 "Hydrides of Praseodymium-Cobalt Compounds" (102)

Cohen, R. L.; West, K. W.; and Buschhow, K. H. J., Solid State Comm., **23** (1978), 293-295, " Degredation of Hydrogen-Absorbing Rare Earth Intermetallics by Cycling"

Darnaudery, J. P.; Pezat, M.; and Darriet, B., J. of Less-Common Metals, **92** (1983), 199-205 "Influence de la Substitution du Cuivre au Nickel dans Mg_2Ni sur le Stockage de l'Hydrogene" (417)

Darnaudery, J. P.; Darriet, B.; and Pezat, M., Int. J. of Hydrogen Energy, **8** (1983), 705-708 "The $Mg_2Ni_{0.75}M_{0.25}$ Alloys (M=3d Element): Their Application to Hydrogen Storage" (418)

Darriet, B.; Pezat, M.; Hbika, A.; and Hagenmuller, P., Int. J. Hydrogen Energy, **5** (1980), 173-178 "Application of Magnesium Rich Rare-Earth Alloys to Hydrogen Storage" (433)

Deschanvres, A.; Desgardin, G., Rev. de Chemie Minerale, **1** (1964), 439-449 "Hydrures ternaires dans le systeme zirconium-argent" (497)

Devillers, M.; Sirch, M.; and Penzhorn, R.-D., Z. Phys. Chem. NF, **164** (1989), 1355-1360 "Hydrogen Isotopes in Pure and Nitrided ZrCo" (399)

Didishiem, J. J.; Zolliker, P.; Yvon, K.; Fischer, P.; Schefer, J.; Grubelmann, M.; and Williams, A. F., Inorg. Chem., **23** (1984), 1953-1957, "Dimagnesium Iron(II) Hydride, Mg_2FeH_6, Containing Octahedral FeH_6^{4-} Anions"

Dillon, A. C.; Jones, K. M.; Bekkedahl, T. A.; Kiang, C. H.; Bethune,D. S.; and Heben, M. J., Nature, **386** (1997), 377-379, "Storage of hydrogen in single-walled nanotubes"

Domizlaff, S., P.M. Magazin, Jan. 1996, 60-63, "Das Super-U-Boot 'made in Germany'"

Drasner, A.; Blazina, J. of Less-Common Metals, **163** (1990), 151-157 "On the Structure and Hydrogen Desorption Properties of the $Zr(Cr_{1-x}Ni_x)_2$ Alloys" (561)

Drasner, A.; Blazina, Z., J. of Less-Common Metals, **168** (1991), 289-294 "Thermodynamic Properties of the $ZrCr_2T_{0.8}$-H_2 Systems (T=Fe,Co,Ni)" (564)

Drasner, A.; Blazina, Z., J. of Alloys and Compounds, **199** (1993), 101-104 "The influence of Si and Ge on the hydrogen sorption properties of the intermetallic compound $ZrCr_2$" (583)

Drulis, H.; Petrynski, W.; Stalinski, B.; and Zygmunt, A., J. of Less-Common Metals, **83** (1982), 87-93 "Hydrogen Absorption Properties of Selected Uranium Intermetallic Compounds" (434)

Drulis, H.; Petrynski, W.; and Stalinski, B., J. of Less-Common Metals, **101** (1984), 229-237 "Magnetic Properties and Electron Paramagnetic Presonace Studies of the $GdXAlH_x$ (X=Fe,Ni) Hydrides" (553)

Dunlap, B. D.; Viccaro, P. J.; and Shenoy, G. K., J. of Less-Common Metals, **74** (1980), 75-79 "Structural Relationships in Rare Earth-Transition Metal Hydrides" (447)

Dutta, K.; N. Srivastava, O., Hydrogen Energy progress VIII, T. N. Veziroglu and P. K. Takahashi, Eds., Pergamon, **2** (1990), 1027-1034 "Investigation on Synthesis, Characterization and Hydrogenation Behavior of La_2Mg_{17} and Related Intermetallics" (442)

Dutta, K.; Mandal, P.; Ramakrishna, K.; and O.N. Srivastava, Int. J. of Hydrogen Energy, **19** (1994), 253-257 "The Synthesis and Hydrogenation Behavior of Some New Composite Storage Materials: Mg-xwt% FeTi(Mn) and La_2Mg_{17}-xwt% $LaNi_5$" (296)

Dymova, T. N.; Eliseeva, N. G.; Bakum, S. I.; and Dergachev, Y. M., Dokl. Akad. Nauk SSSR, **215** (1974), 1369-1372 (trans. 256-259), "Direct Synthesis of Alkali Metal Aluminum Hydrides in the Melt"

Dymova, T. N.; Dergachev, Y. M.; Sokolov, V. A.; and Grechanaya, N. A., Dokl. Akad. Nauk SSSR, **225** (1975), 591-592 (trans. 556-557), "Dissociation Pressure of $NaAlH_4$ and Na_3AlH_6"

Eisenberg, E. G.; Goodell, P. D., J. of Less-Common Metals, **89** (1983), 55-62 "Cycling Response of Reversible Hydriding Alloys in Hydrogen Containing Carbon Monoxide" (208)

Fetcenko, M. A.; Venkatesan, S.; and Ovshinsky, S. R., Hydrogen Storage Materials, Batteries, and Electrochemistry, D. A. Corrigan and S. Srinivasan, Eds., The Electrochemical Soc., **92-5** (1992), 141-167 "Selection of Metal Hydride Alloys for Electrochemical Applications"

Feucht, K.; Hurich, W.; Komoschinski, N.; and Povel, R., Int. J. Hydrogen Energy, **13** (1988), 243-250 "Hydrogen Drive for Road Vehicles - Results from the Fleet test Run in Berlin" (343)

Fickett, A. P., Handbook of Batteries and Fuel Cells, D. Linden, Ed., McGraw-Hill, New York, 1984, Chap. 41 "General Characteristics"

Flanagan, T.B.; Clewley, J. D.; Mason, N. B.; and Chung, H. S., J. of Less-Common Metals, **130** (1987), 309-318 "Thermodynamics of the $ErFe_2$-H(D) System" (358)

Franco, R. J.; Berkowitz, B. J.; and Kaul, B. K., U. S. Patent 4,585,561 (1986) "Low Temperature Heat Pipe Employing Hydrogen Getter" (337)

Freeman, B.; Ryba, E.; Bowman, R.; and Phillips, J., Hydrogen Energy Progress X, D. L. Block and T. N. Veziroglu, Eds., Int. Assoc. Hydrogen Energy (1994), 2031-2041 "Progress towards the Development of Hydrogen Sorption Cryocoolers for Space Applications" (350)

Friedrich, B., International Symp. on Metal Hydrogen Systems, Uppsala, Unpublished, GfE, Hoefener Str. 45, D-8500 Nurnberg (1992), 1-13 "Large Scale Production And Quality Assurance of Hydrogen (Battery)-Storaging Alloys" (342)

Fujii, H.; Pourarian, F.; Sinha, V. K.; and Wallace, W. E., J. Phys. Chem., **85** (1981), 3112-3116 "Magnetic, Crystallographic, and Hydrogen-Storage Characteristicsof $Zr_{1-x}Ti_xMn_2$ Hydrides" (18)

Fujii, F.; Pourarian, F.; and Wallace, W. E., J. of Magnetism and Magnetic Materials, **27** (1982), 215-220 "Effect of Hydrogen Absorption on the Magnetic Properties of $Zr(Fe_{1-x}Al_x)_2$ Compounds" (22)

Fujii, H.; Saga, M.; and Okamoto, T., J. of Less-Common Metals, **130** (1987), 25-31 "Magnetic, Crystallographic and Hydrogen Absorption Properties of YMn_2 and $ZrMn_2$ Hydrides" (369)

Fujii, H.; Orimo, S.; Yamamoto, K.; Yoshimoto, K.; and Ogasawara, T., J. of Less-Common. Met., **175** (1991), 243-257, "New composite materials for hydrogen storage using magnesium as a binder"

Fujii, H.; Orimo, S.; and Ikeda, K., J. Alloys and Compounds,1997, in press, "Cooperative hydriding properties in a nanostructured Mg_2Ni system"

Fujitani, S.; Yonezu, I.; Saito, T.; N; Furukawa; Akiba, E.; Hayakowa, H.; and Ono, S., J. of Less-Common Metals, **172** (1991), 220-230 "Relation between equilibrium hydrogen pressure and lattic parameters in pseudobinary Zr-Mn alloy systems" (368)

Fukai, Y., The Metal-Hydrogen System, Springer Verlag, Berlin, 1993

Gamo, T.; Moriwaki, Y.; Yamashita, T.; and Fukuda, M., U.S. Patent 4144103 (1979) "Method of a Hydrogen Storage Alloy and Product" (33)

Gamo, T.; Moriwaki, Y.; Yamashita, T.; and Fukuda, M., U.S. Patent 4153484 (1979) "Hydrogen Storage Material" (34)

Gamo, T.; Moriwaki, Y.; Yamashita, T.; and Fukuda, M., U.S. Patent 4160014 (1979) "Hydrogen Storage Material" (35)

Gamo, T.; Moriwaki, Y.; Yanagihara, N.; Yamashita, T.; and Iwaki, T., Hydrogen Energy Progress III; Proc. 3rd World Hydrogen Energy Conf., Tokyo, Japan (1980), 2127-2144 "Formation and Properties of Titanium-Manganese Alloy Hydrides" (31)

Gamo, T.; Moriwaki, Y.; Yamashita, T.; and Fukuda, M., U.S. Patent 4195989 (1980) "Hydrogen Storage Material" (36)

Gamo, T.; Moriwaki, Y.; Yamashita, T.; and Fukuda, M., U.S. Patent 4228145 (1980) "Hydrogen Storage Material" (37)

Gamo, T.; Moriwaki, Y.; Yanagihara, N.; and Iwaki, T., J. of Less-Common Metals, **89** (1983), 495-504 "Life Properties of Ti-Mn Alloy Hydrides and Their Hydrogen Purification Effect" (32)

Gao, X.; Song, D.; Zhang, Y.; Wang, G.; and Shen, P., J. of Alloys and Compounds, **223** (1995), 77-80 "Characteristics of the stoichiometric and non-stoichiometric Laves phase alloys and their hydride electrodes" (403)

Gao, X.; Song, D.; Zhang, Y.; Zhou, Z.; Zhang, W.; Wang, M.; and Shen, P., J. of Alloys and Compounds, **229** (1995), 268-273 "Electrochemical and surface properties of the $Zr(V_{0.2}Mn_{0.2}Ni_{0.6})_{2.4}$ alloy electrode" (404)

Gao, X. P.; Zhang, W.; Yang, H.B.; Song, D.Y.; Zhang, Y.S.; Zhou, Z.X.; and P.W. Shen, J. of Alloys and Compounds, **235** (1996), 225-231 "Electrochemical properties of the $Zr(V_{0.4}Ni_{0.6})_{2.4}$ hydrogen storage alloy electrode" (586)

Gavra, Z.; Murray, J. J.; Calvert, L. D.; and Taylor, J. B., J. of Less-Common Metals, **105** (1985), 291-301 "The $EuNi_5$-H System" (280)

Gérard, N.; Ono, S., Hydrogen in Intermetallic Compounds II, L. Schlapbach, Ed., Topics in Appl. Phys., Springer, Berlin, **67** (1992), 165-195 "Hydride Formation and Decomposition Kinetics" (334)

Goodell, P. D.; Sandrock, G. D.; and Huston, E.L., J. of Less Common Metals, **73** (1980), 135-142 "Kinetic and Dynamic Aspects of Rechargeable Metal Hydrides" (6)

Goodell, P. D., J. of Less Common Metals, **74** (1980), 175-184 "Thermal Conductivity of Hydriding Alloy Powders and Comparisons of Reactor Systems" (7)

Goodell, P. D.; Sandrock, G. D.; and Huston, E.L., Rept. SAND79-7095, Sandia N. L., Albuquerque, NM 87185 (1980), 1-176 "Microstructure and Hydriding Studies of AB_5 Hydrogen Storage Compounds" (256)

Goodell, P. D.; Sandrock, G., Report DOE/CS/BNL-51174, U.S. Department of Energy, Washington, April, 1980, "Metallurgical Studies of Hydrogen Storage Alloys"

Goodell, P. D.; Sandrock, G. D.; and Bogdanski, R. R., Rept. for Contract BNL 509926-S, Brookhaven National Laboratory, Dec. 21, 1982, "Development of a Commercial Metal Hydride Process for Hydrogen Recovery: Cyclic Hydrogen Transfer and Adsorption/Poisoning Tests of AB- and AB_5-Type Hydriding Alloys"

Goodell, P. D., J. of Less Common Metals, **89** (1983), 45-54 "Cycling Hydriding Response for $LaNi_5$ in Hydrogen Containing Oxygen as a Minor Impurity" (8)

Goodell, P. D.; Rudman, P. S., J. of Less Common Metals, **89** (1983), 117-125 "Hydriding and Dehidriding Rates of the $LaNi_5$-H_2 System" (9)

Goodell, P. D., J. of Less Common Metals, **99** (1984), 1-14 "Stability of Rechargeable Hydriding Alloys During Extended Cycling" (5)

Goodell, P. D., Rept. DOE/ID/12520, P. D. Goodell, W. J. Rebello and M. R. Ally, Eds., USDOE, Conservation Technologies Div., Ch. 2 (1986) "Literature Survey of Hydriding Alloy Properties" (401)

Goudy, A. J., Thesis, University of Pittsburgh (1976) "Hydrogen Solubility in Rare Earth Intermetallic Compounds" (186)

Groll, M; Supper, W.; Mayer, U.; and Brost, O., Int. J. Hydrogen Energy, **12** (1987), 89, "Heat and Mass Transfer Limitations in Metal Hydride Reaction Beds"

Gross, K. J.; Spatz, P.; Züttel, A.; and Schlapbach, L., J. Alloys and Compounds, **240** (1996), 206-213, "Mechanically milled Mg composites for hydrogen storage, The transition to a steady state composition"

Gruen, D. M.; Mendelsohn, M., J. of Less-Common Metals, **55** (1977), 149-152 "Configurational Entropies and the Stabilities of Intermetallic Hydrides" (162)

Gualtieri, D. M.; Narasimhan, K. S. V. L.; and Wallace, W. E., Magnetism and Magnetic Materials-1976, J. J. Becker and G. H. Lander, Eds., AIP Conf. Series, 34 (1976), 219-221 "Magnetic Properties of the Hydrides of Selected Rare-Earth Intermetallic Compounds with Transition Metals" (516)

Gualtieri, D. M.; Wallace, W. E., J. of Less-Common Metals, **55** (1977), 53-59 "Hydrogen Capacity and Crystallography of $ErFe_2$-Based and $ErCo_2$-Based Ternary Systems" (50)

Gutjahr, M. A.; Bucher, H.; and Beccu, K. D., Power Sources, **4** (1973), 79 "A New Type of Reversible Negative Electrode for Alkaline Storage Batteries Based on Metal Alloy Hydrides" (72)

Han, J. I.; Lee, J.-Y., J. of Less-Common. Met., **152** (1989), 319-327, "Influence of CO Impurity on the Hydrogenation Properties of $LaNi_5$, $LaNi_{4.7}Al_{0.3}$ and $MmNi_{4.5}Al_{0.5}$ During Hydriding-Dehydriding Cycling"

Han, J. I.; Lee, J.-Y., J. of Less-Common. Met., **152** (1989), 329-338, "Influence of Oxygen Impurity on the Hydrogenation Properties of $LaNi_5$, $LaNi_{4.7}Al_{0.3}$ and $MmNi_{4.5}Al_{0.5}$ During Long-Term Pressure-Induced Hydriding-Dehydriding Cycling"

Hata, K.; Sato, H., Nippon Kagaku Kaishi, **16** (1980), 57-83 "Effects of Additional Elements on

the Hydride Formation in TiNi" (74)

Hirata, T.; Matsumoto, T.; Amano, M.; and Sasaki, Y., J. of Less-Common Metals, **89** (1983), 85-91 "Dehydriding Reaction Kinetics in the Improved Intermetallic Mg_2Ni-H System" (427)

Hoffman, K. C.; Winsche, W. E.; Wiswall, R. N.; Reilly, J. J.; Sheehan, T. V.; and Waide, C. H., Paper 690232, Society of Automotive Engineers, New York, 1969, "Metal Hydrides as a Source of Fuel for Vehicular Propulsion"

Hoffman, K. C.; Reilly, J. J.; Salzano, F. J., Waide, C. H.; Wiswall, R. N.; and Winsche, W. E., Int. J. Hydrogen Energy, **1** (1976) 133-151, "Metal Hydride Storage for Mobile and Stationary Applications"

Hoffmann, P., Hydrogen & Fuel Cell Letter, P.O. Box 14, Rhinecliff, NY 12574, 1995-1997 (continuing)

Holtz, R. L.; Imam, M. A., J. Materials Sci., **32** (1997), 2267-2274, "Hydrogen storage capacity of submicron magnesium-nickel alloys"

Hong, C.; Han, D.; and Lin, Q., J. of Less-Common Metals, **171** (1991), 1044-1051 "Characteristics of hydrogen absorption and reactivation of $TiMn_{1.25}Cr_{0.25}$ alloy" (365)

Hong, C.; Zhang, Y.; and Han, D., Z. Phys. Chem. NF, **183** (1994), 169-174 "Hydrogen Absorption Properties of Pseudo-Binary Alloys $Ti_{0.8}Zr_{0.2}Mn_{1.5}M_{0.5}$" (373)

Hong, C.; Zhang, Y.; and Wang, J., J. of Alloys and Compounds, **231** (1995), 546-549 "Second phase and electrode characteristics of rare-earth-based AB_{5+x} alloys" (621)

Huang, P.; Goudy, A. J.; and Koh, J. T., J. of Less-Common. Met., **155** (1989), 111-118, "Hydrogen Absorption-Desorption Kinetics of $MmNi_5$ and Related Compounds"

Huang, B.; Yvon, K.; and Fischer, P., J. of Alloys and Compounds, **178** (1992), 173-179, "Calcium Magnesium Nickel (0) Tetrahydride, $CaMgNiH_4$, Containing Tetrahedral $[NiH_4]^{4-}$ Complex Ions: The First Quaternary Transition Metal Hydride"

Huang, B.; Yvon, K.; and Fischer, P., J. of Alloys and Compounds, **187** (1992), 227-232, "Strontium magnesium iron octahydride, $SrMg_2FeH_8$, containing $[FeH_6]^{4-}$ complex ions"

Huang, B.; Yvon, K.; and Fischer, P., J. of Alloys and Compounds, **197** (1993), 97-99, "Trimagnesium ruthenium (I) heptahydride, Mg_3ReH_7, containing octahedral $[ReH_6]^{5-}$ complex ions"

Huang, B.; Yvon, K.; and Fischer, P., J. of Alloys and Compounds, **210** (1994), 243-246, "$LiMg_2RuH_7$, a new quaternary metal hydride containing octahedral $[Ru(II)H_6]^{4-}$ complex ions"

Huston, E. L.; Sandrock, G. D., J. of Less-Common Metals, **74** (1980), 435-443 "Engineering Properties of Metal Hydrides" (77)

Immamura, H.; Sakasai, N.; and Kajii, Y., J. of Alloys and Compounds, **232** (1996), 218-223, "Hydrogen absorption of Mg-Based composites prepared by mechanical milling: Factors affecting

its characteristics"

Imoto, T.; Satoh, K.; Nishimura, K.; Yonesaki, T.; Fujitani, S.; and Yonetsu, Y., J. of Alloys and Compounds, **223** (1995), 60-64 "Poisoning by air of AB_5 type rare-earth nickel hydrogen-absorbing alloys" (601)

Irvine, S. J. C.; Harris, I. R., Hydrides for Energy Storage, Ed. A. F. Andresen and A. J. Maeland, Pergamon Press (1978), 431-446 "The Effect of Induced Disorder on the Hydrogenation Behaviour of the Phase ZrCo" (70)

Ishikawa, H.; Oguro, K.; Kato, A.; Suzuki, H.; and Ishii, E., J. of Less-Common Metals, **107** (1985), 105-110 "Preparation and Properties of Hydrogen Storage Alloy-Copper Microcapsules" (290)

Ishikawa, H.; Oguro, K.; Kato, A.; Suzuki, H.; and Ishii, E., J. of Less-Common Metals, **120** (1986), 123-133 "Preparation and Properties of Hydrogen Storage Alloys Microencapsulated by Copper" (291)

Ivey, D. G.; Northwood, D. O., J. of Materials for Energy Systems (1982) "Hydrogen Storage Characteristics Of $Zr(BxB^*_{1-x})_2$, B = Fe, Co, B*= Cr, Mn and x = 0.4, 0.5, 0.6" (58)

Ivey, D. G.; Northwood, D. O., J. Materials Sci., **18** (1983), 321-347 "Storing Energy in Metal Hydrides : A Review of the Physical Metallurgy" (251)

Ivey, D. G.; Northwood, D. O., Hydrogen Energy Progress V, T. N. Veziroglu and J. B. Taylor, Eds., Pergamon, New York, **3** (1984), 1395-1406 "Hydrogen Absorption-Desorption Characteristics of $Zr(Fe_xCr_{1-x})_2$" (29)

Ivey, D. G.; Northwood, D. O., Zeit. Phys. Chem. NF, **147** (1986), 191-209 "Storing Hydrogen in AB_2 Laves-Type Compounds" (285)

Ivey, D. G.; Northwood, D. O., Int. J. Hydrogen Energy, **11** (1986), 583-591 "Hydriding Properties of $Zr(Fe_xCr_{1-x})_2$ Intermetallic Compounds" (377)

Jacob, I.; Shaltiel, D.; and Davidov, D., Proc. Second International Congress on Hydrogen in Metals, Paris, France (1977) "Hydrogen Sorption Properties of AB_2 Laves Phase Pseudobinary Compounds" (47)

Jacob, I.; Shaltiel, D., HYDROGEN ENERGY SYSTEM, T. N. Veziroglu and W. Seifritz, Eds., Pergamon Press (1978), 1689-1706 "The Influence of Al on the Hydrogen Sorption Properties of Intermetallic Compounds" (15)

Jacob, I.; Shaltiel, D., Solid State Communications, **27** (1978), 175-180 "Hydrogen Absorption in $Zr(Al_xB_{1-x})_2$, (B = Fe,Co) Laves Phase Compounds" (16)

Jacob, I.; Shaltiel, D., J. of Less-Common Metals, **65** (1979), 117-128 "Hydrogen Sorption Properties of some AB_2 Laves Phase Compounds" (361)

Jacob, I.; Stern, A.; Moran, A.; Shaltiel, D.; and Davidov, D., J. of Less-Common Metals, **73** (1980), 369-376 "Hydrogen Absorption in $(Zr_xTi_{1-x})B_2$ (B = Cr, Mn) and the Phenomenological Model for the Absorption Capacity in Pseudo-Binary" (65)

Jang, T.H.; Han, J. I.; and Lee, J.-Y., J. of Less-Common Metals, **119** (1986), 237-246 "Effect of Substitution of Titanium by Zirconium in TiFe on Hydrogenation Properties" (397)

Jensen, C. M., Proc. 1995 U.S. DOE Program review, Rept. NREL/CP-430-20036, **II** (1995), National Renewable Energy Lab, 437-444, "Polyhydride Complexes for Hydrogen Storage"

Jensen, C. M., Proc. 1996 U.S. DOE Program review, Rept. NREL/CP-430-21968, **II** (1996), National Renewable Energy Lab, 787-793, "Hydrogen Storage via Polyhydride Complexes "

Johnson, J. R.; Reilly, J. J., Proc. International Conf. on Alternative Energy Sources, T. N. Veziroglu, Ed., Univ. Miami (1977), 3739-3769 "The Use of Manganese Substituted Ferrotitanium Alloys for Energy Storage" (393)

Johnson, J. R.; Reilly, J. J., Proc. DOE Contractor Rev. Mtg. on Chem. Energy Storage and Hydrogen Energy Systems, JPL (1978), 171-176 "The Metal Hydride Development Program at Brookhaven National Laboratory" (330)

Johnson, J. R.; Reilly, J. J., Inorg. Chem., **17** (1978), 3101 "The Reaction of Hydrogen with the Low Temperature Form (C15) of $TiCr_2$" (335)

Johnson, J. R., J. of Less-Common Metals, **73** (1980), 345-354 "Reaction of Hydrogen With the High-Temperature (C14) Form of $TiCr_2$" (42)

Joubert, J.-M.; Latroche, M.; Percheron-Guegan, A.; and Bouet, J.: J. Alloys and Compounds, **240** (1996), 219-228, "Improvement of the electrochemical activity of Zr-Ni-Cr Laves phase hydride electrodes by secondary phase precipitation"

Kadel, R.; Weiss, A., Ber. Bunsenges. Phys. Chem., **82** (1978), 1290-1302 "Solubility of Hydrogen in CuTi, CuTi2, PdTi2, and Cu0.5Pd0.5Ti2 - Reactions of Titanium Alloys with Gaseous Hydrogen" (523)

Kadel, R.; Weiss, A., J. of Less-Common Metals, **65** (1979), 89-101 "The Reaction of Gaseous Hydrogen with $CuZr_2$ at Temperatures above 500 C" (429)

Kadir, K, Doctoral Dissertation, Stockholm Univ., 1994 (Chem. Commun., 1994, No.2), "Studies of New Ternary Hydrides with Different d-Electron Content"

Kadir, K.; Noréus, D., Z. Phys. Chem., **179** (1993), 249-253, The Structure of a Sodium-substituted Palladium Hydride $NaPd_3H_2$"

Kanematsu, K.; Sugiyama, T.; Sekine, M.; Okagaki, T.; and Kobayashi, K. I., J. of Less-Common Metals, **147** (1989), 9-18 "Formation and Magnetic Properties of Crystalline and Amorphous $SmCo_2$ Hydrides" (558)

Kesavan, T. R.; Ramesh, R; and Rama Rao, K. V. S., J. of Alloys and Compounds, **226** (1995), 46-50, "Hydrogen absorption studies in $Zr_{0.4}Ho_{0.6}Fe_2$"

Kesavan, T. R.; Ramaprabhu, S.; Rama Rao, K. V. S.; and Das, T. P., J. of Alloys and Compounds, **244** (1996), 164-169, Hydrogen absorption and kinetic studies in $Zr_{0.2}Ho_{0.8}Fe_2$"

Khrussanova, M.; Terzieva, M.; Peshev, P.; Petrov, K.; Pezat, M.; Manaud, J. P.; and Darriet,

B., Int. J. Hydrogen Energy, **9** (1985), 591-594 "Calcium-Substituted Lanthanum-Magnesium Alloys for Hydrogen Storage" (436)

Khrussanova, M.; Terzieva, M.; Peshev, P.; Konstanchuk, I.; and Ivanov, E., Z. Phys. Chem. NF, **164** (1989), 1261-1266 "Hydriding Kinetics of Mixtures Containing Some 3d-Transition Metals Oxides and Magnesium" (293)

Kierstead, H. A.; Viccaro, P. J.; Shenoy, G. K.; and Dunlap, B. D., J. of Less-Common Metals, **66** (1979), 219-222 "Pressure-Composition Phase Diagram for Hydrides of Rare Earth-Fe_2 Laves Compounds" (458)

Kierstead, H. A., L. of Less-Common Metals, **70** (1980), 199-207 "Thermodynamic Properties of $ErFe_2$ and $DyFe_2$ Hydrides" (356)

Kierstead, H. A., J. of Less-Common Metals, **71** (1980), 311-315 "Desorption Isotherms of $DyFe_3$ Hydrides" (449)

Kierstead, H. A., J. of Less-Common Metals, **78** (1981), 29-34 "The Hydrides of $NdCo_3$ and $GdCo_3$" (444)

Kierstead, H. A., J. of Less-Common Metals, **86** (1982), L1-L4 "The Hydrides YFe_2 and $GdFe_2$" (61)

Kierstead, H. A., J. of Less-Common Metals, **85** (1982), 213-219 "Thermodynamic Properties of $TmFe_2$ Hydrides" (374)

Kierstead, H. A., J. of Less-Common Metals, **96** (1984), 133-139 "Thermodynamic Properties of $LuCo_3$ Hydrides" (571)

Kilbourn, B. T., A Lanthanide Lanthology, Molycorp, Inc., White Plains, NY [now Fairfield, NJ] (1993), 1

Kim, Y.-G.; Lee, J.-Y., J. of Less-Common. Met., **132** (1987), 123-132, "Effects of Oxygen on the Hydrogenation Properties of $MmNi_{4.15}Fe_{0.85}$ Upon Pressure Cycling"

Kim, Y.-G.; Lee, J.-Y., J. of Less-Common. Met., **144** (1988), 331-339, "The Changes of Hydrogenation Properties Induced by Thermal Cyclings in $MmNi_{4.5}Al_{0.5}$ and $MmNi_{4.15}Fe_{0.85}$ Upon Pressure Cycling"

Kim, Y.-G.; Lee, S.-M.; and Lee, J.-Y., J. of Less-Common. Met., **169** (1991), 245-256, "Hydrogen-induced amorphization of the Laves compound $CeNi_2$ and the structural and thermal characteristics of the amorphous phase"

Klyamkin, S. N.; Semenenko, K. N.; and Kinas, I. A., J. of Alloys and Compounds, **204** (1994), 65-69 "New hydride formation of $MoSi_2$-type intermetallic compounds at hydrogen pressures up to 2000 atm" (595)

Klyamkin, S. N.; Verbetsky, V. N.; and Karih, A. A., J. of Alloys and Compounds, **231** (1995), 479-482 "Thermodynamic particularities of some $CeNi_5$-based metal hydride systems with high dissociation pressure" (407)

Kohno, T.; Tsuruta, S.; and Kanda, M., J. Electrochem. Soc., **143** (1996), L-198-L199, The Hydrogen Storage Properties of New Mg_2Ni Alloy"

Komozaki, Y.; Uchida, M.; and Suda, S., J. of Less-Common Metals, **89** (1983), 269-274 "Equilibrium Properties of Ti-Zr-Fe-Mn Hydrides" (29)

Kost, M. E.; Raevskaya, M. V.; Shilov, A. L.; Yaropolova, E. I.; and Mikhee, V. I., Russian J. Inorganic Chem., **24** (1979), 1803-1805 "Thermal Stability of the Hydrides of Various Intermetallic Compounds of the Lanthanides Having Structures of the Laves Phase Type" (515)

Konstanchuk, I. G.; Ivanov, E. Y.; Pezat, M.; Darriet, B.; Boldyrev, V. V.; and Hagenmuller, P., J. Less-Common Met., **131** (1987), 181-189, "The Hydriding Properties of a Mechanical Alloy with Composition Mg-25%Fe"

Lakner, J. F.; Steward, S. A.; and Uribe, F., Lawrence Livermore Lab Report UCRL-52039 (1976) "High Pressure Hydrogen Apparatus for PCT Studies up to 700 MPa and 200 C: Preliminary Results on $LaCo_5H_{9.0}$ at 21 C" (166)

Lambert, S. W.; Chandra, D.; Cathey, W. N.; Lynch, F. E.; and Bowman, R. C., J. of Alloys and Compounds, **187** (1992), 113-136 "Investigation of hydriding properties of $LaNi_{4.8}Sn_{0.2}$, $LaNi_{4.27}Sn_{0.24}$ and $La_{0.9}Gd_{0.2}Ni_5$ after thermal cycling and aging" (348)

Lasocka, M., Binary Alloy Phase Diagrams, T. B. Massalski, Ed., ASM International, **3**, 1990, 2629-2631, "Mn-Zr (Manganese-Zirconium"

Lee, J. Y.; Park, J. M., Hydrogen Energy Progress VIII, T. N. Veziroglu and P. K. Takahashi, Eds., Pergamon Press, New York, **2** (1990), 985-993 "A Study on the Sloping Plateaus in the $Zr_{1-x}Ti_xCr_{1-y}Fe_{1+y}$ Laves Phase Alloys" (378)

Lee, S.-M.; Perng, T.-P., Int. J. of Hydrogen Energy, **19** (1994), 259-263 "Effect of the Second Phase on the Initiation of Hydrogenation of $TiFe_{1-x}M_x$ (M=Cr,Mn) Alloys" (391)

Lee, S-G.; Lee, K-Y.; Kim, T-G.; Lee, Z-H.; and Lee, J-Y., Int. J. Hydrogen Energy, **21** (1996), 733-740 "Mathematical Model for the Dynamic P-C-T Curves of the $MmNi_{4.6}Al_{0.2}Fe_{0.2}V_{0.03}$ Alloy in a Tubular Reactor" (451)

Lewis, F. A., Academic Press, London (1967), 1-178 "The Palladium Hydrogen System" (303)

Liang, G; Wang, E.; VFang, S., J. of Alloys and Compounds, **223** (1995), "Hydrogen absorption and desorption characteristics of mechanically milled Mg-35wt.%$FeTi_{1.2}$ powders"

Libowitz, G. G., The Solid State Chemistry of Binary Metal Hydrides, W.A. Benjamin, 1965

Libowitz, G. G.; Hayes, H. F.; Gibb, T. R. P.; and Jr., J. Phys. Chem., **62** (1958), 76-79 "The System Zirconium-Nickel and Hydrogen" (68)

Libowitz, G. G.; Maeland, A. J., J. of Less-Common. Met., **101** (1984), 131-143, " Interaction of Hydrogen with Metallic Glass Alloys"

Libowitz, G. G.; Maeland, A. J.; and Lynch, J. F., Final Report to Brookhaven Nat. Lab., Contract DE-AC02-76CH00016, Allied. Corp., Morristown, NJ 07960 (1985), 1-25 "Advanced

Hydrogen Storage: Modified Vanadium Hydrides" (471)

Libowitz, G. G.; Maeland, A. J., Materials Science Forum, **31** (1988), 177-196 "Hydride Formation by B.C.C. Solid Solution Alloys" (353)

Lim, S. H.; Lee, J.-Y., J. of Less-Common Metals, **97** (1984), 65-71 "The Effects of Aluminum Substitution in TiFe on its Hydrogen Absorption Properties" (547)

Lim, S. H.; Lee, J.-Y., J. of Less-Common Metals, **97** (1984), 59-64 "The Effects of the Addition of Aluminum on the Kinetic properties of the Interemetallic Compound TiFe" (548)

F.-J. Liu; G. Sandrock; and S. Suda, J. Alloys and Compounds, **190** (1992), 57-60, "Activation characteristics of chemically treated $LaNi_{4.7}Al_{0.3}$"

F.-J. Liu; G. Sandrock; and S. Suda: Z. Phys. Chem., **183** (1994), 163-167 "Hydriding Characteristics of Surface Treated Mg_2Ni at 40°C"

Liu, F.-J.; Suda, S., J. of Alloys and Compounds, **231** (1995), 666-669 "F-treatment effect on the hydriding properties of the La-substituted AB_2 compound $(Ti,Zr)(Mn,Cr,Ni)_2$" (415)

Liu, J.; Lundin, C. E., World Pat. WO 82/02214 (1982), 1-12 "Alloys for Hydrogen Storage" (499)

Liu, J.; Huston, E. Lee, J. of Less-Common Metals, **90** (1983), 11-20 "RNi_5 Hydrogen Storage Compounds (R = Rare Earth)" (132)

Lü, M.-Q.; Zhang, H.-F.; Wang, Y.-L.; and Wei, W.-D., J. Alloys and Compounds, **191** (1993), 319-324, "Surface modification of V and its H absorption properties"

Lundin, C. E.; Lynch, F. E., First Annual Technical Report, AFOSR Contract F44620-74-C-0020, Univ. of Denver (1975) "Solid State Hydrogen Storage Materials for Application to Energy Needs" (260)

Lundin, C. E.; Lynch, F. E., Proc. Int. Conf. on Alternate Energy Sources, Ed. T. N. Veziroglu, Univ. of Miami (1978), 3803 "Modification of Hydriding Properties of AB_5 Type Hexagonal Alloys through Manganese Substitution" (272)

Luo, W.; Craft, A.; Kuh, T.; Chung, H. S.; and Flanagan, T. B., J. of Less-Common Metals, **162** (1990), 251-266 "Thermodynamic Characterization of the ZrNi-H System by Reaction Calorimitry and p-c-T Measurements" (550)

Luo, W.; Clewley, J. D.; Flanagan, T. B.; and Oates, W. A., J. of Alloys and Compounds, **185** (1992), 321-338 "Thermodynamic characterization of the Zr-Mn-H system Part 1. Reaction of H2 with single-phase $ZrMn_{2+x}$ C-14 Laves phase alloys" (582)

Lupu, D.; Biris, A.; and Indrea, E., Int. J. of Hydrogen Energy, **7** (1982), 783-785 "Hydrogen Absorption in Beryllium Substituted Mg_2Ni" (419)

Lupu, D.; Sarbu, R.; Biris, A.; Chiriac, G.; and Neda, A., Int. J. Hydrogen Energy, **13** (1988), 239-242. "The Behavior of $Ti_{1.2}Cr_{1.9}Mn_{0.1}$ in Hydrogen Absorption-Desorption Cycling"

Lutz, H. M.; Pous, O. De, Proc. Second International Congress on Hydrogen in Metals, Paris,

Paper 1F5 (1977), 1-8 "Determination of the Hydrogen Absorption Characteristics of Metallic Materials by Thermogravimetric Methods" (420)

Lyman, J. W.; Palmer, G. R., HYDROGEN AND METAL HYDRIDE BATTERIES, P. D. Bennett and T. Sakai, Eds., The Electrochemical Society, **94-27** (1994), 415-431 "Recycling of Nickel-Metal Hydride Battery Scrap"

Lynch, F.E., J. of Less-Common. Met., **74** (1980), 411, "Operating Characteristics of High Performance Commercial Metal Hydride Heat Exchangers"

Lynch, F. E., Phase I Final Report, U.S. Navy Contract N00024-89-C-3817, Hydrogen Consultants, Inc., Littleton, CO, 1989 "Closed Cycle Submersible Power Systems"

Lynch, J. F.; Reilly, J. J.; and Millot, F., J. Phys. Chem. Solids, **39** (1978), 883-890 "The Absorption of Hydrogen by Binary Vanadium-Chromium Alloys" (84)

Lynch, J. F.; Maeland, A. J.; and Libowitz, G. G., Z. Phys. Chem. NF, **145** (1985), 51-59 "Lattice Parameter Variation and Thermodynamics of Dihydride Formation in the Vanadium-Rich V-Ti-Fe/H_2 System" (351)

Machida, Y.; Yamadaya, T.; and Asanuma, M., Hydrides for Energy Storage, A. F. Andresen and A. J. Maeland, Eds., Pergamon Press, Oxford (1978), 329-336 "Hydride Formation of C14-Type Ti Alloy" (371)

Maeland, A. J., Hydrides for Energy Storage, A. F. Andresen and A. J. Maeland, Eds., Pergamon, Oxford (1978), 447-462 "Comparison of Hydrogen Absorption in Glassy and Crystalline Structures" (389)

Maeland, A. J.; Libowitz, G. G., J. of Less-Common Metals, **74** (1980), 295-300 "Hydrogen Absorption in some A2B Intermetallic Compounds with the $MoSi_2$-Type structure ($C11_b$)" (428)

Maeland, A. J.; Tanner, L. E.; and Libowitz, G. G., J. of Less-Common. Met., **74** (1980), 279 (1980), 279-285, "Hydrides of Metallic Glass Alloys"

Maeland, A. J.; Libowitz, G. G., J. of Less-Common Metals, **89** (1983), 197-200 "Hydrides of Beryllium-Based Intermetallic Compounds" (362)

Malik, S. K.; Wallace, W.E., Solid State Comm., **24** (1977), 283-285 "Hydrogen Absorption and its Effect on Structure and Magnetic Behavior of $GdNi_2$" (514)

Mandal, P.; Srivastava, O. N., J. of Alloys and Compounds, **205** (1994), 111-118, "Hydrogenation behavior of the new composite storage material Mg-x% FeTi"

Marmaro, R. W.; Lynch, F. E., Final Report, NAS9-18175, Hydrogen Consultants, Inc., Littleton,CO (1991) "Investigation of Long Term Stability, in Metal Hydrides" (316)

Martin, D. L., U. S. Patent 3,883,346 (1975) "Nickel-Lanthanum Alloy Produced by a Reduction-Diffusion Process" (152)

Matsumoto; T.; Matsushita, A., J. of Less-Common. Met., **123** (1986), 135-144, "A New Intermediate Hydride in the $LaNi_5$-H_2 System Studied by *In Situ* X-Ray Diffractometry"

Matsumoto, T.; Matsushita, A., J. of Less-Common Metals, **132** (1987), 115-121 "Hydrides in

the $PrNi_5$-H_2 System" (568)

Mendelsohn, M. H.; Gruen, D. M.; and Dwight, A. E., J. of Less-Common Metals, **63** (1979), 193-207 "The Effect of Aluminum Additions on the Structural and Hydrogen Absorption Properties of AB_5 Alloys with Particular Reference to the $LaNi_{5-x}Al_x$ Ternary Alloy System" (265)

Mendelsohn, M. H.; Gruen, D. M., J. of Less-Common Metals, **78** (1981), 275-280 "The Pesudo-Binary System $Zr(V_{1-x}Cr_x)_2$: Hydrogen Absorption and Stability Considerations" (21)

Mediati, M.; Tachibana, G. N.; and Jensen, C. M., Inorg. Chem., **29** (1990), 3-5, "Isolation and Characterization of $IrH_2Cl(\eta^2\text{-}H_2)[P(i\text{-}Pr)_3]_2$: A Neutral Dihydrogen Complex of Irridium"

Mediati, M.; Tachibana, G. N.; and Jensen, C. M., Inorg. Chem., **31** (1992), 1827-1832, "Solid-State and Solution Dynamics of the Reversible Loss of Hydrogen from the Iridium Nonclassical Polyhydride Complexes $IrClH_2(PR_3)_2$ (R = Pr^i, Cy, Bu^t)"

Mintz, M. H.; Vaknin, S.; Biderman, S.; and Hadari, Z., J. Appl. Phys., **52** (1981), 463-467 "Hydrides of Ternary $TiFe_xM_{1-x}$ (M=Cr,Mn,Co,Ni) Intermetallics" (390)

Mitrokhin, S. V.; Verbetsky, V. N.; Hong, C.; and Zhang, Y., Z. Phys. Chem. NF, **181** (1993), 283-287 "Hydriding Characteristics of FeTi-Based Ti-Fe-V-Mn Alloy" (396)

Mitrokhin, S. V.; Verbetsky, V. N.; Kajumov, R. R.; Hong, C.; and Zhang, Y., J. of Alloys and Compounds, **199** (1993), 135-160 "Hydrogen sorption properties in FeTi-type Ti-Fe-V-Mn alloys" (593)

Miyamura, H.; Sakai, T.; Kuriyama, N.; Oguro, K.; Uehara, I.; and Ishikawa, H., Z. Phys. Chem. NF, **183** (1994), 347-353 "Hydrogen Absorption and Electrode Characteristics of $(Ti,Zr)(Ni,V,X)_{2+a}$ Alloys" (372)

Morii, K.; Shimizu, T., J. of Alloys and Compounds, **231** (1995), 524-527 "Hydriding characteristics in $(Ti,Zr)(Ni,Mn,X)_2$ alloys" (410)

Moriwaki, Y.; Gamo, T.; Seri, H.; and Iwaki, T., J. of Less-Common Metals, **172** (1991), 1211-1218 "Electrode characteristics of C15-type Laves phase alloys" (367)

Mueller, W. M.; Blackledge, J. P.;Libowitz, G. G., Eds., Metal Hydrides, Academic, New York, 1968

Murray, J. L., Binary Alloy Phase Diagrams, T. B. Massalski, Ed., ASM International, **2**, 1990, 1783-1786, "Fe-Ti (Iron-Titanium)"

Murray, J. L., Binary Alloy Phase Diagrams, T. B. Massalski, Ed., ASM International, **3**, 1990, 2559-2560, "Mg-Ti (Magnesium-Titanium)"

Na, Y.-S.; Kim, Y.-G.; and Lee, J.Y., Int. J. Hydrogen Energy, **19** (1994), 899-903 "A Study of the Hydrogenation Properties of the $MmNi_{4.5}Al_{0.5}Zr_x$ (x=0-0.2) Alloys" (277)

Nagai, H.; Nakatsu, M.; Shoji, K.; and Tamura, H., J. of Less-Common Metals, **119** (1986), 131-142 "Effect of Simultaineous Addition of Oxygen with Copper or Niobium on the Hydriding

Characteristics of FeTi for Hydrogen Storage" (392)

Nakamura, K.; Hoshi, T., J. Vacuum Sci. and Tech. A, **3** (1985), 34-38 "Supply and recovery of hydrogen isotopes in high vacuum systems using ZrNi getter pumps" (338)

Nakamura, Y.; Nakamura, H.; Fujitani, S.; Yonezu, I.; Saito, T.; and Nishizawa, N., J. of Alloys and Compounds, **231** (1995), 898-902 "Characteristics of a hydrogen-absorbing alloy developed for a portable fuel cell" (414)

Nemirovskaya, I. E.; Alekseev, A. M.; and Lunin, V. V., J. of Alloys and Compounds, **177** (1991), 1-15 "Thermodynamics of processes of hydrogen sorption by hydrides of intermetallic compounds of CrB structural type" (606)

Neyeb-Hashemi, A. A.; Clark, J. B.; and Swartzendruber, L. J., Binary Alloy Phase Diagrams, T. B. Massalski, Ed., ASM International, **1**, 1990, 1722-1723, "Fe-Mg (Iron-Magnesium)"

Noreus, D., Z. Phys. Chem. NF, **163** (1989), 575-578 "Properties of Formal Low-Valence Transition Metal-Hydrogen Complexes in Mg_2NiH_4 and Na_2PdH_2" (331)

Notten, P. H. L.; Hokkeling, P., J. Electrochemical Soc., **138** (1991), 1877-1885 "Double-Phase hydride Forming Compounds: A New Class of Highly Electrocatalytic Materials" (294)

Notten, P. H. L.; Einerhand, R. E. F.; and Daams, J. L. C., J. of Alloys and Compounds, **231** (1995), 604-610 "How to achieve long-term electrochemical cycling stability with hydride-forming electrode materials" (412)

Oesterreicher, H.; Clinton, J.; and Bittner, H., Materials Res. Bull., **11** (1976), 1241-1248 "Hydrides of La-Ni Compounds" (524)

Oesterreicher, H.; Ensslen, K.; Kerlin, A.; and Buscher, E., Mat. Res. Bull., **15** (1980), 275-283 "Hydriding Behavior in Ca-Mg-Ni-B" (43)

Ogawa, T.; Ohnishi, K.; and Misawa, T., J. of Less-Common. Met., **133** (1988), 143-154, "Manufacture and Hydriding Characteristics of Unidirectionally Solidified $LaNi_5$-Ni Eutectic Alloys with Disintegration Resistance"

Oguro, K.; Osumi, Y.; Suzuki, H.; Kato, A.; Imamura, Y.; and Tanaka, H., J. of Less-Common Metals, **89** (1983), 275-279 "Hydrogen Storage Properties of $TiFe_{1-x}Ni_yM_z$ Alloys" (78)

Ono, S.; Nomura, K.; and Ikeda, Y., J. of Less-Common Metals, **72** (1980), 159-165 "The Reaction of Hydrogen with Alloys of Vanadium and Titanium" (452)

Orimo, S.; Tabata, M.; Fujii, H.; Yamamoto, K.; Tanioka, S.; and Ogasawara, T., J. of Alloys and Compounds, **203** (1994), 61-65 "Low temperature Formation of MgH_2 in $Ti_{0.6}Zr_{0.4}Mn_{0.8}CrCu_{0.2}$/Mg" (297)

Orimo, S.; Fujii. H.; and Tabata, M., J. of Alloys and Compounds, **210** (1994), 37-43, "Synthesis of fine composite particles for hydrogen storage, starting from Mg-YNi_2 mixture"

Orimo, S.; Fujii, H.; Ikeda, K.; and Kitano, Y., J. Alloys and Compounds,1997, in press, "Hydriding properties of nano-/amorphous-structured Mg-Ni-H System"

Osumi, Y.; Suzuki, H.; Kato, A.; Nakane, M.; and Miyake, Y., J. of Chem. Soc. Japan, Chem. and Industrial Chem. (1978), 1472-1477 "Absorption-Desorption Characteristics of Hydrogen for Mischmetal Based Alloys" (117)

Osumi, Y.; Kato, A.; Suzuki, H.; Nakane, M.; and Miyake, Y., J. of Less-Common Metals, **66** (1979), 67-75 "Hydrogen Absorption-Desorption Characteristics of Mischmetal-Nickel-Aluminum Alloys" (119)

Osumi, Y.; Suzuki, H.; Kato, A.; Nakane, M.; and Miyake, Y., J. of the Chem. Soc. of Japan, Chem. and Idust. Chem., **1** (1979), 45-48 "Absorption-Desorption Characterisitcs of Hydrogen for Mischmetal-Nickel-Manganese Alloys" (120)

Osumi, Y.; Suzuki, H.; Kato, A.; Nakane, M.; and Miyake, Y., J. of the Chem. Soc. of Japan, Chem. and Indust. Chem., **6** (1979), 722-726 "Absorption-Desorption Characteristics of Hydrogen for Mischmetal-Nickel-Cobalt Alloys" (121)

Osumi, Y.; Suzuki, H.; Kato, A.; and Nakane, M., J. of Less-Common Metals, **72** (1980), 79-86 "Hydroge Absorption-Desorption Characteristics of Titanium-Cobalt-Manganese Alloys" (80)

Osumi, Y.; Suzuki, H.; Kato, A.; Oguro, K.; and Nakane, M., J. of Less-Common Metals, **74** (1980), 271-277 "Development of Mischmetal-Nickel and Titanium-Cobalt Hydrides for Hydrogen Storage" (122)

Osumi, Y.; Suzuki, H.; Kato, A.; Oguro, K.; and Nakane, M., Hydrogen Energy Progress, Proc. 3rd World Hydrogen Energy Conf., IAHE (1980), 865-878 "Hydrogen Absorption-Desorption Characteristics of Mischmetal-Nickel Alloys" (123)

Osumi, Y.; Suzuki, H.; Kato, A.; Oguro, K.; and Nakane, M., J. of the Chem. Soc. of Japan, Chem. and Indust. Chem. (1981), 1493-1502 "Effect of Metal-Substitution on Hydrogen Storage Properties for Mischmetal-Nickel Alloys" (124)

Osumi, Y.; Suzuki, H.; Kato, A.; Oguro, K.; and Nakane, M., J. of Less-Common Metals, **79** (1981), 207-214 "Hydrogen Absorption-Desorption Characteristics of Mischmetal-Ni-Cr-Mn Alloys" (126)

Osumi, Y.; Suzuki, H.; Kato, A.; and Nakane, M., J. of Less-Common Metals, **84** (1982), 99-106 "Hydrogen Absorption-Desorption Characteristics of Mischmetal-Nickel-Silicon Alloys" (127)

Osumi, Y.; Suzuki, H.; Kato, A.; Oguro, K.; Kawai, S.; and Kaneko, M., J. of Less-Common Metals, **89** (1983), 287-292 "Hydrogen Absorption-Desorption Characteristics of Mm-Al-M and Mm-Ni-Mn-M Alloys (Mm = Mischmetal)" (133)

Paderets, L. N.; Chertikov, A. A.; and Mikheeva, V. I., Izvestiya Akademii Nauk SSSR, Neorganicheskie Materialy, **14** (1978), 1624-1628 "Synthesis and Properties of Ternary Compounds with Hydrogen in the system Zr-M-H (M is V, Cr, Mn, Fe, Co, or Ni)" (513)

Pan, Y. Y.; Nash, P., Binary Alloy Phase Diagrams, T. B. Massalski, Ed., ASM International, **3**, 1990, 2406-2408, "La-Ni (Lanthanum-Nickel)"

Park, J.-M.; Lee, J.-Y., J. of Less-Common Metals, **160** (1990), 259-271 "Hydrogenation Characteristics of the $Zr_{1-x}TixCr_{1-y}Fe_{1+y}$ Laves Phase Systems" (560)

Park, J.-M.; Lee, J.-Y., J. of Less-Common Metals, **167** (1991), 245-253 "Thermodynamic Properties of the $Zr_{0.8}Ti_{0.2}(Mn_xCr_{1-x})Fe$-$H_2$ System" (562)

Park, J.-M.; Lee, J.Y., J. of Alloys and Compounds, **182** (1992), 43-54 "Effect of alloying element on the sloping hydrogen plateaux in zirconium-based Laves phase systems" (581)

Pebler, A.; Gulbransen, E. A., Electrochemical Technology, **4** (1966), 211-215 "Thermochemical and Structural Aspects of the Reaction of Hydrogen with Alloys and Intermetallic Compounds of Zirconium" (12)

Pebler, A.; Gulbransen, E. A., Transactions TMS AIME, **239** (1967), 1593-1596 "Equilibrium Studies on the Systems $ZrCr_2$-H_2, ZrV_2-H_2, and $ZrMo_2$-H_2 Between 0 and 900 C" (13)

Pedziwiatr, A. T.; Craig, R. S.; Wallace, W. E.; and Pourarian, F., J. of Solid State Chem., **46** (1983), 336-341 "Calorimetric Enthalpies of Formation and Decomposistion of Hydrides $ZrMn_2$, $ZrCr_2$, and Related Systems" (28)

Percheron-Guegan, A.; Welter, J.-M., Hydrogen in Intermetallic Compounds I, L. Schlapbach, Ed., Topics in Appl. Phys., **63** (1988), 11-48, "Preparation of Intermetallics and Hydrides"

Perevesenzew, A.; Lanzel, E.; Elder, O. J.; Tuscher, E.; and Weinzierl, P., J. of Less-Common Metals, **143** (1988), 39-47 "Thermodynamics and Kinetics of Hydrogen Absorption in the Intermetallic Compounds $Zr(Cr_{1-x}V_x)_2$" (557)

Philipp, S.; Schmidt, P. C.; and Weiss, A., J. of Less-Common Metals, **172** (1991), 136-143 "Solubility of hydrogen in CsCl-type Group Ib-Erbium alloys XEr (X = Cu, Ag, Au)" (384)

Pourarian, F.; Wallace, W. E.; Elattar, A.; and Lakner, J. F., J. of Less-Common Metals, **74** (1980), 161-165 "$DyFe_2$-H2 System: Magnetism and Pressure-Composition Isotherms to 1400 atm" (357)

Pourarian, F.; Fujii, H.; Wallace, W. E.; Sinha, V. K.; and Smith, H. Kevin, J. Phys. Chem., **85** (1981), 3105-3111 "Stabillity and Magnetism of Hydrides of Nonstoichiometric $ZrMn_2$" (19)

Pourarian, F.; Sinha, V. K.; and Wallace, W. E., J. Phys. Chem., **82** (1982), 4956-4958 "Hydrogen Absorption by $ZrMn_2Mn_yFe_x$" (512)

Pourarian, F.; Sinha, V. K.; and Wallace, W. E., J. of Less-Common Metals, **96** (1984), 237-248 "Hydrogen Sorption Properties of Non-Stoichiometric $ZrMn_2$-based Systems" (551)

Qian, S.; Northwood, D. O., Z. Phys. Chem. NF, **164** (1989), 1349-1354 "Hysteresis in the $Zr(Fe_xCr_{1-x})_2$-H Systems" (376)

Qian, S.; Northwood, D. O., J. of Less-Common Metals, **147** (1989), 149-159 "Thermodynamic Characterization of $Zr(Fe_xCr_{1-x})_2$-H Systems" (559)

Ramesh, R.; Rao, K. V. S. Rama, J. of Alloys and Compounds, **191** (1993), 101-105 "Hydrogen absorption characteristics of the $Zr_{1-x}Ho_xCo_2$ system in the pressure range 0-40 bar" (363)

Reilly, J.; Wiswall, R., Annual Report, Nuclear Engineering Dept., Brookhaven National

Laboratory, W. E. Winsche and F. T. Miles, Eds., BNL 50023 (1966), 36-38 "Metal Hydrides" (489)

Reilly, J. J.; Wiswall, R. H., Inorganic Chem., **6** (1967), 2220-2223 "The Reaction of Hydrogen with Alloys of Magnesium and Copper" (87)

Reilly, J. J.; Wiswall Jr., R. H., Inorganic Chem., **7** (1968), 2254-2256 "The Reaction of Hydrogen with Alloys of Magnesium and Nickel and the Formation of Mg_2NiH_4" (88)

Reilly, J. J.; Wiswall, R. H., BNL Report 17136, Brookhaven National Laboratory (1972) "Hydrogen Storage and Purification Systems" (195)

Reilly, J. J.; Wiswall, R. H., Rept. BNL-16546, Brookhaven Nat. Lab. (1972), 1-25 "The Effect of Minor Constituents on the Properties of Vanadium and Niobium Hydrides" (314)

Reilly, J. J.; Wiswall Jr., R. H., U. S. Patent 3,825,418 (1974) "Alloys for the Isolation of Hydrogen" (153)

Reilly, J. J.; Wiswall, Inorg. Chem., **13** (1974), 218-222 "Formation and Properties of Iron Titanium Hydride" (319)

Reilly, J. J.; Johnson, J. R., Proc. 1st World Hydrogen Energy Conference, T. N. Veziroglu, Ed., IAHE, Coral Gables, **II** (1976), 8B-3-8B-26 "Titanium Alloy Hydrides; Their Properties and Applications" (383)

Reilly, J. J.; Wiswall, R. H., Report BNL 21322, Brookhaven National Lab (1976) "Hydrogen Storage and Purification Systems III" (490)

Reilly, J. J., Hydrogen: Its Technology and Implications, K. E. Kox and K. D. Williamson, Eds., CRC Press, **II** (1977), 13-48 "Metal Hydrides as Hydrogen Storage Media and Their Applications" (281)

Reilly, J. J., Hydrides for Energy Storage, A. F. Andresen and A. J. Maeland, Eds., Pergamon Press, Oxford (1978), 301-322, "Synthesis and Properties of Useful Metal Hydrides"

Reilly, J. J.; Sandrock, G. D., Scientific American, **242** (No.2), Feb. 1980, 118-129, "Hydrogen Storage in Metal Hydrides"

Rodriguez, D.; Meyer, G.; Peretti, H. A.; and Bolcich, J. C., HYDROGEN ENERGY PROGRESS XI, T.N. Veziroglu, C.-J. Winter, J.P. Baselt and G. Kreysa, Eds., Int. Assoc. of Hydrogen Energy, **2** (1996), 1305-1309 "Hydrogen absorption/desorption characterization of $Mm_{0.8}Ca_{0.2}Ni_{5-x}Al_x$ alloys" (632)

Ron, M., J. of Less-Common. Met., **74** (1980), 445, "Preparation and Properties of Porous Metal Hydride Compacts"

Ron, M.; Joshepy, Y., J. of Less-Common Metals, **131** (1987), 51-59 "Dynamic Characteristics of the Hydrogen Sorption Process in $MmNi_{4.15}Fe_{0.85}H_x$ Compacts" (276)

Ryan, D. H.; Dumias, F.; Patel, B.; Kycia, J.; and Ström-Olsen, J. O., J. of Less-Common. Met., **172-174** (1991), 1246-1251, "A rechargeable cell based on amorphous Ni-Zr"

Sai Raman, S. S.; Srivastava, O. N., J. of Alloys and Compounds, **241** (1996), 167-174,

"Hydrogenation behavior of the new composite storage materials Mg-x% CFMmNi$_5$"

Sakai, T.; Yoshinaga, H.; Miyamura, H.; Kuriyama, N.; and Ishikawa, H., J. Alloys and Compounds, **180** (1992), 37-54 "Rechargeable hydrogen batteries using rare-earth-based hydrogen storage alloys" (278)

Sakai, T.; ,; Muta, K.; Miyamura, H.; Kuriyama, N.; and Ishikawa, H., Hydrogen Storage Materials, Batteries, and Electrochemistry, D. A. Corrigan and S. Srinivasan, Eds., The Electrochemical Soc., **92-5** (1992), 59-91 "Nickel-Metal Hydride Batteries using Rare-Earth Based Hydrogen Storage Alloys" (345)

Sakai, T; Matsuoka, and M; Iwakura, C., Handbook on the Physics and Chemistry of Rare Earths, K. A. Gschneidner and L. Eyring, Eds., **21**, Elsevier Science, 1995, Chapt. 142, 133-178, "Rare Earth Intermetallics for Metal-Hydrogen Batteries"

Sakai, T., Osaka National Research Institute, Private Communication, May, 1996

Sakamoto, Y.; Nakamura, R.; and Ura, M., J. of Alloys and Compounds, **231** (1995), 533-536 "Hydrogen solubility in $PdLi_{0.94}$ and $Pd_2Li_{1.04}$ compounds" (411)

Sandrock, G. D., Final Report, Contract BNL 352410S, Brookhaven National Laboratory, Upton, NY, June 30, 1976, "The Interrelations among Composition, Microstructure, and Hydriding Behavior for Alloys Based on the Intermetallic Compound FeTi"

Sandrock, G. D.; Reilly, J. J.; and Johnson, J. R., Proc. of the Eleventh Intersociety Energy Conversion Engineering Conference, **I** (1976), 965-971 "Metallurgical Considerations in the Production and Use of FeTi Alloys for Hydrogen Storage" (76)

Sandrock, G. D., Proc. 12th Intersociety Energy Conversion Engineering Conference, Am. Nuclear Soc., **I** (1977), 951-958 "A New Family of Hydrogen Storage Alloys Based on the System Nickel-Mischmetal-Calcium" (106)

Sandrock, G. D.; Trozzi, C. J., Final Report, Contract BNL 352410S (Second Year), Brookhaven National Laboratory, Upton, NY, Dec. 30, 1977, "Thermodynamic, Economic and Metallurgical Studies of Various Techniques for the Large Scale Production of Hydriding Grade FeTi and Related Compounds"

Sandrock, G. D., Proc. Miami Int. Conf. on Alt. Energy Sources, Univ. Miami (1977), 3713-3738 "A Survey of the Hydrogen Storage Properties of Nickel-Copper-Mischmetal-Calcium Alloys" (107)

Sandrock, G. D., HYDROGEN ENERGY SYSTEM, T. N. Vezeroglu and W. Seifritz, Eds., Pergamon Press, **3** (1978), 1625-1656 "Development of Low Cost Nickel-Rare Earth Hydrides for Hydrogen Storage" (113)

Sandrock, G. D., Hydrides for Energy Storage, A. F. Andresen and A. J. Maeland, Eds., Pergamon Press, Oxford (1978), 353-393 "The Metallurgy and Production of Rechargeable Hydrides" (321)

Sandrock, G. D.; Goodell, P. D., J. of Less-Common Metals, **73** (1980), 161-168 "Surface Poisoning of $LaNi_5$, FeTi, and (Fe,Mn)Ti by O_2, CO, and H_2O" (203)

Sandrock, G. D., Hydrogen Energy, G. Hambraeus and B. Belfrage, Eds., Rapport 199,

Injenjörsvetenskapsakademien, Stockholm, 1981, 67-151, "Hydrogen Storage"

Sandrock, G. D.; Murray, J. J.; Post, M. L.; and Taylor, J. B., Materials Res. Bull., **17** (1982), 887-894 "Hydrides and Deuterides of $CaNi_5$" (326)

Sandrock, G. D.; Goodell, P. D., J. of Less-Common Metals, **104** (1984), 159-173 "Cyclic Life of Metal Hydrides with Impure Hydrogen: Overview and Engineering Considerations" (4)

Sandrock, G. D., U. S. Patent 4,668,424 (1987) "Low Temperature Reusable Hydrogen Getter" (336)

Sandrock, G. D.; Goodell, P. D.; Huston, E. L.; and Golben, P. M., Z. Phys. Chem. NF, **164** (1989), 1285, "On the Disproportionation of Intermetallic Hydrides"

Sandrock, G. D.; Huston, E. L., RARE EARTHS, Resources Science, Technology and Applications, R. G. Bautista and N. Jackson, Eds., The Minerals, Metals & Materials Soc., 1991, 423-447, "Rare Earths and Rechargeables - The Role of REE's in Reversible Metal Hydrides"

Sandrock, G.; Suda, S.; and Schlapbach, L., Hydrogen in Intermetallic Compounds II, L. Schlapbach, Ed., Topics in Appl. Phys., Springer, Berlin, **67** (1992), 197-258 "Applications" (322)

Sandrock, G., Hydrogen Energy System - Production and Utilization of Hydrogen and Future Aspects, Y. Yürüm, Ed., Kluwer Academic, Dordrecht, 1995 (a), 135-166, "Hydrogen-Metal Systems"

Sandrock, G., Hydrogen Energy System - Production and Utilization of Hydrogen and Future Aspects, Y. Yürüm, Ed., Kluwer Academic, Dordrecht, 1995 (b), 253-280, "Applications of Hydrides"

Sandrock, G; Thomas, G., SNL Hydrogen Information Center, http://hydpark.ca.sandia.gov/, 1997 (continuing), "IEA/DOE/SNL Hydride Databases"

Sandrock, G; Thomas, G., Report Series IEA/H2/TR-97, International Energy Agency, Paris, 1997, "Compilation of IEA/DOE/SNL Hydride Databases"

Sasai, T.; Oku, K.; Konno, H.; Onouwe, K.; and Kashu, S., J. of Less-Common Metals, **89** (1983), 281-285 "Hydrogen Storage Characteristics of Fe-Ti-Zr-Nb Alloys" (79)

Sasaki, Y.; Amano, M., Hydrogen Energy Progress, T. N. Veziroglu, K. Fueki, and T. Ohta, Eds., Pergamon, Oxford, **2** (1981), 891-895 "Hydrogen Storage Properties of $Fe_{1-x}Nb_xTi$" (394)

Schlapbach, L.; A.Seiler; H.C.Siegmann; T.V.Waldkirch; P.Zurcher; and C.Brundel, Int. J. Hydrogen Energy, **4** (1979), 21-28 "Self Restoring of the Active Surface in $LaNi_5$" (230)

Sapru, K.; Reichman, A. R.; and Ovshinsky, S. R.; US Pat. 4 623 597. Nov. 18, 1986, "Rechargeable Battery and Electrode used Therein"

Schlapbach, L.; Riesterer, T., Appl. Phys. A, **32** (1983), 169-182, "The Activation of FeTi for Hydrogen Absorption"

Schlapbach, L., Ed., Hydrogen in Intermetallic Compounds I & II, Topics in Appl. Phys., **63** &

67 (1988 & 1992)

Schober, T.; Wenzl, H; Hydrogen in Metals II, G. Alefeld and J. Völkl, Eds., Topics in Appl. Phys., **29** (1978), 11-71, "The Systems NbH(D), TaH(D), VH(D): Structure, Phase Diagrams, Morphologies, Methods of Preparation"

Selvam, P.; Viswanathan, B.; Swamy, C. S.; and Srinivasan, V., Int. J. Hydrogen Energy, **11** (1986), 169-192, "Magnesium and Magnesium Alloy Hydrides"

Selvam, P.; Yvon, K., Int. J. of Hydrogen Energy, **9** (1991), 615-617 "Synthesis of Mg_2FeH_6, Mg_2CoH_5 and Mg_2NiH_4 by High-Pressure Sintering of the Elements" (426)

Shaltiel, D.; Jacob, I.; and Davidov, D., J. of Less-Common Metals, **53** (1977), 117-131 "Hydrogen Absorption and Desorption Properties of AB_2 Laves-Phase Pseudobinary Compounds" (14)

Shaltiel, D., J. of Less-Common Metals, **62** (1978), 407-416 "Hydride Properties of AB_2 Laves Phase Compounds" (66)

Shaltiel, D.; Davidov, D.; and Jacob, I., U. S. Patent 4,163,666 (1979) "Hydrogen Charged Alloys of $Zr(A_{1-x}B_x)_2$ And Method of Hydrogen Storage" (51)

Shenoy, G. K.; Dunlap, B. D.; Viccaro, P. J.; and Niarchos, D., Mossbauer Spectroscopy: Its Chemical Applications, Adv. in Chem. Series, **194** (1981), 501-521 "Hydrogen Storage Materials" (445)

Shilov, A. L.; Kost, M. E., Russian J. Inorganic Chem., **28** (1981), 163-166 "The Stability of Intermetallic Hydrides" (530)

Shitikov, V.; Hilscher, G.; Stampfl, H.; and Kirchmayr, H., J. of Less-Common Metals, **102** (1984), 29-40 "Thermodynamics and Kinetics of $Zr(Fe_{1-x}Mn_x)_2H_x$ and the Storage Compound $Ti_{0.8}Zr_{0.2}MnCrH_3$" (552)

Siegmann, H. C.; Schlapbach, L.; and Brundle, C. R., Phys. Rev. Lett., **14** (1978), 972-975, "Self-Restoring of the Active Surface in the Hydrogen Sponge $LaNi_5$"

Singh, A. K.; Singh, A. K.; Srivastava, O.N.; Int. J. Hydrogen Energy, **18** (1993), 567-570, Synthesis of $MmNi_{4.5}Al_{0.5}$ by Mechanical Alloying"

Singh, A. K.; Singh, A. K.; and Srivastava, J. Alloys and Compounds, **227** (1995) 63-68, "On the synthesis of the Mg_2Ni alloy by mechanical alloying"

Sinha, V. K.; Wallace, W. E., J. of Less-Common Metals, **87** (1982), 297-303 "$Zr_{0.7}Ti_{0.3}Mn_2Fe_{0.8}$ As a Material for Hydrogen Storage" (20)

Sinha, V. K.; Pourarian, F.; and Wallace, W. E., J. of Less-Common Metals, **87** (1982), 283-296 "Hydrogenation Characteristics of $Zr_{1-x}Ti_xMnFe$ Alloys" (25)

Sinha, V. K.; Pourariam, F.; and Wallace, W. E., J. Phys. Chem., **86** (1982), 4952-4956 "Hydrogen Absorption by $ZrMn_2Fe_x$" (509)

Sinha, V. K.; Wallace, W. E., J. of Less-Common Metals, **91** (1983), 229-237 "The Hyperstoichiometric $ZrMn_{1+x}Fe_{1+y}$-H_2 System, I: Hydrogen Storage Characteristics" (23)

Sinha, V. K.; Yu, G. Y.; and Wallace, W. E., J. of Less-Common Metals, **106** (1985), 67-77 "Hydrogen Storage in some Ternary and Quaternary Zirconium-Based Alloys with the C14 Structure" (554)

Slattery, D. K., Int. J. Hydrogen Energy, **20** (1995), 971-973 "The Hydriding-Dehydriding Characteristics of La_2Mg_{17}" (443)

Someno, M.; Arita, M.; Kinaka, R.; and Ichinose, Y., Hydrogen in Metals, Trans. Japan Inst. of Metals (Supplement), **21** (1980), 325-328 "Hydrogen Absorption and Hydriding of Ti-Based Intermetallic Compounds" (381)

Song, M. Y.; Lee, J. Y., Int. J. Hydrogen Energy, **8** (1983), 363-367, "A Study of the Kinetics of Mg-(10-20 w/o) $LaNi_5$"

Song, M. Y.; Ivanov, E. I.; Darriet, B.; Pezat, M.; and Hagenmueller, P., Int. J. Hydrogen Energy, **10** (1985), 169-178, "Hydriding Properties of a Mechanically Alloyed Mixture with a Composition Mg_2Ni"

Song, M.Y.; Ivanov, E.; Darriet, B.; Pezat, M.; and Hagenmuller, P., J. Less-Common Met., **131** (1987), 71-79, "Hydriding and Dehydriding Characteristics of Mechanically Alloyed Mixtures Mg-xwt.%Ni (x=5, 10, 25, and 55)"

Spada, F. E.; Bowman, R. C.; and Cantrell, J. S., J. of Less-Common Metals, **129** (1987), 261-270 "Hydrogen Absorption by $LaCu_5$ and Nuclear Magnetic Resonance (NMR) Studies of Hydrogen Diffusion in beta-$LaCu_5$ Hydride" (255)

Spada, F. E.; Bowman, R. C.; and Cantrell, J. S., J. of Less-Common Metals, **129** (1987), 197-205 "Hydride Phase Coposition and Crystal Structure in Zr_2PdH_x" (424)

Spit, F. H. M.; Drijver, J. W.; and Radelarr, S., Scripta Metallurgica, **14** (1980), 1071-1076, " Hydrogen Sorption by the Metallic Glass $Ni_{64}Zr_{36}$ and by its Related Crystalline Compounds"

Spit, F. H. M., Doctor's Thesis, Rijksuniversiteit Utrecht (1982), 1-137 "The Thermodynamics and Kinetics of Hydrogen Solution in Some Metallic Glasses" (446)

Stepanov, A.; Ivanov, E.; Konstanchuk, I; and Boldyrev, V, J. Less-Common Met., **131** (1987), 89-97, "Hydriding Properties of Mechanical Alloys Mg-Ni"

Stetson, N. T.; Yvon, K.; and Fischer, P., Inorg. Chem., **33** (1994), 4598-4599, "On the Structure of the Complex Hydride $BaReH_9$"

Suda, S.; Uchida, M., Hydrides for Energy Storage, A. F. Andresen and A. J. Maeland, Eds., Pergamon Press, Oxford (1978), 515-525, "Mixing Effects of Two Different Types of Hydrides"

Suda, S.; Komazaki, Y.; and Kobayashi, N., Hydrogen Energy Progress, T. N. Veziroglu, K. Fueki, and T. Ohta, Eds., Pergamon Press, Oxford, **4** (1981), 2169-2183 "Mixing Effects of Metal Hydrides on Equilibrium Behavior and Reaction Kinetics" (288)

S. Suda, Research Reports of Kogakuin University, **74** (Apr.1993), 29-34, "Mechanism of Hydrogen Uptake on the F-Treated Surface of the $LaNi_{4.7}Al_{0.3}$-alloy"

Sullivan, E. A.; Wade, R. C., Kirk-Othmer Encyclopedia of Chemical Technology, **12** (1980), 772-792, "Hydrides"

Suzuki, H.; Osumi, Y.; Kato, A.; Oguro, K.; and Nakane, M., J. of Less-Common Metals, **80** (1981), 179-185 "Hydrogen Absorption-Desorption Characteristics of Ti-Co-Fe Alloys" (82)

Suzuki, H.; Osumi, Y.; Kato, A.; and Nakane, M., J. of the Chem. Soc. of Japan, Chem. and Indust. Chem., **7** (1981), 1069 "Hydrogen Absorption-Desorption Characterisitcs of Mischmetal-Nickel-Chromium Alloys" (125)

Suzuki, A.; Nishimiya, N.; Ono, S.; Higano, S.; and Kamino, K., Chem. Letters (Japan) (1982), 75-78 "Hydriding Behaviors of $Zr_xTi_{1-x}(Fe_yMn_{1-y})_z$ Alloys" (26)

Suzuki, A.; Nishimiya, N.; and Ono, S., Chem. Letters (Japan) (1982), 205-208 "Hydriding Behaviors of $Zr(Fe_xMn_{1-x})_2$ Alloys" (27)

Suzuki, A.; Nishimiya, N.; and Ono, S., J. of Less-Common Metals, **89** (1983), 263-268 "Thermodynamic Properties of $Zr(Fe_xMn_{1-x})_2$-H_2 Systems" (30)

Suzuki, J.; Abe, M.; Yamaguchi, T.; and Terazawa, S., J. of Less-Common Metals, **131** (1987), 301-309 "Hydrogen Absorption Properties of $FeTi_{(1+x)}$-Rare Earth Oxide Composite Materials" (292)

Takeshita, T.; Gschneider Jr., K. A.; and Lakner, J. F., J. of Less-Common Metals, **78** (1981), P43-P47 "High Pressure Hydrogen Absorption Study on YNi_5, $LaPt_5$ and $ThNi_5$" (128)

Takeya, K.; Tsugita, Y.; Okajima, Y.; Sakai, T.; Miyamura, H.; and et al, J. of Alloys and Compounds, **192** (1993), 167-169 "Hydrogen storage alloy powder produced by reduction-diffusion process and their electrode properties" (279)

Tauber, A.; Finnegan, R. D.; Schwartz, A.; Rothwarf, F.; and Wallace, W. E., Proc. 12th Rare Earth Research Conf., C. E. Lundin, Ed. (1976), 1073-1082 "Some Light Rare Earth Intermetallic Hydrides" (529)

Thomas, G. J.; Guthrie, S. E.; Bauer, W.; Yang, N. Y. C.; and Sandrock, G., Proc. 1996 U.S. DOE Hydrogen Program Review, Rept. NREL/CP-430-21968, **II** (Oct.1996), National Renewable Energy Laboratory, Golden, CO, 807-818, "Hydride Development for Hydrogen Storage"

Thomas, G. J.; Guthrie, S. E., Proc. 1997 U.S. DOE Hydrogen Program Review, in press, National Renewable Energy Laboratory, Golden, CO, " Lightweight Hydride Development"

Toepler, J.; Bernauer, O.; and Buchner, H., J. of Less-Common. Met., **74** (1980), 385, "The Use of Hydrides in Motor Vehicles"

Trzeciak, M. J.; Dilthey, D. F.; and Mallett, M. W., Rept. BMI-1112, Battelle Memorial Institute, Columbus, OH (1956), 1-32 "Study of Hydrides" (483)

Tsukahara, M.; Takahashi, K.; Mishima, T.; Sakai, T.; Miyamura, H.; Kuriyama, N.; and Uehara, I., J. Alloys and Compounds, **226** (1995), 203-207, "Metal hydride electrodes based on solid solution type alloy TiV_3Ni_x ($0 \leq x \leq 0.75$)"

Tsukahara, M.; Takahashi, K.; Mishima, T.; Isomura, T.; and Sakai, T., J. Alloys and Compounds, **236** (1996), 151-155, "V-based solid solution alloys with Laves phase network: hydrogen absorption properties and microdtructure"

Uchida, H.; Tada, M.; and Huang, Y. C., J. of Less-Common Metals, **88** (1982), 81-87 "The Influence of Cerium, Praseodymium, Neodymium and Samarium on Hydrogen Absorption in $LaNi_5$ Alloys" (131)

Uchida, M.; Bjurstrom, H.; Suda, S.; and Matsubara, Y., J. of Less-Common Metals, **119** (1986), 63-74 "On the Equilibrium Properties of some $ZrMn_2$-Related Hydride-Forming Metals" (370)

van Essen, R. M.; Buschow, K. H. J., J. of Less-Common Metals, **64** (1979), 277-284 "Hydrogen Absotption in Various Zirconium- and Hafnium-Based Intermetallic Compounds" (386)

van Essen, R. M.; Buschow, K. H. J., Mat. Res. Bull., **15** (1980), 1149-1155 "Composition and Hydrogen Absorption of C14 Type Zr-Mn Compounds" (17)

van Essen, R. H.; Bushow, K. H. J., J. of Less-Common Metals, **70** (1980), 189-198 "Hydrogen Sorption Characteristics of Ce-3d and Y-3d Intermetallic Compounds" (355)

van Mal, H. H.; Buschow, K. H. J.; and Kuijpers, F. A., J. of Less-Common Metals, **32** (1973), 289-296 "Hydrogen Absorption and Magnetic Properties of $LaCo_{5x}Ni_{5-5x}$ Compounds" (97)

van Mal, H. H.; Buschow, K. H. J.; and Miedema, A. R., J. of Less-Common Metals, **35** (1974), 65-76 "Hydrogen Absorption in $LaNi_5$ and Related Compounds: Experimental Observations and Their Explanation" (98)

van Mal, H. H., Thesis, University of Delft, Netherlands (1976) "Stabilty of Ternary Hydrides and Some Applications" (44)

van Vucht, J. H. N., Philips Res. Repts., **18** (1963), 1-20 "Equilibrium Pressures in the System Th_2Al-Hydrogen" (492)

van Vucht, J. H. N.; Kuijpers, F. A.; and Bruning, H. C. A. M., Philips Res. Repts., **25** (1970), 133-140 "Reversible Room-Temperature Absorption of Large Quantities of Hydrogen by Intermetallic Compounds" (93)

Verbetsky, V. N.; Klyamkin, S. N.; Kovriga, A. Yu.; and Besphalov, A. P., Int. J. Hydrogen Energy, **21** (1996), 997-1000 "Hydrogen Interaction with RNi_3 Type Intermetallic Compounds at High Gaseous Pressure" (636)

Viccaro, P. J.; Shenoy, G. K.; Niarchos, D.; and Dunlap, B. D., J. of Less-Common Metals, **73** (1980), 265-271 "^{166}Er Mossbauer and X-Ray Diffraction Study of $ErMn_2$ Hydrides" (359)

Vivano, A. M.; Stroud, R. M.; Gibbons, P. C.; McDowell, A. F.; Conradi, M. S.; and Kelton, K. F., Phys. Rev. B, **51** (1995), 12026-12029, "Hydrogenation of titanium-based quasicrystals"

Vivano, A. M.; McDowell, A. F.; Conradi, M. S.; Gibbons, P. C.; and Kelton, K. F., Proc. 5th Int. Conf. in Quasicrystals, Avignon, France, May 1995, "Hydrogen in Quasicrystalline TiZrNi"

Wallace, W. E.; Karlicek, R. F.; and Immamura, H., J. Phys Chem., **83** (1979), 1708

Wallace, W. E.; Craig, R. S.; and Rao, V. U. S., Solid State Chemistry: A Contemporary Overview, Adv. in Chemistry Series, S. L. Holt, J. B. Milstein, and M. Robbins, Eds., ACS, **186** (1980), 207-240 "Hydrogen Absorption by Intermetallic Compounds" (439)

Wallace, W. E.; Pourarian, F.; and Sinha, V. K., U. S. Pat. 4,406,874 (1983) "$ZrMn_2$-Type Alloy Partially Substituted with Cerium/Praeseodymium/Neodymium and Characterized by AB_2 Stoichiometry" (528)

Wang, J. C.; Chen, F. C.; and Murphy, R. W., Proc. 1996 U.S. DOE Hydrogen Program Review, Rept. NREL/CP-430-21968, **II** (Oct.1996), National Renewable Energy Laboratory, Golden, CO, 819-829, "Thermal Management Technology for Hydrogen Storage: Fullerene Option"

Wang, Q.-D.; Wu, J.; and Chen, C.-P., Zeit. Phys. Chem. NF, **164** (1989), 1293-1304 "Development of New Mischmetal-Nickel Hydrogen Storage Alloys According to the Specific Requirements of Different Applications" (267)

Wang, X. L.; Suda, S., Int. J. Hydrogen Energy, **15** (1990), 569-577 "Reaction Kinetics of Hydrogen-Metal hydride systems" (324)

Wang, X.; Chen, C.; Wang, C.; and Wang, Q., J. of Alloys and Compounds, **232** (1996), 192-196 "Hydrogen storage properties of $M1_{1-x}Ca_xNi5$ pseudobinary intermetallic compounds" (592)

Wernick, J. H., Intermetallic Compounds, J. H. Westbrook, Ed., 1967, John Wiley, 197-216, "Topologically Close-Packed Structures"

Westlake, D. G., J. of Less-Common Metals, **91** (1983), 275-292 "A Geometric Model for the Stoichiometry and Interstitial Site Occupancy in Hydrides (Deuterides) of $LaNi_5$, $LaNi_4Al$ and $LaNi_4Mn$" (154)

Willems, J. J. G., Philips J. of Research, Supplement No. 1, **39** (1984), 1-94 "Metal Hydride Electrodes: Stability of $LaNi_5$-Related Compounds" (340)

Willems, J. J. G.; Buschow, K. H. J., J. of Less-Common Metals, **129** (1987), 13-30 "From Permanent Magnets to Rechargeable Hydride Electrodes" (354)

Wiswall, R. H.; Reilly, J. J., Inorg. Chem., **11** (1972), 1691-1696 "Inverse Hydrogen Isotope Effects in Some Metal Hydrides" (318)

Withers, J. C.; Loutfy, R. O.; and Lowe, T. P., Fullerine Sciench and Technology, **5** (1997), 1-31, "Fullerene Commercial Vision"

Yajima, S.; Kayano, H.; and Toma, H., J. of Less-Common Metals, **55** (1977), 139-141 "Hydrogen Sorption in La_2Mg_{17}" (188)

Yamaguchi, M.; Ikeda, H.; Ohta, T.; Katayama, T.; and Goto, T., J. of Less-Common Metals, **106** (1985), 165-173 "Influence of Hydrogen on the Magnetic Properties of Y-Co Compounds" (573)

Yamaguchi, M.; Yamamoto, I.; Fujita, Y.; and Goto, T., Zeit. Phys. Chem. NF, **163** (1989), 677-682 "Magnetic Moments in the Hydrides of YCo_3-Related Compounds" (615)

Yamamoto, T.; Kayano, H.; Sinaga, S.; Ono, F.; Tanaka, S.; and Yamawaki, M., J. of Less-Common Metals, **172** (1991), 71-78 "Hydrogen absorption-desorption properties of UCo" (398)

Yamanaka, K.; Saito, H.; and Someno, M., J. Chem. Soc. Japan, **8** (1975), 1267-1272 "Hydride Formation of Intermetallic Compounds of Titanium-Iron, Titanium- Cobalt, Titanium-Nickel, and Titanium Copper" (73)

Yang, H. W.; Jenq, S. N.; Wang, Y. Y.; and Wan, C. C., J. of Alloys and Compounds, **227** (1995), 69-75 "Hydrogen absorption-desorption characteristics of $Ti_{0.35}Zr_{0.65}Ni_xV_{2-x-y}Mn_y$ alloys with C14 Laves phase for nickel/metal hydride" (402)

Ye, Z.; Erickson, L. C.; and Hjörvarsson, B., J. of Alloys and Compounds, **209** (1994), 117-124, Hydride formation in Mg-$ZrFe_{1.4}Cr_{0.6}$ composite material"

Yonezu, I.; Fujitani, S.; Furukawa, A.; Nasako, K.; T; Yonesaki; Sato, T.; and Furukawa N., J. of Less-Common Metals, **168** (1991), 201-209 "Characteristics of Hydrogen-Absorbing Zr-Mn Alloys for Heat Utilization" (563)

Yoshida, M.; Bonhomme, F.; Yvon, K.; and Fischer, P., J. of Alloys and Compounds, **190** (1993), L45-L46 "On the composition and structure of the cubic δ-phase in the Mg-Co-H system" (594)

Yoshida, M.; Yvon, K.; and Fischer, P., J. of Alloys and Compounds, **194** (1993), L11-L13, "$LiSr_2PdH_5$, the first mixed alkali-alkaline earth transition metal hydride"

Yoshida, M.; Akiba, E.; Shimojo, Y.; Morii, Y.; and Izumi, F., J. of Alloys and Compounds, **231** (1995), 755-759 "Hexagonal ZrNiAl alloy and its hydride (deuteride) with the Fe_2P-type structure" (622)

Yoshinaga, H.; Wada, M.; Sakai, T.; Miyamura, H.; Kuriyama, N.; and Uehara, I., Denki Kagaku, **63** (1995), 847-852 "Metal Hydride Electrodes Made by Dry Powder Process Using Flake Copper and Flake Nickel Powders" (298)

Yu, G. Y.; Pourarian, F.; and Wallace, W. E., J. of Less-Common Metals, **106** (1985), 79-87 "The Crystallographic, Thermodynamic and Kinetic Properties of the $Zr_{1-x}Ti_xCrFe$-H_2 System" (555)

Yvon, K.; Fischer, P., Hydrogen in Intermetallic Compounds, L. Schlapbach, Ed., Topics in Appl. Phys., Springer, Berlin, **63** (1988), 87-138 "Crystal and Magnetic Structures of Ternary Metal Hydrides" (320)

Yvon, K.; University of Geneva, private communication, 1997

Zaluski, L.; Tessier, P.; Ryan, D. H.; Donner, C. B.; Zaluska, A.; and Ström-Olsen, J. O., J.

Materials Res., **8** (1993), 3059-3068, "Amorphous and nanocrystalline Fe-Ti prepared by ball milling"

Zaluski, L.; Zaluska, A.; and Ström-Olsen, J. O., J. Alloys and Compounds, **217** (1995), 245-249, "Hydrogen absorption in nanocrystalline Mg_2Ni formed by mechanical alloying"

Zaluski, L.; Zaluska, A.; Tessier, P.; Ström-Olsen, J. O.; and Schultz, R, J. Alloys and Compounds, **217** (1995), 295-300, "Catalytic effect of Pd on hydrogen absorption in mechanically alloyed Mg_2Ni, $LaNi_5$ and FeTi"

Zaluski, L.; Zaluska, A.; and Ström-Olsen, J. O., J. Alloys and Compounds, 1997, in press, "Nanocrystalline Metal Hydrides"

Zhan, F.; Bao, D.; Jiang, L.; Zhang, L.; Yu, X.; and Zhou, Y., J. of Alloys and Compounds, **231** (1995), 907-909 "Metal hydride compressor and its application in cryogenic technology" (627)

Zhang, D. X.; Wang, X. L.; and Wang, G. S., Zeit. Phys. Chem. NF, **164** (1989), 1441-1446 "Recovery of Efficacy-Lost $LaNi_5$ by Chemical Preparation Method" (262)

Zidan, R. A.; Rocheleau, R. E.; and Jensen, C. M., Proc. 1996 U.S. DOE Program review, Rept. NREL/CP-430-21968, **II** (1996), National Renewable Energy Lab, 795-805, "Thermodynamic Characterization of Polyhydride Complexes"

Zijlstra, H.; Westendorp, F. F., Solid State Comm., **7** (1969), 857-859 "Influence of Hydrogen on the Magnetic Properties of $SmCo_5$" (148)

Zolliker, P.; Yvon, K.; Fischer, P.; and Schefer, J., Inorg. Chem., **24** (1985), 4177-4180, "Dimagnesium Cobalt(I) Pentahydride, Mg_2CoH_5, Containing Square Pyramidal CoH_5^{4-} Anions"

Zolliker, P.; Yvon, K.; Jorgensen, J. D.; and Rotella, F. J., Inorg. Chem., **25** (1986), 3590-3593, "Structural Studies of Hydrogen storage Material Mg_2NiH_4. 2. Monoclinic Low Temperature Structure"

APPENDIX
LISTING OF HYDRIDE R&D FACILITIES IN VARIOUS COUNTRIES

This Appendix gives abbreviated listings of hydride R&D facilities in five countries selected by the sponsor of this study: Australia, Canada, New Zealand, United Kingdom and United States. These lists concentrate on hydride activities and generally exclude dilute hydrogen in metals activities such as hydrogen permeation, embrittlement, etc., although there may be some overlap. A few entries on carbons are included. The entries are mostly from the reviewer's personal contacts and additional limited research from recent conferences. Acknowledgements are hereby made to Dr. Evan Gray (Griffith University) and Prof. D. Keith Ross (University of Salford) for extensive help with the Australia and UK sections, respectively. In the case of New Zealand, I am unaware of any hydride activity. The lists are certainly not 100% complete and the author would be grateful to hear of any activities not listed for the surveyed countries.

AUSTRALIA

Organization	Contact	Topics
Australian Defence Force Academy Department of Physics Canberra ACT 2600	S. Campbell Tel: +61-6-268-8767 Fax: +61-6-268-8786 s-campbell@adfa.oz.au	Structures, neutron scattering, Mössbauer
ANSTO Private Mail Bag 1 Menai NSW 2234	S. Kennedy Tel: +61-2-9717-3610 Fax: +61-2-9717-3606 sjk@ansto.gov.au	Structures, neutron scattering
Flinders University of South Australia School of Physical Sciences GPO Box 2100 Adelaide SA 5001	N. Clark Tel: +61-8-8201-2096 Nevill.Clark@flinders.edu.au	Structures, XRD
Griffith University Scool of Science Brisbane QLD 4111	E. Gray Tel: +61-7-3875-7240 Fax: +61-7-3875-7656 E.Gray@sct.gu.edu.au	Structures, neutron and X-ray diffraction, hysteresis, kinetics, magnetism
University of Newcastle Dept. of Mechanical Engineering Callaghan NSW 2308	E. Kisi Tel: +61-49-21-6213 Fax: +61-49-21-6946 meehk@cc.newcastle.edu.au	Structures, neutron and x-ray
University of New England Physics Department Armidale NSW 2351	C. Sholl Tel: +61-67-73-2387 Fax: +61-67-73-3413 csholl@metz.une.edu.au	Diffusion, NMR

Organization	Contact	Topics
University of New South Wales Department of Physics Kensington NSW 2033	S. Cadogan Tel: +61-2-9385-5203 Fax: +61-2-9385-6060 jmc@newt.phys.unsw.edu.au	H in magnet alloys
The University of Sydney School of Chemistry Sydney NSW 2006	B. Kennedy Tel: +61-2-9351-2742 Fax: +61-2-9351-3329 B.Kennedy@chem.usyd.edu.au	Structure, neutron and x-ray diffraction, PCT, electrochemistry
University of Wollongong Centre for Superconducting and Electronic Materials Wollongong NSW 2522	S.X. Dou Tel: +61-42-21-4559 Fax: +61-42-21-4577 S.Dou@uow.edu.au	MH battery alloys

CANADA

Organization	Contact	Topics
A.E.C.L. Research Reactor Materials Division Chalk River, Ontario K0J 1J0	D. Khatamian Tel: +1-613-584-3311 Fax: +1-613-584-3250 khatamid@crl5.crl.aecl.ca	Zr alloys, corrosion
Electrolyzer Corporation, Ltd. 122 The West Mall, Etobicoke Toronto, Ontario M9C 1B9	M. Fairlie Tel: +1-416-621-9140 Fax: +1-416-621-9380	Stationary and vehicular H-storage
Glenmont Consulting Box 838 Deep River, Ontario K0S 1P0	C. Ells Tel: +1-613-584-2819 Fax: +1-613-584-1802	Consulting
Hydrogen Research Institute Université du Québec à Trois-Rivières 3351, Boul des Forges Trois-Rivières, Québec G9A 5H7	T.K. Bose Tel: +1-819-376-5139 Fax: +1-819-376-5164 Tappan_Bose@uqtr.uquebec.ca	H-storage, cryoadsorbants
Hydro-Québec Technologies Emergentes de Production 1800 Bld. Lionel-Boulet Varennes, Québec J3X 1S1	R. Schultz J. Huot Tel: +1-514-652-8134 Fax: +1-514-652-8905 jhuot@ireq.ca	Mg alloys, nanocrystalline alloys
INCO Specialty Powder Products J. Roy Gordon Research Lab Mississauga, Ontario L5K 1Z9	V.A. Ettel	MH batteries

Organization	Contact	Topics
INRS-Energie et Materiaux 1650 Bld. Lionel-Boulet Varennes, Québec J3X 1S2	D. Guay Tel: +1-514-929-8141 Fax: +1-514-929-8102 guay@inrs-ener.uquebec.ca	Mg alloys, nanocrystalline alloys
McGill University Dept. of Physics 3600 University St. Montreal, Québec H3A 2T8	J. Ström-Olsen Tel: +1-514-398-6527 Fax: +1-514-398-6526 jso@physics.mcgill.ca	Amorphous and nanocrystalline alloys, PCT, microstructure, kinetics, DTA
Natural Resources Canada MTL/MTB/MMS 205A - 568 Booth St. Ottawa, Ontario K1A 0E4	Z. Wronski Tel: +1-613-992-0160 Fax: +1-613-992-8735 zwronski@NRCan.gc.ca	MH batteries
Ontario Hydro Technologies 800 Kipling Ave. Toronto, Ontario M8Z 5S4	N.P. Kherani Tel: +1-416-207-6683 Fax: +1-416-207-5551 KheraniN@oht.hydro.on.ca	Tritium handling, storage and tritide R&D, microstructure, hydride R&D
University of Ottawa Chemistry Dept. 10 Marie Curie St. Ottawa, Ontario K1N 6N5	B.E. Conway Tel: +1-613-562-5481 Fax: +1-613-562-5170	Electrodes, surface effects
University of Sherbrooke Dept. of Chemistry 2500 Bld. Université Sherbrooke, Québec J1K 2R1	G. Jerkiewicz Tel: +1-819-821-7085 Fax: +1-819-821-8017 gregoryJ@structure.chimie.usherb.ca	Electrodes, surface effects
University of Winsor Dept. of Mechanical and Materials Eng. Winsor, Ontario N9B 3P4	D.O. Northwood	Alloy PCT, AB_2 intermetallics, hysteresis

NEW ZEALAND

No apparent R&D activities on hydrides.

UNITED KINGDOM

Organization	Contact	Topics
CERAM Research Queens Road Penkhall Stoke-on-Trent ST4 7LQ		MH batteries
Defence Evaluations Research Agency Farnborough Structural Materials Centre Room 7, R50 Bldg. Farnborough, Hampshire GU14 6TD	S. Dodds Tel: +44-1252-392846 Fax: +44-1252-394135	Alloy synthesis and evaluation
Defence Evaluations Research Agency Haslar Haslar Road Gosport, Hampshire PO12 2AG	P. Jones	Battery alloys
Queens University School of Chemistry David Keir Building Belfast, Northern Ireland BT9 5AG	F. Lewis Tel: +44-1232-245133 Fax: +44-1232-245133 fa.lewis@qub.ac.uk	Pd and Pd alloys, PCT, diffusion, microstructure,
University of Birmingham School of Metallurgy and Materials Edgbaston Birmingham B15 2TT	I.R. Harris Tel: +44-121-4143659 Fax: +44-121-4145247 i.r.harris@bham.ac.uk	H-processing of magnet alloys, PCT, microstructure
University of Salford Chemical Engineering Salford M5 4WT	R. Hughes	Pd membranes
University of Salford Joule Laboratory of Physics Salford M5 4WT	D.K. Ross Tel: +44-161-2955881 Fax: +44-161-2955903 d.k.ross@physics.salford.uk	Structure, neutron scattering, PCT, TGA, muon spectroscopy
University of Sheffield Physics Dept. Housnsfield Road Hicks Bldg. Sheffield S3 7RH	J. Titman Tel: +44-114-2824287 Fax: +44-114-2728079 j.titman@scheffield.ac.uk	Diffusion, NMR, muon spectroscopy
University of Strathclyde Dept. of Chemistry 295 Cathedral St. Glasgow, Scotland G1 1XL	L.E. Berlouis Tel: +44-141-5484244 Fax: +44-141-5525664 l.berlouis@strath.ac.uk P.J. Hall Tel: +44-141-5484084 p.j.hall@strath.ac.uk	Positron annihilation, DSC, TGA

UNITED STATES

Organization	Contact	Topics
Arthur D. Little, Inc. Acorn Park Cambridge, MA 02140	S. Hynek Tel: +1-617-498-6578 Fax: +1-617-498-7206 hynek.s@adlittle.com	Mg-alloys, heat storage, coatings
Brookhaven National Laboratory Dept. of Applied Science Bldg. 815 Upton, NY 11973	J.J. Reilly Tel: +1-516-344-4502 Fax: +1-516-344-3137 jreillys@bnl.gov	Alloys, PCT, electrodes, hydride slurries, general properties
California Inst. of Technology Pasadena, CA 91125	B. Fultz Tel: +1-818-356-2170 Fax: +1-818-795-6132 btf@hyperfine.caltech.edu	MH batteries, alloy properties
Colorado State University Dept. of Physics Fort Collins, CO 80523	R.G. Leisure Tel: +1-970-491-5370 Fax: +1-970-491-7947 leisure@lamar.colostate.edu	Ultrasonic studies
Duracell, Inc. 37 A St. Needham, MA 02194	W. Luo Tel: +1-617-445-9465 Fax: +1-617-449-3970 weifang_luo@duracell.com	MH batteries
Energizer Power Systems Highway 441 North Gainesville, FL 32614	E.L. Huston Tel: +1-904-462-4455 FAX: +1-904-462-3677	MH batteries and alloys
Ergenics, Inc. 247 Margaret King Ave. Ringwood, NJ 07456	D. DaCosta Tel: +1-973-962-4480 Fax: +1-973-962-4325 mail_us@ergenics.com	Commercial, HY-STOR™ alloys, H-storage tanks, HY-STOR™ batteries, contract R&D
Energy Conversion Devices 1675 West Maple Road Troy, MI 48084	K. Sapru Tel: +1-810-362-4780 Fax: +1-810-362-0012 ksapru@rust.net	Mg alloys, amorphous and nanocrystalline alloys, PCT, MH battery alloys
Georgia Inst. of Technology School of Physics Atlanta, GA 30332	M.-Y. Chou Tel: +1-404-894-4688 Fax: +1-404-894-9958 ph279mc@prism.gatech.edu	Structure
G.G. Libowitz, Inc. P.O. Box 392 Morristown, NJ 07963	G.G. Libowitz Tel: +1-973-984-1691 Fax: +1-973-984-1691 libowitz@worldnet.att.net	Consulting

Organization	Contact	Topics
Hydrogen Components, Inc. 12420 N. Dumont Way Littleton, CO 80125	F.E. Lynch Tel: +1-303-791-7972 Fax: +1-303-791-7975 h2comp@aol.com	Commercial, H-storage tanks, PCT, alloys, H-fueled vehicles, contract R&D
Indiana Univ.-Purdue at Ft. Wayne Dept. of Chemistry 2101 Ciliserm Blvd. E Fort Wayne, IN 46805	D.E. Lynn Tel: +1-219-481-6813 Fax: +1-219-481-6880 linn@in.ipfw.indiana.edu	Complex hydrides
Iowa State University Ames Laboratory 242 Spedding Ames, IA 50011	V.K. Pecharsky Tel: +1-515-294-8220 Fax: +1-515-294-9579 vitkp@ameslab.gov J. Ting ting@ameslab.gov	Alloy synthesis, atomization
Los Alamos National Lab Center for Materials Science Los Alamos, NM 87545	R.O Schwartz Tel: +1-505-667-8454 Fax: +1-505-665-2992 rxzs@lanl.gov	Theory, hysteresis (other activities, mostly classified)
MER Corporation 7960 S. Kolb Road Tucson, AZ 85706	R.O. Loutfy Tel: +1-602-574-1980 Fax: +1-602-574-1983 rloutfy@opus1.com	Fullerene carbon
Miami University Chemistry Dept. Oxford, OH 45056	J. Cantrell Tel: +1-513-529-2834 Fax: +1-513-529-5715 jscantrel@miamiu.muohio.edu	Structure, XRD
NASA Jet Propulsion Laboratory California Inst. of Technology 4800 Oak Grove Drive Pasadena, CA 91109	R.C. Bowman Tel: +1-818-354-7941 Fax: +1-818-393-4206 robert.c.bowman-jr@jpl.nasa.gov	Alloy properties, absorption cryocoolers
NASA Jet Propulsion Laboratory California Inst. of Technology 4800 Oak Grove Drive Pasadena, CA 91109	B.V. Ratnakumar Tel: +1-818-354-0110 Fax: +1-818-393-6951 ratnakumar.v.bugga@jpl.nasa.gov	MH battery alloys
National Institute of Standards & Technology Bldg. 235 Gaithersburg, MD 20899	T.J. Udovic Tel: +1-301-975-6241 Fax: +1-301-921-9847 udovic@rrdstrad.nist.gov	Neutron scattering
National Renewable Energy Lab 1617 Cole Blvd. Golden, CO 80401	M. Heben Tel: +1-303-384-6641 Fax: +1-303-384-6490 mikeh@nrel.gov	Nanotube carbon

Organization	Contact	Topics
Naval Research Laboratory Code 6320 Washington, DC 20375	M.A. Imam Tel: +1-202-767-2185 Fax: +1-202-767-2623 imam@anvil.nrl.navy.mil	Mg-alloys, nanocrystalline alloys, PCT, kinetics, microstructure
Oak Ridge National Laboratory P.O. Box 2008 Oak Ridge, TN 37831	R. Murphy Tel: +1-423-576-7772 Fax: +1-423-574-9331 rim@ornl.gov	Fullerene carbon
Oak Ridge National Laboratory Lockheed Martin Energy systems P.O. Box 2009 Oak Ridge, TN 37831	G.L. Powell Tel: +1-615-574-1717 Fax: +1-615-574-2582 plg@onrl.gov	Hydrides, isotope-storage, corrosion
Sandia National Laboratories P.O. Box 969 Livermore, CA 94551	G. Thomas Tel: +1-510-294-3224 Fax: +1-510-294-3410 gthomas@sandia.gov	Mg alloys, PCT, kinetics, metallography, H-storage, IEA/DOE/SNL on-line database server
SunaTech, Inc. 113 Kraft Pl. Ringwood, NJ 07456	G. Sandrock Tel: +1-973-962-1158 Fax: +1-973-962-1158 sandrock@warwick.net	Consulting, contract R&D, IEA/DOE/SNL on-line databases, IEA Task 12 Operating Agent
Trinity College Chemistry Dept. 300 Summit St. Hartford, CT 06106	R.O. Moyer Tel: +1-860-297-2217 Fax: +1-860-297-5129 ralph.moyer@trincoll.edu	Complex hydrides
University of Hawaii Dept. of Chemistry 2545 The Mall Honolulu, HI 96822	C.M. Jensen Tel: +1-808-956-6721 Fax: +1-808-956-5908 jensen@gold.chem.hawaii.edu	Polyhydrides
University of Illinois Materials Research Laboratory 104 South Goodwin Ave.	H.K. Birnbaum Tel: +1-217-333-1370 Fax: +1-217-244-2278 hbirnbau@uiuc.edu	Hydride precipitation in alloys, metallurgy, metallography
University of Memphis Physics Dept. Memphis, TN 38152	J.W. Hanneken Tel: +1-901-678-2417 Fax: +1-901-678-4733 jhannekn@cc.memphis.edu	Misc. properties
University of Nevada-Reno Mackay School of Mines Dept. of Chem. and Met. Eng. Reno, NV 89557	D. Chandra Tel: +1-702-784-4960 Fax: +1-702-784-4316 dchandra@scs.unr.edu	Alloys, PCT, cyclic stability

Organization	Contact	Topics
University of Vermont Dept. of Chemistry Burlington, VT 05405	T.B. Flanagan Tel: +1-802-656-0199 Fax: 1-802-656-8705 flanagan@emba.uvm.edu	Alloys, PCT, calorimetry, Pd and Pd-alloys, thermodynamics
Washington University One Brookings Drive St. Louis, MO 63130	K.F. Kelton Tel: +1-314-935-6228 Fax: +1-314-935-6219 kfk@wuphys.wustl.edu	Quasicrystals, NMR
West Chester University Chemistry Dept. West Chester, PA 19383	A. Goudy Tel: +1-610-436-2675 Fax: +1-610-436-2890 agoudy@wcupa.edu	H/D kinetics
Westinghouse Savannah River Co. P.O. Box 616 Aiken, SC 29802	T. Motyka Tel: +1-803-725-3665 Fax: +1-803-725-2756 ted.motyka@srs.gov	Applications, isotope handling, H-storage, compression, tritium, H-vehicle, hydride composites

ATTACHMENT

REPORTS AND REPORT DISTRIBUTION

REPORT TYPES

(b) Final Technical Report, issued at completion of Grant.
Note: Technical Reports must have a SF-298 accompanying them.

REPORTS DISTRIBUTION		
ADDRESSEES	REPORT TYPES	NUMBER OF COPIES
Office of Naval Research Program Officer John A. Sedriks ONR 332 Ballston Center Tower One 800 North Quincy Street Arlington, VA 22217-5660	(b) w/(SF-298's)	7
MIAC Newsletter MIAC/CINDAS Purdue University 2595 Yeager Road West Lafayette, IN 47906-1398	(b) w/(SF-298)	1
Director, Naval Research Laboratory Attn: Code 2627 4555 Overlook Drive Washington, DC 20375-5326	(b) w/(SF-298)	1
Defense Technical Information Center 8725 John J. Kingman Road STE 0944 Ft. Belvoir, VA 22060-6218	(b) w/(SF-298's)	2

If the Program Officer directs, the Grantee shall make additional distribution of technical reports in accordance with a supplemental distribution list provided by the Program Officer. The supplemental distribution list shall not exceed 250 addresses.